ABSTRACT

SUAREZ, VINICIO A. Implementation of Direct Displacement-Based Design for Highway Bridges. (Under the direction of Dr. Mervyn Kowalsky).

In the last decade, seismic design shifted towards Displacement-Based methods. Among the several methodologies that have been devolved, the Direct Displacement-Based Design Method (DDBD) has been shown to be effective for performance-based seismic design of bridges and other types of structures.

The main objective of this Dissertation is to bridge the gap between existing research on Direct Displacement-Based Design (DDBD) and its implementation for design of conventional highway bridges.

Real highway bridges have complexities that limit the application of DDBD. This research presents new models to account for: limits in the lateral displacement capacity of the superstructure, skewed configurations, P-Δ effects, expansion joints and different types of substructures and abutments. Special interest is given to the definition of predefined displacement patterns that can be used for direct application of DDBD to several types of bridges.

The results of the research show the effectiveness of the proposed models. One of the most relevant conclusions is that bridge frames of bridges with seat-type abutments, which comply with the balanced mass and stiffness requirements of AASHTO, can be designed with DDBD using rigid body translation patters, which greatly simplifies the application of DDBD.

Another objective of the research was to compare the execution and outcome of DDBD to the design method in the new AASHTO Guide Specifications for LRFD Seismic Bridge Design. This was accomplished by a comparative study of four real bridges designed with the two methods. Results of that study indicate that DDBD is compatible with the new AASHTO Guide Specification and furthermore, it has several advantages over the design method in that specification.

Important products of this research are the computer programs DDBD-Bridge and ITHA-Bridge for design and assessment of highway bridges.

Implementation of Direct Displacement Based Design for Highway Bridges

by
Vinicio A. Suarez

A dissertation submitted to the Graduate Faculty of
North Carolina State University
in partial fulfillment of the
requirements for the Degree of
Doctor of Philosophy

Civil Engineering

Raleigh, North Carolina

2008

APPROVED BY:

_____	_____
Dr. Vernon Matzen	Dr. James Nau
_____	_____
Dr. Mohammed Gabr	Dr. Lewis Reynolds

_____

Dr. Mervyn Kowalsky

Chair of Advisory Committee

BIOGRAPHY

Vinicio Suarez was born in Cuenca, Ecuador on February 23th, 1975. He received his BS in Civil Engineering, in December 2000, from Universidad Tecnica Particular de Loja (UTPL), in Ecuador. After graduating, he jointed the School of Engineering at UTPL as faculty member and taught courses on Strength of Materials and Reinforced Concrete. In August of 2004, he came to Raleigh and joined North Carolina State University to obtain a Master of Science Degree in 2005. After that, he started Doctoral studies, which he completed in 2008, obtaining the Degree of Doctor of Philosophy in Civil Engineering. His research interests include but are not limited to the seismic analysis and design bridges and buildings, soil-structure interaction and software development. After completion of his PhD, Vinicio will return to Ecuador as a Professor, Director of the Civil Engineering School and Director of the Civil Engineering, Geology and Mining Research Center at UTPL.

ACKNOWLEDGMENTS

I wish to thank my advisor, Dr. Mervyn Kowalsky, for his continuous support and generosity in passing on his knowledge to me. I also want to thank the other members of the Advisory Committee, Dr. Vernon Matzen, Dr. Mohammed Gabr, Dr. James Nau and Dr. Lewis Reynolds.

I would not have done this without the love of my wife, María del Rocío and the support of of UTPL and its Chancellor Dr. Luis Miguel Romero. I also thank my friends in NCSU especially Brent Robinson and Luis Mata for their continuous support.

Finally, I would like to thank the financial support provided by NCSU, UTPL and SENACYT.

TABLE OF CONTENTS

LIST OF TABLES

PART IV

PART V

PART VI

LIST OF FIGURES

PART I

PART II

PART III

PART IV

PART V

PART VI

APPENDICES

PART I

INTRODUCTION AND RESEARCH OBJETIVES

1. INTRODUCTION

Ideally, seismic resistant structures are designed with a simple configuration, such that their behavior can be easily modeled and analyzed, while aiming that energy dissipation takes place in well defined parts of the structure. In contrast with the seismic design of buildings, highway overpasses are usually designed to limit their capacity to the lateral capacity of the piers, therefore, bridge columns must be designed and detailed carefully to assure ductile behavior and capacity which is in excess of seismic demand.

Seismic design of bridges can be accomplished following different approaches. The conventional procedure, currently found in the LRFD Bridge Design Specification (AASHTO, 2004), is "force based" since damage in the structure is controlled by the provision of strength. The procedure uses strength reduction factors to reduce the elastic force demand to a design level demand while considering the importance, assumed ductility capacity, over-strength and redundancy in the structure.

After the Loma Prieta earthquake in 1989, extensive research has been conducted to develop improved seismic design criteria for bridges, emphasizing the use of displacements rather than forces as a measure of earthquake demand and damage in the structures (Priestley, 1993; ATC, 1996; Caltrans, 2006; ATC, 2003). Extensive work on the application of capacity design principles to assure ductile mechanisms and concentration of damage in specified regions has also been conducted.

Several Displacement-Based Design (DBD) methodologies have been proposed, among them, the Direct Displacement-Based Design Method (DDBD) (Priestley, 1993) has proven to be effective for performance-based seismic design of bridges, buildings and other types of structures (Kowalsky, 1995; Calvi and Kingsley, 1997; Kowalsky 2002; Dwairi, 2005; Ortiz, 2006; Suarez and Kowalsky, 2007).

The main objective of this research is to bridge the gap between existing research on DDBD and its implementation for design of conventional highway bridges with all their inherent complexities. This research addresses issues such as: limited displacement

superstructure capacity, skew in bents and abutments, displacement patterns, P-Δ effects, and different types of substructures, increasing the scope and applicability of DDBD substantially.

2. DISSERTATION ORGANIZATION

The Dissertation has seven parts. The first one contains the introduction and objectives of the research. It also includes a review of DDBD and other displacement based procedures.

Part II deals with the implementation of DDBD. In this part the DDBD method is presented with new features such as: the determination of a superstructure target displacement, the determination of a stability-based target displacement for piers, the design of skewed bents and abutments. Also included is a description of different design algorithms and their application to different types of bridges.

Part III contains a comparative study of bridges designed with DDBD and with the method in the AASHTO Guide Specification for LRFD Seismic Design of Bridges. The study looks at differences in the execution and outcome of the two methods.

Part IV contains a paper entailed "Displacement Patterns for Direct Displacement Based Design of Conventional Highway Bridges"**.** This paper focuses on determining under what conditions predefined displacement patterns can be used for DDBD of different types of bridges. This is an extension of previous work done by Dwairi (2006).

Part V contains a paper entailed "Determination of a Stability-Based Target Displacement for Direct Displacement-Based Design of Bridges". In designs controlled by P-Δ effects, the determination of a target displacement that accounts for these effects eliminates the need for iteration in DDBD. This part contains the derivation of a model to compute the target displacement and also contains examples that demonstrate its application.

Part VI contains the paper "Direct Displacement-Based Design as an Alternative Method for Seismic Design of Bridges". This paper compares DDBD to the method in the AASHTO Guide Specification for LRFD Seismic Bridge Design. Finally, the summary and conclusions of the research are presented in Part VII.

3. REVIEW OF THE FUNDAMENTALS OF DBD

Displacement Based Design (DBD) has gained popularity in the last decade, as it addresses several shortcomings of the conventional Force Based Design (FBD) procedure, while serving as a useful tool for performance-based seismic engineering. FBD is currently found in the AASHTO LRFD Bridge Design Specification (AASHTO, 2004).

The primary difference between DBD and FBD is that the first uses displacement as a measure of seismic demand and also as an indicator of damage in the structure. DBD takes advantage of the fact that displacement correlates better with damage than force. DBD also overcomes serious problems of FBD such as ignoring the proportionality between strength and stiffness and the generalization of ductility capacity through the use of force reduction factors (Priestley et al, 2007).

Several Displacement Based Design (DBD) methodologies have been developed including:

- The Direct Displacement Based Design Method (DDBD) (Priestley, 1993)
- The Seismic Design Criteria of Caltrans (Caltrans, 2006)
- The Bridge Design Specification of South Carolina DOT (SCDOT, 2002)
- MCEER/ATC-49 Recommended LRFD guidelines for seismic design of bridges (ATC, 2003)
- The Proposed AASHTO Guide Specification for LRFD Seismic Bridge Design (Imbsen, 2007)

DDBD and the other procedures show similarities such as:

- The use of displacement as a measure of damage and seismic demand.
- They require the computation of specific values of ductility for each bridge. This contrasts with the FBD approach in which ductility capacity is generalized by specification of force reduction factors.
- Capacity Design principles are used to assure damage will only occur in predefined locations in the structure.

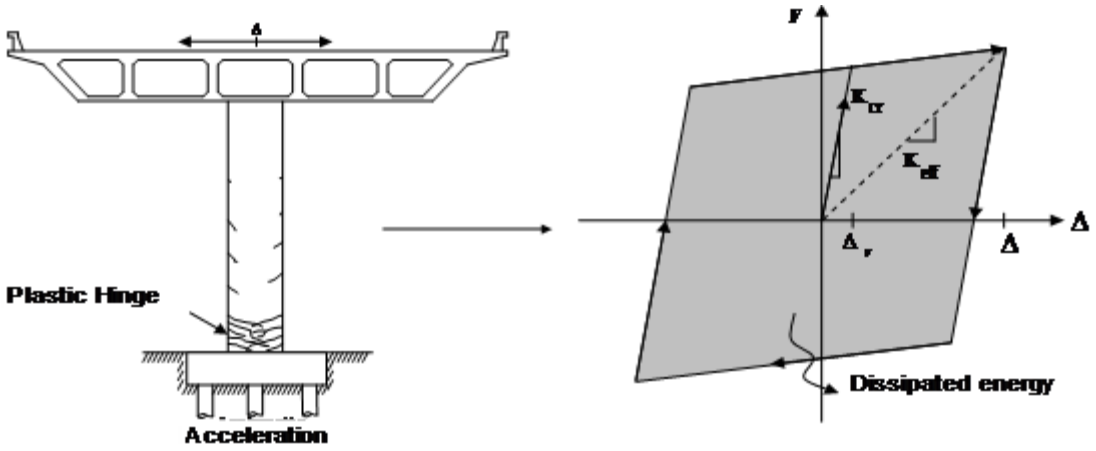

(a)

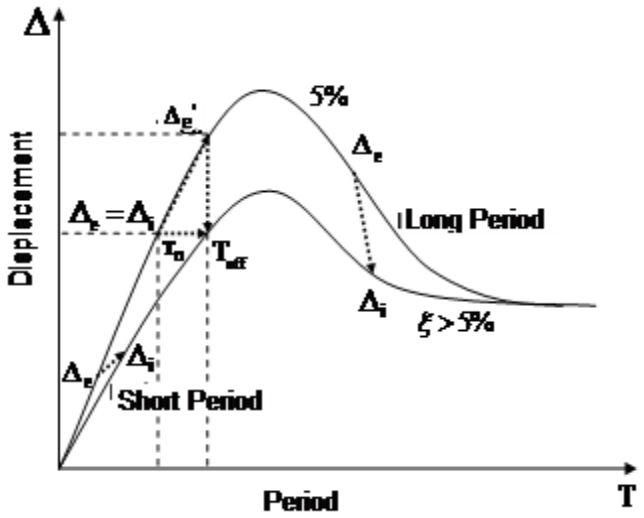

(b)

Figure 1 - Effects of earthquake motion on inelastic SDOF

Despite the similarities, DDBD and the other DBD methods differ in several aspects:

- DDBD goes directly from target displacement to required strength, while the other methods require an iterative process in which strength is assumed and then displacement demand is checked against displacement capacity.
- DDBD uses equivalent linearization, while the other methods use displacement modification, which leads to the use of the equal displacement approximation

(Newmark and Hall, 1982) for systems in the constant velocity region of the design spectra.

The use of equivalent linearization in DDBD versus the use of displacement modification in the other methods, it is believed by the author to be a fundamental source of difference between both approaches. The origin and effects of this difference are discussed in the following section.

3.1 Linearization of Inelastic Response of SDOF Systems

When a structure under seismic excitation is taken beyond its elastic limit, its maximum response is influenced by two phenomena: stiffness degradation and energy dissipation, as shown in Fig. (1.a). The degradation in stiffness is caused by yielding of sections in the structure and its primary effect is the increase of the displacement demand due to lengthening of the fundamental period. At the same time, the hysteretic behavior of the yielding sections results in energy dissipation, which reduces the displacement demand due to an increase of damping in the system. These effects can be visualized for different regions of the design spectrum in Fig. (1.b). If a Single Degree of Freedom (SDOF) system with initial period T_n is considered of infinite strength and 5% damping, it responds with a peak elastic displacement Δ_e. But, if a reduced strength is considered, yielding occurs, stiffness degrades, period lengthens to T_{eff} and displacement demand increases to Δ'_e. However, this tendency to displace more is counteracted by the increase in damping that in turn, reduces the displacement demand to the final maximum inelastic displacement Δ_i. In a certain section of the spectrum, Δ_e and Δ_i coincide, meaning that the effect of stiffness degradation is fully counteracted by the increase in damping. This observation has resulted in the "equal displacement rule" for elasto-plastic SDOF systems (Newmark and Hall , 1982). For SDOF with short periods the stiffness effect is greater than the damping effect, which results in an increase of the displacement demand. The contrary effect happens for SDOF with long periods of vibration.

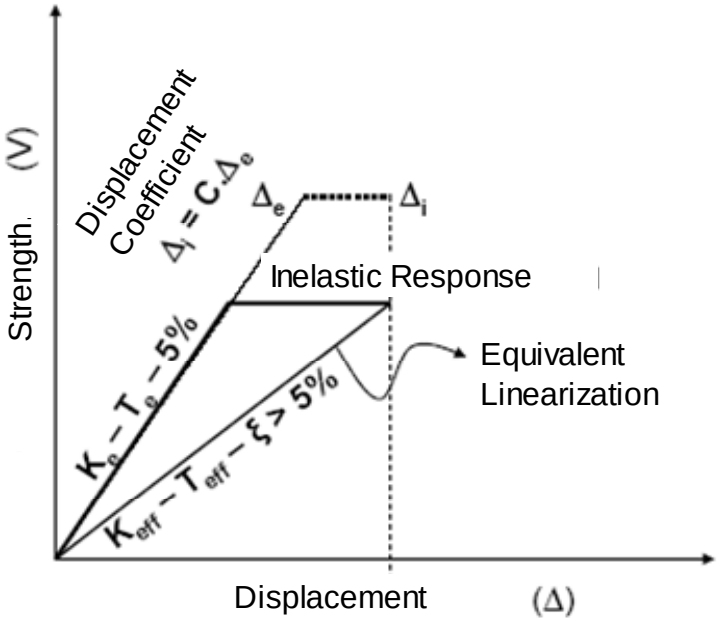

Figure 2 - Linearization Methods

For design purposes, since seismic hazard is usually presented in the form of elastic spectra, it is convenient to substitute the real inelastic system for an elastic one such that both systems reach the same peak displacement. There are two widely known approaches to linearize inelastic SDOF systems: The Displacement Modification Method and the Equivalent Linearization Method.

Displacement Modification Method (DMM)

This method is used by AASHTO (Imbsen, 2007) and Caltrans (2006) to replace the inelastic system by an elastic one, with the same level of elastic-damping and fundamental-elastic period. The peak response of the substitute system is modified to match the peak displacement of the inelastic system by application of the displacement coefficient *C* (Fig. 2).

The coefficient *C* has been studied extensively (Newmark and Hall, 1982; Miranda, 2000; FEMA, 2005), concluding that assuming C = 1 (i.e. equal displacement approximation) is appropriate for structures in which the fundamental period is longer than a

characteristic period, T*, equal to 1.25 times the period, T_s, at the end of the spectral acceleration plateau (Fig. 3). For short period structures, C is increased as given by Eq. 1 (Imbsen, 2007), where R equals the maximum ductility demand expected in the structure, and T* equals 1.25 T_s (Fig.3).

$$C = \left(1 - \frac{1}{R}\right)\frac{T^*}{T} + \frac{1}{R} \geq 1.0 \qquad \text{(Eq.1)}$$

Equivalent Linearization Method (ELM)

This method is used in DDBD. In this approach, an inelastic SDOF is substituted by an elastic system with secant stiffness and equivalent viscous damping which, under earthquake excitation, reaches the same maximum displacement as the original inelastic SDOF (Fig.2) (Shibata and Sosen, 1976).

Several studies have been conducted to obtain models of equivalent damping, $\xi_{eq,}$ for different types of structural elements such as RC beams, unbonded-postensioned walls, steel members, drilled shafts and piles and isolation/dissipation devices. (Dwairi, 2005 ; Blandon, 2004 ; Suarez, 2007) . Table 1 shows some of these models where ξ_v is the viscous damping in the elastic range, *r* Is the ratio between second and first slopes in a bilinear force-deformation response, μ is the ductility demand, T_{eff} is the effective period that corresponds to secant stiffness and *a,b,c,d*, and *A,B,C,D,G,H,I,J* are coefficients that depend on the hysteresis model.

The models in Table 1 allow the linearization of the response of inelastic SDOF using a combination of period and equivalent damping. The ATC-40 (ATC, 1996) model utilizes the area of hysteresis as an indication of equivalent damping, as first proposed by Jacobson (1930). Recently, work done by Dwairi (2005) has indicated that when utilizing effective period based on secant stiffness to maximum response, the area approach overestimates damping. Instead, Dwairi obtained hysteretic damping by determining the optimum value of damping to be combined with secant stiffness such that the resulting response matches an Inelastic Time History Analysis (ITHA). A similar approach has been followed by Blandon

and Priestley (2004) and Suarez and Kowalsky (2007) to obtain models that can be used with DDBD.

Table 1 - Models for equivalent linearization

Source	Model	Applicable to:
Blandon, 2004	$\xi_{eff} = \frac{a}{\pi}\left(1-\frac{1}{\mu^b}\right)\cdot\left(1+\frac{1}{(T_{eff}+c)^d}\right)\cdot\frac{1}{N}$ $T_{eff} = T_o\sqrt{\frac{\mu}{1+\alpha\mu-\alpha}}$	**RC Columns**
Dwairi, 2005	$\xi_{eff} = \xi_v + C_{ST}\left(\frac{\mu-1}{\pi\mu}\right)\%$ $C_{sT} = 50+40(1-T_{eff}),\ T_{eff}<1$ $C_{ST} = 50\ ,\ T_{eff}>1$ $T_{eff} = T_o\sqrt{\frac{\mu}{1+\alpha\mu-\alpha}}$	**RC Columns**
Suarez, 2007	$\xi_{eff} = \xi_v\mu^{-0.376} + 13.7 + 10.9\frac{\mu-1}{\pi\mu}$ $T_{eff} = T_o\sqrt{\frac{\mu}{1+\alpha\mu-\alpha}}$	**Drilled Shafts in soft clay**
FEMA-440	If $1<\mu<4$: $\xi_{eff} = A(\mu-1)^2 + B(\mu-1)^3 + \xi_v$ $T_{eff} = \left[G(\mu-1)^2 + H(\mu-1)^3 + 1\right]T_o$ If $4\le\mu\le6.5$: $\xi_{eff} = C + D(\mu-1) + \xi_v$ $T_{eff} = \left[I + J(\mu-1) + 1\right]T_o$	**Stiffness degrading systems**
ATC-40	$\xi_{eff} = 0.05 + K\frac{2}{\pi}\frac{(\mu-1)(1-\alpha)}{\mu(1+r\mu-\alpha)}$ $T_{eff} = T_o\sqrt{\frac{\mu}{1+r\mu-\alpha}}$	**Bilinear response**

In 2005 FEMA published FEMA-440 updating the equivalent linearization model initially proposed by ATC-40. In this model equivalent damping is related to an effective

period based on stiffness which is not secant to maximum response. According to FEMA, using such definition of period reduces the variability in the determination of equivalent damping.

Comparative analysis of the linearization approaches

As it was mentioned before, the inelastic response of a SDOF system is affected by stiffness degradation and increased damping. The equivalent linearization approach, used in DDBD, accounts for these two phenomena in a rational and independent way. Conversely, with the displacement modification, these effects are mixed together, without considering the relation between damping and ductility and the energy dissipation characteristics of different materials. Furthermore, most of the research on coefficient C has been based on the response of elastic perfectly-plastic SDOF with mass proportional viscous damping, even though that type of response is not observed in reinforced concrete piers. (Priestley et al, 2007)

For a quantitative comparison of the two linearization methods, a displacement coefficient *C* is derived from an equivalent damping model. Based on its definition,

$$C = \frac{\Delta_i}{\Delta_e} \qquad \text{(Eq. 2)}$$

where Δ_i is the inelastic displacement and Δ_e is the elastic displacement of a SDOF system with the same fundamental period T_n and 5% viscous damping. Δ_i can be found in terms of effective period T_{eff} and equivalent damping ξ_{eq} as (Eurocode , 1998):

$$\Delta_{i(T_{eff})} = \Delta_{e(T_{eff})}\sqrt{\frac{7}{2+\xi_{eff}}} \qquad \text{(Eq. 3)}$$

Replacing Eq.3 in Eq.2, *C* is found as the ratio of elastic displacement for initial and effective periods times a damping reduction factor:

$$C = \frac{\Delta_{e(T_{eff})}}{\Delta_{e(T_n)}}\sqrt{\frac{7}{2+\xi_{eff}}} \qquad \text{(Eq.4)}$$

For the two point acceleration response spectra shown in Fig. 3, Eq.4 can be simplified for three cases:

a) When $T_o < T_n < T_s$ y $T_o < T_{eff} < T_s$

$$\Delta_e = \frac{S_{DS} T^2}{4\pi^2} \qquad \text{(Eq.5)}$$

$$C = \frac{T_{eff}^2}{T_n^2} \sqrt{\frac{7}{2 + \xi_{eff}}} \qquad \text{(Eq.6)}$$

b) When $T_o < T_n < T_s$ y $T_{eff} > T_s$

$$\Delta_e = \frac{S_{D1} T}{4\pi^2} \qquad \text{(Eq.7)}$$

$$C = \frac{T_S T_{eff}}{T_n^2} \sqrt{\frac{7}{2 + \xi_{eff}}} \qquad \text{(Eq.8)}$$

c) When $T_n > T_s$ y $T_{eff} > T_s$

$$C = \frac{T_{eff}}{T_n} \sqrt{\frac{7}{2 + \xi_{eff}}} \qquad \text{(Eq.9)}$$

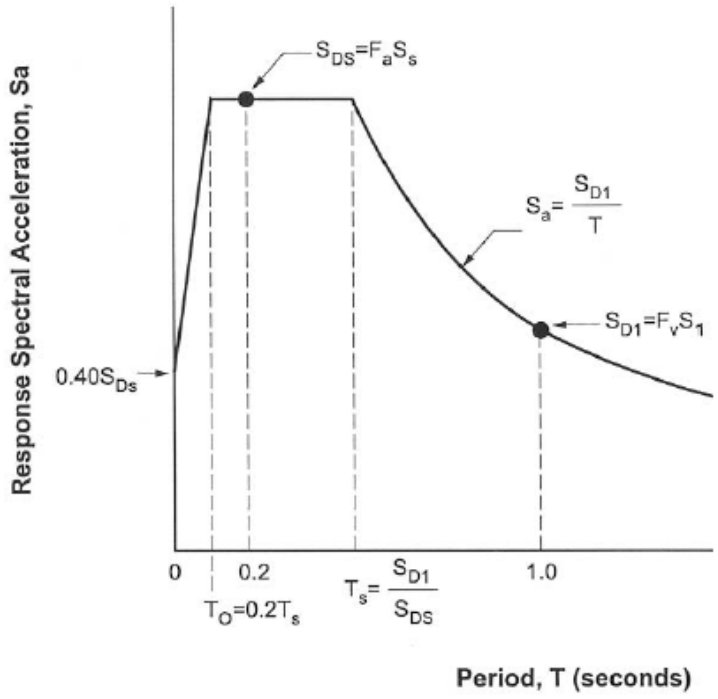

Figure 3 - Acceleration Response spectrum

Using Eq. 9, C has been found for SDOF systems with $T_n > 1$ s using the equivalent linearization models presented in Table 1. The results are shown in Fig.4. Following an inverse approach, and also for the sake of comparison, the equal displacement approximation has been translated into an equivalent damping model, with results as shown in Fig. 5

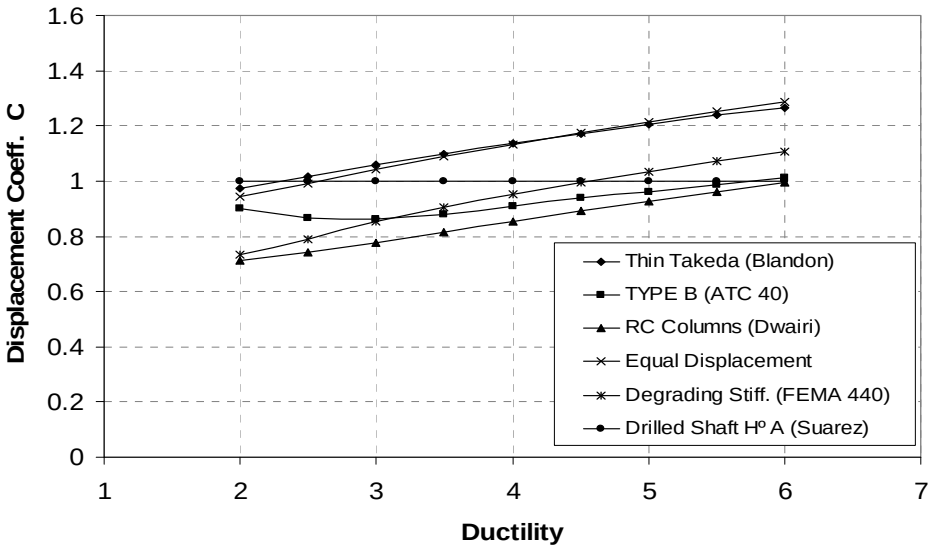

Figure 4 - Equivalent damping models translated to displacement coefficient

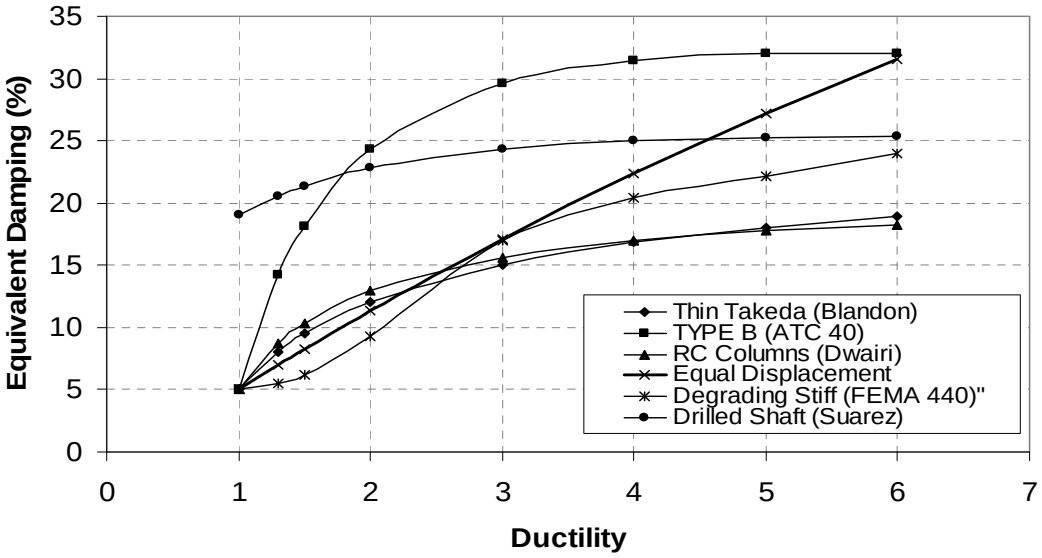

Figure 5 - Displacement coefficient models translated to equivalent damping

It has been shown that for SDOF systems, equivalent linearization can be converted to displacement modification or vice versa, and as a result the two approaches are valid to linearize the inelastic response of SDOF systems. In addition, from observation of Figs. 4 and 5, important conclusions can be advanced:

- The equivalent damping models translate into displacement coefficient models that increase with ductility, whereas the equal displacement approximation implies C = 1, independently from ductility. Fig. 6 shows C coefficient from FEMA-440 (2006) as a function of T_n and the force reduction factor, R, which for elastoplastic response can be assumed equal to ductility. This graph shows that in reality, C increases with ductility as predicted by the equivalent damping models. Assuming C = 1 seems to be a gross average of response.

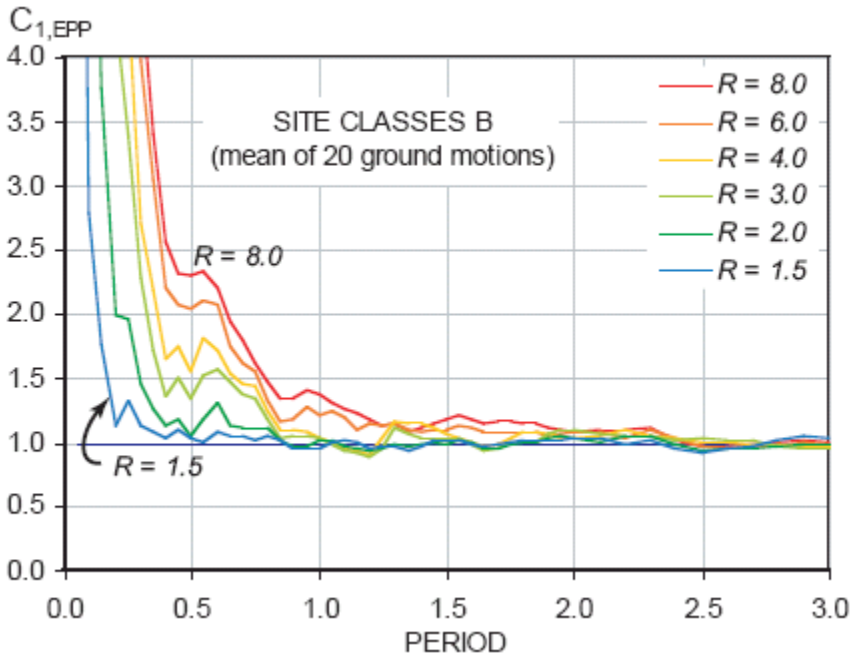

Figure 6 - C coefficient for elastoplastic systems in sites class B. (FEMA, 2006)

- By comparing the equivalent damping model derived from the equal displacement approximation with the equivalent damping models proposed by Blandon and Dwairi; it is observed that the equal displacement approximation implies less damping for

ductility less than 2.5 and more damping for higher ductility. That means that bridge piers with ductility less than 2.5 require less strength if designed based on Dwairi or Blandon equivalent damping models.

- The equivalent damping model in FEMA 440 can not be compared to other damping models since this model is meant to be used with combination with an effective period that is not base on stiffness secant to maximum response.
- Fig. 5 shows that the equal displacement approximation is conservative for design of drilled shafts bents, since ignores soil damping.

4. DISPLACEMENT BASED DESIGN METHODS

4.1 Seismic Design Criteria by Caltrans

The Seismic Design Criteria (SDC) by Caltrans (2006) shifted towards displacement based design in 1999 consolidating ATC-32 recommendations (American Technology Council, 1996). The SDC is currently used for design of ordinary bridges in the state of California.

The SDC of Caltrans presents an iterative design procedure in which the lateral strength of the system (size and reinforcement of the substructure sections) is assumed at the beginning of the process. Then, by means of displacement demand analysis and displacement capacity verification, it is confirmed that the bridge with the assumed strength has an acceptable performance, otherwise, the strength is revised and the process repeated.

In the demand analysis, the peak inelastic displacement demands are estimated from a linear elastic response spectrum analysis of the bridge with cracked (secant to yield point) section stiffness. Then, elastic peak displacements are converted to peak inelastic displacements using the Displacement Modification Method described in Section 3.1.

Once the displacement demands are estimated, the procedure requires the verification of the displacement capacity of each pier by means of a pushover analysis. Finally, the substructure sections and protected elements are designed and detailed according to capacity design principles.

4.2 Proposed AASHTO Guide Specification for LRFD Seismic Bridge Design

The AASHTO LRFD Bridge Design Specifications (2004) and the AASHTO Standard Specifications are essentially the recommendations that were completed by the Applied Technology Council (ATC-6) in 1981 and adopted by AASHTO as a "Guide Specification" in 1983. Recognizing the availability of improvements since ATC-6 as documented in NCHRP 12-49, Caltrans Seismic Design Criteria (SDC) 2006, SCDOT – Seismic Design Specifications for Highway Bridges (2002) and related research projects, the T-3 AASHTO committee for seismic design started a project to update the LRFD guidelines that yielded the proposed AASHTO Guide Specification for LRFD Seismic Bridge Design (Imbsen, 2007).

The LRFD Seismic guide recognizes the variability of seismic hazard over the US territory and specifies different Seismic Design Categories. For category A no design is required, for categories B, C and D, demand analysis and capacity verification is required. The design procedure is in concept similar to the procedure by Caltrans, described in the previous section. For regular bridges, the demand analysis is performed by the uniform load method for regular bridges, while the spectral modal analysis can be used for all bridges. The capacity verification can be done using implicit equations for seismic design category B or C and by pushover analysis for categories D. As in Caltrans SDC, and with the exception of seismic category A, the proposed guide requires the application of capacity design principles for the detailing of the substructure sections and protected elements.

4.3 Direct Displacement Based Design

The Direct Displacement Based Design Method can be used for performance-based design of bridges, buildings and other types of structures (Priestley et al, 2007). DDBD uses the equivalent linearization approach described in section 3.1. The procedure starts with a target displacement and returns strength required to meet the target displacement under earthquake attack. The main steps involved in the application of DDBD are:

1) Determination of a target displacement profile for the bridge.
2) Evaluation of a substitute SDOF system, including the determination of equivalent damping based on ductility demand at target displacement.
3) Determination of required stiffness and strength using displacement design spectra.
4) Distribution of strength and application of capacity design principles.

DDBD requires no iteration when the target displacement profile can be accurately estimated at the beginning of the process. That is the case when a continuous bridge is designed in the longitudinal direction. No iteration is neither required for transverse design when the superstructure is formed by simply supported spans or when the superstructure displaces transversely as a rigid body. The DDBD method for bridges is covered in detail in Part II.

5. RESEARCH OBJECTIVES

The main objective of this research is to bridge the gap between existing research DDBD and its implementation for design of conventional highway bridges, with all their inherent complexities.

Since it was first proposed by Priestley in 1993, DDBD has been under constant development. Despite the important and extensive progress of DDBD in the last decade, several items require specific attention to fully implement DDBD for conventional highway bridges. The specific objectives of this dissertation are:

- Determine under what conditions predefined displacement patterns can be used for DDBD of different types of bridges.
- Propose a model for determination of a stability-based target displacement for piers.
- Propose models to account for: displacement capacity of the superstructure and skew.
- Define a general DDBD procedure for conventional highway bridges
- Determine the scope and applicability of DDBD
- Compare DDBD to the recently proposed AASHTO LRFD Seismic Design Guide

- Develop software for the application of DDBD

6. REFERENCES

AASHTO, 2004, LRFD Bridge design specifications, fourth edition, American Association of State Highway and Transportation Officials, Washington, D.C.

ATC, 2003, NCHRP 12-49 Recommended LRFD Guidelines for the Seismic Design of Highway Bridges, http://www.ATCouncil.org, (accessed June, 2008)

ATC-40. "Seismic Evaluation and Retrofit of Concrete Buildings/Volume 1". 1996, http://www.ATCouncil.org, (accessed June, 2008)

Blandon Uribe C., Priestley M. 2005, Equivalent viscous damping equations for direct displacement based design, "Journal of Earthquake Engineering", Imperial College Press, London, England, 9, SP2, pp.257-278.

Caltrans, 2006, Seismic Design Criteria, Caltrans, http://www.dot.ca.gov/hq/esc/earthquake_engineering, (accessed April 18, 2008)

Calvi G.M. and Kingsley G.R., 1995, Displacement based seismic design of multi-degree-of-freedom bridge structures, Earthquake Engineering and Structural Dynamics 24, 1247-1266.

Dwairi, H. and Kowalsky, M.J., 2006, Implementation of Inelastic Displacement Patterns in Direct Displacement-Based Design of Continuous Bridge Structures, Earthquake Spectra, Volume 22, Issue 3, pp. 631-662

Dwairi, H., 2004. Equivalent Damping in Support of Direct Displacement - Based Design with Applications To Multi - Span Bridges. PhD Dissertation, North Carolina State University

EuroCode 8, 1998, Structures in seismic regions – Design. Part 1, General and Building", Commission of European Communities, Report EUR 8849 EN

FEMA, 2006. "FEMA 440, Improvement Of Nonlinear Static Seismic Analysis Procedures", http://www.fema.gov, (accessed June, 2008)

Imbsen, 2007, AASHTO Guide Specifications for LRFD Seismic Bridge Design, AASHTO, http://cms.transportation.org/?siteid=34&pageid=1800, (accessed April 18, 2008).

Kowalsky M.J., 2002, A Displacement-based approach for the seismic design of continuous concrete bridges, Earthquake Engineering and Structural Dynamics 31, pp. 719-747.

Kowalsky M.J., Priestley M.J.N. and MacRae G.A. 1995. Displacement-based Design of RC Bridge Columns in Seismic Regions, Earthquake Engineering and Structural Dynamics 24, 1623-1643.

Miranda E. Inelastic displacement ratios for structures on Brm sites. Journal of Structural Engineering 2000; 126:1150–1159.

Newmark NM, Hall WJ. Earthquake Spectra and Design. Earthquake Engineering Research Institute, Berkeley, CA, 1982.

Ortiz, J., 2006, Displacement-Based Design of Continuous Concrete Bridges under Transverse Seismic Excitation". European School for Advanced Studies in Reduction of Seismic Risk (ROSE School).

Priestley, M. J. N., 1993, Myths and fallacies in earthquake engineering-conflicts between design and reality, Bulletin of the New Zealand Society of Earthquake Engineering, 26 (3), pp. 329–341

Priestley, M. J. N., Calvi, G. M. and Kowalsky, M. J., 2007, Direct Displacement-Based Seismic Design of Structures, Pavia, IUSS Press

Shibata A. and Sozen M. Substitute structure method for seismic design in R/C. Journal of the Structural Division, ASCE 1976; 102(ST1): 1-18.

South Carolina Department of Transportation (2002), Seismic Design Specifications for Highway Bridges, First Edition 2001, with October 2002 Interim Revisions

Suarez, V.A. and Kowalsky M.J. 2007, Displacement-Based Seismic Design of Drilled Shaft Bents with Soil-Structure Interaction, Journal of Earthquake Engineering, Volume 11, Issue 6 , pp. 1010 – 1030

PART II

IMPLEMENTATION OF THE DIRECT DISPLACEMENT-BASED DESIGN METHOD FOR SEISMIC DESIGN OF HIGHWAY BRIDGES

Vinicio A. Suarez and Mervyn J. Kowalsky

Department of Civil, Construction and Environmental Engineering, North Carolina State University, Campus-Box 7908, Raleigh, NC-27695, USA

ABSTRACT

This paper presents the DDBD method with all the details required for its application to the design of conventional highway bridges. The method presented here includes new features such as: the incorporation of the displacement capacity of the superstructure as a design parameter, the determination of a stability-based target displacement for piers the design of skewed bents and abutments, among others.

1. INTRODUCTION

After the Loma Prieta earthquake in 1989, extensive research has been conducted to develop improved seismic design criteria for bridges, emphasizing the use of displacements rather than forces as a measure of earthquake demand and damage in bridges. (Priestley, 1993; ATC, 1996; Caltrans, 2006; ATC, 2003; Imbsen, 2007)

Several Displacement Based Design (DBD) methodologies have been proposed. Among them, the Direct Displacement-Based Design Method (DDBD) (Priestley, 1993) has proven to be effective for performance-based seismic design of bridges, buildings and other types of structures (Priestley et al, 2007). Specific research on DDBD of bridges has focused on design of bridge piers (Kowalsky, 1995), drilled shaft bents with soil-structure interaction (Suarez and Kowalsky, 2007) and multi-span continuous bridges (Calvi and Kingsley, 1997; Kowalsky 2002; Dwairi, 2005; Ortiz, 2006).

DDBD differs from other DBD procedures for bridges, such as the Seismic Design Criteria of Caltrans (2005) or the newly proposed AASHTO Guide Specification for LRFD Seismic Bridge Design (Imbsen, 2007), in the use of an equivalent linearization approach and in its execution. While the other methods are iterative and require strength to be assumed at the beginning of the process, DDBD directly returns the strength required by the structure to meet a predefined target performance.

The purpose of this report is to present the DDBD method with all the details required for its application to the design of conventional highway bridges. The method presented here includes new features such as: the incorporation of the displacement capacity of the superstructure as a design parameter, the determination of a stability-based target displacement for piers, the design of skewed bents and abutments, among others.

2. FUNDAMENTALS OF DDBD

DDBD was first proposed by Priestley (1993) as a tool for Performance-Based Seismic Engineering. The method allows designing a structure to meet any level of performance when subjected to any level of seismic hazard. DDBD starts with the definition of a target

displacement and returns the strength required to meet the target displacement under the design earthquake. The target displacement can be selected on the basis of material strains, drift or displacement ductility, either of which is correlated to a desired damage level or limit state. For example, in the case of a bridge column, designing for a serviceability limit state could imply steel strains to minimize residual crack widths that require repair or concrete compression strains consistent with incipient crushing.

DDBD uses an equivalent linearization approach (Shibata and Sozen, 1976) by which, a nonlinear system at maximum response, is substituted by an equivalent elastic system. This system has secant stiffness, $K_{eff,}$ and equivalent viscous damping, ξ_{eq}, to match the maximum response of the nonlinear system (Fig 1). In the case of multi degree of freedom systems, the equivalent system is a Single Degree of Freedom (SDOF) with a generalized displacement, $\Delta_{sys,}$ and the effective mass, $M_{EFF,}$ computed with Eq. 1 and Eq. 2 respectively (Fig.2) (Calvi and Kingsley, 1995). In these equations, $\Delta_1 \ldots \Delta_i \ldots \Delta_n$ are the displacements of the piers and abutments (if present) according to the assumed displacement profile, and $M_1 \ldots M_i \ldots M_n$ are effective masses lumped at the location of piers and abutments (if present).

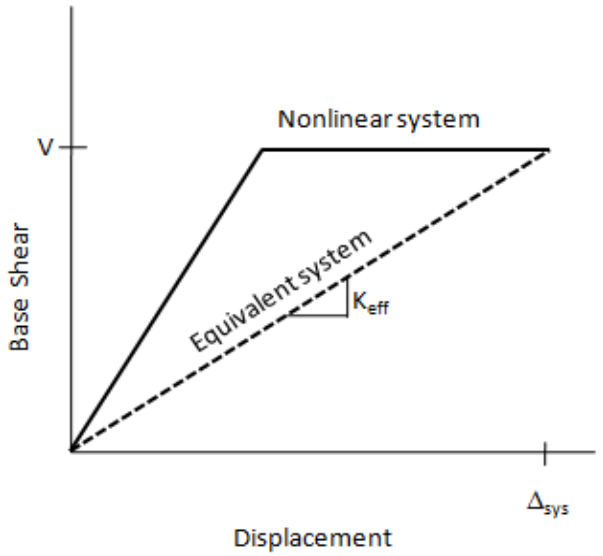

Figure 1 – Equivalent linearization approach used in DDBD

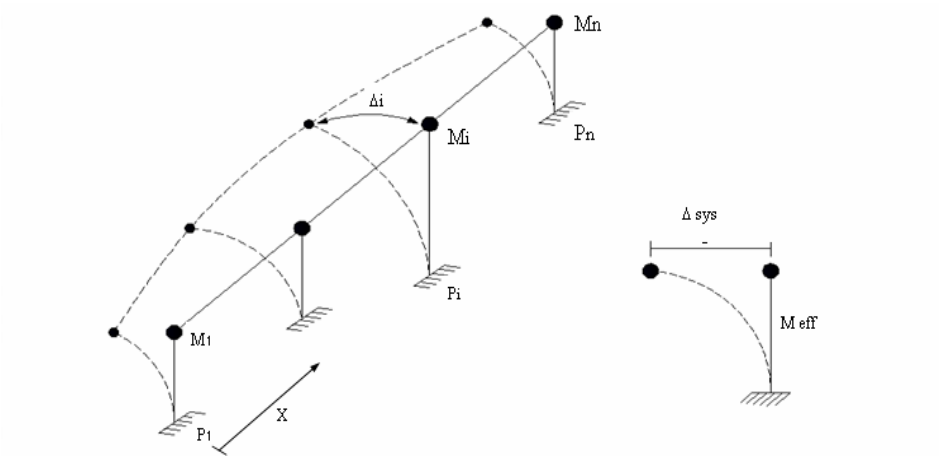

Figure 2 - Equivalent single degree of system.

$$\Delta_{sys} = \frac{\sum_{i=1}^{i=n} \Delta_i{}^2 M_i}{\sum_{i=1}^{i=n} \Delta_i M_i} \tag{1}$$

$$M_{eff} = \frac{\left(\sum_{i=1}^{i=n} \Delta_i M_i \right)^2}{\sum_{i=1}^{i=n} \Delta_i{}^2 M_i} \tag{2}$$

The energy dissipated by inelastic behavior in the bridge is accounted for in the substitute elastic system by the addition of equivalent viscous damping ξ_{eq}. With the seismic hazard represented by a displacement design spectrum that has been reduced to the level of damping in the bridge, the required effective period, T_{eff}, is easily found by entering in the displacement spectrum curve with Δ_{sys} (Fig. 3). Once T_{eff} is known, the stiffness, K_{eff}, and required strength, V, for the structure are computed from the well known relation between period, mass and stiffness for SDOF systems. Finally, V is distributed among the elements

that form the earthquake resisting system, and the elements are designed and detailed following capacity design principles to avoid the formation of unwanted mechanisms.

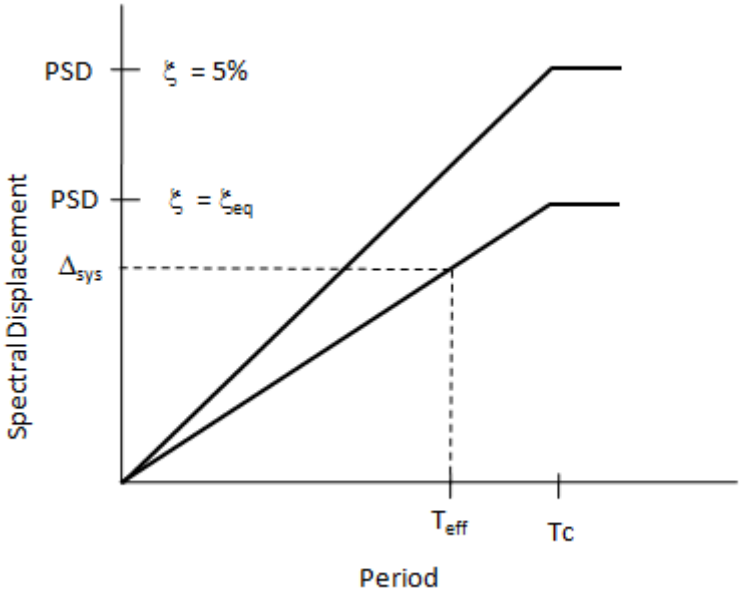

Figure 3 – Determination of effective period in DDBD

2.1 Equivalent damping

Several studies have been performed to obtain equivalent damping models suitable for DDBD (Dwairi 2005, Blandon 2005, Suarez 2006, Priestley et al 2007). These models relate equivalent damping to displacement ductility in the structure.

For reinforced concrete columns supported on rigid foundations, ξ_{eq}, is computed with Eq. 3 (Priestley, 2007).

$$\xi_{eq} = 5 + 44.4\frac{\mu_t - 1}{\pi\mu_t} \qquad \text{(Eq. 3)}$$

For extended drilled shaft bents embedded in soft soils, the equivalent damping is computed by combination of hysteretic damping, $\xi_{eq,h}$, and tangent stiffness proportional viscous damping, ξ_v, with Eq. 4 (Priestley and Grant, 2005). The hysteretic damping is computed with Eq. 5 as a function of the ductility in the drilled shaft. The values of the parameters *p* and *q* are given in Table 1 for different types of soils and boundary conditions (Suarez 2005). In Table 1, clay-20 and clay-40 refer to saturated clay soils with shear strengths of 20 kPa and 40 kPa respectively. Sand-30 and Sand-37 refer to saturated sand with friction angles of 30 and 37 degrees respectively. A fixed head implies that the head of the extended drilled shaft displaces laterally without rotation, causing double bending in the element. A pinned head implies lateral displacement with rotation and single bending. To use Eq. 4, ξ_v should be taken as 5%, since this value is typically used as default to develop design spectra.

$$\xi_{eq} = \xi_v \mu^{-0.378} + \xi_{eq,h} \qquad \mu \geq 1 \qquad \text{(Eq. 4)}$$

$$\xi_{eq,h} = p + q\frac{\mu - 1}{\mu} \qquad \mu \geq 1 \qquad \text{(Eq. 5)}$$

Table 1. Parameters for hysteretic damping models in drilled shaft - soil systems

HEAD	SOIL	p	q
Fixed	Clay-20	6.70	8.10
Fixed	Clay-40	5.60	8.70
Fixed	Sand-30	2.40	10.20
Fixed	Sand-37	2.00	9.60
Pinned	Clay-20	15.80	9.40
Pinned	Clay-40	13.70	10.90
Pinned	Sand-30	9.40	11.20
Pinned	Sand-37	8.50	10.40

All damping models are plotted in Fig. 4. It is observed that when ductility equals one, the equivalent damping for the column on rigid foundation equals 5% (i.e. the elastic viscous damping level) whereas the equivalent damping for the drilled shafts is higher than 5%. The additional damping comes from the soil which performs inelastically and dissipates energy at displacements that are less than the yield displacement of the reinforced concrete section. In

cases where the target displacement is less than the yield displacement of the element, a linear relation between damping and ductility is appropriate. Such relation is given by Eq. 6.

$$\xi_{eq} = \xi_v + (q - \xi_v)\mu \qquad \mu < 1 \tag{Eq. 6}$$

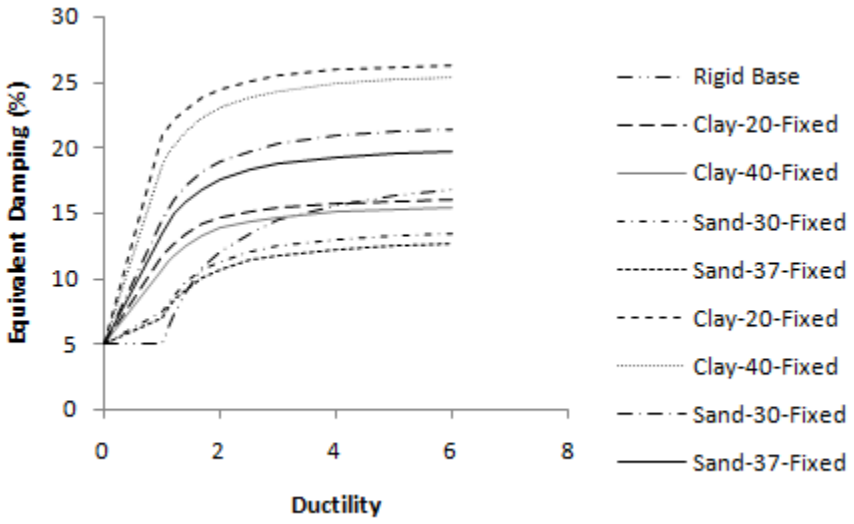

Figure 4. Equivalent damping models for bridge piers

3. GENERAL DDBD PROCEDURE FOR BRIDGES

The main steps of the design procedure are presented in Fig. 5. The bridge is previously designed for non-seismic loads and the configuration, superstructure section and foundation are known. A design objective is proposed by defining the expected performance and the seismic hazard. Then, the target displacement profile for the bridge is determined, and DDBD is applied in the longitudinal and transverse axes of the bridge. Finally the results are combined, P-Δ effects are checked and reinforcement is designed and detailed following Capacity Design principles (Priestley et al, 2007).

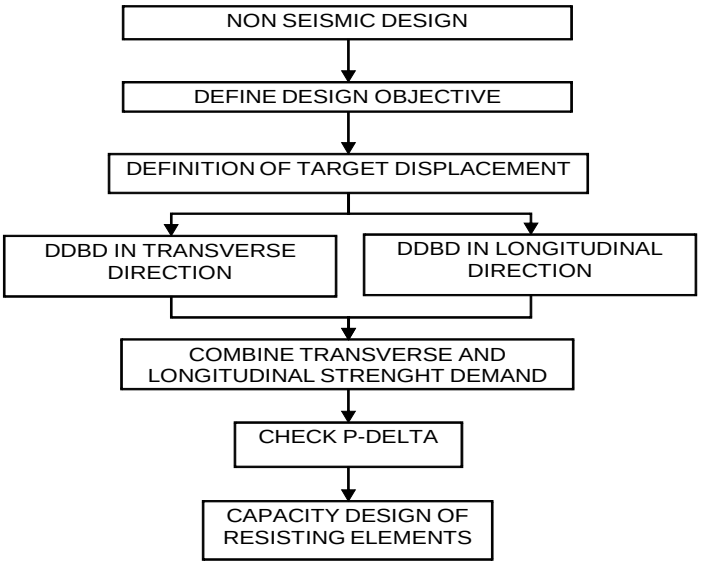

Figure 5 - DDBD main steps flowchart

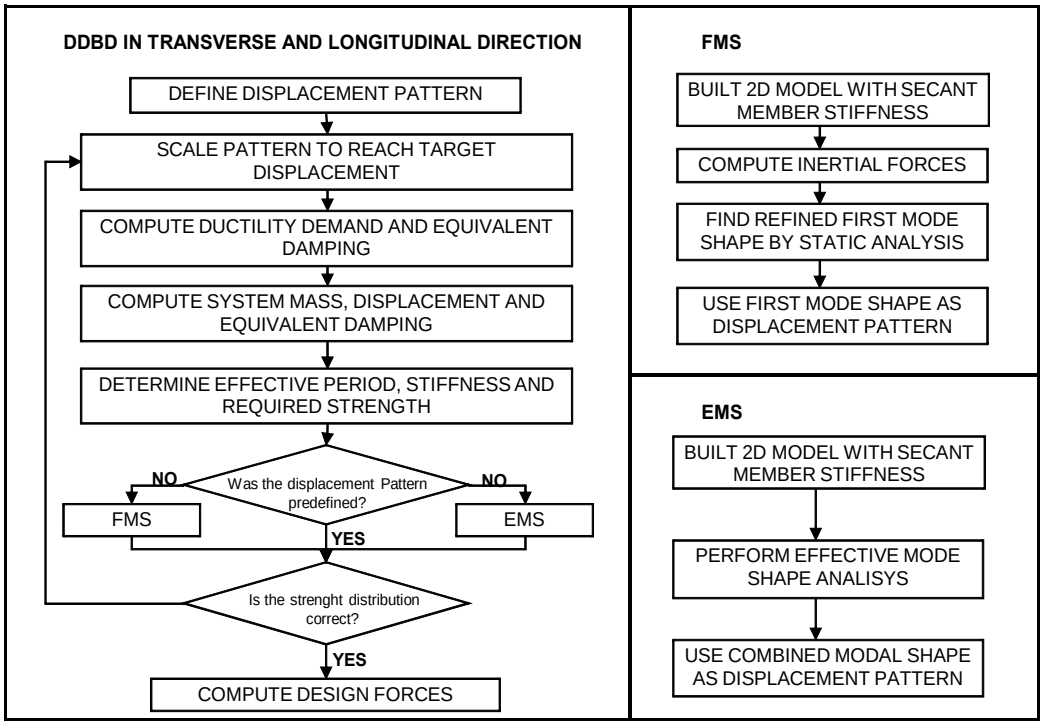

Figure 6 - Complementary DDBD flowcharts

The flowcharts in Fig. 6 show the procedure for DDBD in the transverse and longitudinal direction, as part of the general procedure shown in Fig. 5. As seen in Fig. 6, there are three variations of the procedure: (1) If the displacement pattern is known and predefined, DDBD is applied directly; (2) If the pattern is unknown but dominated by the first mode of vibration, as in the case of bridges with integral or other type of strong abutment, a First Mode Shape (FMS) iterative algorithm is applied; (3) If the pattern is unknown but dominated by modal combination, an Effective Mode Shape (EMS) iterative algorithm is applied. The direct application of DDBD, when the displacement pattern is known, requires less effort than the application of the FMS or EMS algorithms. Recent research by the author (Suarez and Kowalsky, 2008a) showed that predefined displacement patterns can be effectively used for design of bridge frames, bridges with seat-type of other type of weak abutments and bridges with one or two expansion joints. These bridges must have a balanced distribution of mass and stiffness, according to AASHTO (Ibsen, 2007). A summary of the design algorithms applicable to common types of highway bridges is presented in Table 2.

Table 2. Displacement patterns for DDDBD of bridges

BRIDGE	BALANCED MASS AND STIFFNESS	NO BALANCED MASS AND STIFFNEES
FRAME	**RBT or EMS**	**EMS**
WEAK ABUTMENTS	**RBT or EMS**	**EMS**
STRONG ABUTMENTS	**FMS or EMS**	**FMS**
ONE EXPANSION JOINT	**LDP1 or EMS**	**EMS**
TWO EXPANSION JOINTS	**LDP2 or EMS**	**EMS**
MORE THAN TWO EXPANSION JOINTS	**EMS**	**EMS**
		

A detailed explanation of all the steps involved in the application of DDBD is presented next.

3.1 Design Objective

In DDBD, a design objective or performance objective is defined by specification of the seismic hazard and the design limit state to be met under the specified seismic hazard. The seismic hazard is represented by an elastic displacement design spectrum (Fig 3). The design spectrum is characterized by a Peak Spectral Displacement, *PSD*, and a corner period, T_c. The design limit state can be based on material strain limits, ductility, drift or any other damage or stability index. DDBD allows any combination of seismic hazard and design limit state; therefore, it can be used as a tool for Performance Based Seismic Engineering. Some of the most common design limit states are:

Life safety

This limit is used in the AASHTO Guide Specifications for LRFD Seismic Bridge Design (Imbsen, 2007) for bridges in Seismic Design Category (SDC) "D". It is intended to protect human life during and after a rare earthquake. This limit implies that the bridge has low probability of collapse but may suffer significant damage in piers and partial or complete replacement may be required. To compute pier displacements to meet the life safety limit the ductility limits proposed in the AASHTO LRFD Guides (Imbsen, 2007) can be used. For single column bents ductility equals five. For multiple column bents, ductility equals six. For pier walls is the weak direction, ductility equals five. For pier walls in the strong direction, ductility equals one.

Damage control.

This limit is more restrictive than the life safety limit state. It sets the limit, beyond which damage in piers is not longer economically repairable due to failure of the transverse reinforcement (Kowalsky, 2000). For circular reinforced concrete columns typical strains related to this limit state are 0.018 for concrete in compression and 0.06 for steel in tension.

Specific values of compression strain for the confined concrete can be estimated using the energy balance approach developed by Mander (1988). In this model (Eq. 7), the damage-control concrete strain, $\varepsilon_{c,dc}$, is a function of volumetric transverse steel ratio, ρ_v , yield stress of the transverse steel reinforcement, f_{yh}, ultimate strain of the transverse steel reinforcement , ε_{su},, compressive strength of the confined concrete, $f'_{cc,}$(Eq. 8) compressive strength of the unconfined concrete, f'_c, and the confinement stress f_1 (Eq. 9).

$$\varepsilon_{c,dc} = 0.004 + 1.4\frac{\rho_v f_{yh}\varepsilon_{su}}{f'_{cc`}} \qquad \text{(Eq. 7)}$$

$$f'_{cc} = f'_c\left(2.254\sqrt{1+\frac{7.94 f_1}{f'_c}} - 2\frac{f_1}{f'_c} - 1.254\right) \qquad \text{(Eq. 8)}$$

$$f_1 = 0.5\rho_v f_{yh} \qquad \text{(Eq. 9)}$$

The damage control displacement for single column or multiple column bents can then be computed based on the damage control strains using the plastic hinge method (Priestley and Calvi, 1993). This method is covered in Section 3.2.4.

Serviceability

This limit is more restrictive than the damage control limit state. It sets the limit beyond which damage in piers needs repair (Kowalsky, 2000). For circular reinforced concrete columns, typical strains related to this limit state are 0.004 for concrete in compression and 0.015 for steel in tension. The steel tension strain is defined as the strain at which residual cracks widths would exceed 1 mm. Serviceability pier displacement can be computed with the plastic hinge method covered in Section 3.2.4.

Stability limit

In addition to damage-based limit states, a stability criterion must also be specified as part of the design objective. According to the AASHTO guide specification (Imbsen, 2007), P-Δ

effects can be neglected in the design of piers when the stability index is less that 25%. For application in DDBD, Priestley et al (2007) suggest that if the stability index is higher that 8%, P-Δ effects should be counteract by an increase in the strength of the pier. However, stability index should not exceed 30%.

3.2 Determination of target displacement

Perhaps the most important step of the DDBD procedure is to determine the target displacement profiles in the transverse and longitudinal directions of the bridge. This process is executed in two steps: (1) Target displacements are computed for all earthquake resisting elements; (2) Target profiles for transverse and longitudinal response are proposed so that one or more elements meet their target displacements. No element must exceed its target displacement. The proposed target profiles must be consistent with the expected dynamic response of the bridge. Therefore in most cases, it will not be possible that all elements meet their target displacements and there will be one or two elements controlling the displacement profiles of the bridge. A detailed explanation on how to determine the target displacements for superstructures, abutments and piers, and the target displacement profiles for a bridge is presented next.

3.2.1 Plan Curvature

This feature cannot be explicitly accounted for in DDBD. Plan curvature complicates the definition of two principal design axes, and makes it difficult to apply of DDBD, since the method requires the determination of target displacement profiles in each principal direction independently.

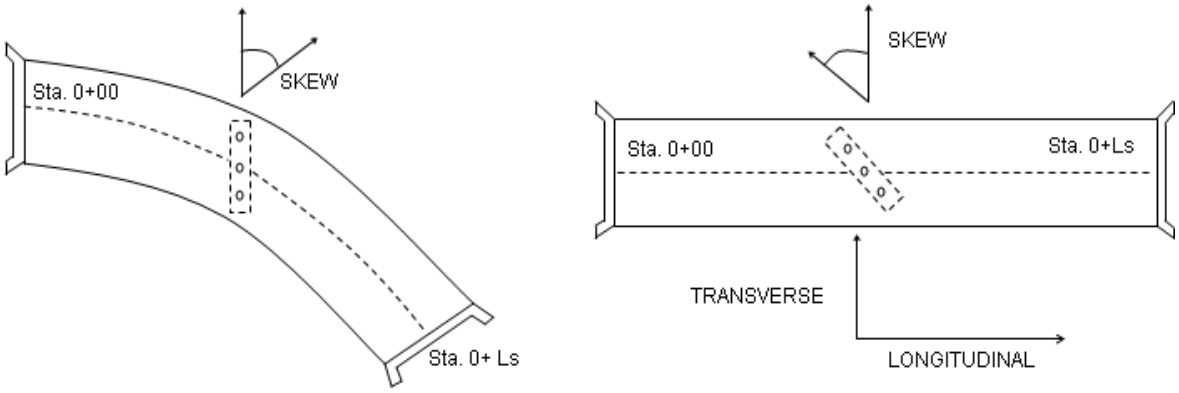

Figure 7. Curve bridge unwrapped to be designed as straight

A practical solution suggest that bridges with subtended angles of 90 degrees or less can be unwrapped and designed as straight bridges (Fig. 7). This is currently recommended in other bridge design codes (Caltrans, 2004; Ibsen 2007). Span lengths and skew angles in the equivalent straight bridge must be the same as in the curved bridge. Gravity induced forces, especially those resulting from the curved geometry, must be carefully considered and combined with seismic actions. (see Section 3.8.1).

3.2.2 Superstructure target displacement

It is a common strategy to design bridges in which damage and energy dissipation take place in the piers and abutments while the superstructure is protected and designed to remain elastic. The reason is that the substructure elements can be effectively designed to be ductile and dissipate energy while most superstructures cannot.

Current displacement-based practice (Ibsen, 2007; Caltrans, 2004) focuses on a displacement demand-capacity check for piers and ignores the limited displacement capacity of the superstructure. The implication of this is that while piers can have enough displacement capacity to cope with seismic demand, the superstructure might not. Therefore, a design based purely on pier displacement capacity could lead to bridges in which the superstructure suffers unaccounted damage.

If a target displacement is determined for the superstructure, this should meet the serviceability or other more restrictive strain limits or should by controlled by the displacement capacity of expansion joints. This discussion applies only to DDBD of bridges in the transverse direction. Bridge superstructures are usually stiff and strong in their axis, so their performance is not an issue when designing in the longitudinal direction.

Determining a superstructure target displacement is important for design of bridges responding with a flexible transverse displacement pattern, including: bridges with strong abutments, bridges with weak and flexible superstructures, bridges with unbalanced mass and stiffness.

The DDBD framework allows easy inclusion of superstructure transverse target displacement into the design procedure. The transverse target displacement profile of the bridge must be defined accounting for the target displacement of the piers, abutments and target displacement of the superstructure.

The determination of a target displacement for the superstructure requires moment curvature analysis of the superstructure section and double integration of the curvature profile along the length of the superstructure. Moment curvature analysis should account for expected material properties and strains caused by gravity loads. The result of the moment curvature analysis is the target curvature to meet the specified strain limits. Other important result is the flexural stiffness of the superstructure, which is also needed in design.

If it is believed that the target displacement of the superstructure should be controlled by yielding of the longitudinal reinforcement of a concrete deck, a yield curvature as target curvature can be estimated with Eq. 10. Where w_s is the width of the concrete deck and ε_y is the yield strain of the steel reinforcement. The yield curvature of a section in mainly dependent on its geometry and it is insensitive to its strength and stiffness (Priestley, 2007).

$$\phi_{ys} = \frac{2\varepsilon_y}{w_s} \qquad \text{(Eq. 10)}$$

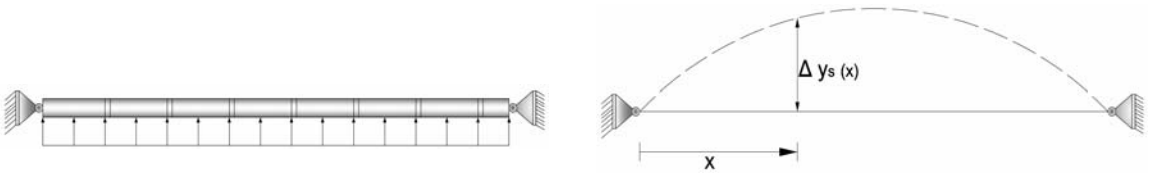

Figure 8 - Assumed superstructure displacement pattern

Assuming that the superstructure responds in the transverse direction as a simply supported beam, with the seismic force acting as a uniform load (Fig. 8), the curvature along the superstructure, $\phi_{s(x)}$, as a function of the target curvature of the superstructure, ϕ_{sT}, is given by Eq. 11. Double integration of the curvature function results in the target displacement function shown as Eq. 12. Where L_s is the length of the superstructure and x is the location of the point of interest.

$$\phi_{s(x)} = \frac{4\phi_{ys}x}{L_s} - \frac{4\phi_{ys}x^2}{L_s^{\,2}} \qquad \text{(Eq. 11)}$$

$$\Delta_{Ts} = \phi_{Ts}\left[\frac{2x^4 - 4L_s x^3 + 2L_s^{\,3}x}{6L_s^{\,2}}\right] \qquad \text{(Eq. 12)}$$

Eq. 12 gives the target displacement relative to the abutments. However, since the abutments are also likely to displace, Eq. 13 should be added to Eq. 12 to obtain a total target displacement. In Eq. 13, Δ_1 and Δ_n are the displacements of the initial and end abutment respectively.

$$\Delta_A = \Delta_1 + \frac{\Delta_n - \Delta_1}{L_s}x \qquad \text{(Eq. 13)}$$

$$\Delta_{Tsi} = \phi_{Ts}\left[\frac{2x_i^{\,4} - 4L_s x_i^{\,3} + 2L_s^{\,3}x_i}{6L_s^{\,2}}\right] + \Delta_1 + \frac{\Delta_n - \Delta_1}{L_s}x_i \qquad \text{(Eq. 14)}$$

In Eq. 14, x is replaced by the location of each pier, x_i, to get the target displacement of the superstructure Δ_{Tsi} at that specific point. If Δ_{Tsi} is less than the target displacement of the pier,

then Δ_{Tsi} controls design and becomes the design target displacement for the pier. An example that illustrates the application of this model is presented in Section 5.1

3.2.3 Abutment target displacement

Due to specific configurations and design details, an appropriate estimation of lateral target displacement will in most cases require a nonlinear static analysis of the abutment that has been previously designed for non-seismic loads. Instead of such analysis, a gross estimation of the displacement that will fully develop the strength of the fill behind the back or wing walls can be obtained with Eq. 15 (Imbsen, 2008). In this equation, f_h is a factor taken as 0.01 to 0.05 for soils ranging from dense sand to compacted clays and H_w is the height of the wall. This relation might be useful in the assessment of a target displacement for integral abutments or seat-type abutments with knock-off walls.

$$\Delta_T = f_h H_w \qquad \text{(Eq. 15)}$$

Table 3 - Parameters for DDBD of common types of piers

PIER TYPE	Effective Height Hp		Yield Disp. Factor α		Shear Height Hs	
	Transv.	Long.	Transv.	Long.	Transv.	Long.
Single column integral bent	H+Hsup+Lsp	H+2Lsp	1/3	1/6	Hp	Hp/2
Single extended drilled shaft integrall bent	Le+Hsup	Le+Lsp	varies	varies	Hp	Hp/2
Single column non-integral bent pinned in long direction	H+Hsup+Lsp	H+Lsp	1/3	1/3	Hp	Hp
Single extended-drilled-shaft non-integral bent pinned in long direction	Le+Hsup	Le	varies	varies	Hp	Hp/2
Multi column integral bent	H+2Lsp	H+2Lsp	1/6	1/6	Hp/2	Hp/2
Multi extended-drilled-shaft integrall bent	Le+Lsp	Le+Lsp	varies	varies	Hp/2	Hp/2
Multi column integral bent with pinned base	H+Lsp	H+Lsp	1/3	1/3	Hp	Hp
Multi column bent pinned in longitudinal direction	H+2Lsp *	H+Lsp *	1/6 *	1/3 *	Hp/2 *	Hp *
Multi extended-drilled-shaft non-integral bent pinned in long direction	Le *	Le *	varies *	varies *	Hp/2 *	Hp *

* These are in-plane and out-of-plane values and must be corrected for skew to get transverse and longitudinal values

3.2.4 Pier target displacement

Any type of bridge pier can be designed with DDBD as long as: (a) a target displacement can be easily estimated prior design; b) a relation between displacement and equivalent damping

can be established. The first requirement is usually easy to comply knowing that the relation between strain in the plastic hinge region and displacement at the top of a pier is independent from the strength and stiffness of the pier.

The second item requires an assessment of design ductility and the use of an existing ductility-damping model such as those presented in Section 2.1. The determination of ductility demand requires knowledge of yield displacement which is calculated as part of the target displacement determination. As a result of this, the design of most common types of piers used in highway bridges can be easily implemented in DDBD. This includes piers with isolation/dissipation devices and piers with soil-structure interaction.

A graphic description of common types of reinforced concrete piers used in conventional bridges is presented in Fig. 9. In relation to that figure, Table 3 shows values for: the effective height of the pier H_p, yield displacement factor α, and shear height H_s.

These parameters are given for design in transverse and longitudinal axes of the bridge. In Table 3, H is the height of column, L_e is the effective height of drilled shaft, H_{sup} is the height from the soffit to the centroid of the superstructure and L_{sp} is the strain penetration length. The parameters L_e and α for drilled shaft bents are shown in Fig. 10 in terms of the type of soil, above ground height of the bent, L_a, and diameter of the drilled shaft section D.

Plastic Hinge Method

Strain-based target displacements are determined using the plastic hinge method (Priestley et al, 2007). For any type of pier listed in Table 3, the target displacement, Δ_t, along the transverse and longitudinal axis of the bridge is estimated with Eq. 16. In this equation, Δ_y is the yield displacement of the pier, ϕ_t and ϕ_y are the target and yield curvature respectively, L_p is the plastic hinge length and H_p is the effective height of the pier defined in Table 3.

$$\Delta_T = \Delta_y + (\phi_t - \phi_y) L_p H_p \qquad \text{(Eq. 16)}$$

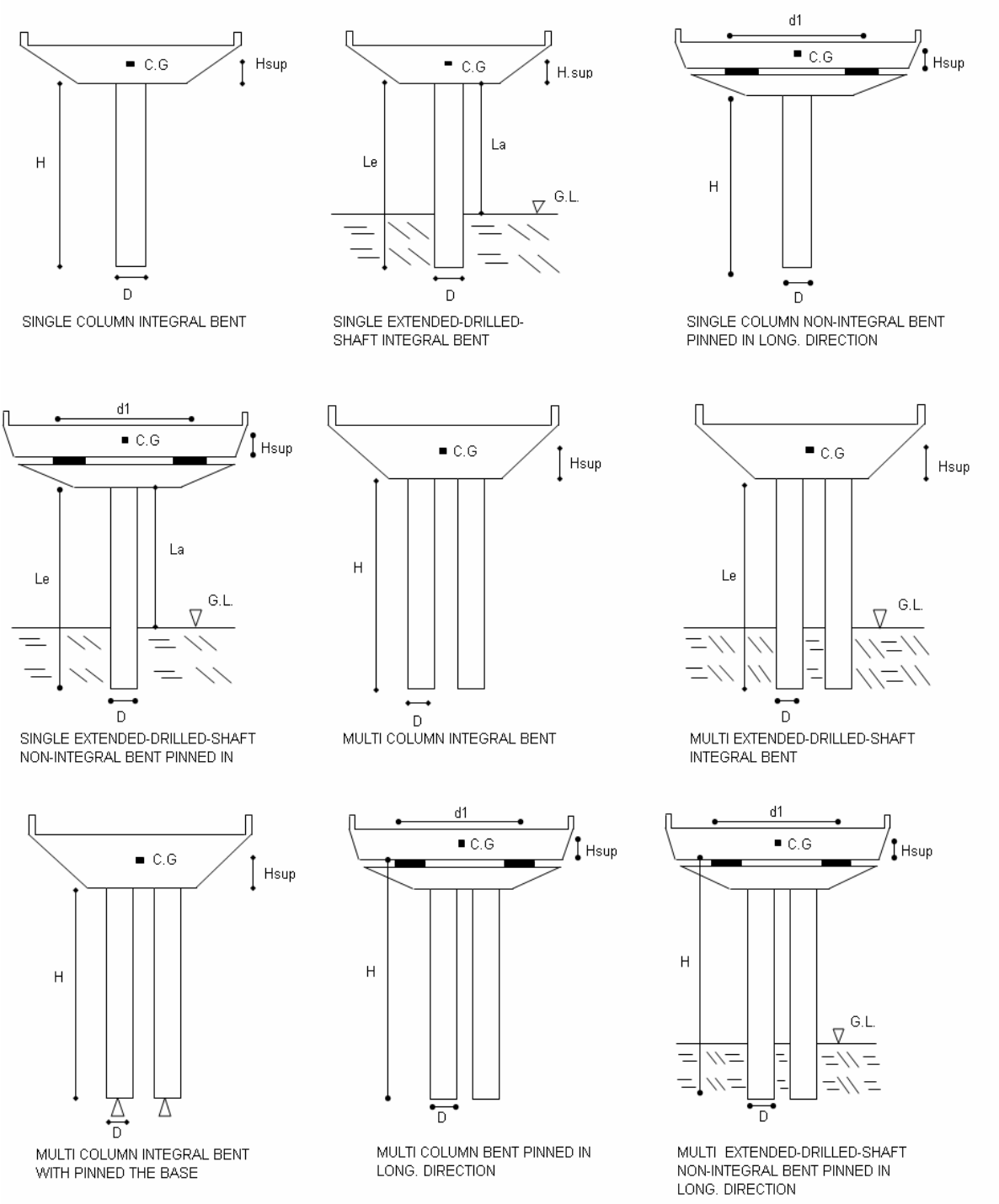

Figure 9 - Common types of piers in highway bridges

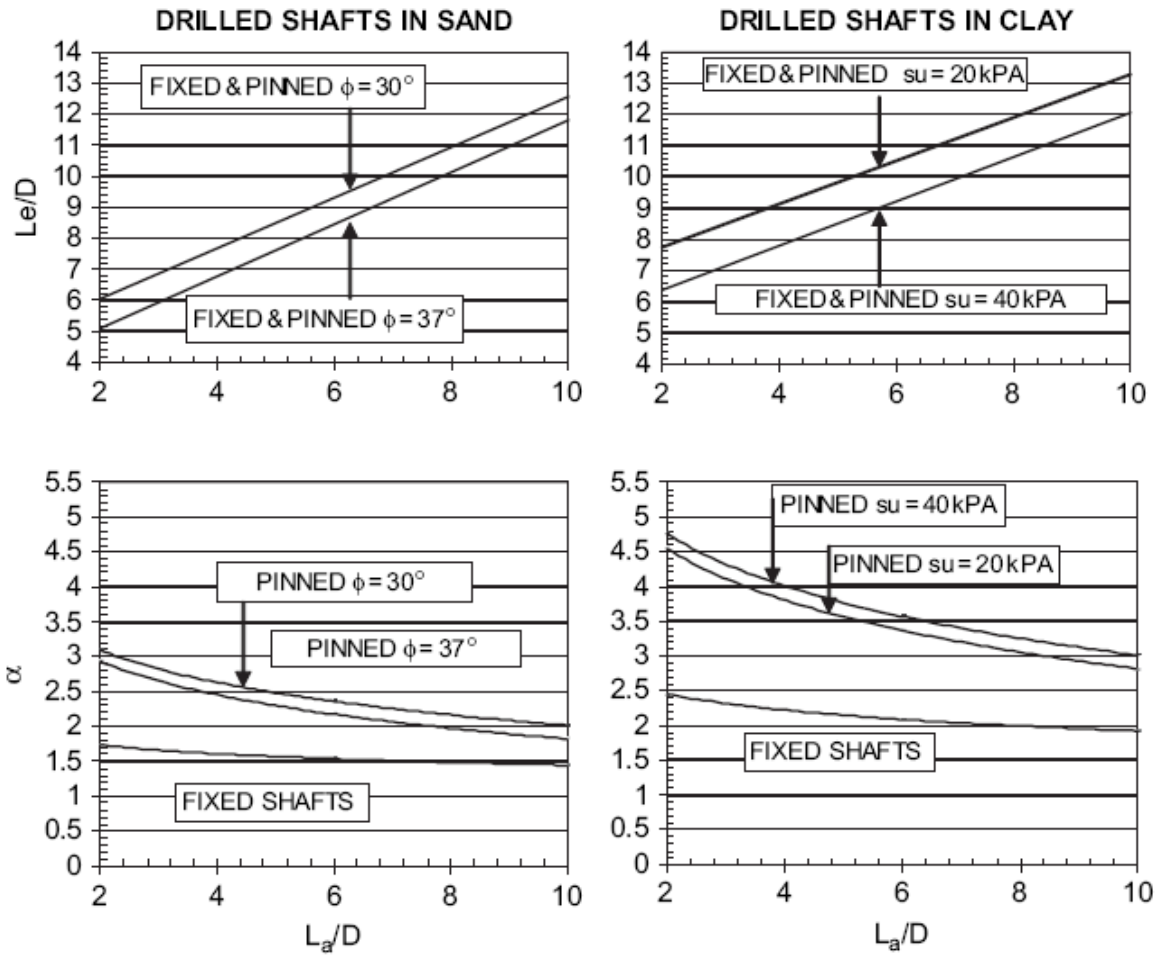

Figure 10 - Le and a for definition of the equivalent model for drilled shaft bents (Suarez and Kowalsky, 2007)

The target curvature is determined in terms of the target concrete strain, $\varepsilon_{c,T}$, target steel strain, $\varepsilon_{s,T}$, and neutral axis depth, *c*, with Eq. 17. The target curvature can be controlled by the concrete reaching its target strain in compression or the flexural reinforcement reaching its target strain in tension.

$$\phi_{dc} = \min\left[\frac{\varepsilon_{c,T}}{c}, \frac{\varepsilon_{s,T}}{D-c}\right] \qquad \text{(Eq. 17)}$$

The neutral axis depth can be estimated with Eq. 18, where *P* is the axial load acting on the element and A_g is the gross area of the section (Priestley et al, 2007)

$$c = 0.2D\left(1 + 3.25\frac{P}{f'_{ce}A_g}\right) \quad \text{(Eq. 18)}$$

The yield curvature ϕ_y is independent of the strength of the section and can be determined in terms of the yield strain of the flexural reinforcement ε_y and the diameter of the section D with in Eq. 19 (Priestley et al, 2007)

$$\phi_y = 2.25\frac{\varepsilon_y}{D} \quad \text{(Eq. 19)}$$

The yield displacement Δ_y is given by Eq. 20, where α is given in Table 3 for transverse and longitudinal directions. For extended drilled shaft bents, α is shown in Figure 10.

$$\Delta_y = \alpha\phi_y\left(H_p\right)^2 \quad \text{(Eq. 20)}$$

Life safety target displacement

Is computed introducing the ductility limits given in Section 3.1 in Eq. 21.

$$\Delta_T = \Delta_y\mu \quad \text{(Eq. 21)}$$

Damage control target displacement

The damage control concrete compression strain $\varepsilon_{c,dc}$ must be first computed with Eq. 7. The damage control tension strain for the flexural reinforcement is $\varepsilon_{s,dc}$ = 0.06 (Kowalsky, 2000) (See Section 3.1). These values are used in Eq. 17 to find ϕ_t and finally Eq. 16 is used to get the target displacement.

Serviceability target displacement

The strain limits in Section 3.1 are used to compute a target curvature and then a target displacement with Eq. 16

Target displacements for SDC "B" and "C"

For these SDCs, the equations given in AASHTO (Ibsen, 2007) for the assessment of displacement capacity for moderate plastic action (Eq. 23) and minimal plastic action (Eq. 24) can also be used in DDBD to get a target displacement. In Eq. 23 and Eq. 24, H_c is the clear height of the columns and Λ is 1 for columns in single bending and 2 for columns in double bending.

$$\Delta_c = 0.003 H_c \left(-2.32 \ln\left(\frac{D}{H_c} \Lambda \right) - 1.22 \right) \geq 0.003 H_c \qquad \text{(m)} \qquad \text{(Eq. 23)}$$

$$\Delta_c = 0.003 H_c \left(-1.27 \ln\left(\frac{D}{H_c} \Lambda \right) - 0.32 \right) \geq 0.003 H_c \qquad \text{(m)} \qquad \text{(Eq. 24)}$$

Stability-based target displacement

A target displacement for a bridge pier to meet a predefined value of the stability index, θ_s, can be estimated with Eq. 25 (Suarez and Kowalsky 2008b), where the parameters *a*, *b*, *c* and *d* are given in Tables 4 and 5 for piers on rigid foundations and extended drilled shaft bents in different types of soils. Table 4 gives the parameters for near fault sites and Table 5 for far fault sites. The parameter *C* in Eq. 25 is computed with Eq. 26 in terms of the peak spectral displacement, *PSD*, the corner period, T_c, the axial load acting on the pier, *P*, the effective mass on the pier, M_{eff} , and the height of the pier *H*.

$$\mu_{\theta_s} = a + bC + c\frac{C-d}{C} \qquad \text{(Eq. 25)}$$

$$C = \frac{T_c \Delta_y}{2\pi PSD}\sqrt{\frac{P}{\theta_s M_{eff} H}} \qquad \text{(Eq. 26)}$$

If a bridge pier is designed as a stand-alone structure, M_{eff} can be computed taking a tributary area of superstructure and adding the mass of the cap-beam and a portion of the mass of the pier itself (1/3 is appropriate). If the target displacement is being determined for a pier that is part of a continuous bridge, M_{eff} is computed with Eq. 27 as a fraction of the effective mass of the bridge, M_{EFF}. The effective mass of the bridge is computed as with Eq. 2 and v_i is computed with Eq.31

$$M_{eff} = v_i M_{EFF} \qquad \text{(Eq. 27)}$$

Table 4 - Parameters to define Eq.15 for far fault sites

	Rigid Base	Clay-20 Pinned	Clay-20 Fixed	Clay-40 Pinned	Clay-40 Fixed	Sand-30 Pinned	Sand-30 Fixed	Sand-37 Pinned	Sand-37 Fixed
a	1.256	0.839	0.885	0.961	0.909	1.010	1.468	1.105	1.053
b	-0.127	-0.021	-0.034	-0.042	-0.043	-0.047	-0.078	-0.055	-0.061
c	-0.766	-0.657	-0.693	-0.737	-0.697	-0.774	-1.160	-0.847	-0.792
d	0.731	0.724	0.860	0.644	0.877	0.677	0.546	0.620	0.852

Table 5 - Parameters to define Eq.15 for near fault sites

	Rigid Base	Clay-20 Pinned	Clay-20 Fixed	Clay-40 Pinned	Clay-40 Fixed	Sand-30 Pinned	Sand-30 Fixed	Sand-37 Pinned	Sand-37 Fixed
a	1.146	0.803	0.924	0.868	0.912	0.963	1.210	0.966	1.053
b	-0.112	0.000	-0.013	-0.015	-0.023	-0.028	-0.035	-0.019	-0.061
c	-0.799	-0.728	-0.833	-0.754	-0.793	-0.814	-1.058	-0.850	-0.792
d	0.917	0.965	0.939	0.920	0.980	0.869	0.759	0.869	0.852

The target ductility obtained from Eq. 25 is multiplied to the yield displacement of the pier to get the stability-based target displacement. The target ductility obtained from Eq. 25 is plotted in Figs 11 and 12 for a range of values of C. In both figures it is observed that ductility is very sensitive to changes in C when C is less than 0.5. The differences in ductility for the different models come from the differences in equivalent damping (see Section 2.1). If two piers have the same value of C, the one with more damping develops less ductility to reach the stability limit. The reason is that the pier with less damping requires more strength.

The different damping models have less effect in the relation between $\mu_{\theta s}$ and C for near fault sites.

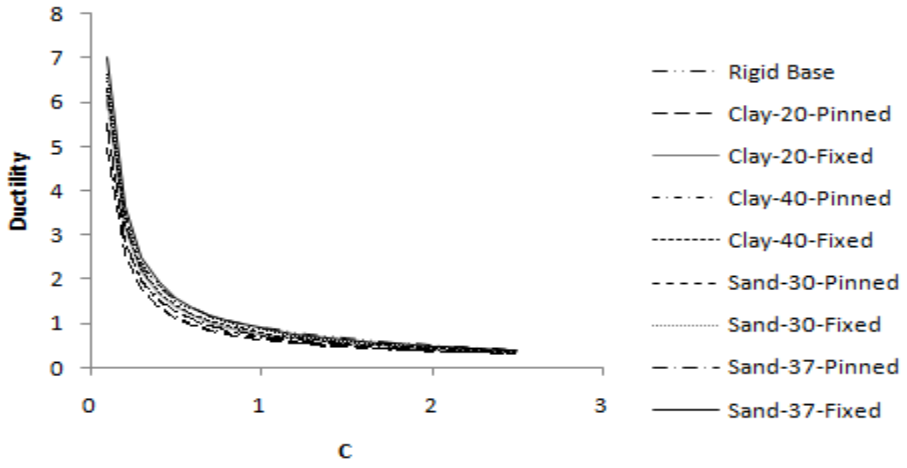

Figure 11. Ductility vs. C for far fault sites

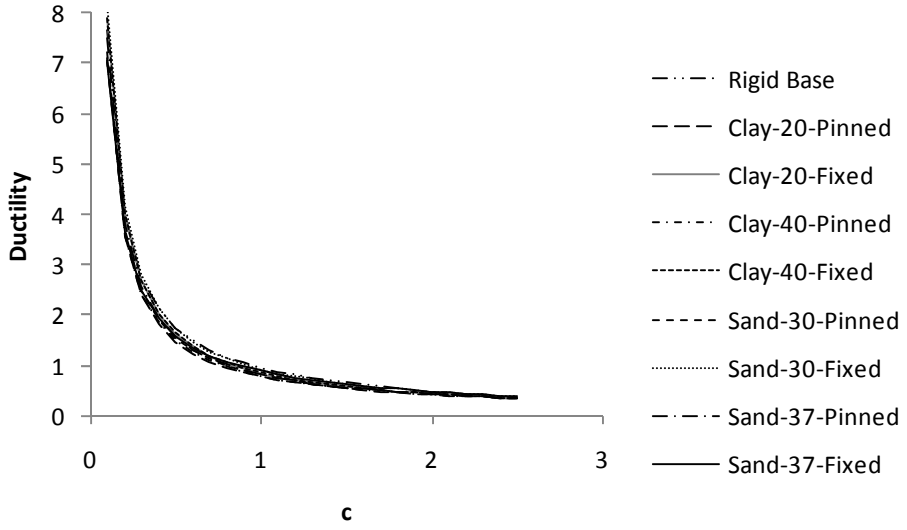

Figure 12. Ductility vs. C for near fault sites

The use of Eq. 25 avoids the need of iteration in DDBD for designs controlled by P-Δ effects. The proposed model is accurate for design of piers as stand-alone structures or in the case of regular bridges with a balanced distribution of mass and stiffness. If the model is used with

irregular bridges, it will produce conservative estimates of target displacement (Suarez and Kowalsky, 2008b). An example that illustrates the application of this model is presented in Section 5.2

3.3 Skewed piers or abutments

From a design perspective, the effect of a skewed configuration is that in-plane and out-of-plane response parameters of abutments and piers are no longer oriented in the principal design directions of the bridge (Fig. 13).

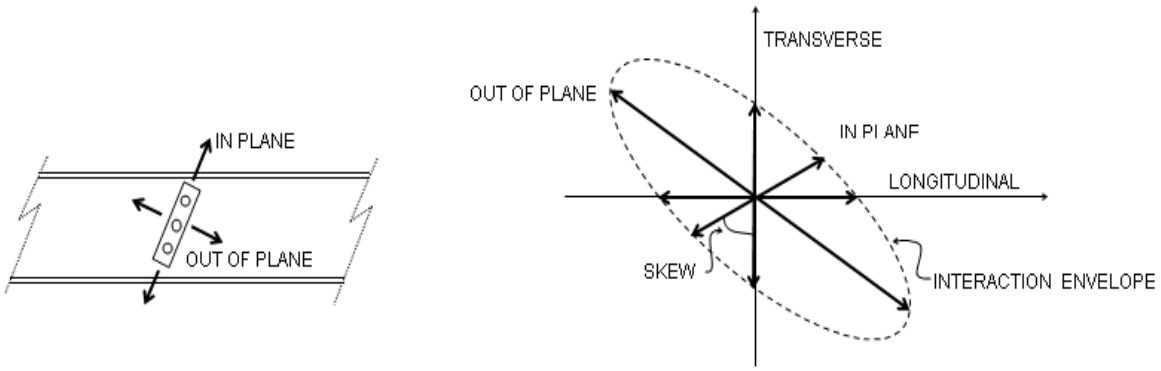

(a) Skewed bent **(b) Element and bridge design axis**

Figure 13 - Design axes in skewed elements

The effects of skew can be considered in DDBD by determining the projection of any response parameter such as yield displacement Δ_y, target displacement Δ_T, shear height H_s and others, with respect to the transverse and longitudinal direction of the bridge. Such determination can be done using an elliptical interaction function between the in-plane and out-of-plane response, as given by the following equations:

$$rp_T = rp_{IN} + skew\frac{rp_{OUT} - rp_{IN}}{90} \quad \text{(Eq. 28)}$$

$$rp_L = rp_{OUT} + skew\frac{rp_{IN} - rp_{OUT}}{90} \quad \text{(Eq. 29)}$$

Where, rp_{IN} is the value of the response parameter in the in-plane direction of the element, rp_{OUT} is the response parameter in the out-of-plane direction of the element, rp_T is the projection of the response parameter in the transverse direction of the bridge and rp_L is the projection of the response parameter in the longitudinal direction of the bridge. An example that illustrates the application of this model is presented in Section 5.3.

3.4 Determination of target displacement profiles

Once the target displacement has been determined for the superstructure, abutments and piers, considering skew if necessary, the next step is to propose a target displacement profile along the transverse and longitudinal directions of the bridge.

3.4.1 Transverse displacement profiles

As was mentioned before, much of the effort in the application of DDBD for transverse design of bridges is in the selection or determination of the target displacement profile. Previous research conducted by Dwairi and Kowalsky (2006) focused on the identification of displacement patterns for symmetric and asymmetric bridge configurations using Inelastic Time History Analysis (ITHA). Three types of displacement patterns were identified, namely: Rigid Body Translation (RBT), Rigid Body Translation with Rotation (RBTR) and flexible pattern. These patterns were found to be highly dependent on the superstructure to substructure stiffness ratio, bridge regularity and type of abutment. It was also found that only symmetrical regular bridges with stiff superstructures and free abutments respond with a RBT pattern.

Recent research (Suarez and Kowalsky, 2008) has shown that bridges frames and bridges with weak abutments that comply with balanced mass and stiffness requirements of the AASHTO guide specification (Imbsen, 2007) can be designed in the transverse direction assuming a rigid body translation pattern. The Balanced Mass and Stiffness (BMS) index is computed with Eq. 30, where m_i and m_j are the lumped mass at piers i and j and K_{pi} and K_{pj} are the stiffness of piers i and j. This index is computed in two ways, BMS1 is the least value

that results of all combinations of any two piers and BMS2 is the least value that results from all combinations of adjacent piers. If BMS1 > 0.50 and BMS2 > 0.75 the bridge is considered regular.

$$BMS = \frac{M_i K_{p\,j}}{M_j K_{p\,i}} \qquad \text{(Eq. 30)}$$

AASHTO (Imbsen, 2007) and Caltrans (1996) recommend bridges to comply with the balanced mass and stiffness requirements described above. This is to avoid torsion and uneven distribution of damage in the structures. Therefore, it is likely that most conventional highway bridges can be designed with DDBD using a rigid body displacement pattern. In such a case, it is expected that the transverse displacement of all piers be the same and thereof, the amplitude of displacement profile is controlled by the pier or abutment with the least target displacement (See Table 2). When a rigid body displacement pattern is used, the application of DDBD is direct as shown in Fig. 6 This process is cover in detail in Section 3.5.1.

In the case of bridges with integral abutments or other types of strong abutments, designed to limit the displacement of the superstructure, the transverse displacement pattern is flexible and its shape depends mainly on the relation between the stiffness of the superstructure, abutments and piers (See Table 2). Since the stiffness of the piers and abutments depends on their strength, which is not know at the beginning of the process, the shape of the displacement pattern of this type of bridges must be assumed and refined iteratively. This is done using the First Mode Shape (FMS) or the Effective Mode Shape (EMS) algorithms shown in Fig. 6 and described in detail in Sections 3.5.2 and 3.5.3. The amplitude of the displacement profiles is set so that no element exceeds their target displacement.

For bridges with up to two internal expansion joints in the superstructure, research by the authors (Suarez and Kowalsky, 2008a) indicated that predefined linear displacement patterns can be used to execute DDBD directly. Such displacement patterns are shown in

Table 2 and Fig. 14, the amplitude of the displacement profiles is set so that no element exceeds their target displacement.

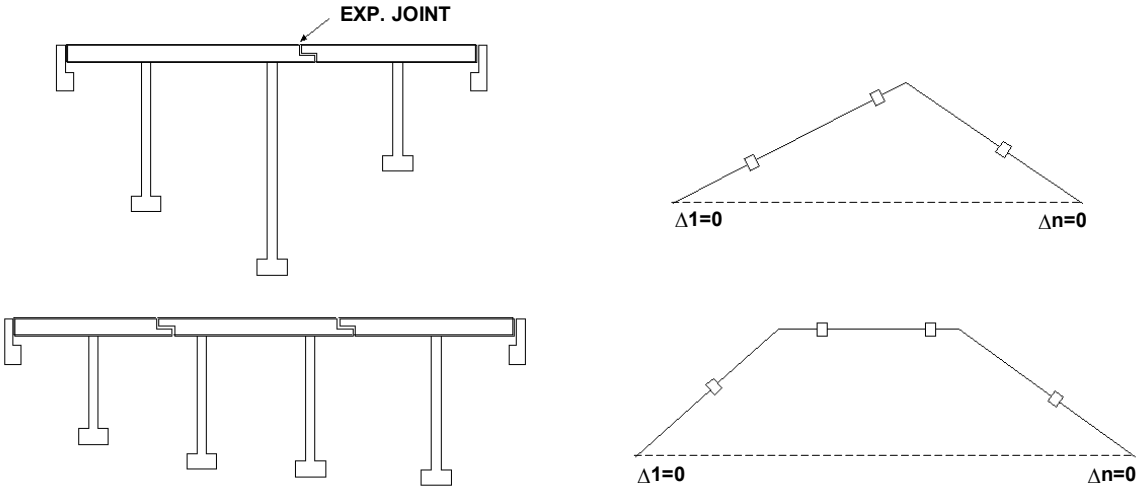

(a) Elevation view **(b) displacement pattern**

Figure 14 - Displacement patterns for bridges with expansion joints

3.4.2 Longitudinal displacement profiles

Continuous superstructures are usually strong and axially rigid, therefore it is reasonable to assume that the superstructure displaces longitudinally as a rigid body, constraining the displacements of all piers to be the same. In this case, the amplitude of the displacement profile is controlled by the pier or abutment with the least target displacement and DDBD is applied directly as shown in Fig. 6.

For superstructures with expansion joints, two possible displacement patterns must be considered (Fig. 15), one with the expansion joint gaps closing towards one end of the bridge and the other with the joints closing towards the opposite end of the bridge. These two alternative patterns are likely to result in different generalized displacement for the bridge (See Section 2, Eq. 1). The least generalized displacement controls design.

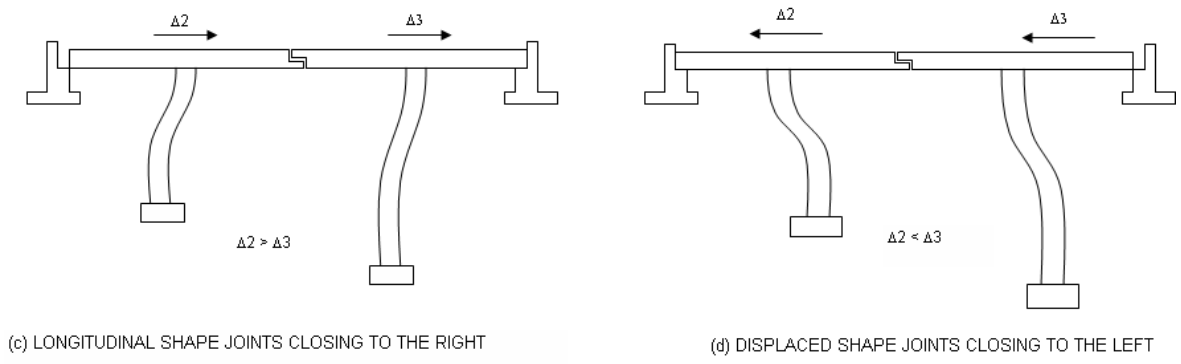

Figure 15 – Longitudinal displacement pattern for bridges with expansion joints

3.5 DDBD IN THE TRANSVERSE DIRECTION

DDBD is applied in the transverse direction as part of the overall procedure showed in Fig. 5. A summary of the steps involved in the transverse design is presented in Fig. 6. In this figure it is shown that there are three different design algorithms. A detailed description of the general steps and algorithms is presented next.

Strength Distribution

If a bridge is designed to suffer damage during the design earthquake, it is possible that most of its piers and abutments (if present) develop their nominal strength and behave inelastically. Therefore, the distribution of strength among bents and abutments is not longer a unique matter of initial stiffness but a designer's choice constrained by equilibrium.

In most bridges, there are two load paths for the inertial forces developed during an earthquake, one is from the superstructure through the abutments and the other is from the superstructure through the piers to the foundation soil (Fig. 16). The ratio of total base shear V taken by the superstructure to the abutments v_s is generally unknown and must be assumed at the beginning of the design process. The ratio of base shear taken by the piers, $v_p=1-v_s$, must be distributed among them satisfying equilibrium. Some of the possible distributions of strength are:

- A distribution to obtain pier columns with the same flexural reinforcement ratio, which is practical and leads to construction savings.
- A distribution with equal shear demand in all piers, which is appropriate for bridges with seismic isolation, to use the same device in all piers

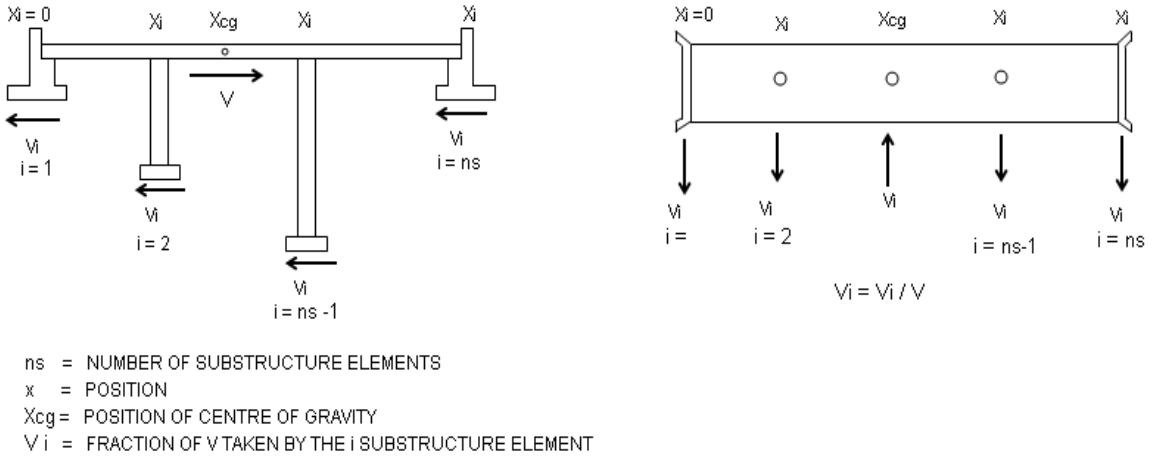

Figure 16 – Strength distribution in the longitudinal and transverse directions

Strength Distribution for columns with same reinforcement ratio

Since reinforced concrete sections with the same reinforcing ratio show similar ratios of cracked to gross section stiffness, a distribution of strength to get the same reinforcement ratio in all columns of the bridge can be computed with Eq. 31. This equation gives the ratio of total strength, v_i, taken by bent i, with n_i columns of diameter D_i, shear height Hs_i and ductility μ_i, required to satisfy force equilibrium. Table 3 defines H_s for different types of piers.

$$v_i = (1 - vs)\frac{\frac{n_i \mu_i D_i^3}{H_{si}}}{\sum \frac{n_i \mu_i D_i^3}{H_{si}}} \qquad \mu_i \le 1 \qquad \text{(Eq. 31)}$$

Strength Distribution for equal shear in bents

Strength among piers can be distributed equally. This alternative is practical when designing bridges with isolation/dissipation devices on top of the bents. The reason is that the same device can be use in all bridge piers.

3.5.1 Direct procedure

This procedure applies to cases where a rigid body or other predefined displacement profile has been adopted for design (see Section 3).

Step1. Determine Target displacement profile

Follow Section 3.4

Step2. Determine properties of equivalent SDOF system

Using Eq. 1 and Eq. 2 the generalized displacement Δ_{sys} and the Effective mass M_{EFF} are found.

Step3. Compute ductility and equivalent damping

For each pier and abutment the ductility is computed as the ratio of the displacement in the target profile Δ_i and the yield displacement Δ_{yi} of the element. If the yield displacement Δ_y was not computed during the determination of target displacement, it should be computed with Eq. 20, with reference to Table 3.

Once ductility is known, the equivalent damping for each pier is computed with an appropriate model. See Section 2.1. For the abutments it is recommended to use equivalent damping values between 5% and 10%. The higher value of damping is appropriate when full soil mobilization is expected. Higher values of damping can be computed with Eq. 3 when plastic hinges are expected to develop in piles supporting the abutment at the target displacement level. If elastic response is expected in the superstructure, damping between 2% and 5% should be used.

The equivalent damping computed for each element must be combined to obtain the equivalent damping for the substitute SDOF system. The combination is done in terms of the work done by each element (Kowalsky, 2002). The work done by the superstructure is computed with Eq. 32. The work done by each abutment is computed with Eq. 33 and Eq. 34. The work done by each pier is computed with Eq. 35. Finally the combined damping is computed with Eq. 36.

$$ws = \left[\Delta_{sys} - \frac{(\Delta_1 + \Delta_{nb})}{2} \right] v_s \qquad \text{(Eq. 32)}$$

$$wa_1 = \Delta_1 v_1 \qquad \text{(Eq. 33)}$$

$$wa_n = \Delta_n v_n \qquad \text{(Eq. 34)}$$

$$wp_i = \Delta_i v_i \qquad \text{(Eq. 35)}$$

$$\xi_{sys} = \frac{wa_1\xi_1 + wa_n\xi_n + ws\xi_s + \sum_{2}^{n-1} wp_i\xi_i}{wa_1 + wa_n + ws + \sum_{2}^{n-1} wp_i} \qquad \text{(Eq. 36)}$$

Step 4. Determine the required strength

First the 5% damping elastic displacement spectrum is reduced to the level of damping of the structure (ξ_{sys}). To do this, a demand reduction factor is computed with Eq. 37 (Eurocode, 1998), where α = 0.25 for near fault sites and α = 0.5 for other sites. Then, the reduced displacement design spectra is entered with Δ_{sys} to find the required period, T_{eff}, for the structure. This is shown schematically in Fig. 3. This process has been synthesized in Eq. 38.

$$R_\xi = \left(\frac{7}{2 + \xi_{sys}} \right)^\alpha \qquad \text{(Eq. 37)}$$

$$T_{eff} = \frac{\Delta_{sys}}{PSD \cdot R_{\xi}} T_c \qquad \text{(Eq. 38)}$$

Based on the well know relation between stiffness, mass and period of a single degree of freedom system, the stiffness, $K_{eff,}$ and then the strength, V, required for the equivalent system are obtained with Eq. 39 and Eq. 40 respectively.

$$K_{eff} = \frac{4\pi^2 M_{eff}}{T_{eff}^{\ 2}} \qquad \text{(Eq. 39)}$$

$$V = K_{eff} \Delta_{sys} \qquad \text{(Eq. 40)}$$

Step 5. Distribute required strength

The required strength V_i is determined for each substructure element with Eq. 41. Finally, the design flexural strength, M_i, for the columns in each pier is computed according to the type of pier (Table 3) with Eq. 42.

$$V_i = v_i V \qquad \text{(Eq. 41)}$$

$$M_i = \frac{H_{si} V_i}{n_i} \qquad \text{(Eq. 42)}$$

3.5.2 First mode shape algorithm

This algorithm is applicable to cases where a flexible displacement pattern has been adopted and the response of the bridge is controlled by its first mode of vibration (See Table 3). This procedure is iterative and use elastic analysis of refine the assumed displacement pattern. This algorithm converges to the first mode inelastic shape of the structure.

Step1. Determine Target displacement profile

Follow Section 3.4

Step 2. Apply direct procedure

Conduct all the steps 2- 4 of the direct solution presented in Section 3.5.1

Step 3. Find a best estimate of the displacement pattern

Inertial forces consistent with the assumed displacement pattern are applied to a bridge model with stiffness secant to maximum response. This static analysis results in a displacement pattern that is a best approximation to the first mode shape of the bridge.

To perform the static analysis, a 2D model of the bridge is built (Fig. 17). In this model, the substructure elements are springs with secant stiffness computed with Eq.43. The superstructure is modeled as a series of frame elements. The loads apply to the model are the inertial forces, F_i, are computed with Eq. 44.

$$K_{effi} = \frac{V_i}{\Delta_i} \quad \text{(Eq. 43)}$$

$$F_i = \frac{m_i \Delta_i}{\sum_1^n m_i \Delta_i} V \quad \text{(Eq. 44)}$$

Once performed, the outcome of this analysis includes the displacements for each substructure element, Φ_i, and new estimates of the proportion of the total shear taken by the abutments, v_{r1} and v_{rn}. These values are computed with Eq. 45 and Eq. 46. If v_1 and v_n where assumed at the beginning of the process, an error between the new and assumed values can be computed with Eq. 47 and Eq. 48.

$$v_{r1} = \frac{\Phi_1 K_1}{V} \quad \text{(Eq. 45)}$$

$$v_{rn} = \frac{\Phi_n K_n}{V} \quad \text{(Eq. 46)}$$

$$ERR_{v1} = abs\left(\frac{v_1 - v_{r1}}{v_{r1}}\right) \quad \text{(Eq. 47)}$$

$$ERR_{vn} = abs\left(\frac{v_n - v_{rn}}{v_{rn}}\right) \quad \text{(Eq. 48)}$$

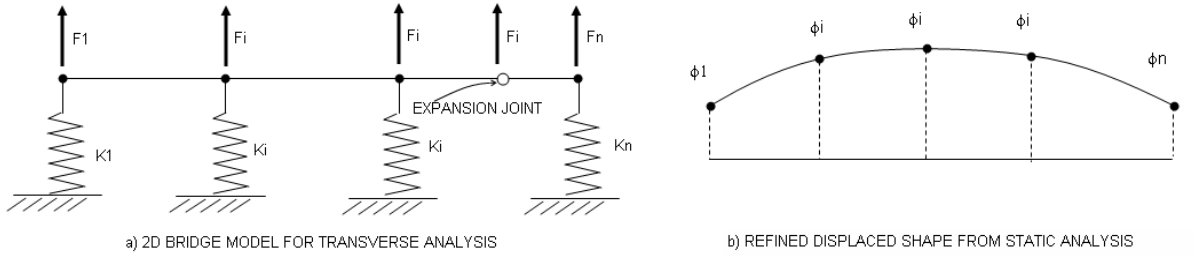

Figure 17 – 2D model of bridge with secant stiffness.

Step 4. Scaling the first mode shape to meet the design objective

This process must assure that no element in the bridge exceeds their previously calculated target displacement. This step is accomplished by calculating a scaling factor, $Sf_{i,}$ for each element as shown in Eq. 49. Then, the least of the scaling factors is applied to the displacements computed in Step 3 to get a refined displacement profile (Eq. 50).

$$Sf_i = \frac{\Delta_{Ti}}{\Phi_i} \quad \text{(Eq. 49)}$$

$$\Delta_{ri} = \Phi_i \min_{1}^{n} Sf_i \quad \text{(Eq. 50)}$$

If the abutments are elastic, their target displacements must be enforced in the displaced shape, that is $\Delta_{r1} = \Delta_{y1}$ and $\Delta_{rn}=\Delta_{yn}$. An error between the previous displacement profile and the new displacement profile can be estimated with Eq. 51

$$ERR_{dp} = \sum_{i=1}^{i=n} (\Delta_{ri} - \Delta_i)^2 \quad \text{(Eq. 51)}$$

Step 5. Check convergence and iterate

When applying this algorithm two assumptions are made: (1) The shape of the displacement pattern, (2) The proportion of total shear carried by the abutments (if present). If errors ER_{v1} and ER_{vn} and ER_{dp} are greater than a predefined tolerance, the procedure must be repeated from Step 2 the number of times required to get the errors within the tolerance. In each iteration the proportion of base shear taken by the abutments and the displacement profile must be updated (i.e. $v_1 = v_{r1}$, $v_n = v_{rn}$ and $\Delta_i = \Delta_{ri}$)

3.5.3 Effective mode shape algorithm

This algorithm is applicable to all cases (See Table 3), however due to its increased complexity, it is recommended to cases where a flexible displacement pattern is used and the response of the bridge is controlled by the combination of several modes of vibration.

This procedure is more complex and requires more effort than the First Mode Shape algorithm. However, this procedure captures the effects of higher modes of vibration in the displacement profile and in the element forces. This procedure is iterative and uses response spectrum analysis to refine the assumed displacement pattern. Its application follows the steps presented next:

Step1. Determine Target displacement profile

Follow Section 3.4

Step 2. Apply direct procedure

Conduct all the steps 2- 4 of the direct procedure presented in Section 3.5.1

Step 3. Find a best estimate of the displacement pattern

A response spectrum analysis is conducted with a model of the bridge in which the substructure elements have secant stiffness computed with Eq. 43. A composite acceleration response spectrum is used such as the one shown in Fig. 18. In the composite spectrum, the spectral ordinates corresponding to the effective period (T_{eff}) of the bridge are reduced by the

factor R_{ξ} computed with Eq. 38 in Step 4 of the direct procedure. The spectral ordinates for periods shorter than T_{eff} are not reduced since the higher modes are likely to be elastic modes of response in the structure.

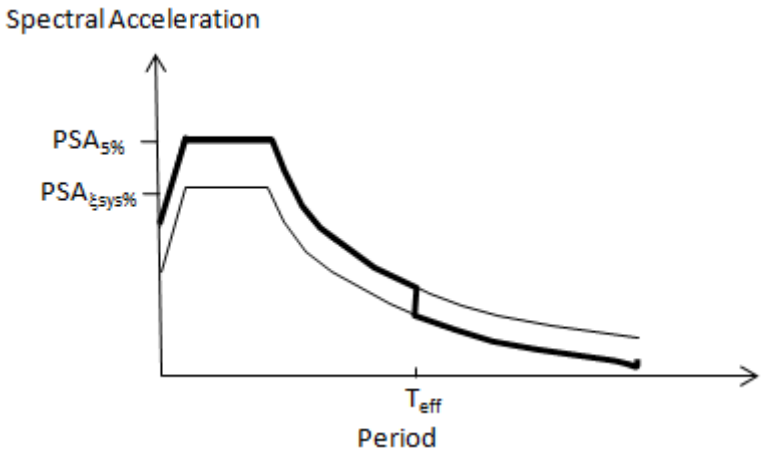

Figure 18 – Composite acceleration response spectrum

The outcome of this analysis includes the displacements for each substructure element, Φ_i , new estimates of the proportion of the total shear taken by the abutments, v_{r1} and $v_{rn,}$ and forces in the superstructure and abutments. Forces in inelastic piers are not considered since any demand in excess of the capacity of the piers is only a result of the elastic analysis. The proportion of shear taken by the abutments is computed with Eq. 45 and Eq. 46. If v_1 and v_n where assumed at the beginning of the process, an error between the new and assumed values can be computed with Eq. 47 and Eq. 48.

Step 4. Scaling the first mode shape to meet the design objective

This process must assure that no element in the bridge exceeds their previously calculated target displacement. This step is accomplished by calculating a scaling factor, $Sf_{i,}$ for each element as shown in Eq. 49. Then the least of the scaling factors is applied to the displacements computed in Step 3, to get a refined displacement profile (Eq. 50).

If the abutments are elastic, their target displacements must be enforced in the displaced shape, that is $\Delta_{r1} = \Delta_{y1}$ and $\Delta_{rn}=\Delta_{yn}$. An error between the previous displacement profile and the new displacement profile can be estimated with Eq. 51

Step 5. Check convergence and iterate

When applying this algorithm to two assumptions basic are made: (1) The shape of the displacement pattern, (2) The proportion of total shear carried by the abutments. If errors ER_{v1} and ER_{vn} and ER_{dp} are greater than a predefined tolerance, the procedure must be repeated from Step 2 the number of times required to get the errors within the tolerance. In each iteration the proportion of base shear taken by the abutments and the displacement profile must be updated (i.e. $v_1 = v_{r1}$, $v_n = v_{rn}$ and $\Delta_i = \Delta_{ri}$)

3.6 DDBD in the longitudinal direction

Applying DDBD in the longitudinal direction of the bridge is generally simpler than doing it in the transverse direction. The steps involved are detailed next:

Step1. Determining target displacement profile

Due to high axial stiffness of the superstructure, a target displacement profile can be determined at the beginning of the process. There are two possibilities that must be considered:

a) If there are not expansion joints in the superstructure nor at the abutments (if exist), all substructure elements are constrained to displace the same amount. Therefore, the substructure element with the least target displacement will control the target displacement of the bridge.

b) If there are expansion joints in the bridge, two target displacement profiles must be considered, one with the bridge being pushed towards the end pier or abutment and the other with the bridge being pushed towards the initial pier or abutment (Fig. 14)

In any case then target profile must be scaled keeping in mind that no substructure element should exceed its target displacement.

Step 2. Computing system displacement and mass

The same as step 2 of the procedure for DDBD in the transverse direction using the direct procedure.

Step 3. Computing ductility demand and equivalent damping

The same as step 3 of the procedure for DDBD in the transverse direction using the direct procedure.

Step 4. Determining the effective period, secant stiffness and required strength

The same as step 4 of the procedure for DDBD in the transverse direction using the direct procedure.

Step 5. Checking the assumed strength distribution

If the bridge has abutments with known strength, the assumed values of v_1 and v_n, must be verified. New refined values for v_{r1} and v_{rn} can be computed with Eq. 52 and Eq. 53. An error between the new and assumed values can be computed with Eq. 47 and Eq. 48.

$$v_{r1} = \frac{K_{eff,1}}{K_{eff}} \qquad \text{(Eq. 52)}$$

$$v_{r1} = \frac{K_{eff,n}}{K_{eff}} \qquad \text{(Eq. 53)}$$

If errors ER_{v1} and ER_{vn} and ER_{dp} are greater than a predefined tolerance, the procedure must be repeated from Step 2 the number of times required to get the errors within the tolerance. In each iteration the proportion of base shear taken by the abutments must be updated (i.e. $v_1 = v_{r1}$, $v_n = v_{rn}$)

3.7 Concurrent orthogonal excitations

Real earthquakes induce three dimensional displacements with two horizontal components that could cause damage in the earthquake resisting components of the bridge. For this

reason, DDBD must be applied in the two principal directions of the bridge and the results must be combined to produce a design capable of performing satisfactorily when attacked in any direction. Strength demands along principal directions can be combined using the well known 100%-30% rule, currently used most seismic design codes (Imbsen, 2007; Caltrans, 2006). Application of this rule is presented in the following section.

3.8 Element Design

3.8.1 Pier design

The design of piers is based in Capacity Design principles to assure that all inelastic behavior take place in well detailed sections. The flexural design of reinforced concrete circular pier columns requires knowledge of moment, axial force and design concrete strain in the critical section of the element. The moments in the transverse, $M_{t,}$ and longitudinal direction, $M_{l,}$ are given by Eq. 54 and Eq. 55, in terms of the design shear that resulted of the application of DDBD, the shear height given by Table 3 and the number of columns in the pier, n_c.

$$M_t = \frac{V_t H_{st}}{n_c} \qquad \text{(Eq. 54)}$$

$$M_l = \frac{V_l H_{sl}}{n_c} \qquad \text{(Eq. 55)}$$

The 100%-30% rule for combination of forces caused by concurrent orthogonal combinations can be used to determine the design moment, M_E. In which case M_E is the grater of the two combinations of transverse M_t and longitudinal M_l moment demands given by Eq. 56 or Eq. 57.

$$M_E = \sqrt{Mt^2 + 0.3Ml^2} \qquad \text{(Eq. 56)}$$

$$M_E = \sqrt{Ml^2 + 0.3Mt^2} \qquad \text{(Eq. 57)}$$

The axial load P_G comes from a dead load analysis. The design strain ε_D must be reached when M_E is developed in the section. When designing for minimal or moderate inelastic actions, ε_D can be taken as 0.003 for nominal strength. When designing for the damage-control or life-safety limit states, ε_D is taken as the least of the strains calculated in the critical section at the transverse or longitudinal design displacement. The strain ε_D is given by Eq. 58.

$$\varepsilon_D = \left(\frac{\Delta - \Delta_y}{L_p H_p} + \phi_y \right) c > 0.003 \qquad \text{(Eq. 58)}$$

Once P_G, M_E and ε_D are known, the amount of flexural reinforcement is determined by section analysis. This analysis should be based on realistic material models and expected rather than specified material properties. In practice, a moment-curvature analysis program could be used to determine by iteration the amount of flexural reinforcement required.

The shear design is based on a demand capacity analysis. The shear demand is based on the flexural over-strength of the section and must be computed in the design direction with the least shear height (H_s). The shear demand is given by Eq. 59, where Φ is an over-strength factor and H_s is the shear height given in Table 3 for different types of piers. If strain hardening was considered in the flexural design, $\Phi = 1.25$ is appropriate (Priestley et al, 2007). The shear capacity of the section can be determined using the modified UCSD model (Kowalsky and Priestley, 2000).

$$V_D = \frac{\Phi M_E}{H_s} \qquad \text{(Eq. 59)}$$

Combination of seismic and non-seismic loads

Element design in DDBD aims to provide the required strength to the earthquake resisting system so the design objective is met. The resulting structure should be capable of resisting gravity loads, other non-earthquake actions and the design earthquake attacking in any

direction. Design for non-earthquake loads should follow LRFD practice specified by AASHTO (2004).

When designing piers in DDBD, it is not generally necessary to combine seismic with non-seismic moment demand. It is also not generally necessary to consider the axial loads generated by the earthquake. The reason is that combining seismic with non-seismic moment and accounting for earthquake induced axial forces might lead to unnecessary over-strength in the structure.

For example, if the columns in the bent shown in Fig. 19a are only designed for gravity axial loads P_G and earthquake moments M_E, the strength developed by the bent in a Pushover analysis (Fig. 19b) will match the design strength V. If the seismic induced axial loads P_E are considered, the windward column, with less axial load, requires more reinforcement. However due to seismic reversal, the two columns must be provided with the same reinforcement, causing the bent to have more lateral strength than required, as shown in the pushover curve in Fig. 19b. If gravity load moments are included, the moment demand on the leeward column is increased, increasing also the amount of required reinforcement. Due to seismic reversal, the two columns should be detailed with the same amount of reinforcement, although only one really needs that much strength. The excess of reinforcement in one column, as in the previous case, causes unnecessary over-strength.

Lateral over-strength is believed to be unnecessary unless it is required to accommodate non-seismic loads. For the example presented previously, if the columns are designed for M_E and P_G only, after the unavoidable gravity loads act, the lateral capacity of one column is reduced while the capacity of the other column is increased. Under lateral loading, one column might experience more damage than the other; however the overall response of the bent will be as planned. In the other hand, if the bent has over-strength in an attempt to limit the damage in a critical section of the bent, due to the over-strength, the bent will have a conservative response and not even the critical section will reach the design limit sate, which is thought to be uneconomical.

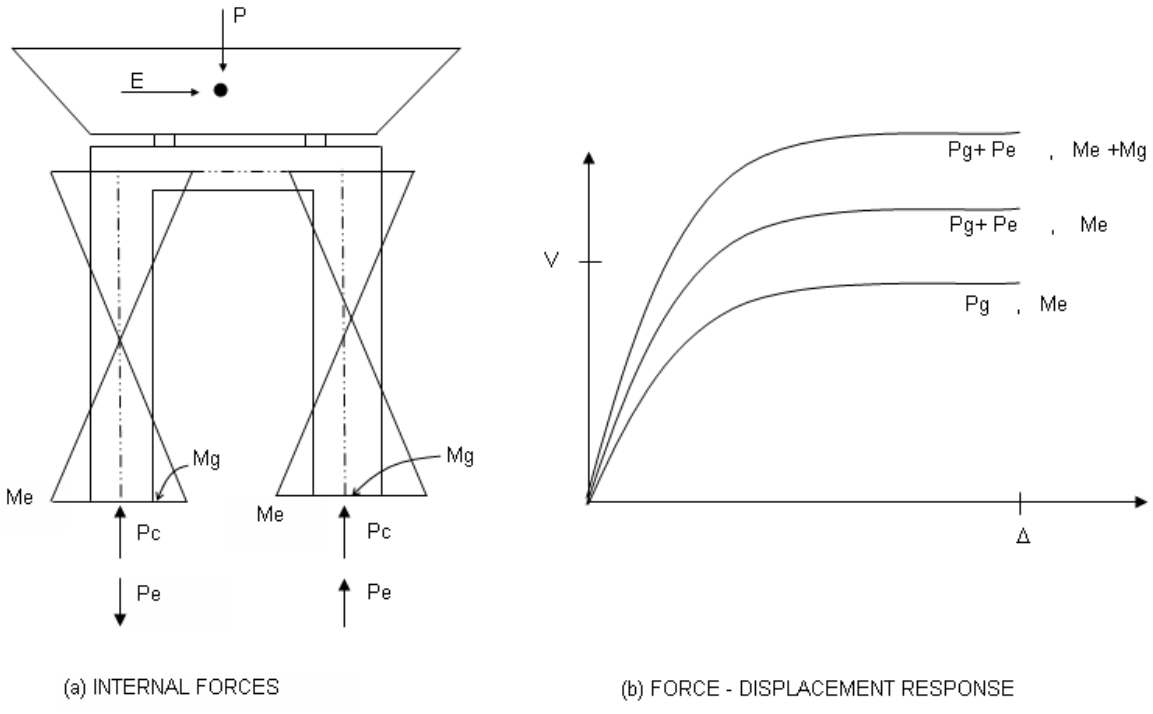

Figure 19 – Force-displacement response of bents designed for combinations of seismic and non-seismic forces.

The arguments presented above apply to all design situations where the gravity loads produce moments that increase the lateral capacity of some columns and reduce the capacity of others. No consideration of gravity moments and seismic induced axial forces is especially appropriate for cases where design is controlled by P-Δ effects rather than damage-based limit states. Caution must be exercised in the case of curved bridge frames with integral single column piers, where gravity loads reduce the lateral capacity of all columns. Seismic axial loads should not be ignored in columns with high axial load ratios, where additional axial loads could lead to brittle failures.

3.8.2 Abutment design

The effects that the abutments have in the response of the bridge depend on their contribution of strength and stiffness. Seat-type abutments have sacrificial shear keys and knock off walls

and generally contribute little to the strength of the bridge. Integral abutments are monolithic with the superstructure and must be strong enough to restrain superstructure displacement and avoid excessive damage. DDBD can be used to obtain the design actions for these types of abutments, as explained next:

Integral Abutments

Generally, abutments have less displacement capacity than the adjacent bents. Therefore, integral abutments must be effective in restraining the displacement of the superstructure at their ends to avoid excessive damage. To do this, integral abutments must be strong and stiff.

To design integral abutments with DDBD, the designer specifies, a maximum displacement to be reached by the abutments in the in-plane and out-of-plane directions. The designer must also specify the amount of viscous damping and a skew angle if any. The amount of damping should be between 5 and 10%, as recommended by AASHTO (Imbsen, 2007) for continuous bridges, in which there is considerable soil mobilization at the abutments. If plastic hinges are expected to develop in the supporting piles, the amount of viscous damping could be further increased as a function of ductility demand (See section 2.1).

Continuous bridges with integral abutments are expected to respond in the transverse direction with a flexible displacement pattern. The shape of the pattern is unknown before design and is generally given by the first mode of vibration. Therefore DDBD is applied with the FMS algorithm or the EMS algorithm (Table. 2) (see Section 3.5).

If the target displacement is less than their yield displacement, the abutments will perform elastically during the earthquake. If that is the case, it is important to consider the additional demands generated by higher modes of vibration. Such determination can be accomplished using the EMS algorithm or by the application of a dynamic amplification factors. Analyses performed by the authors on a set of ten bridges with integral abutments,

showed that the shear demand in the abutments can be increase up to 2.5 times the forces derived from the FMS design (Suarez and Kowalsky, 2008a)

The application of DDBD in the longitudinal direction is direct for bridges with integral type of abutments. The ratio of the total base shear taken by the abutments can be decided by the designer at the beginning of design.

Seat type abutments

This type of abutments are typically designed for non-seismic loads and protected from seismic demands by the provision of sacrificial shear keys and knock off walls that are designed to fuse. In the in-plane direction, contribution to the strength of the bridge is given by passive pressure of the soil that is mobilized behind the wing walls and residual strength or friction after the shear keys fail. In the longitudinal direction, the strength contribution comes from passive pressure of the soil mobilized behind the back-walls that is compressed. Methods for determining the strength and yield displacement of these elements are well known and presented in detail in AASHTO Guide Specification for LRFD Seismic Bridge Design (Ibsen, 2007).

When designing a continuous bridge with seat-type abutments, their contribution to the strength and the effect on the response of the bridge can be easily accounted for in DDBD. The force-displacement response of the abutment must be known in both direction of design. In this case, DDBD will limit the response of the abutment to the specified target displacement by allocating the appropriate level of strength in the bridge piers. Since the ratio of the total base shear taken by the abutments is not known at the beginning design, DDBD requires iteration. The study of higher mode effects is unnecessary for elasto-plastic abutments since demand cannot exceed capacity.

4. COMPUTERIZATION OF DDBD

The computer program DDBD-Bridge has been developed for automation of the DDBD method for highway bridges. In most design cases DDBD can be applied with manual or spreadsheet calculations using the direct procedure. However, time in the application of the FMS or EMS algorithms and section design could be saved by programming the algorithms into a computer code.

DDBD-Bridge has been programmed following the general procedure presented in this report. The program has the following features:

- DDBD of highway bridges in the transverse and longitudinal directions
- Design using the direct, FMS and EMS algorithms
- Continuous superstructures or superstructures with expansion joints
- Integral or seat-type abutments
- All types of piers shown in Table 3
- Automated section design by moment-curvature analysis

The program and its documentation can be accessed and used on-line though the Virtual Laboratory for Earthquake Engineering (www.utpl.edu.ec/vlee)

4.1 DDBD using commercially available structural analysis software

Any frame analysis program capable of performing static and response spectrum analysis can be used to perform the Step 3 of the FMS or EMS algorithms presented in Section 3.5.

Even though static analysis is not required in the direct solution (Section 3.5.1.), inertia forces can be calculated (Eq. 44) and applied to an elastic model of the bridge to get element forces and easy element design. This is equivalent to apply the FMS algorithm (Section 3.5.2) without iteration.

When applying the iterative design algorithms, the secant stiffness of the elements must be updated in the model in each iteration. If a 3D model is used with the piers modeled using frame elements, Eq. 60 can be used to compute inertia reduction factors, I_{rf}, for each element. In this equation, E is the elastic modulus used in the analysis program, I_g is the gross moment of inertia of the section and γ is 1/3 for pinned head columns and 1/12 for fixed head columns. Inertia reduction factors are accepted in most analysis programs to modify the gross section properties of frame elements.

$$I_{rf} = \frac{K_i H^3}{\gamma E I_g} \qquad \text{(Eq. 60)}$$

4.1 Evaluation of DDBD with Inelastic Time History Analysis

Inelastic Time History Analysis (ITHA) is considered to be the most accurate tool to assess structural performance. Other assessment methods based on nonlinear static analysis (Pushover) such as the Capacity Spectrum Method (FEMA, 2005) or the Displacement Coefficient Method (FEMA, 2005) should not be used for assessment of structures designed with DDBD since these methods also use equivalent linearization and an assumed pattern of displacement. Therefore, there is no reason to believe that the performance predicted by assessment methods based on Pushover analysis is more accurate than the target performance used in DDBD.

Research on DDBD of bridges (Kowalsky, 2002; Dwairi and Kowalsky, 2006; Ortiz, 2006; Suarez and Kowalsky, 2008a) has shown good agreement between the target performance used in DDBD and the performance simulated by ITHA. This has proven that DDBD is an effective design method and therefore, in general, designs done with DDBD do not require evaluation by ITHA or other method. Exemptions to this are the cases were the bridges have characteristics that cannot be captured by DDBD or have not yet been studied for their implementation in DDBD. Additionally, ITHA may be required by the owner for important/essential bridges. The conditions under which ITHA may be required for design evaluation are:

- Bridges with more than six spans
- Bridges with more than two internal expansion joints in the superstructure
- Curves bridges where the subtended angle is greater than 90^o
- Highly irregular configurations
- When the target displacement and target ductility of critical components cannot be accurately assessed. This may happen for some substructures that are not considered in Table 3 or for drilled shaft bents when soil conditions are different of those assumed for the definition of the equivalent model

The program ITHA-Bridge has been developed to perform ITHA of highway bridges. This program is a pre-processor and post-processor of OpenSees (Mazoni et al, 2006) and has the following features:

- From a basic input automatically generates the bridge model files for OpenSees.
- Supports the substructures shown in Table 3, integral and seat-type abutments. Also supports superstructure joints and plan curvature.
- Multiple acceleration records can be run in batch mode automatically.
- Checks convergence errors in solution and adjusts the analysis time step if necessary to achieve convergence.
- Produces and output file combining the output of the different acceleration records that were run.

ITHA-Bridge and its documentation can be accessed and used on-line though the Virtual Laboratory for Earthquake Engineering (www.utpl.edu.ec/vlee).

5. APPLICATION EXAMPLES

5.1 Superstructure target displacement

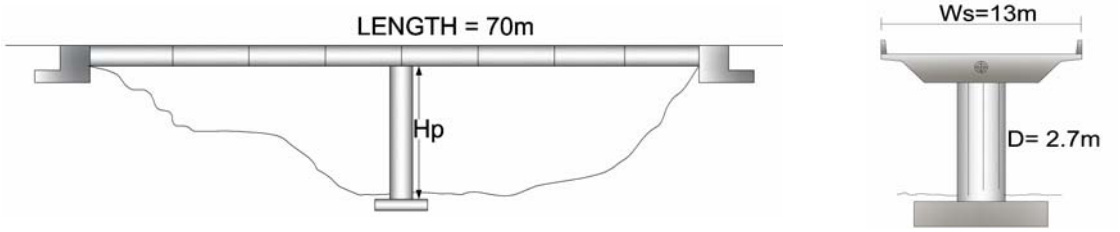

Figure 20 – Two span continuous bridges

This example illustrates the effect of superstructure displacement capacity in the ductility of the central pier of the bridge shown in Fig. 19. It is assumed that the displacement capacity of the continuous superstructure is controlled by the yielding of the longitudinal reinforcement in the concrete deck. The yield displacement of the superstructure is computed at the location of the central pier. The length of the bridge is Ls = 70 m and the width of the superstructure deck is w_s = 13 m, as shown in Fig. 20.

$$\mu_{\Delta i} = \frac{\Delta_{ysi}}{\Delta_{ypi}} \qquad \text{(Eq. 61)}$$

The ductility of the central pier is computed with reference to the yield displacement of the superstructure using Eq. 61, for a range of pier heights H_p. The yield displacement of the superstructure computed with Eq. 14 is Δ_{ys2} = 0.207 m. This is based on $\Delta_1 = \Delta_3$ = 0.05 m. The yield displacement of the central pier, Δ_{yp2}, is computed with Eq. 20. The yield curvature of the superstructure is computed with Eq. 10 and the yield curvature of the pier is computed with Eq. 19. In both cases the yield strain of steel is ε_y = 0.002.

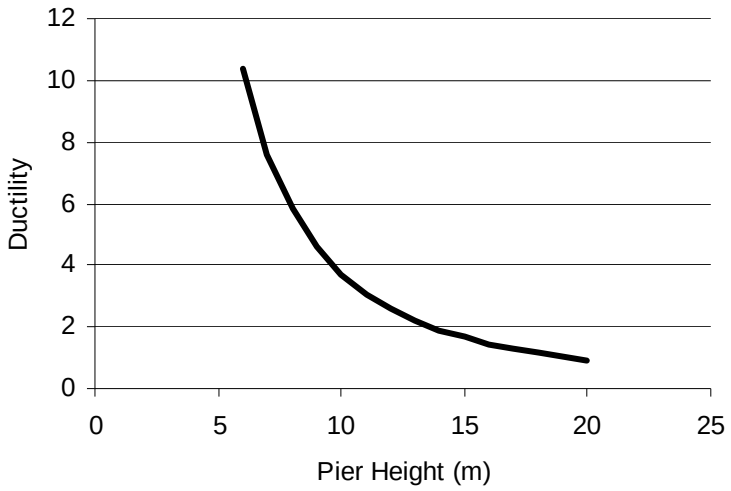

Figure 21 – Target ductility of central pier of two span bridge

If the height of the pier H_p is varied from 6 m to 20 m, the target ductility of the pier, limited by target displacement of the superstructure, varies as shown in Fig. 21. Well confined piers designed for the life-safety limit state have a target ductility of 6 (See section 3.1). Therefore, if the height of the central pier is greater than 10 m, the target displacement of the pier is governed by the yield displacement of the superstructure rather than by target displacement of the pier itself. If the pier is 20 m tall, the yield displacement of the pier equals the yield displacement of the superstructure.

5.2 Stability-based target displacement model

To assess the effectiveness of the proposed model, Eq. 25 was used in the single column pier shown in Fig. 22, to find the target ductility to meet a stability index, $\theta_s = 0.3$. The diameter of the reinforced concrete column is 1.8 m. The axial load is P = 6107 kN and the mass is M_{eff} = 622.5 t. The height of the column is varied between 5.4 m and 27 m so the aspect ratio ranges from 3 to 15. The pier is designed for a displacement spectra with T_c = 3.5 s and the *PSD* = 0.71 m. The results are presented in Fig. 23

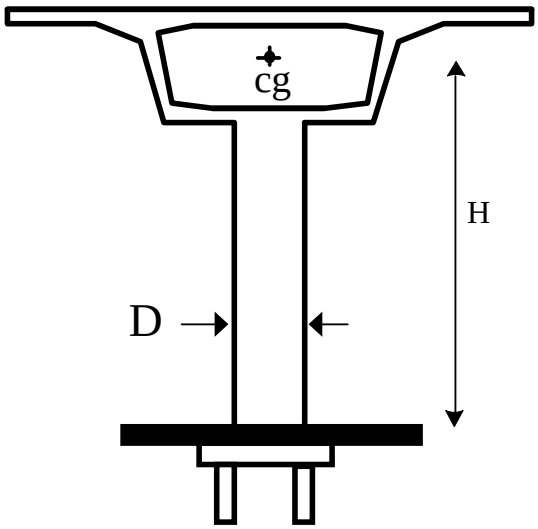

Figure 22 - Single Column Bent

Results in Fig. 23a indicate that the target ductility reduces fast when the aspect ratio increases. If the life-safety ductility for the pier is six, P-Δ controls design when the aspect ratio is higher than five.

Continuing design, using the stability-based ductility as target ductility, P-Δ effects are checked at the end and θ_s can be plotted against ductility as shown in Fig. 23b. This figure shows that the proposed model can effectively predict the target ductility to meet the specified stability index.

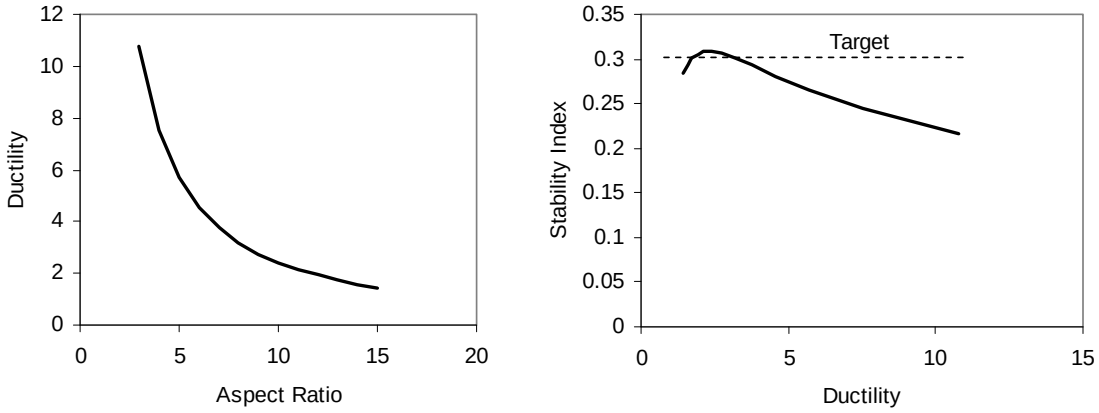

(a) Ductility vs. Aspect Ratio **(b) Stability index vs. Ductility**

Figure 23 - Stability based ductility vs. aspect ratio for a single column pier

5.3 Skewed bent design

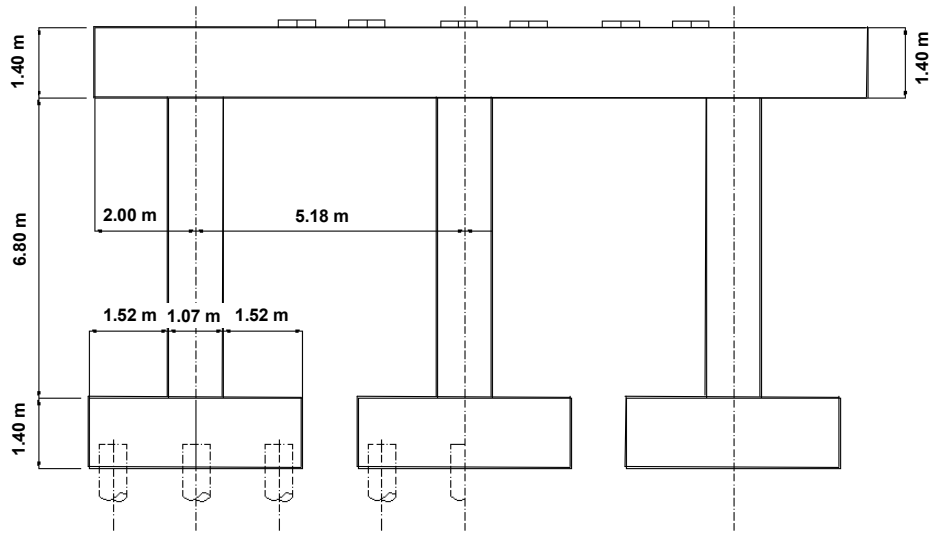

Figure 24 - Multi column bent

The multi column bridge bent shown in Fig. 24 was designed with 0, 15, 30 and 45 degrees of skew. Once designed, the performance of the bent was assessed by ITHA. This multi-column bent supports simply supported spans of a highway bridge. The tributary weight of the superstructure is 6408 kN, the weight of the cap-beam is 562 kN. The bent has three

circular, 1.05 m diameter, reinforced concrete columns, with height equal to 6.80 m. The height of the cap-beam is 1.37 m. To meet detailing requirements regarding to minimum reinforcement and spacing, the columns are reinforced with longitudinal bars of 25 mm and hoops of 13 mm spaced 150 mm. f'_{ce} = 34.45 MPa, ε_y = 0.0022, ε_{su} = 0.06, f_{yh} = 414 MPA.

The bent was designed to meet the damage control limit state under the earthquake represented by the displacement spectrum shown in Fig. 24, where T_c = 3.5 s and the *PSD* = 0.71 m. The damage-control concrete compression strain computed with Eq. 7 is ε_{dc} = 0.017. The damage control displacement of the bent is $\Delta_{T,in}$ = 146 mm in the in-plane direction and $\Delta_{T,out}$ = 317 mm in the out-of-plane direction. These values were calculated with Eq. 16 with reference to Table 3. The yield displacement is $\Delta_{y,in}$ = 43 mm in the in-plane direction and $\Delta_{y,out}$ = 115 mm in the out-of-plane direction. These values are computed with Eq. 20, with reference to Table 3. The effective height of the bent is $H_{p,in}$ = 6.8 m in the in-plane direction and $H_{p,out}$ = 8.17 m in the out-of-plane direction.

Using Eq. 23 and Eq. 24, the in-plane and out-of-plane design parameters are projected in the transverse and longitudinal directions of the bridge for the different skew angles. The results are presented in Table 6.

Table 6 - Design parameters from local to global axes

Skew	Δ_t (mm)	Δ_l (mm)	Δ_{yt} (mm)	Δ_{yl} (mm)	H_t (m)	H_l (m)
0	146	317	43	115	6.8	8.17
15	174	288	55	103	7	7.94
30	203	260	67	91	7.26	7.71
45	231	231	79	79	7.49	7.49

For each target displacement in the transverse and longitudinal directions, design was continued to get the required strengths V_t and V_l and design moments M_t and M_l. Finally the amount of longitudinal reinforcement was obtained by section analysis using the axial load and the combined moment M_E. This process was done as explained in Section 3.8. The design results are summarized in Table 7, where ρ is the longitudinal steel ratio required in the section.

Table 7 - Design results for multi-column bent

Skew	V_t (kN)	V_l (kN)	M_t (kN.m)	M_l (kN.m)	M (kN.m)	ρ %
0	3341	1624	3786	4423	4566	2.61
15	2840	1776	3327	4702	4807	2.83
30	2470	1959	2987	5039	5118	3.06
45	2185	2185	2726	5453	5514	3.4

It is observed in Table 7 that as the skew increases, the displacement capacity in the longitudinal direction decreases. This causes the strength demand in that direction to increase. The required reinforcement also increases and since design is controlled by response in longitudinal direction.

To assess the response of the skewed bent, ITHAs were conducted using OpenSees (Mazzoni et al, 2005). The columns were modeled using fiber sections, with nonlinear stress-strain models for reinforcing steel, confined and unconfined concrete. The cap-beam was modeled with elastic frame elements.

Six finite element models were built. Three models had skew angles of 15 ^{o}, 30 ^{o} and 45^{o}, but the columns were reinforced as for 0 skew. The other models had the different skew angles and the reinforcement required for each level of skew. All models were subjected to the two horizontal components of the seven earthquake compatible records shown in Fig. 25.

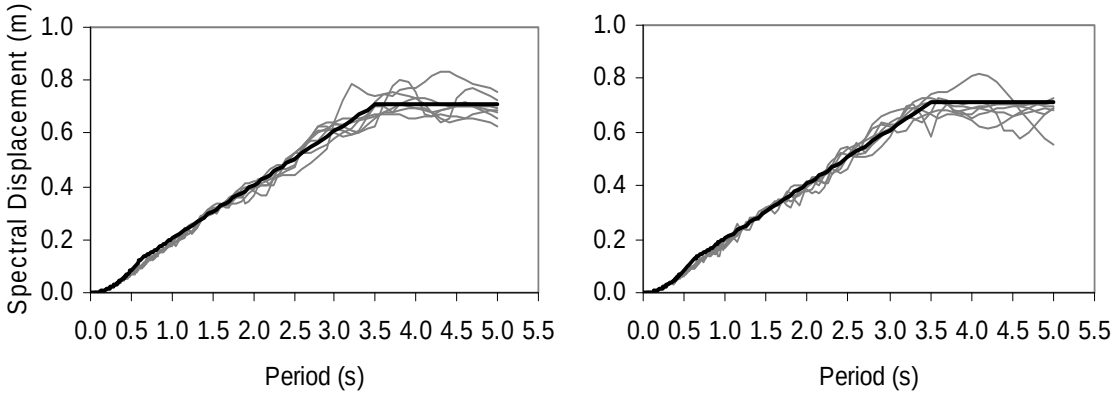

(a) North-South components **(b) East-West components**

Figure 25 - Displacement spectrum and displacement spectra of 7 earthquake compatible records

During the displacements in the local axes of the bent were recorded at the time in which maximum concrete strains were reached. These results were averaged with results from the other records. The final results are presented in Table 8. It is observed that the response in longitudinal direction controls design in all cases. In the models were the reinforcement was not increased with skew, the demand increases as the skew increases. In the models were the reinforcement was increased with skew, the demand was maintained. It is concluded then, that the proposed method is capable of capturing the effects of skew in this types of bents.

Table 8 - Design results for multi-column bent

	Design for 0 skew		Designed for skew	
Skew	Δ_{in} (mm)	Δ_{out} (mm)	Δ_{in} (mm)	Δ_{out} (mm)
15	32	264	17	250
30	29	276	15	269
45	28	297	16	256

5.4 DDBD of a three span continuous bridge with seat-type abutments

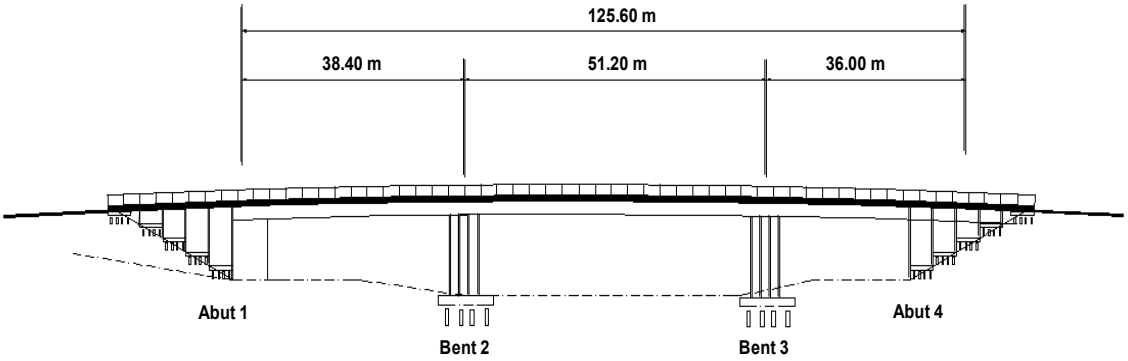

Figure 26 - Elevation view three span bridge

This bridge has three spans of 38.41 m, 51.21 m and 35.98 m respectively and a total length of 125.60 m. The superstructure is a continuous prestressed reinforced concrete box girder. The two bents have two 1.83 m diameter columns supported on piles. Column height varies

from 13.40 m at bent two to 14.30 m at bent three. The columns are pinned at the bottom and fixed to an integral bent in the superstructure. The abutments are seat type with brake-off walls. An elevation view of the bridge is presented in Fig. 26 and the superstructure section and substructure configuration are shown in Fig. 27. The reinforced concrete in piers has the following properties: f'_{ce} = 36 MPA, f_{ye} = 455 MPa, ε_y = 455/200000 = 0.0022, ε_{su} = 0.1, f_{yh} = 414 MPA.

The seismic hazard at the bridge site is given by the design spectra, with 5% damping, shown in Fig. 27. The corner period of the displacement spectra is 8 s (FEMA, 2003), and the maximum spectral displacement is 1.92 m.

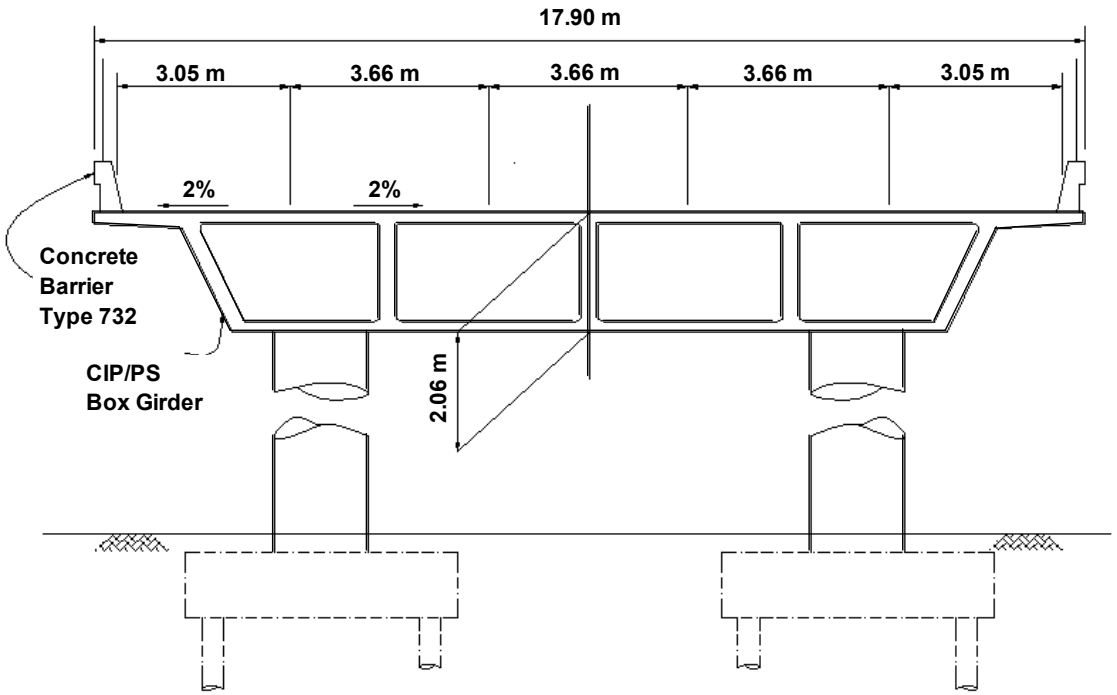

Figure 27 - Superstructure section and interior bent

Design Objective

Under the design earthquake represented by the displacement spectra shown in Fig. 28, the bridge shall meet one or more of the following performance limits: 1) damage control strains in the columns, 2) stability index less than 30%

Assessment of Target Displacement

Complying with min reinforcement requirements of AASHTO (Imbsen, 2007), D44 longitudinal bars and a D25 spiral spaced 130 mm are chosen for the columns.

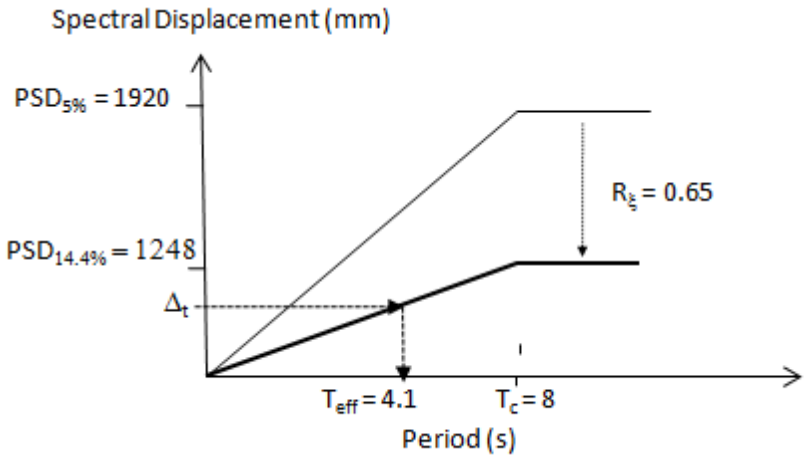

Figure 28 – Displacement Spectra

1. The damage control displacement Δ_{DC} of the bents is determined with the plastic hinge method (Eq. 16), assuming single bending in the columns. These calculations are valid for the two directions of design. The yield displacement Δ_y (Eq. 20) and damage-control displacement Δ_{DC} are shown in Table 9. The damage control compression strain for concrete is $\varepsilon_{c,dc} = 0.018$ and controls the determination of $\Delta_{DC.}$

2. The stability based target displacement is computed with Eq. 25 and Eq. 26. The results are shown in Table 9. It is observed in this table that stability-based displacement controls design and becomes target design displacement.

Table 9 - Target displacements Trial design CA-1

	H (m)	D (m)	P (kN)	Δ_y (m)	Damage Control Δ_C (m)	P-Δ Δ_C (m)
Bent 2	13.4	1.83	6714	178	656	640
Bent 3	14.3	1.83	6557	202	737	650

Strength Distribution.

The strength is be distributed among the bents so that all columns have the same reinforcement (See Section 3.5). The proportion of the total base shear taken by each bent in computed with Eq. 31, assuming that the abutments will contribute 10% of the total strength in the transverse and longitudinal directions (i.e. v_s = 0.1 in Eq. 31). Applying Eq. 31 it is found that v_2 = 0.46 and v_3 = 0.44

Design in Transverse Direction

Design in the transverse direction will account for interaction between the superstructure, bents and abutments. The superstructure section shown in Fig. 26 has an out-of-plane inertia I = 222 m4, an elastic modulus E_s = 26500 MPa, and a weight W_s = 260 kN/m.

The abutments are assumed to have an elasto-plastic response. The transverse strength or yield force of the abutments is computed considering there are sacrificial shear keys that will brake during the design earthquake. The residual strength in the abutment comes from friction between the superstructure and the abutment. Assuming a friction coefficient of 0.2, with a normal force equal to the tributary superstructure weight carried by the abutments, the transverse strength of the abutments is 1300 kN. It is assumed that the yield displacement is 50mm.

Step 1. Target displacement profile. Since the bridge is regular and the superstructure is stiff, the abutments are not expected to restrain the displacement of the superstructure and a rigid body displacement patter will be used (Section 3.4.1) (Suarez and Kowalsky, 2008a). As a result of this, all substructures displace the same amount and the amplitude of the displacement profile is given by the bent 2, which is the one with the least target displacement (Table 12).

Step 2. Equivalent single degree of freedom system. With the bents and abutments displacing the same amount in the transverse direction Eq. 1 and Eq. 2 reduce to Eq. 62 and Eq. 63. The generalized displacement equals the target design displacement of bent 2 so Δ_{sys} = 640 mm. Also the effective mass of the bridge is the sum of the total mass of the superstructure, integral bent-caps and one third of the weight of the columns, M_{eff} = 3808 t.

$$\Delta_{sys} = \Delta_T \qquad \text{(Eq. 62)}$$

$$M_{eff} = \sum_{i=1}^{i=n} M_i \qquad \text{(Eq. 63)}$$

Step 3. Equivalent damping. The ductility at the target displacement level is μ_1 = 12.80, μ_2 = 3.59, μ_3 = 3.16, μ_4 = 12.80. These values are obtained as ratios between Δ_{sys} and the yield displacement of each substructure. Equivalent damping is computed for each bent as a function of ductility using Eq. 3. Assuming the abutments respond with 10% of critical damping, ξ_1 = 10%, ξ_2 = 15.2%, ξ_3 = 14.7%, ξ_4 = 10%. The damping combined with Eq. 36 in terms of work done by each element, results in ξ_{sys} = 14.4%.

Step 4. Required strength. The level of damping in the bridge results in a displacement demand reduction factor R_ξ = 0.65 (Eq. 37). As shown in Fig. 27, by entering the reduced displacement spectrum with Δ_{sys}, the required period is T_{eff} = 4.1 s (Eq. 38). Finally, the required strength for the bridge in the transverse direction is V = 5700 kN (Eq. 40).

Step 5. Checking assumed strength distribution. Since the abutments yield at 50 mm, at the target displacement, both abutments develop their full strength, V_a = 2600 kN. Therefore the proportion of the total strength taken by the abutments is v_a = 2600/5700 = 45% (Eq. 42). This is 4.6 times the value assumed at the beginning of the process, therefore ξ_{sys} must be re-evaluated to obtained a new V. After a few iterations V = 6447 kN and the participation of the abutments is 39 %, as shown in Table 10.

It is important to note that iteration was required since it was chosen to consider the strength of the abutments. Accounting for the strength of the abutments has significantly reduced the demand on the piers. However whether the abutments are able to contribute this strength after several cycles of displacements as large as 0.6 m might be questioned.

Table 10 - Transverse design parameters

Iteration	Δ_{sys}	M_{eff}	ξ_{sys}	T_{eff}	V	(V1+V4)/V
1	0.64	3808.1	14.4	>Tc	5879.8	0.1
2	0.64	3808.1	13.3	3.9	6313.3	0.45
3	0.64	3808.1	13.1	3.87	6417.2	0.38
4	0.64	3808.1	13	3.86	6447.8	0.39

Longitudinal Direction

The design process along the longitudinal direction is similar to design in transverse direction. Since the columns are pinned to the foundation and they are integral with the superstructure, the target displacement in the longitudinal direction is the same as the target displacement in the transverse direction. Also, since the superstructure is stiff and continuous, the displacement at the location of the bents and abutments are constrained to be the same. Therefore, Δ_{sys} and M_{eff} are the same as in transverse direction.

Since the longitudinal direction the abutments are designed with knock-off walls, their strength comes from soil mobilization behind the wall pushed by the superstructure. For a wall 14 m wide and 2.5 m tall, assuming a passive pressure of 70 kPa/m (Imbsen, 2007), the strength of the backfill is 6080 kN. Also, using Eq. 15, the yield displacement can be

taken as 75 mm. An elasto-plastic compression only response based on these values is used for this design. The equivalent damping of the abutments is assumed constant, equal to 10%

Table 11 - Longitudinal design parameters

Iteration	Δ_{sys}	M_{eff}	ξ_{sys}	T_{eff}	V	(V1+V4)/V
1	640	3808.1	14.5	>Tc	5699.9	0.1
2	640	3808.1	11	3.69	7247.1	0.8
3	640	3808.1	10.8	3.66	7349.5	0.84
4	640	3808.1	10.9	3.67	7316	0.82

Table 11 summarizes the values of the parameters for longitudinal design. A few iterations were required as it was found that the abutments contribute with as much as 82% of the total strength in this direction. In the first iteration, it was assumed that the contribution of the abutments was 10%. This yielded a total required strength of 5699 kN, which is actually less than the capacity of the abutment that resist the movement of the superstructure. Therefore that solution is not possible. Repeating the process but starting with 80% as abutment contribution, increases the strength demand since the damping is reduced. After three iterations the solution converges, V = 7316 kN and the contribution of the abutments is 82%.

Element Design

In DDBD, the flexural reinforcement is designed using moment-curvature analysis to provide the required strength at a level of curvature compatible with the ductility demand in the element. Table 12 shows the design moments in the transverse M_t and longitudinal direction M_l that resulted from DDBD. It is observed that these values are the same for bents 2 and 3, as it was chosen in the strength distribution. These values are followed by the combined moment M_E. This resulted from the largest of the values obtained with Eq. 56 and Eq. 57, using the 100%-30% combination rule.

Also shown in Table 12 are the P-Δ moments in the transverse P-Δ_t and longitudinal P-Δ_l direction along with the stability indexes calculated as the ratio of the P-Δ moments and the combined moment. In DDBD the stability index should be less than 30%. However, if the

stability index is larger than 8%, the design moment must be increased adding 50% of the P-Δ moment to account for strength reduction caused by P-Δ effects (Priestley et al, 2007). These increased moments are shown in Table 12 along with the design axial force, P,that results from gravity loads only.

Table 12 – Element design parameters

BENT	M_T (kN.m)	M_L (kN.m)	$M_{t\ P\text{-}\Delta}$ (kN.m)	$M_{l\ P\text{-}\Delta}$ (kN.m)	θ_t	θ_l	M_E (kN.m)	P (kN)	ρ (%)	Shear D/C ratio
2	14975	4446	4408	4408	0.29	0.29	17238	7547	1.1	0.24
3	14975	4446	4304	4304	0.29	0.29	17238	7547	1.1	0.25

At the design displacements, the strain in the concrete reaches values of 0.011 for bent 2 and 0.010 for bent 3 (Eq. 58). By section analysis at the design strains, it is found that all columns in the bridge require 20D44 bars as flexural reinforcement, which is a 1.1% steel ratio.

Finally, using the modified UCSD shear model (Kowalsky and Priestley, 2000), the shear capacity of the section is computed and compared to shear demand at flexural over-strength. The shear demand/capacity ratios are shown in Table 12. Since the shear demand capacity ratios are less than one, it is concluded that the amount of adopted shear reinforcement is conservative.

8. REFERENCES

Caltrans, 2006a, Seismic Design Criteria, Caltrans, http://www.dot.ca.gov/hq/esc/earthquake_engineering, (accessed April 18, 2008)

Caltrans, 2006b, LRFD Design Example B November 3, 2006 – Version 1.1, AASHTO, http://cms.transportation.org/?siteid=34&pageid=1800, (accessed April 18, 2008).

Calvi G.M. and Kingsley G.R., 1995, Displacement based seismic design of multi-degree-of-freedom bridge structures, Earthquake Engineering and Structural Dynamics 24, 1247-1266.

Dwairi, H. and Kowalsky, M.J., 2006, Implementation of Inelastic Displacement Patterns in Direct Displacement-Based Design of Continuous Bridge Structures, Earthquake Spectra, Volume 22, Issue 3, pp. 631-662

EuroCode 8, 1998, Structures in seismic regions – Design. Part 1, General and Building", Commission of European Communities, Report EUR 8849 EN

Imbsen, 2007, AASHTO Guide Specifications for LRFD Seismic Bridge Design, AASHTO, http://cms.transportation.org/?siteid=34&pageid=1800, (accessed April 18, 2008).

Kowalsky M.J., 2002, A Displacement-based approach for the seismic design of continuous concrete bridges, Earthquake Engineering and Structural Dynamics 31, pp. 719-747.

Kowalsky M.J., Priestley M.J.N. and MacRae G.A. 1995. Displacement-based Design of RC Bridge Columns in Seismic Regions, Earthquake Engineering and Structural Dynamics 24, 1623-1643.

Mander, J.B., Priestley, M.J.N. and Park, R., 1988a, Theoretical Stress Strain Model of Confined Concrete Journal of Structural Engineering, ASCE, Vol. 114, No.8, August, 1988

Mazzoni, S., McKenna, F., Scott, M. and Fenves, G., 2004, OpenSees command language manual, http://opensees.berkeley.edu, (accessed April 18, 2008)

Paulay, T, Priestley, M.J.N., 1992, Seismic Design of Reinforced Concrete and Masonry Buildings, Wiley, 978-0-471-54915-4

Priestley, M. J. N., 1993, Myths and fallacies in earthquake engineering-conflicts between design and reality, Bulletin of the New Zealand Society of Earthquake Engineering, 26 (3), pp. 329–341

Priestley, M. J. N., Calvi, G. M. and Kowalsky, M. J., 2007, Direct Displacement-Based Seismic Design of Structures, Pavia, IUSS Press

Priestley, M. J. N., Verma, R., Xiao, Y., 1994, Seismic Shear Strength of Reinforced Concrete Columns, Journal of Structural Engineering 120(8) (1994) pp. 2310–2328

Shibata A. and Sozen M. Substitute structure method for seismic design in R/C. Journal of the Structural Division, ASCE 1976; 102(ST1): 1-18.

Suarez, V.A. and Kowalsky M.J., Displacement-Based Seismic Design of Drilled Shaft Bents with Soil-Structure Interaction, Journal of Earthquake Engineering, Volume 11, Issue 6 November 2007 , pp. 1010 – 1030

Suarez, V.A., 2008, Implementation of Direct Displacement Based Design for Highway Bridges, PhD Dissertation, North Carolina State University.

Veletzos, A. and Newmark, N. M., 1960, Effect of inelastic behavior on the response of simple systems to earthquake motions, Proceedings of 2nd World Conference on Earthquake Engineering, pp. 895 – 912.

PART III

COMPARATIVE STUDY OF BRIDGES DESIGNED WITH THE AASHTO GUIDE SPECIFICATION FOR LRFD SEISMIC BRIDGE DESIGN AND DDBD

Vinicio A. Suarez and Mervyn J. Kowalsky

Department of Civil, Construction and Environmental Engineering, North Carolina State University, Campus-Box 7908, Raleigh, NC-27695, USA

ABSTRACT

This paper is intended to show differences in the execution and outcomes of the Direct Displacement-Based Design method and the design method in the recently proposed AASHTO Guide Specification for LRFD Seismic Bridge Design. The comparison is based on the results of the application of the DDBD method to four bridges that were previously designed by others, as trial designs for the implementation of the LRFD Seismic guide. The selected bridges are typical highway bridges with two and three spans and continuous superstructures.

1. INTRODUCTION

The seismic design procedure in AASHTO LRFD Bridge Design Specification (2004) is Force-Based and was adopted by AASHTO in 1983. In the last decade, recognizing the availability of improvements documented in NCHRP 12-49 and the Caltrans Seismic Design Criteria SDC (2006), the T-3 AASHTO committee for seismic design started a project to update the LRFD guidelines. This resulted in the proposed AASHTO Guide Specification for LRFD Seismic Design Guide (Imbsen, 2007).

The main improvement in the newly proposed LRFD Seismic guide is the use of displacements rather than forces to assess the demand and capacity of the structure. Therefore, the design method within the specification can be classified as "Displacement-Based" in contrast to the previous methodology that was essentially "Force-Based".

Another Displacement-Based method is the Direct Displacement-Based Design Method (DDBD) proposed Priestley in 1993 (Priestley, 1993). This method has undergone extensive research and has been shown to be effective for performance-based seismic design of bridge piers (Kowalsky et al, 1995; Suarez and Kowalsky, 2007), continuous bridges (Calvi and Kingsley, 1997; Dwairi and Kowalsky, 2006; Ortiz 2006, Suarez and Kowalsky, 2008a), buildings and other types of structures (Priestley et al, 2007).

Although these two methods are displacement-based, they differ in several aspects:

- DDBD follows directly from a target displacement to required strength, while LRFD-Seismic requires an iterative process in which strength is assumed and then displacement demand is checked against displacement capacity.
- DDBD uses equivalent linearization to determine seismic demand, while the LRFD Seismic guide uses displacement modification, which leads to the use of the equal displacement approximation (Veletzos and Newmark, 1960) for systems in the constant velocity region of the design spectra. While the equal displacement approximation is acceptable in some cases, past research has shown that its application is often invalid (Kowalsky, 2001; Priestley et al, 2007).

The purpose of this research is twofold: to show differences in execution and to compare the outcome of these two methods. The comparison is based on the designs obtained with DDBD for four bridges that have been designed with the LRFD Seismic guide elsewhere as trial designs for the implementation of that guide specification.

2. REVIEW OF THE DDBD METHOD

2.1 Fundamentals of DDBD

DDBD was first proposed by Priestley (1993) as a tool for Performance-Based Seismic Engineering. The method allows designing a structure to meet any level of performance when subjected to any level of seismic hazard. DDBD starts with the definition of a target displacement and returns the strength required to meet the target displacement under the design earthquake. The target displacement can be selected on the basis of material strains, drift or displacement ductility, either of which is correlated to a desired damage level or limit state. For example, in the case of a bridge column, designing for a serviceability limit state could imply steel strains to minimize residual crack widths that require repair or concrete compression strains consistent with incipient crushing.

DDBD uses an equivalent linearization approach (Shibata and Sozen, 1976) by which, a nonlinear system at maximum response, is substituted by an equivalent elastic system. This system has secant stiffness, $K_{eff,}$ and equivalent viscous damping, ξ_{eq}, to match the maximum response of the nonlinear system (Fig 1). In the case of multi degree of freedom systems, the equivalent system is a Single Degree of Freedom (SDOF) with a generalized displacement, $\Delta_{sys,}$ and the effective mass, $M_{EFF,}$ computed with Eq. 1 and Eq. 2 respectively (Fig.2) (Calvi and Kingsley, 1995). In these equations, $\Delta_1 \ldots \Delta_i \ldots \Delta_n$ are the displacements of the piers and abutments (if present) according to the assumed displacement profile, and $M_1 \ldots M_i \ldots M_n$ are effective masses lumped at the location of piers and abutments (if present).

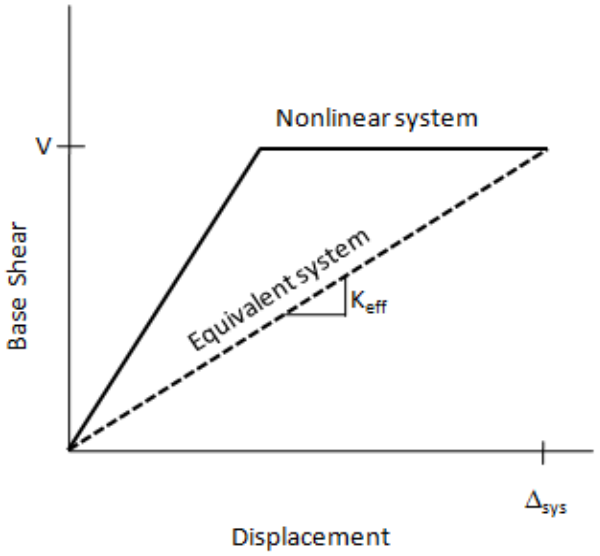

Figure 1 – Equivalent linearization approach used in DDBD

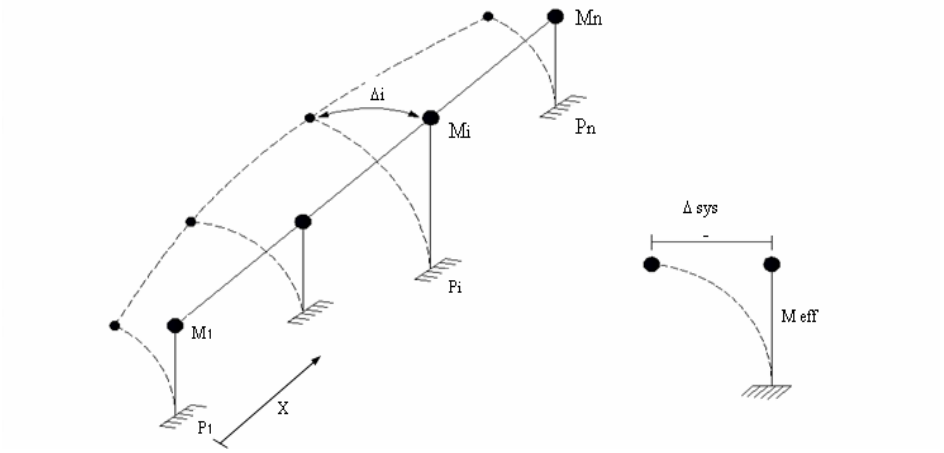

Figure 2 - Equivalent single degree of system.

$$\Delta_{sys} = \frac{\sum_{i=1}^{i=n} \Delta_i^{\,2} M_i}{\sum_{i=1}^{i=n} \Delta_i M_i} \qquad (1)$$

$$M_{eff} = \frac{\left(\sum_{i=1}^{i=n} \Delta_i M_i\right)^2}{\sum_{i=1}^{i=n} \Delta_i^{\,2} M_i} \qquad (2)$$

The energy dissipated by inelastic behavior in the bridge is accounted for in the substitute elastic system by the addition of equivalent viscous damping ξ_{eq}. With the seismic hazard represented by a displacement design spectrum that has been reduced to the level of damping in the bridge, the required effective period, T_{eff}, is easily found by entering in the displacement spectrum curve with Δ_{sys} (Fig. 3). Once T_{eff} is known, the stiffness, K_{eff}, and required strength, V, for the structure are computed from the well known relation between period, mass and stiffness for SDOF systems. Finally, V is distributed among the elements that form the earthquake resisting system, and the elements are designed and detailed following capacity design principles to avoid the formation of unwanted mechanisms.

Equivalent damping

Several studies have been performed to obtain equivalent damping models suitable for DDBD (Dwairi 2005, Blandon 2005, Suarez 2006, Priestley et al 2007). These models relate equivalent damping to displacement ductility in the structure.

For reinforced concrete columns supported on rigid foundations, ξ_{eq}, is computed with Eq. 3 (Priestley, 2007).

$$\xi_{eq} = 5 + 44.4\frac{\mu_t - 1}{\pi \mu_t} \qquad \text{(Eq. 3)}$$

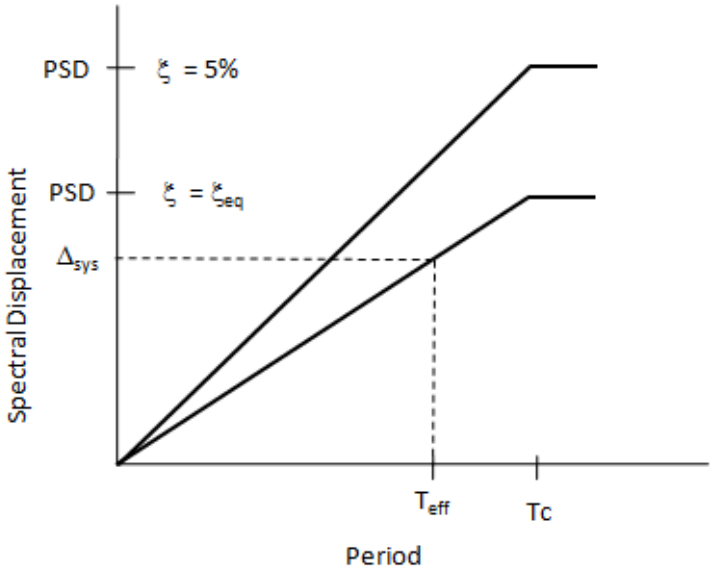

Figure 3 – Determination of effective period in DDBD

For extended drilled shaft bents embedded in soft soils, the equivalent damping is computed by combination of hysteretic damping, $\xi_{eq,h}$, and tangent stiffness proportional viscous damping, ξ_v, with Eq. 4 (Priestley and Grant, 2005). The hysteretic damping is computed with Eq. 5 as a function of the ductility in the drilled shaft. The values of the parameters *p* and *q* are given in Table 1 for different types of soils and boundary conditions (Suarez 2005). In Table 1, clay-20 and clay-40 refer to saturated clay soils with shear strengths of 20 kPa and 40 kPa respectively. Sand-30 and Sand-37 refer to saturated sand with friction angles of 30 and 37 degrees respectively. A fixed head implies that the head of the extended drilled shaft displaces laterally without rotation, causing double bending in the element. A pinned head implies lateral displacement with rotation and single bending. To use Eq. 4, ξ_v should be taken as 5%, since this value is typically used as default to develop design spectra.

$$\xi_{eq} = \xi_v \mu^{-0.378} + \xi_{eq,h} \qquad \mu \geq 1 \qquad \text{(Eq. 4)}$$

$$\xi_{eq,h} = p + q\frac{\mu - 1}{\mu} \qquad \mu \geq 1 \qquad \text{(Eq. 5)}$$

Table 1. Parameters for hysteretic damping models in drilled shaft - soil systems

HEAD	SOIL	p	q
Fixed	Clay-20	6.70	8.10
Fixed	Clay-40	5.60	8.70
Fixed	Sand-30	2.40	10.20
Fixed	Sand-37	2.00	9.60
Pinned	Clay-20	15.80	9.40
Pinned	Clay-40	13.70	10.90
Pinned	Sand-30	9.40	11.20
Pinned	Sand-37	8.50	10.40

All damping models are plotted in Fig. 4. It is observed that when ductility equals one, the equivalent damping for the column on rigid foundation equals 5% (i.e. the elastic viscous damping level) whereas the equivalent damping for the drilled shafts is higher than 5%. The additional damping comes from the soil which performs inelastically and dissipates energy at displacements that are less than the yield displacement of the reinforced concrete section. In cases where the target displacement is less than the yield displacement of the element, a linear relation between damping and ductility is appropriate. Such relation is given by Eq. 6.

$$\xi_{eq} = \xi_v + (q - \xi_v)\mu \qquad \mu < 1 \qquad \text{(Eq. 6)}$$

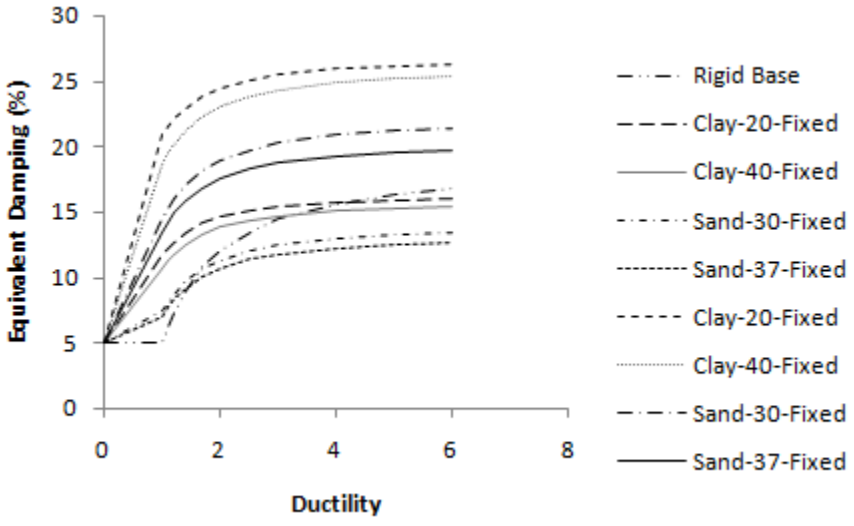

Figure 4. Equivalent damping models for bridge piers

2.2 General DDBD procedure for bridges

The main steps of the design procedure are presented in Fig. 5. The bridge is previously designed for non-seismic loads and the configuration, superstructure section and foundation are known. A design objective is proposed by defining the expected performance and the seismic hazard. Then, the target displacement profile for the bridge is determined, and DDBD is applied in the longitudinal and transverse axes of the bridge. Finally the results are combined, P-Δ effects are checked and reinforcement is designed and detailed following Capacity Design principles (Priestley et al, 2007).

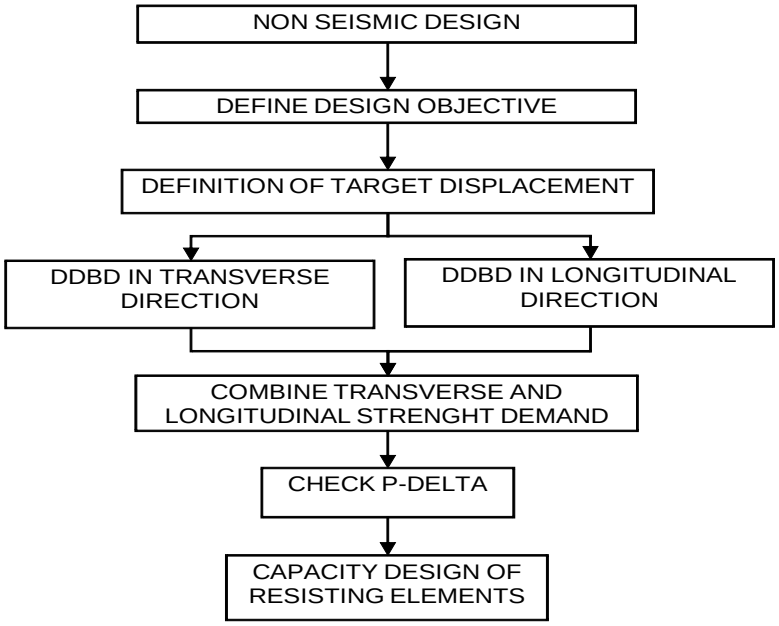

Figure 5 - DDBD main steps flowchart

The flowcharts in Fig. 6 show the procedure for DDBD in the transverse and longitudinal direction, as part of the general procedure shown in Fig. 5. As seen in Fig. 6, there are three variations of the procedure: (1) If the displacement pattern is known and predefined, DDBD is applied directly; (2) If the pattern is unknown but dominated by the first mode of vibration, as in the case of bridges with integral or other type of strong abutment, a First Mode Shape (FMS) iterative algorithm is applied; (3) If the pattern is unknown but dominated by modal combination,

an Effective Mode Shape (EMS) iterative algorithm is applied. The direct application of DDBD, when the displacement pattern is known, requires less effort than the application of the FMS or EMS algorithms. Recent research by the author (Suarez and Kowalsky, 2008a) showed that predefined displacement patterns can be effectively used for design of bridge frames, bridges with seat-type of other type of weak abutments and bridges with one or two expansion joints. These bridges must have a balanced distribution of mass and stiffness, according to AASHTO (Ibsen, 2007). A summary of the design algorithms applicable to common types of highway bridges is presented in Table 2.

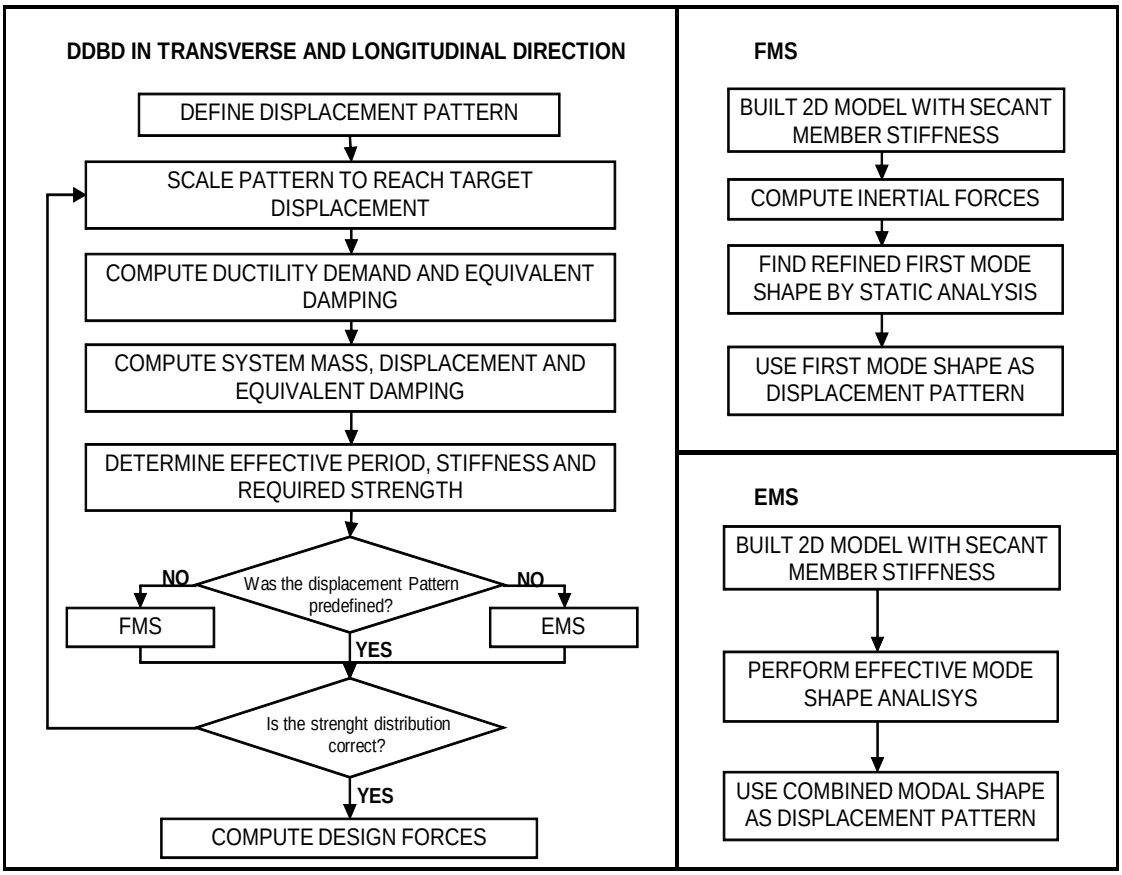

Figure 6 - Complementary DDBD flowcharts

Table 2 - Displacement patterns for DDDBD of bridges

BRIDGE	BALANCED MASS AND STIFFNESS	NO BALANCED MASS AND STIFFNEES
FRAME	**RBT or EMS**	**EMS**
WEAK ABUTMENTS	**RBT or EMS**	**EMS**
STRONG ABUTMENTS	**FMS or EMS**	**FMS**
ONE EXPANSION JOINT	**LDP1 or EMS**	**EMS**
TWO EXPANSION JOINTS	**LDP2 or EMS**	**EMS**
MORE THAN TWO EXPANSION JOINTS	**EMS**	**EMS**
		

2.3. Trial designs

In the following sections, four bridges (Table 3) that were design by others as trial designs for the implementation of the AASHTO Guide Specification for LRFD Seismic Bridge Design (Imbsen, 2007) are also designed with DDBD. The purpose of this is twofold: to show differences in the execution of the two methods and to compare the outcome of the two methods.

Since specific details about the LRFD Seismic designs are available in the design reports posted in the AASHTO web site (bridges.transportation.org/sites/bridges), more details are given for DDBD designs, which are not available elsewhere. DDBD designs are based on the general procedure briefly discussed in the previous section. For more detailed information about DDBD, the readers are referred to Priestley et al (2007) and Suarez (2008)

Table 3 -Summary of bridges used for trial designs

BRIDGE	SPANS	SUBSTRUCTURE	ABUTMENT
Bridge Over Rte. 60, Missouri (MO-1)	4	Multi-column bent	Seat-type
Missouri Bridge MO-2	3	Multi-column bent	Integral
Illinois Bridge IL-2	3	Multi-column bent	Integral
Typical California Bridge. CA-1	3	Single-column bent	Seat-type

The bridges in Table 3, were designed for different Seismic Design Categories (SDC) according to the seismic hazard of each location. The acceleration design spectra used for the LRFD Seismic design and the corresponding displacement design spectra used in DDBD are shown in Fig. 7. The corner or long transition period was obtained from the NEHRP Recommended Provisions for Seismic Regulations for new Buildings and other Structures (FEMA 450) (FEMA, 2003). In the following sections, each of the bridges is described and the LRFD seismic and DDBD designs are presented and compared.

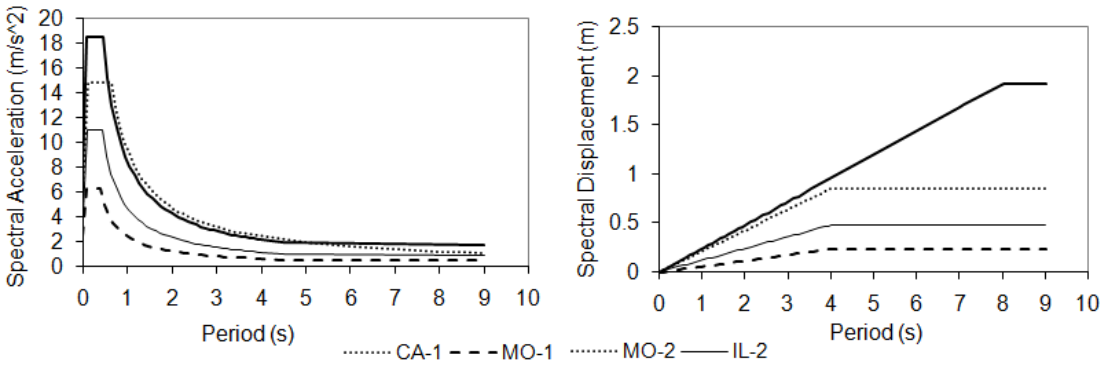

(a) Acceleration spectra **(b) Displacement spectra**

Figure 7. Design spectra

3. BRIDGE OVER RTE. 60, MISSOURI MO-1

This is a four span bridge, with span lengths of 8.99 m - 38.20 m -38.20 m - 8.99 m and a total length of 94.38 m. The external spans are integral with the abutments and the contiguous bent. The superstructure is continuous over the two central spans and is comprised of steel plate girders with a composite concrete deck. The width of the superstructure is 13.41 m. The central bent has three reinforced concrete columns supported on pile groups. The connection between the central bent and the superstructure is pinned. The abutments are seat type supported on a pile cap. All substructure elements are skewed 18 degrees. An elevation view is provided in Fig. 8

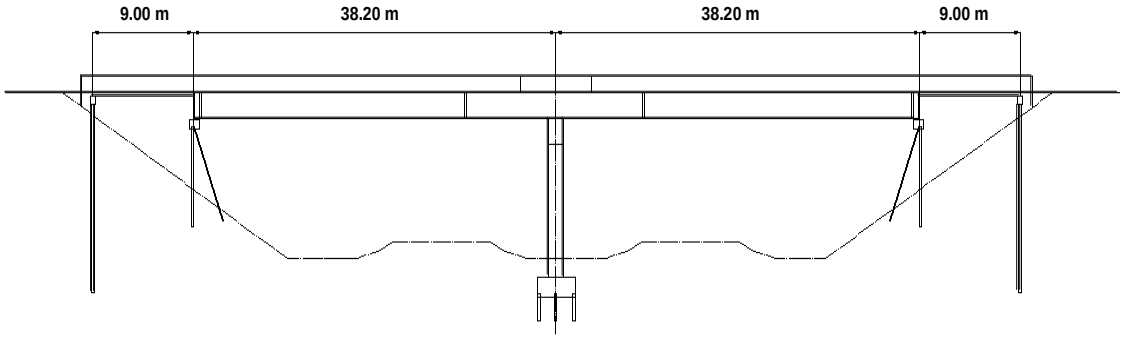

Figure 8 - Elevation view MO-1 bridge

The seismic hazard at the bridge site is given by the acceleration and displacement design spectra shown in Fig.7. The Peak Spectral Acceleration (PSA) is 6.30 m/s^2, the Peak Ground Acceleration (PGA) is 2.5 m/s^2. The corner period of the displacement spectra is 4 s (FEMA, 2003), the Peak Spectral Displacement (PSD) is 0.24 m. According to the LRFD Seismic guide the Seismic Design Category is “B”.

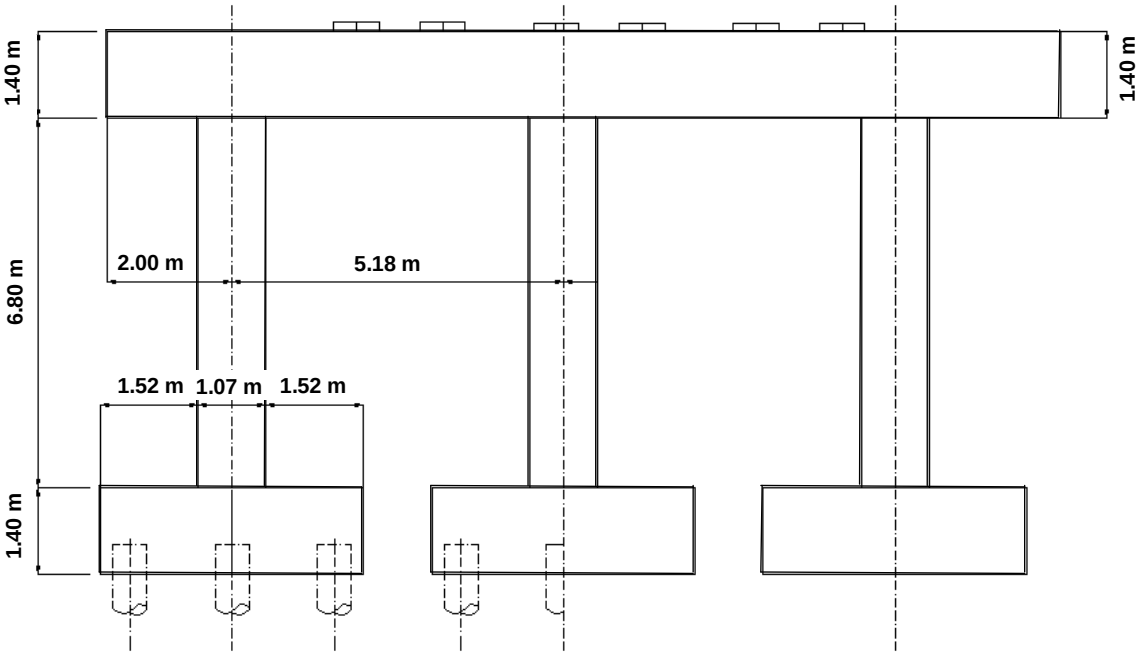

Figure 9 - Central bent MO-1 bridge

3.1 Review of design based on LRFD-Seismic

This design focused on the transverse response of the central bent shown in Fig. 9. The mass used to determine displacement demand corresponds to the tributary dead load that the bent supports. No design was reported for the external bents or abutments.

The design strategy was to design the central bent for full ductile response, with plastic hinges forming at the ends of the columns only. This bent has three reinforced concrete circular columns of diameter D = 1.05 m, height H = 6.80 m, spaced 5.18 m from center to center. The cap-beam has a rectangular section of 1.37 m in height and width of 1.21 m. The columns are supported on rigid pile caps. The cap-beam, columns and pile-caps are monolithically connected.

Guess of longitudinal rebar configuration

Design began assuming that the columns could work with 18D25 longitudinal bars and D16 hoops spaced 90 mm. The amount of reinforcement complies with the min requirements of the AASHTO LRFD seismic guide.

Section analysis

A moment-curvature analysis was conducted to determine the yield moment, M_y, yield curvature, ϕ_y, and ultimate curvature, ϕ_u, for the three columns, using expected material properties. These analyses accounted for different axial loads in each column as a result of the combination of the weight of the superstructure and seismicity induced axial forces.

The moment-curvature analysis was performed using XTRACT (http://www.imbsen.com/xtract.htm). This program uses the stress-strain models proposed by Mander et al (1988). The ultimate curvature was reached at a steel tension strain of 0.06. A summary of the results of these analyses is presented in Table 4. The axial load in the columns was computed as if the bent was pushed from left to right.

Table 4 – Moment curvature analysis results for bent in bridge MO-1

Column:	Left	Center	Right
M_y	2226.15	2470.50	2685.15
ϕ_y	0.0044	0.0043	0.0044
ϕ_u	0.0754	0.0787	0.0768

A cracked section stiffness, K_{cr}, and yield displacement, Δ_y, were computed for the bent using the results of moment-curvature analysis. These computations assumed a pinned connection between the columns and pile-caps. A yield displacement of 69 mm was computed using Eq. 7, where H is the free height of the bent.

$$K_{cr} = 3\frac{M_y / \phi_y}{H^3} \qquad \text{(Eq. 7)}$$

$$\Delta_y = \frac{M_p / H}{K_{cr}} \qquad \text{(Eq. 8)}$$

Displacement Demand

Displacement demand, $\Delta_{D,}$ was computed using the natural period of vibration of the bent and the design spectra (Fig. 10). The assessment of the fundamental period was based on lateral stiffness and a mass that corresponds to the tributary dead load on the bent as given by Eq. 9. The dead load is W_D = 6480 kN. The period was estimated as 1.28s and the displacement demand was 79 mm. The ductility demand, computed as the ratio between the Δ_D and the Δ_y, did not exceeded 1.2 for any column. According to the LRFD Seismic Guide, this value must be less than six, for a life safety design.

$$T = 2\pi\sqrt{\frac{W_D}{g \cdot K_{cr}}} \qquad \text{(Eq. 9)}$$

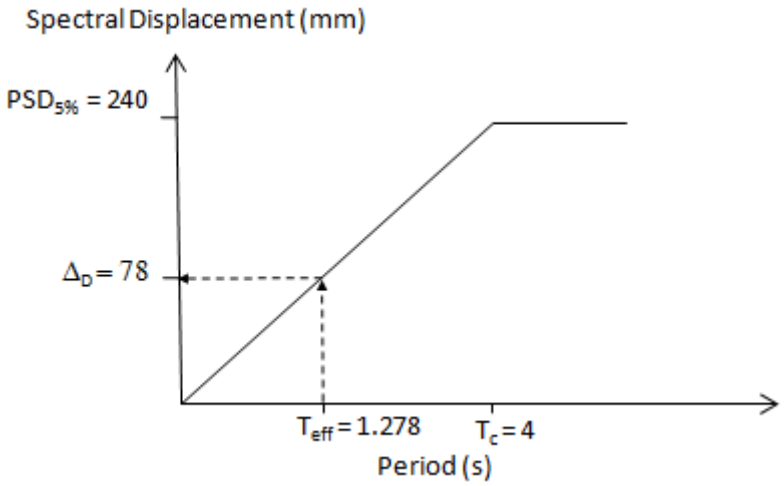

Figure 10 – Determination of displacement demand for LRFD Seismic design of bridge MO-1

Displacement Capacity check

The displacement capacity, $\Delta_{C,}$ of the bent was determined using the plastic hinge method, using Eq. 10. In this equation, Δ_P is the plastic displacement given by Eq. 11, where L_p is the plastic hinge length. A pined connection was assumed between the columns and pile caps. This computation resulted in a displacement capacity of 430 mm for the bent. This is 5.46 times grater than displacement demand; therefore the amount of assumed reinforcement was considered appropriate. This is clearly not an optimal design; however, AASHTO does not require that the design be refined. A ultimate ductility capacity of 6.24 was computed as the ratio of Δ_C and Δ_y. According to the design specification this value qualifies this structure as fully ductile.

$$\Delta_D = \Delta_P + \Delta_y \qquad \text{(Eq. 10)}$$

$$\Delta_P = (\phi_u - \phi_y) L_p H \qquad \text{(Eq. 11)}$$

Shear Design

The design/assessment of the columns was finished by checking the shear demand versus the shear capacity of the sections. Shear demand, $V_{D,}$ was computed using the over-strength moment capacity of the columns, with Eq.12, where H_s is the shear height and 1.2 is the overstregth factor. In this design, H_s was taken equal to the height of the column assuming there is a pinned connection between column and pile-cap. This is not appropriate since the top and bottom sections of the columns are detailed to develop plastic hinges, therefore the H_s should be taken as H/2 resulting in an increase in V_D.

$$V_D = 1.2\frac{M_y}{H_s} \qquad \text{(Eq. 12)}$$

The shear capacity, $V_{n,}$ was computed with Eq. 11, adding the contributions of the concrete, V_c, and of the shear reinforcement, V_s, according to the model in the AASHTO LRDF Guide. At the end, a demand-capacity ratio of 0.21 was computed for the critical column, which is conservative.

$$V_n = V_c + V_s \qquad \text{(Eq. 13)}$$

Stability check

According to the LRFD Seismic Guide, if P-Δ effects exceed 25% of the flexural capacity of the columns, an Inelastic Time History Analysis is required to properly account for these effects. Therefore, P-Δ moments were computed with Eq. 12 for all columns, checking that the P-Δ limit was not exceeded.

$$M_{P-\Delta} = P\Delta_D \qquad < 0.25M_y \qquad \text{(Eq. 14)}$$

Design of protected elements

Cap-beam and joints were designed with base on the flexural over strength of columns. The foundation capacity was also checked assuming full continuity between columns and pile-caps. A minimum seat width was computed for the design of the abutments. This calculation was based on the calculated displacement demand.

3.2 Direct Displacement Based Design

In order to obtain results comparable to those that resulted in the application of LRFD Seismic, DDBD is used to perform a stand-alone design of the central pier in the transverse direction.

Design Objective

Under the design earthquake represented by the displacement spectra shown in Fig.7 the central bent must meet one or more of the following limit states: 1) strain in columns equal to or less than the damage-control strains, 2) stability index equal to or less than 30% and, 3) superstructure displacement equal to or less than its yield displacement. Calculation of these three will follow below.

Assessment of Target Displacement

The determination of a target displacement for the bent requires the assessment of the displacements that will cause the bent to reach the performance limits specified in the design objective.

1. The damage-control limit state sets the limit beyond which damage cannot be economically repaired (Kowalsky, 2000). This limit is characterized by failure of the shear confinement. The damage-control displacement Δ_{DC} of the bent is determined with the plastic hinge method, with Eq. 15, assuming double bending in the columns. In Eq. 16, Δ_y is the yield displacement given by Eq. 16, which is derived from the moment-area method. ϕ_{dc} and

ϕ_y are the damage-control and yield curvatures, L_p is the plastic hinge length given by Eq. 17 (Priestley et al, 2007), H is the height of the columns and L_{sp} is the strain penetration length given in Eq. 18 (Priestley et al, 2007) in terms of the effective yield strength of the longitudinal reinforcement f_{ye} and the diameter of the reinforcement, d_{bl}.

$$\Delta_{DC} = \Delta_y + (\phi_{dc} - \phi_y) L_p H \quad \text{(Eq. 15)}$$

$$\Delta_y = \frac{\phi_y (H + 2L_{sp})^2}{6} \quad \text{(Eq. 16)}$$

$$Lp = k\frac{H}{2} + L_{sp} \qquad k = 0.2\left(\frac{f_u}{f_y} - 1\right) \leq 0.07 \quad \text{(Eq. 17)}$$

$$L_{sp} = 0.022 f_y d_{bl} \quad \text{(MPa)} \quad \text{(Eq. 18)}$$

The yield curvature, ϕ_y, is computed with Eq. 19, where D is the diameter of the section and ε_y is the yield strain of the flexural reinforcement. This equation was derived from the results of moment-curvature analysis that shown that ϕ_y depends on the geometry of the section and is insensitive to the level of reinforcement and axial load (Priestley et al, 2007).

$$\phi_y = 2.25\frac{\varepsilon_y}{D} \quad \text{(Eq. 19)}$$

The damage-control curvature ϕ_{dc} is estimated with Eq. 20 and can be controlled by the concrete reaching the damage-control strain, $\varepsilon_{c,dc,}$ in compression or the flexural reinforcement reaching the damage-control strain, $\varepsilon_{s,dc}$, in tension.

$$\phi_{dc} = \min\left[\frac{\varepsilon_{c,dc}}{c}, \frac{\varepsilon_{s,dc}}{D - c}\right] \quad \text{(Eq. 20)}$$

The damage control strain of the confined concrete core is computed with (Eq. 21) with base on the energy balance approach proposed by Mander (1988). In this equation, ε_{su} is strain at maximum stress of steel , f_{yh} is the yield stress of the transverse steel, ρ_v is the transverse reinforcement ratio, f'_{ce} is the expected compressive strength of the unconfined concrete and

f'_{cc} is compressive strength of the confined concrete (Eq. 22). An estimate of the neutral axis depth *c* is given in Eq.23 (Priestley et al, 2007), where A_g is the area of the section and P is the axial load. The damage-control steel strain, $\varepsilon_{s,dc,}$ can be taken as 0.06 (Kowalsky, 2000)

$$\varepsilon_{c,dc} = 0.004 + 1.4\frac{\rho_v f_{yh}\varepsilon_{su}}{f'_{cc`}} \qquad \text{(Eq. 21)}$$

$$f'_{cc} = f'_{ce}\left(2.254\sqrt{1+\frac{7.94 f_1}{f'_{ce}}} - 2\frac{f_1}{f'_{ce}} - 1.254\right) \quad f_1 = 0.5\rho_v f_{yh} \qquad \text{(Eq. 22)}$$

$$c = 0.2D\left(1+3.25\frac{P}{f'_{ce}A_g}\right) \qquad \text{(Eq. 23)}$$

Complying with the requirements in the LRFD Seismic Guide (Imbsen, 2007) for minimum reinforcement and maximum spacing of reinforcement in column sections, D25 bars are selected for flexural reinforcement and a D13 spiral spaced 150mm is selected for shear and confinement. This results in a volumetric ratio of shear reinforcement, ρ_v = 0.33%.

According to the LRDF Seismic design report, f'_{ce} = 34.45 MPa, ε_y = 0.0022, ε_{su} = 0.06, D = 1.05 m, H = 6.80 m, P = 2461 kN (on each column), f_{yh} = 414 MPA. Therefore, the yield displacement is Δ_y = 43 mm and the damage-control displacement is Δ_{DC} = 146 mm. These values are almost half of the values of yield displacement and displacement capacity computed in the LRFD Seismic design. The reason is that in this design, double bending is considered in the columns, where as single bending was considered in LRFD-Seismic. Considering double bending seems to be appropriate since the columns are detailed to develop plastic hinges at top and bottom.

2. The target ductility to meet the stability criteria is computed with Eq. 24 (Suarez and Kowalsky, 2008b), where C is given in Eq. 25. For θ_s = 0.3, with an axial load P = 2323 kN, an effective mass M_{eff} = 241.5 t and other predefined parameters, C = 0.25 and $\mu_{\theta s}$ = 2.7. Multiplying ductility by yield displacement, the stability-based target displacement is $\Delta_{\theta s}$ = 116 mm.

$$\mu_{\theta s} = 1.256 - 0.127C - 0.766\frac{C - 0.731}{C} \quad \text{(Eq. 24)}$$

$$C = \frac{T_c \Delta_y}{2\pi PSD}\sqrt{\frac{P}{\theta_s M_{eff} H}} \quad \text{(Eq. 25)}$$

3. Assuming that the yield displacement of the superstructure is controlled by yielding of the longitudinal reinforcement in the concrete deck, the yield curvature of the superstructure, ϕ_{ys} , can be estimated with Eq. 26 as a function of the width of the concrete deck w_s and the yield strain of the longitudinal reinforcement in the deck, ε_y,. Then, assuming the superstructure displace transversely like a simply supported beam, at yield, the displacement at any location is given by Eq. 27 (Suarez, 2008). Where x_i is the location of the point of interest, L_s is the length of the superstructure, Δ_1 and Δn are the initial and end abutment displacements. With Δ_1 and Δ_n = 50 mm, L = 94.38, x_i = 47.19 m, w_s = 13.41 m and ε_y = 0.002, the displacement of the superstructure at the location of the bent is $\Delta_{ys,3}$ = 327 mm.

$$\phi_{ys} = 2\frac{\varepsilon_y}{w_s} \quad \text{(Eq. 26)}$$

$$\Delta_{ys,i} = \phi_{ys}\left[\frac{2x_i^{\,4} - 4L_s x_i^{\,3} + 2L_s^{\,3} x_i}{6L_s^{\,2}}\right] + \Delta_1 + \frac{\Delta_n - \Delta_1}{L_s} x_i \quad \text{(Eq. 27)}$$

Since the stability based target displacement is less than the displacements based on other limit states, this displacement becomes the target design displacement.

Equivalent damping

The equivalent damping for reinforced concrete column with ductility μ is given by Eq. 28 (Priestley et al, 2007). For μ_t = 2.70, ξ_{eq} = 13.4%

$$\xi_{eq} = 5 + 44.4\frac{\mu_t - 1}{\pi\mu_t} \qquad \text{(Eq. 28)}$$

Required Strength

The displacement design spectrum gives the maximum displacement demand for single degree of freedom systems with 5% damping. If the spectrum is reduced to the level of damping of the bent, entering the spectrum with the Δ_t ,as displacement demand, results in the effective period T_{eff} required by the structure to meet its target displacement (Fig. 11). This has been synthesized in Eq. 29, where R_ξ is the spectral reduction due to damping and α is 0.25 for near fault sites and 0.5 in other cases (Eurocode,1998).

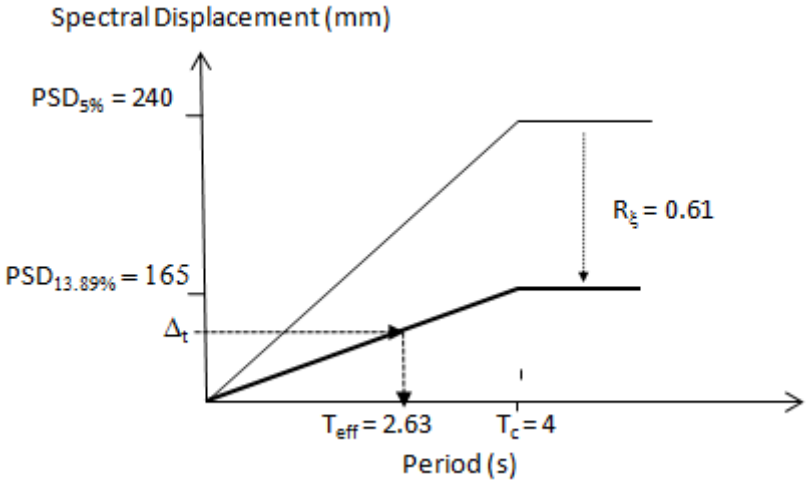

Figure 11- Determination of effective period for DDBD of bridge MO-1

$$T_{eff} = \frac{\Delta_t}{PSD \cdot R_\xi} T_c \qquad R_\xi = \left(\frac{7}{2 + \xi_{eq}}\right)^\alpha \qquad \text{(Eq. 29)}$$

From Eq. 29, R_ξ = 0.69 and T_{eff} = 2.63s. Then, using the dynamic properties of single degree of freedom systems, the required secant stiffness K_s is computed with Eq. 30 and the required strength with Eq. 31. This results in V = 130 kN for each column, which is close to 6% of P.

The design moment assuming double bending in the column is M_E = 130 kN $_x$ 6.40m / 2 = 441 kN-m.

$$K_s = \frac{4\pi^2 M_{eff}}{T_{eff}^{\ 2}} \qquad \text{(Eq. 30)}$$

$$V = K_s \Delta_t \qquad \text{(Eq. 31)}$$

Flexural Design

The flexural reinforcement of the columns is obtained by section analysis under the effects of M_E and axial forces due to gravity loads, using the expected material properties. Since strain limits do not control design, there is no need to consider seismic induced axial forces and gravity induced moments. This is because these actions increase lateral capacity in one external column while reducing capacity by approximately the same amount in the opposite column, with an overall balancing effect. By conducting the section analysis it is found that the section with 1% ratio of flexural reinforcement develops a yield moment M_y = 2467 kN.m, which is greater than M_E (Fig. 10). Therefore, the minimum steel ratio of 1% controls design and all columns are provided with 18D25 bars.

Shear Design

Once the flexural design has been obtained, the next step is to assess the shear capacity of the columns and compare to a shear demand based on the over-strength flexural capacity of the sections. The shear demand cannot be computed from M_E since the section was provided with more strength than required. Instead, the shear demand is computed with Eq. 10 with M_y = 2467 kN.m and H_s = H/2 = 3.4m . This results in V_D = 870.7 kN per column.

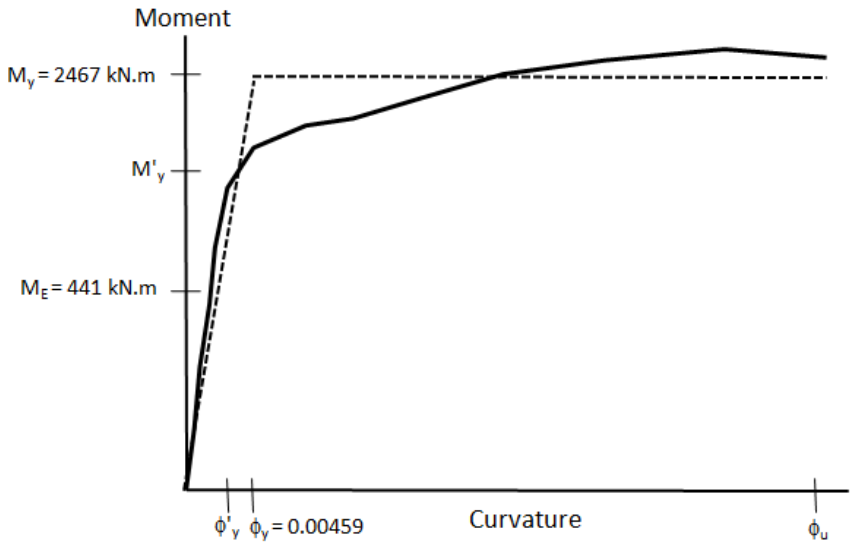

Figure 12 – Moment curvature response of RC column of diameter 1.07 m with 1% steel ratio

The shear strength can be computed using the modified UCSD model (Kowalsky and Priestley, 2000). In this model, the shear capacity, V_n, results from the combination of the strength attributed to the steel truss mechanism, V_s, the strength attributed to the concrete shear mechanism, V_c, and the strength attributed to the axial load, V_p (Eq. 32-35). The factors α β and γ required to compute V_c are given in Fig. 13.

$$V_n = V_s + V_c + V_p \qquad \text{(Eq. 32)}$$

$$V_s = \left(A_v f_y \frac{D'}{s} \right) \qquad \text{(Eq. 33)}$$

$$V_c = \alpha\beta\gamma \sqrt{f'_c}\left(0.8 A_g\right) \qquad \text{(Eq. 34)}$$

$$V_p = P\frac{(D-c)}{2L} \quad \text{for } P > 0 \qquad \text{(Eq. 35)}$$

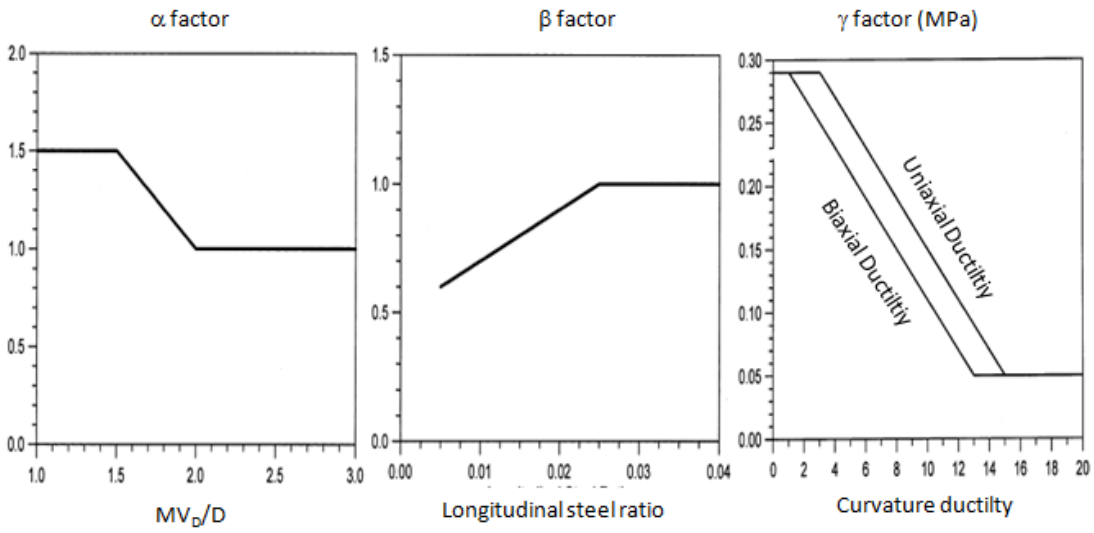

Figure 13 – α β γ factors of UCSD modified model

The application of the modified UCSD model resulted in V_n = 2071 kN, which gives a demand capacity ratio of 0.4. Therefore it is concluded that the selected amount of shear reinforcement is conservative. The design of this bent could be optimized by reducing the diameter of the columns.

Design of protected elements

The design of the foundation and cap-beam is not covered in this example. The design of these elements should follow Capacity Design principles (Priestley et al, 2007).

3.3 Analysis of results and comparison

The two methods resulted in the same design and both required the same effort for this particular bridge. The effort required to obtain an optimum design using the method in the LRFD Seismic Guide relies in the experience of the designer to start with a good guess of the reinforcement in the column. This is not an issue in DDBD since strength is the result of the design process and is not assumed at any point.

Table 5. Design results for MO-1

	D (m)	$\Delta_{c\ (mm)}$	$\Delta_{D\ (mm)}$	ρ %
LRFD-Seismic	1.05	430	79	1%
DDBD	1.05	116	116	1%

The most important design parameters are summarized in Table 5. Since the columns are provided with more strength that required by DDBD, the target displacement of 116 mm it is not likely to be reached during the design earthquake.

Although the bent was design by the two methods for the same level of damage, it is observed in Table 2 that the displacement capacity in LRFD Seismic is much larger that the target displacement in DDBD. The reason is that in the LRFD Seismic design single bending was assumed in the columns in spite of the fact that columns are detailed to develop plastic hinges at the top and bottom.

In the LRFD Seismic design, the stiffness, displacement capacity and shear demand calculations for the central pier assumed that the columns are pinned to the pile caps. However the design drawings show continuity of reinforcement and monolithic construction. This apparent contradiction might be considered conservative from a flexural design perspective. However, as detailed, the bent can develop as much as twice shear demand that was not accounted in the demand capacity checks.

4. Missouri Bridge MO-2

This bridge has three spans with lengths 18.05 m, 18.30 m, 18.05 m with a total length of 54.40 m. The superstructure has preestressed concrete I girders supporting a composite deck. The width of the superstructure is 11.84 m. The abutments are supported on piles and are integral with the superstructure. The intermediate bents have three reinforced concrete columns supported by pile groups. The connection between the superstructure and the bents is pinned. An elevation view of the bridge is presented in Fig. 14.

The seismic hazard at the bridge site is given by the acceleration and displacement design spectra, with 5% damping, shown in Fig. 7. The peak spectral acceleration is 18.54

m/s^2, the peak ground acceleration is 7.36 m/s^2, the corner period of the displacement spectrum is 4 s (FEMA, 2003) and the maximum spectral displacement is 0.85 m. The Seismic Design Category is "D", according to the LRFD Seismic Guide (Imbsen, 2007).

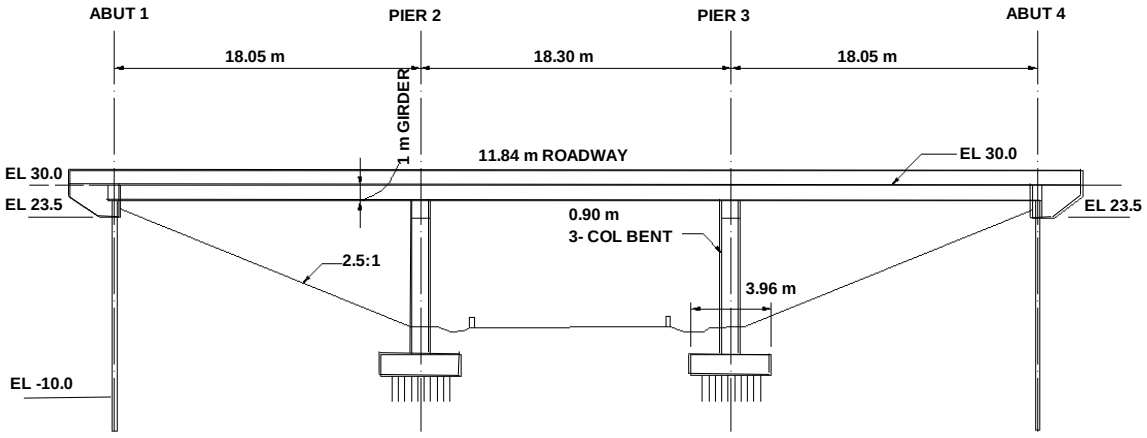

Figure 14 - Elevation view MO-2 Bridge

4.1 Review of design based on LRFD-Seismic

The design focused on the transverse response of the two intermediate bents. The mass used to determine the demand on the bents corresponds to the tributary dead load that the bents support. No design was reported for the abutments.

The bents are identical. A sketch of one of the bents is shown if Fig. 15. Both have three circular columns of 0.91 m in diameter and 8.07 m in height, spaced 4.4m. The cap-beam is 1.00 m in height and 1.07 m in width. The centre of gravity of the superstructure is located 1.93 m on top of the cap-beam. The RC columns are supported on rigid pile caps. The cap-beam, columns and pile-caps are monolithically connected. A stand-alone design was performed for one of the bents. The steps followed during the design are similar to those followed for design of Bridge MO-1.

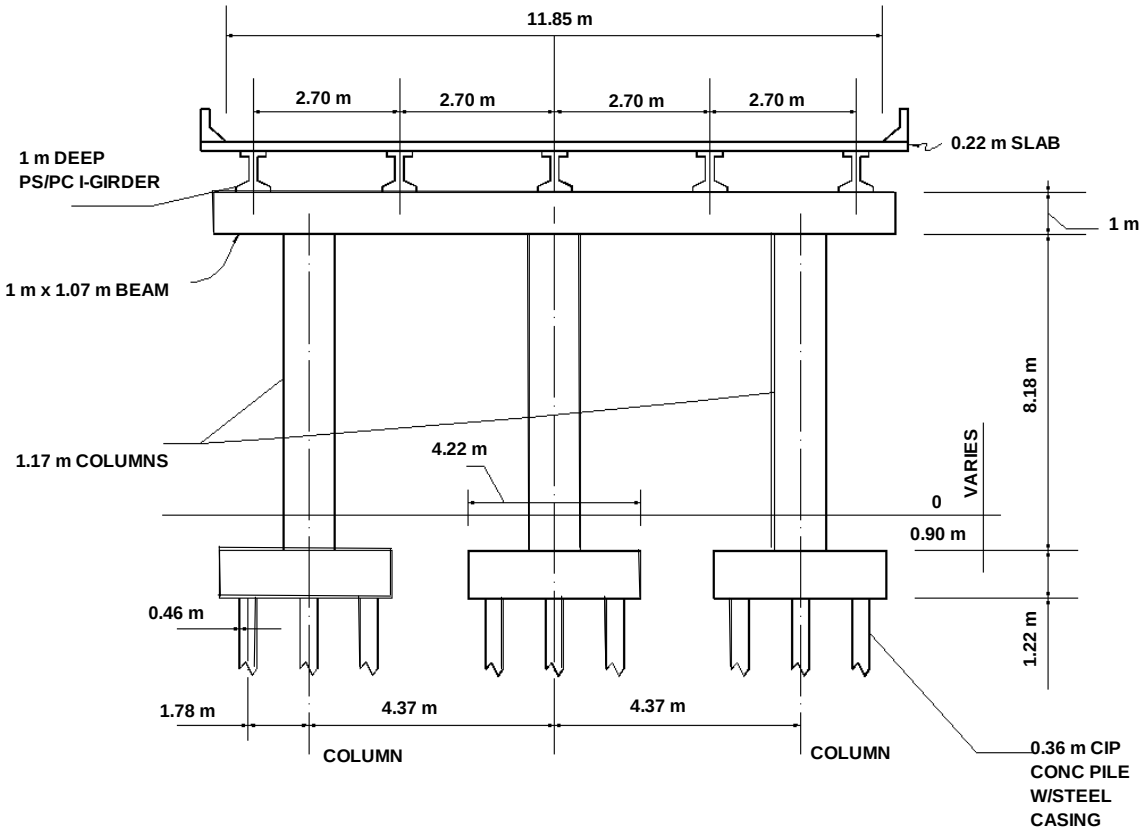

Figure 15. Interior bent in MO-2 Bridge

Guess of longitudinal rebar configuration

The design according to the method in the LRFD Seismic Guide began guessing the reinforcement of the columns. 13D25 bars were selected for flexural reinforcement (1% flexural reinforcement ratio) and D16 hoops spaced 75 mm were selected for confinement and shear reinforcement.

Section analysis

Moment-curvature analyses were conducted with XTRACT, using expected material properties, to determine the yield moment, M_y, yield curvature, ϕ_y and ultimate curvature ϕ_u,

for the three columns, with the results shown in Table 6. The axial load was computed as if the bent was pushed from left to right. The ultimate curvature was reached when the confined concrete reached a compression strain of 0.015

Table 6 – Moment-Curvature analysis results for LRFD Seismic design of bent in Bridge MO-2

Column:	Left	Center	Right
M_y	1117.80	1227.15	1325.70
ϕ_y	0.0053	0.0052	0.0054
ϕ_u	0.1019	0.0833	0.0793

Displacement Demand

Next, cracked section stiffness, $K_{cr,}$ and yield displacement, Δ_y were computed for the bent with Eq. 7 and Eq 8, using the results of the M-ϕ analyses. These computations assumed a pinned connection between the columns and pile-caps. The yield displacement was found to be Δ_y = 139 mm.

For determination of the displacement demand, Δ_D, the natural period of vibration T was calculated with Eq. 9. The seismic weight, W = 3026 kN and corresponds to the tributary dead load acting on the bent. This calculation resulted in T = 1.80 s . Then, using the design spectra and the equal displacement approximation, Δ_D = 370 mm as shown in Fig. 16

The ductility demand μ_D was computed as the ratio of Δ_D and Δ_Y, and did not exceed 2.7. This value must be less than six according to the design specification.

Displacement Capacity check

The displacement capacity, $\Delta_{C,}$ of the bent was computed using the plastic hinge method (Eq. 10-11) with the ultimate curvature values computed previously. A pined connection was assumed between the columns and pile caps and Δ_C was 647 mm. Since this is 1.74 times

grater than Δ_D, the assumed reinforcement was considered satisfactory, although is not optimum.

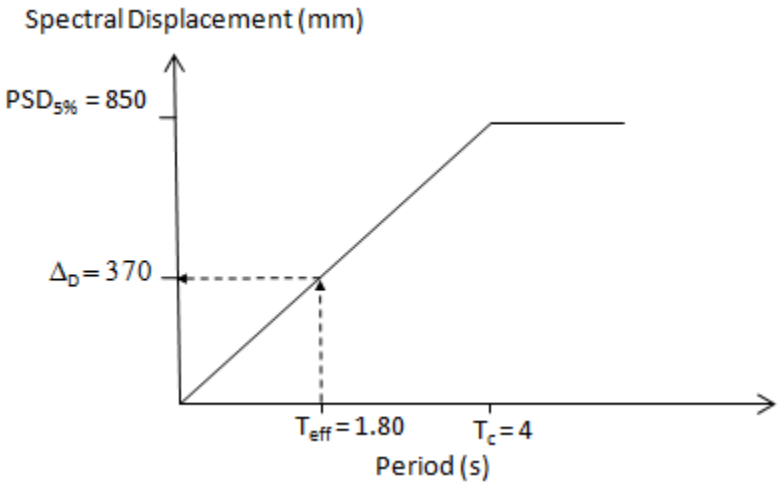

Figure 16 – Determination of displacement demand for bridge MO-2

Shear Design

The design/assessment of the columns was finished by checking the shear demand versus the shear capacity of the column sections. Using the same procedure as for bridge MO-1, the shear demand was computed using the over-strength moment capacity of the columns but assuming pinned connection between column and pile-cap. Since the shear demand-capacity ratio was low, the shear reinforcement was reduced to a D13 spiral spaced 75mm. The final demand-capacity ratio was 0.3 for the critical column.

Stability check

As for Bridge MO-1, P-Δ induced moments were checked to be less than 25% of the flexural capacity of the columns.

Design of protected elements

Cap-beam and joints were designed with base on the flexural over strength of columns. The foundation capacity was also checked assuming full continuity between columns and pile-caps.

4.2 Direct Displacement Based Design

With base on the reported configuration and geometry of the bridge and in order to obtain comparable results, DDBD is used to perform a transverse stand-alone design of one of the intermediate bents.

Design Objective

Under the design earthquake represented by the displacement spectra shown in Fig.7 the intermediate bents must meet one or more of the following limits: 1) strain in columns equal to or less than the damage-control strains, 2) stability index equal to or less than 30% and 3) superstructure displacement is equal to or less than yield displacement. The calculation of target displacement to meet the design limit states is presented next.

Assessment of Target Displacement

The definition of a target displacement for the bent requires the assessment of the displacements that will cause the bent to meet the performance specified in the design objective.

1. The damage-control displacement Δ_{DC} is determined with the plastic hinge method (Eq. 10-11), assuming double bending in the columns.

First, in order to comply with the minimum reinforcement requirements in the LRFD Seismic guide, D25 bars were chosen for the main reinforcement and a D13 spiral spaced 150 mm for shear and confinement.

Then, the yield curvature ϕ_y and damage-control curvatures ϕ_{dc} are estimated with Eq. 19 and Eq. 20. According to the LRDF-Seismic design report, f'_{ce} = 34.45 MPa, ε_y = 0.0022, ε_{su} = 0.06, D = 0.91 m, H = 8.07 m, P = 883 kN (on each column), f_{yh} = 414 MPa. Therefore, the yield displacement is Δ_y = 69 mm and the damage-control target displacement is Δ_{DC} = 252 mm. These displacements are almost half the values obtained in the LRFD Seismic design. The reason is that in DDBD double bending is considered in the columns, where as single bending was considered in LRFD-Seismic. Considering double bending seems to be appropriate since the columns are detailed to develop plastic hinges at top and bottom.

2. The target displacement to meet the stability limit is computed with Eq. 24 and Eq. 25. With M_{eff} = 94.2 t , C = 0.10, $\mu_{\theta s}$ = 5.7 and $\Delta_{\theta s}$ = 395 mm.

3. Assuming the abutment displacement $\Delta_1 = \Delta_4$ = 50 mm and for L=54.4 m, *ws* = 11.83 m and x_2= 18.05 m, εy = 0.002, the yield displacement of superstructure at the location of the bent is $\Delta_{ys,2}$ = 140 mm. (Eq. 26 and Eq. 27).

Since the target displacement for superstructure yielding is the less than the target displacements to meet other limit states, this displacement becomes the target design displacement for the bent. Therefore the target ductility is μ_t = 140 mm / 69 mm = 2.03

Required Strength

For the target ductility, ξ_{eq} = 13.4% (Eq. 3). At the target displacement, Eq. 29 gives T_{eff} = 0.94 s (Fig. 17). With an effective mass of 95.16 t acting of each column, the required lateral strength calculated with Eq. 31 is V = 592 kN per column. For double bending in the columns, V generates a design moment M_E = 1487 kN.m.

Flexural Design

Section analysis was performed to determine the amount of flexural reinforcement required in the columns. It was found that the columns must be provided with 28D25 bars, that is a

2.6% flexural steel ratio, to develop the required strength and at the nominal design strain ε_c = 0.003 (Fig. 18).

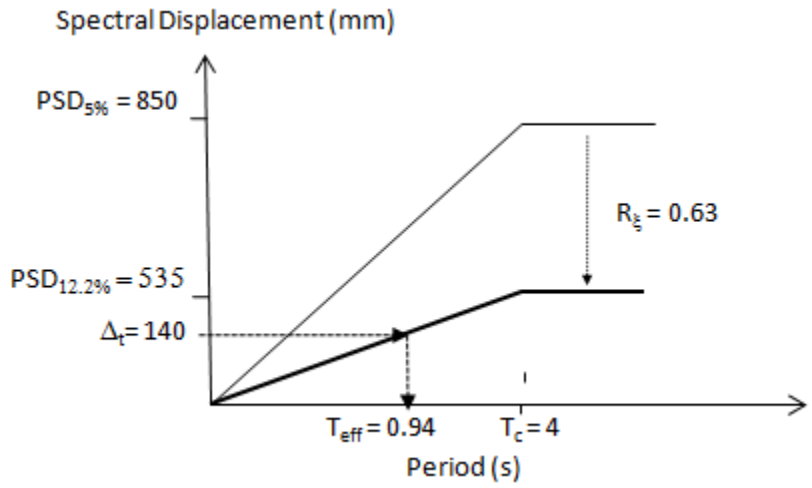

Figure 17 - Effective period for interior bent of bridge MO-2

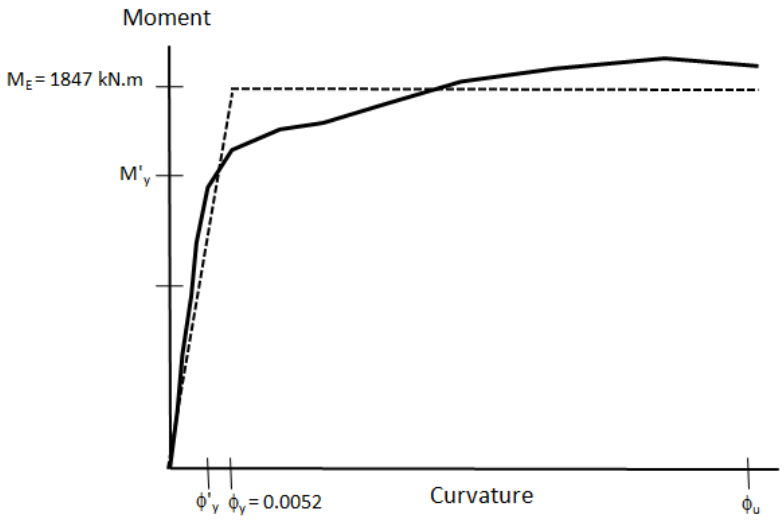

Figure - 18 Moment curvature response of 0.9 diameter RC section with 2.6% reinforcement.

Shear Design

The shear demand in the column was computed with Eq. 12 using a 1.2 overstregth factor with $H_s = H/2 = 4.09$ m. That resulted in $V_D = 437$ kN per column.

The Modified UCSD shear model (Kowalsky and Priestley, 2000) was used to determine the shear capacity of the columns. Using Eq. 32, $V_n = 705$ kN, which results in a demand capacity ratio of 0.62. It is concluded that the selected amount of transverse reinforcement is conservative.

4.3 Analysis of results and comparison

The most important design results are shown in Table. 7. The LRFD-Seismic design is based on the displacement capacity of the bent only and assumes the bent columns are pinned to the foundation. LRFD-Seismic predicts a displacement demand of 370 mm, which can not be actually allowed without accepting damage in the superstructure and or in the integral abutments. If the displacement capacity of the superstructure was accounted for in LRFD then, more reinforcement in the columns would be required to lower the displacement demand. That is the case in DDBD, where the displacement capacity of the superstructure and abutments has controlled design.

Table 7. Design Results for MO-2

	D (m)	$\Delta_{c\ (mm)}$	$\Delta_{D\ (mm)}$	ρ %	ρ_v %	Shear D/C
LRFD-Seismic	0.91	647	370	1%	0.86	0.30
DDBD	0.91	140	140	2.60%	0.43	0.64

The solution obtained by DDBD, although accounts for displacement capacity of the superstructure, is still approximate since the stiffness of the superstructure and abutments was not considered to determine the effective mass acting in the bent. Calculating the effective mass from the dead load carried by the bent has probably lead to a conservative design, since it is reasonable to assume that the system formed by the superstructure and

abutments is stiffer than the bents and the effective mass acting on the bents is, in reality, less than it was considered.

Another observation to the LRFD-Seismic design is that the stiffness, displacement capacity and shear demand calculations for the bent assume that the columns are pinned to the pile caps. However the design drawings show continuity of reinforcement and monolithic construction. This apparent contradiction might be considered conservative from a flexural design perspective. However, as detailed, the bent can develop as much as twice shear demand that was not accounted in the demand capacity checks.

5. Illinois Bridge IL-2

In this trial design, a typical bridge was designed four times varying the height of the columns. The bridge has three spans with lengths of 18.90 m, 23.47 m, 18.90 m and a total length of 61.27 m. The superstructure is continuous with steel girders and a concrete deck. An elevation view is presented in Fig. 19. The total width of the superstructure is 12.80 m. The intermediate bents have four reinforced concrete columns supported on piles, as shown in Fig. 20. The connection between the cap-beam and the superstructure is pinned. The abutments are integral with the superstructure and have a transverse stiffness of 175200 kN/m. The abutments do not contribute any strength in the longitudinal direction

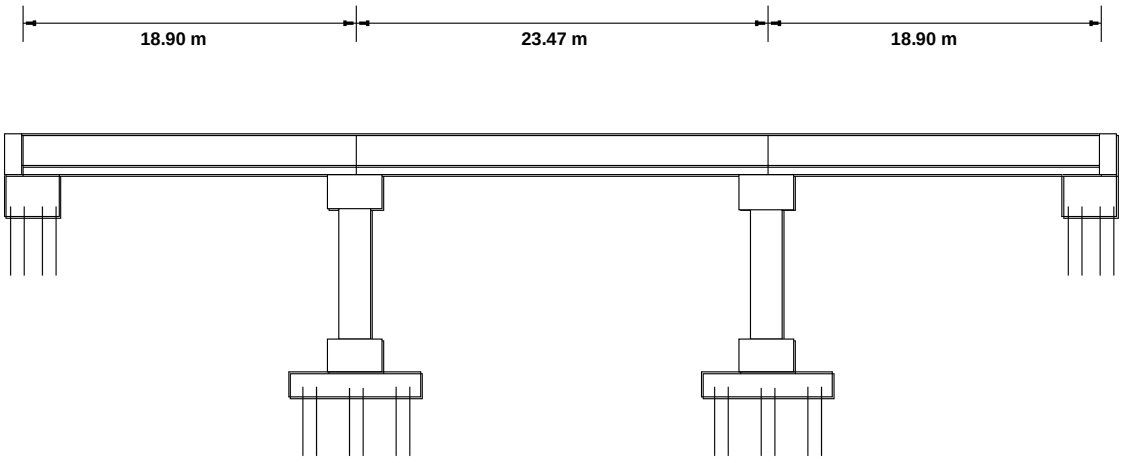

Figure 19. Elevation view of trial design IL-2

The seismic hazard at the bridge site is given by the acceleration and displacement design spectra, with 5% damping, shown in Fig.7 .Where, PSA is 11.06 m/s^2, PGA is 4.42 m/s^2, Tc is 4 s (FEMA, 2003) and PSD is 0.48 m. The Seismic Design Category is "C", according to the LRFD Seismic Guide (Imbsen, 2007).

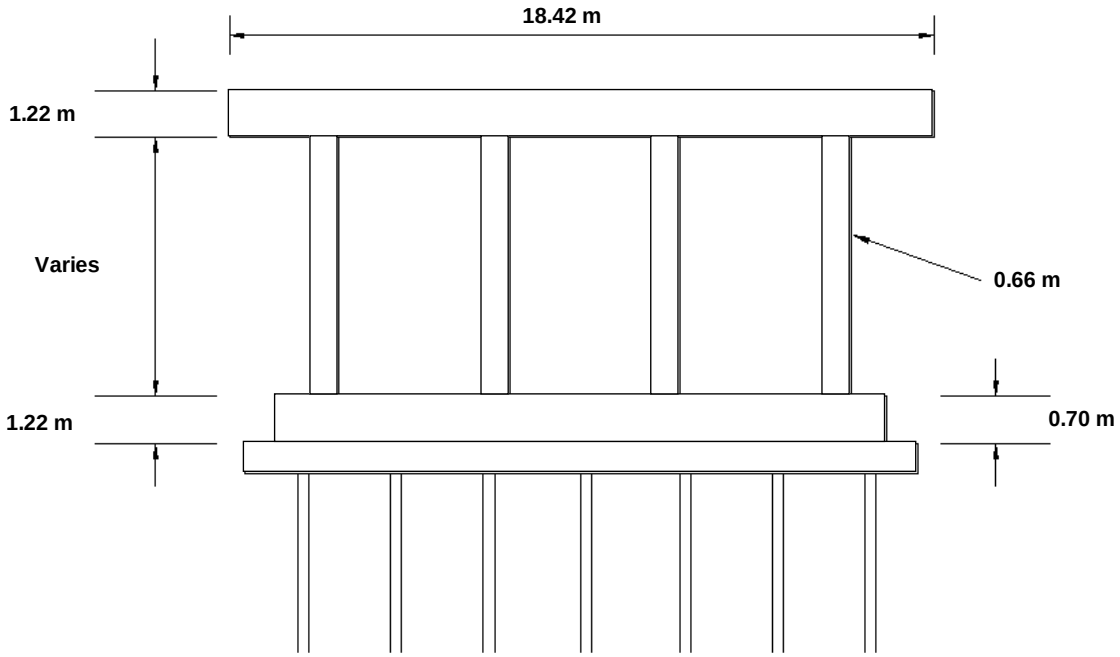

Figure 20. Interior bent trial design IL-02

5.1 Review of design based on LRFD-Seismic

The bridge was designed four times for different column heights: 3.05 m, 4.57 m, 6.10m and 7.62 m. Each design was performed in the longitudinal and transverse directions.

Guess of longitudinal rebar configuration

Design started assuming the amount of longitudinal reinforcement in the 0.66 m diameter reinforced concrete columns. Flexural steel ratios of one, two, three and four percent were tried.

Section analysis

Instead of moment curvature analyses, a cracked to gross inertia ratio was estimated using Fig. 21, in terms of the steel ratio and axial load ratio. Then the stiffness of the bents was computed in transverse and longitudinal direction for columns of different heights and different reinforcement, 16 cases in total.

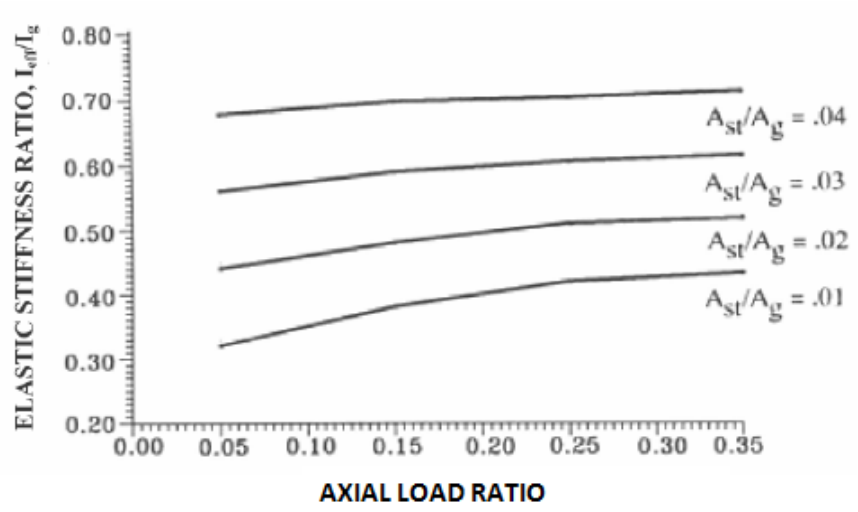

Figure 21 – Cracked to gross inertia ratio for circular RC sections (Imbsen, 2007)

Displacement Demand

The fundamental period of vibration was computed for transverse response using the Uniform Load Method (Imbsen, 2007), for all 16 cases. These analyses accounted for the flexibility of superstructure, abutments and bents.

Then using the displacement spectra with 5% damping, the maximum transverse displacement demand at the location of each bent was evaluated. Similarly, the displacement demand in the longitudinal direction was found for each combination of column length and steel ratio. In the longitudinal demand assessment, the abutments were not considered.

Displacement Capacity check

The displacement capacity of the bents in the transverse and longitudinal directions was computed using the Implicit Method in the LRFD-Seismic Guide. With this procedure Δ_C is computed with Eq. 36, where H_c is the clear height of the columns and Λ is 1 for columns in single bending and 2 for columns in double bending.

$$\Delta_c = 0.003 H_c \left(-2.32 \ln\left(\frac{D}{H_c} \Lambda \right) - 1.22 \right) \geq 0.003 H_c \qquad \text{(m)} \qquad \text{(Eq. 36)}$$

Then, the displacement demand in the orthogonal directions was combined as well as the displacement capacity. For each column length, the appropriate amount of reinforcement was chosen such that displacement capacity slightly exceeded the displacement demand. The table below shows the displacement capacity, displacement demand values and column flexural reinforcement ratio for the designs that satisfied the demand capacity check. It is observed that longitudinal demand controls design.

Table 8. LRFD-Seismic design summary for trial design IL-2

Column Height (m)	Displacement Capacity		Displacement Demand		Design Steel Ratio
	Transverse (mm)	Longitudinal (mm)	Transverse (mm)	Longitudinal (mm)	
3.05	30	71	22	71	4%
4.57	76	149	36	145	2%
6.10	142	240	43	241	1%
7.62	217	339	45	329	1%

5.2 Direct Displacement Based Design

This design is based on the geometry, configuration, materials and section properties as reported in the LRFD Seismic design. Transverse and longitudinal responses are considered.

Design Objective

Under the design earthquake represented by the displacement spectra shown in Fig. 7, the four bridges considered must meet one or more of the following limits: 1) lateral displacement of bents equal to or less than the specified in LRFD seismic for SDC "C" (moderate plastic action), 2) stability index equal to or less than 30%, 3) superstructure displacement equal to or less than its yield displacement, 4) displacement of the abutments limited to 100mm to avoid excessive damage.

Target displacement

1. According to LRFD-Seismic design report, the reinforced concrete in the intermediate bents has the following properties: f'_e = 31 MPA, f_{ye} = 454 MPA, ε_y = 454/200000 = 0.0022. Choosing d_{bl} = 22 mm to satisfy minimum reinforcement requirement to LRFD-Seismic, the yield displacement Δ_y of the bent is computed with Eq. 16 and Eq. 37. for the transverse and longitudinal directions respectively. These equations assume double bending of the columns in the transverse direction and single bending in the longitudinal direction. H is taken as the clear column height in the transverse direction while in the longitudinal direction is the clear length plus the height of the cap-beam, which is 1.2m. The estimated yield displacement for the different column heights are shown in Table 9.

$$\Delta_y = \frac{\phi_y (H + L_{sp})^2}{3} \qquad \text{(Eq. 37)}$$

The damage-based target displacement Δ_t for the bent is determined with the implicit formula given in LRFD-Seismic for bridges in SDC "C". The use of Eq. 36 implies moderate plastic action that may require closure or limited usage. The resulting target displacements for bents of different heights are given in Table 9.

2. The stability-based target displacement is calculated with Eq. 24 and Eq. 25, with results shown in Tables 9. In these calculations P = 593 kN and M_{eff} = 61.3 t for column.

3. The yield displacement of the superstructure is computed with Eq. 26 and Eq. 27 as shown in Table 9. In this calculation, w_s = 18.4 m, x_i = 18.90 m, L = 61.28 m, ε_y = 0.002 and the displacement of the abutments were 100 mm.

The displacement that satisfies all performance limits is the design target displacement for the bent. This value is shown at the end of Table 9.

Table 9. Displacement capacity of interior bents. Trial design IL-2

Column Height (m)	Δ_y (mm)		Damage-Based Δc (mm)		P–Δ Δc (mm)		Superstructure Δc (mm)		Target Δ (mm)	
	Transv.	Long.	Transv.	Long.	Transv.	Long.	Transv.	Long.	Transv.	Long.
3.05	11	46	30	71	145	207	185	-	30	71
4.57	27	86	76	149	197	260	185	-	76	149
6.10	48	137	142	239	243	310	185	-	142	239
7.62	75	200	217	339	288	358	185	-	185	339

Strength Distribution.

During an earthquake, inertia forces that developed due to the mass of the superstructure can reach the foundation soil through the abutments or through the piers. As it will be explained later, the calculation of the combined damping for the bridge requires knowledge of the distribution of strength in the bridge. Therefore, it will be assumed that in the transverse direction, each abutment takes 45% of the total base shear and that each bent takes 5%. This assumption will be verified later. In the longitudinal direction, the abutments do not contribute with strength; therefore each bent takes 50% of the total shear.

Design in Transverse Direction

These designs account for the interaction among bents, superstructure and abutments, therefore each bent cannot be longer treated as a single degree of freedom system. Since the bridge is symmetrical, with strong abutments, the displacement pattern is not known and DDBD will be applied using the First Mode Shape algorithm (FMS) described in Section 2.2.

The design of the bridge with columns of height equal to 7.62 m is described next. The design of the bridges with other column heights follows the same approach.

Step 1: Target displacement profile. For the bridge with columns of 7.62 m, the target displacement profile is defined with the two bents displacing their target displacement, $\Delta_2 = \Delta_3 = 185$ mm (Table 9), and the abutments displacing their target displacement, $\Delta_1 = \Delta_4 = 100$ mm.

Step 2: Equivalent single degree of freedom system. Using Eq. 1 and Eq. 2 a generalized displacement $\Delta_{sys} = 170$ mm and an effective mass $M_{eff} = 645.3\ t$ are calculated for the bridge (See Section 2.1). One third of the mass of the columns was included in these calculations.

Next, the equivalent damping is determined as a combination of bent damping, superstructure damping and abutment damping. The combination is done in terms of the work done by each element as shown in Eq. 38 (Priestley et al, 2007). Where, ξ_a is the abutment damping and ξ_s is the superstructure damping, both taken as 5% in this design, ξ_i is the equivalent damping for the bents, calculated with Eq. 3 as a function of their ductility, and v_i is the fraction of base shear taken by each element and assumed at the beginning of the design.

$$\xi_{sys} = \frac{\Delta_a v_a \xi_a + (\Delta_{sys} - \Delta_a) v_a \xi_s + \sum_{i=1}^{i=\#bents} \Delta_i v_i \xi_i}{\Delta_a v_a + (\Delta_{sys} - \Delta_a) v_a + \sum_{i=1}^{i=\#bents} \Delta_i v_i} \qquad \text{(Eq. 38)}$$

If the yield displacement of these bents is 75 mm, then $\mu = 185\text{mm} / 75\text{ mm} = 2.46$ and $\xi_2 = \xi_3 = 13.38\%$. Finally ξ_{sys} is 5.9%.

Step 3: Required strength. For the level of damping in the bridge, the spectral reduction factor $R_\xi = 0.80$, the effective period is $T_{eff} = 1.52$ s (Eq. 29) and the required strength is $V = 1894$ kN (Eq. 31).

Step 4. Checking the proposed force distribution. Inertial forces consistent with the diplacement shape assumed before can be computed with Eq. 39. If these forces are applied to an elastic model of the bridge, the outcome will be a best estimate of the first inelastic shape. This static analysis will also provide a best estimate of the base shear that is being taken by the abutments.

$$F_i = \frac{m_i \Delta_i}{\sum_1^n m_i \Delta_i} V \qquad \text{(Eq. 39)}$$

For a simple bridge as the one that is being designed, a two dimensional model of the bridge, such as the one shown in Fig. 22 is appropriate. The superstructure is modeled with elastic beam elements of inertia I = 64.5 m4 and elastic modulus E = 21532 MPa. The abutments are modeled as springs with stiffness K = 175200 kN/m. These values were also used for the LRFD Seismic design. The bents are modeled also as springs but with stiffness secant to design displacement. According to the strength distribution assumed before, each bent takes 5% of V. The stiffness of the bents given by Eq. 40 is 511 kN/m.

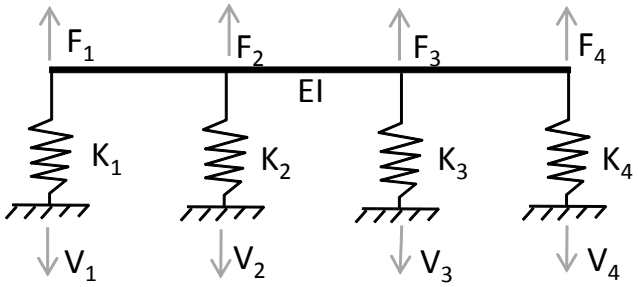

Figure 22- 2D bridge model for static analysis

$$K_{effi} = \frac{V_i}{\Delta_i} \qquad \text{(Eq. 40)}$$

$$v_a = \frac{\Delta_1 K_1 + \Delta_n K_n}{V} \qquad \text{(Eq. 41)}$$

The elastic analysis results in displacements of 4 mm for the abutments and 7 mm for the bents. By Eq. 41, it is also found that the force taken by the abutments is 99.8% of the total shear. This is because the super and the abutments are much stiffer than the bents at this level of displacement. At this point it is concluded that, at the target displacement level, the abutments and the superstructure will attract (due to their high stiffness) most of the seismic forces in the transverse direction. Therefore, the strength demand on the bents will be small and no further iteration is required since it is anticipated that longitudinal direction will control design.

DDBD was applied in the same way for the bridges with other column heights, obtaining the same results.

Design in the longitudinal direction

All strength in this direction is provided by the bents. Since the superstructure is continuous and with a high axial stiffness, it is reasonable to assume that both bents will displace the same amount. Since the bents are equal, and will be provided with the same reinforcement, they will develop the same strength, equal to 50% of the total base shear.

Step 1. Target displacement profile. Since no displacement limit is given for the abutments, the target displacement of the bridge in this direction is given by the damage control displacement of the bents. Therefore, for the bridge with columns of 7.62 m, Δ_t = 339 mm (Table. 9).

Step 2. Equivalent single degree of freedom. Since the bents and abutments displace the same amount $\Delta_{sys} = \Delta_t$ = 339 mm, and the effective mass M_{eff} is the total mass of the bridge, equal to 679.8 t. The equivalent damping comes entirely from the columns, so with Eq. 3, ξ_{eq} is 10.8%.

Step 3. Required Strength. For the level of damping in the bridge, $R_\xi = 0.66$, the effective period is $T_{eff} = 3.82$ s (Eq. 29). Finally the required strength in the system is V = 624.0 kN (Eq. 31), which generate a moment demand in the base of the columns $M_E = 687$ kN.m.

Step 4. Pdelta check. With an axial load acting on the top of the column P = 593 kN, the P-Δ moment is 201 kN and the stability index is θs = 28.7%. If the stability index is less than 30% but more than 8%, it is recommended to increase the flexural strength of the element by one half of the P-Δ induced moments to counteract its effects (Priestley et al, 2007). Therefore the final seismic design moment is $M_E = 802$ kN.

Step 5. Flexural Design. . Moment-curvature analysis is performed to provide the required strength at a level of curvature compatible with the ductility demand in the element. In this example, since the ductility demand is low, design is simplified and reinforcement is designed for a concrete compression strain $\varepsilon_c = 0.003$ (i.e. nominal strength). For the bent with H = 7.62 m, flexural design then results in a steel ratio of 1.8% provided as 20D20 bars. M_E must be used in combination with the axial force in the base of the column, P = 654 kN, to design the flexural reinforcement.

The results of flexural design of the columns are presented in the Table 10. The shear capacity is not checked for this trial design.

Table 10. DDBD results for trial design IL-2

Equivalent Damping ξ_{eq} (%)		Required Strength V (kN)		Seismic Moment M_s (kN.m)		Combined Actions		Steel Ratio ρ (%)
Transv.	Long.	Transv.	Long.	Transv.	Long.	P (kN)	M_s (kN.m	
5	9.8	0	1593	0	1689	617.74	1689	> 4
5	11	0	689	0	994.78	630.04	994.78	2.6
5	11	0	430	0	784.95	642.26	784.95	2.0
5	11	0	312.01	0	687.97	654.56	687.97	1.8

5.3 Analysis and Comparison

This example confirms the observation made before about the method is the LRFD Seismic guide. An optimum design, in which displacement demand equals displacement capacity, can only be achieved iteratively, assuming different levels of reinforcement. Therefore, generally DDBD will require less effort in its application than the method in the LRFD Seismic guide.

Table 11. Comparison of design results for trial design IL-2

Column Height (m)	LRFD-Seismic		DDBD	
	Δ_D (mm)	Steel Ratio	Δ_t (mm)	Steel Ratio
3.05	71	4%	71	4.3
4.57	145	2%	149	2.6
6.10	241	1%	239	2.0
7.62	329	1%	339	1.8

For all column heights considered in this trial design, DDBD requires higher strengths than LRFD-Seismic, as shown in Table 11. The reason for this is that in the LRFR-Seismic design, the amount of reinforcement in the section was related to the stiffness of the section using Fig. 2, without moment-curvature analysis. Section analysis performed during DDBD suggested that the ratios between cracked and gross inertia used in LRFD-Seismic were high and therefore the stiffness of the piers was over-predicted and displacement demand was under-predicted. That explains why less reinforcement is needed in LRFD-Seismic, even though the target displacement in DDBD is similar to the displacement demand in LRFD-Seismic.

6. TYPICAL CALIFORNIA BRIDGE. CA-1

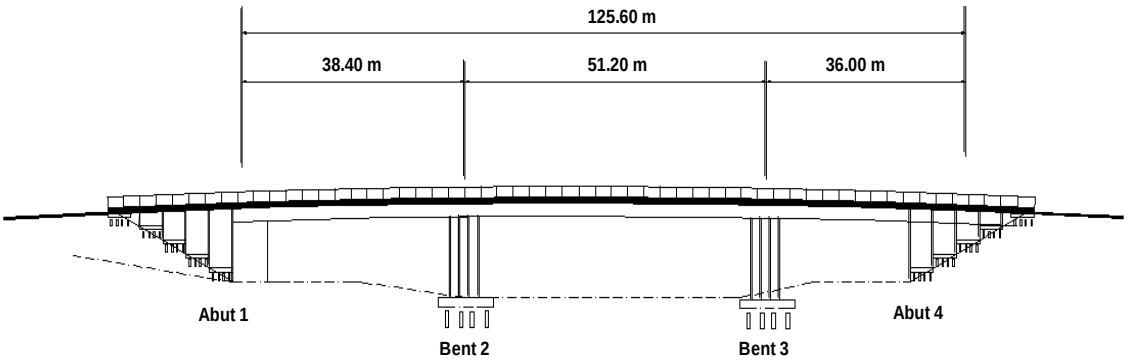

Figure 23 - Elevation view trial design CA-1

This bridge has three spans of 38.41 m, 51.21 m and 35.98 m respectively and a total length of 125.60 m. The superstructure is a continuous prestressed reinforced concrete box girder. The two bents are skewed 20^{o} and have two 1.83 m diameter columns supported on piles. Column height varies from 13.40 m at bent two to 14.30 m at bent three. The columns are pinned at the bottom and fixed to an integral bent in the superstructure. The abutments are seat type with brake-off walls and therefore are not considered part of the earthquake resisting system. An elevation view of the bridge is presented in Fig. 23 and the superstructure section and substructure configuration are shown in Fig. 24

The seismic hazard at the bridge site is given by the acceleration and displacement design spectra, with 5% damping, shown in Fig. 7. The PSA is 14.91 m/s^2, the PGA is 5.88 m/s^2. The corner period of the displacement spectra is 8 s (FEMA, 2003), and the maximum spectral displacement is 1.92 m. The Seismic Design Category is “D”.

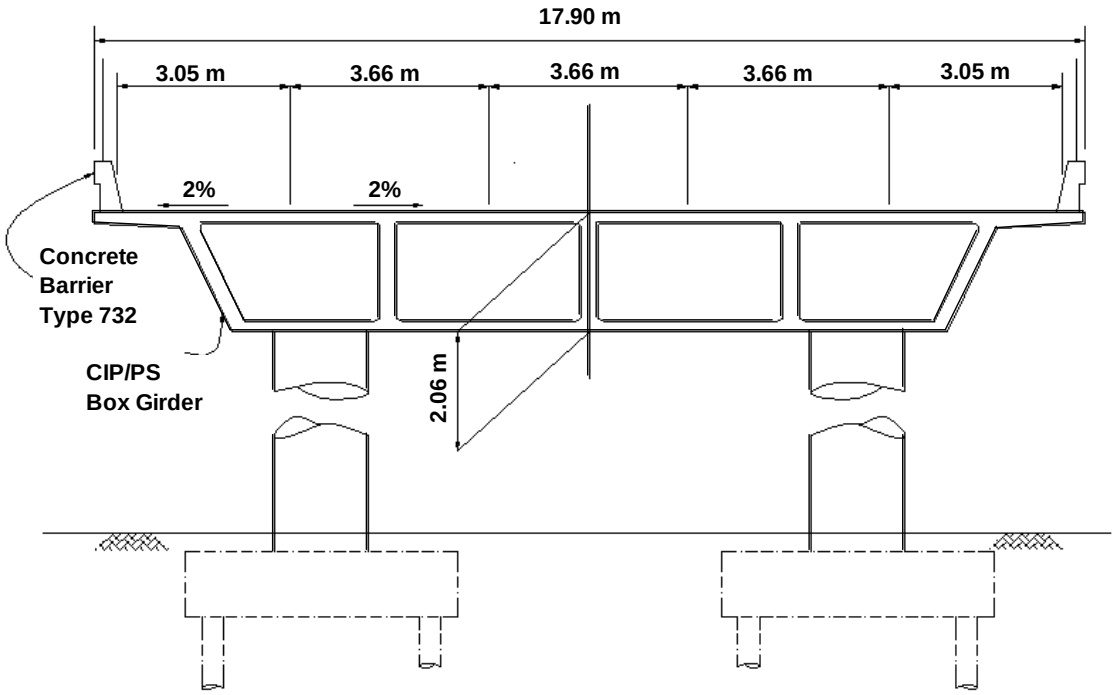

Figure 24 - Superstructure section and interior bent, trial design CA-1

6.1 Review of design based on LRFD-Seismic

Design in transverse direction is carried for each bent independently (stand-alone design). In the longitudinal direction, the bents were considered linked by the superstructure. In both cases any participation of the abutments was ignored.

Guess of longitudinal rebar configuration

Design began assuming the columns are reinforced with 26D44 bars and a D25 spiral spaced 125 mm. Next, it was checked that the bridge complies with the balanced mass and stiffness criteria given by LRFD-Seismic

Preliminary demand capacity assessment

Moment-curvature analysis was performed to determine response of the 1.83 m diameter RC section with 1.5% reinforcement. The yield moment, M_y = 18640 kN.m, yield curvature, ϕ_y = 0.000256, ultimate curvature, ϕ_u = 0.003434, and cracked inertia, I_{cr} = 0.21. The ultimate curvature was reached when the confined concrete reached a strain 0.0185 in compression.

Then the plastic hinge method (Eq. 10-11) was used to estimate the yield displacement, Δ_y, and displacement capacity, Δ_c, of each bent. For bent 2, Δ_y = 184 mm and Δ_c = 908 mm and for bent 3, Δ_y = 210 mm and Δ_c = 1026 mm. These values are valid for transverse and longitudinal response. The ductility capacity of these bents is close to 5 exceeds the minimum 3 specified in LRFD-Seismic.

Displacement Demand

Next, displacement demand was computed in the transverse direction of the bridge. Each bent was treated separately; the mass that was used corresponded to the weight supported by each bent. These calculations resulted in displacement demands of 478 mm and 524 mm for bents 2 and 3 respectively. The ductility demand is 2.6 and 2.5 for bents 2 and 3 respectively. These values are significantly less than the ductility capacity and less than maximum ductility allowed by LRFD-Seismic. Therefore, it was concluded that the sections satisfied the minimum design requirements and design was continued with more detailed analyses.

Displacement Capacity check

Pushover analyses were then used to get a best estimate of the displacement capacity and stiffness of the bents in the transverse and longitudinal directions of the bridge. This time accounting for the flexibility of the integral cap-beam and considering that the columns are partially embedded in soil. In the transverse direction, Δ_c = 882 mm and Δ_D= 564 mm for bent 2. For bent 3, Δ_C = 988 mm and Δ_D= 601 mm. A P-Δ check showed that the stability index was close to 25%. Since 25% is the limit allowed in LRFD-Seismic, it was concluded

that the assumed reinforcement was appropriate and that design was controlled by P-Δ effects rather than by displacement capacity.

The pushover analysis in the longitudinal direction considered all columns in the bridge lumped together and all the mass of the bridge. First, the strength and stiffness of the abutments were considered. A pushover analysis was conducted to determine the stiffness. Then a displacement demand equal to 376 mm was estimated. Next, following Caltrans recommendations (Caltrans, 2006), it was decided that since the ductility demand in the abutments is higher than 4, the model is insensitive to abutment stiffness and also that the contribution of the abutments is insignificant to the longitudinal performance of the structure.

The pushover was then repeated without the abutments, Δ_y = 210 mm and Δc = 947 mm for bent two. Δ_y = 229 mm and Δ_C = 1063 mm for bent three. The displacement demand was 599 mm for the two bents since the superstructure acts as a rigid link between them. The ductility demand is 3.11 for bent two and 2.76 for bent three. With base on the displacement demand, P-Δ moments are 24% of the flexural capacity of the columns, which is in the limit allowed by LRFD-seismic. Therefore, the longitudinal design was also controlled by P-Δ effects.

The skew in the bents was ignored in design. Demand and capacity in the two directions were not combined, each direction was treated separately. As part of the design checks, it was verified that the bents are provided with a lateral strength of at least 10% of the supported weight, per LRFD-Seismic.

Shear design

Finally, a shear demand-capacity check was performed for the columns. The shear demand was based on the over-strength flexural capacity of the columns, the integral cap-beams were designed and seismic forces developed in the superstructure due to longitudinal displacement of the bridge were determined.

6.3 Direct Displacement Based Design

This design is based on the geometry, configuration, materials and section properties as reported in the LRFD-Seismic Design. Transverse and longitudinal responses are considered.

Design Objective

Under the design earthquake represented by the displacement spectra shown in Fig. 7, the bridge must meet one or more of the following limits: 1) damage control strains in the columns, 2) stability index less than 30%

Assessment of Target Displacement

According to LRFD-Seismic design report, the reinforced concrete in the bents has the following properties: f'_{ce} = 36 MPA, f_{ye} = 455 MPa, ε_y = 455/200000 = 0.0022, ε_{su} = 0.1, f_{yh} = 414 MPA. Complying with min reinforcement requirements, D44 longitudinal bars and a D25 spiral spaced 130 mm are chosen for the columns.

1. The damage control displacement Δ_{DC} of the bents is determined with the plastic hinge method (Eq. 15), assuming single bending in the columns. These calculations are valid for the two directions of design. The yield displacement Δ_y (Eq. 37) and damage-control displacement Δ_{DC} are shown in Table 12. The damage control compression strain for concrete is $\varepsilon_{c,dc}$ = 0.018 and controls the determination of $\Delta_{DC.}$

2. The stability based target displacement is computed with Eq. 24 and Eq.25. The results are shown in Table 12. It is observed in this table that stability-based displacement controls design and becomes target design displacement.

Table 12 - Target displacements Trial design CA-1

	H (m)	D (m)	P (kN)	Δ_y (m)	Damage Control Δ_C (m)	P-Δ Δ_C (m)
Bent 2	13.4	1.83	6714	178	656	640
Bent 3	14.3	1.83	6557	202	737	650

Strength Distribution.

The application of DDBD results in the total strength V, required in each design direction, to meet performance specified in the design objective. The strength of seat-type abutments V_a is generally known or can be estimated before design. The contribution of the abutments to the total strength of the bridge, v_a, is given by Eq. 42 Therefore, satisfying equilibrium of forces, the contribution of the piers, v_p, to the strength of the bridge is given by Eq. 43

$$v_a = \frac{V_a}{V} \qquad \text{(Eq. 42)}$$

$$v_p = 1 - v_a \qquad \text{(Eq. 43)}$$

Since RC columns with same reinforcement ratio have similar ratios of cracked to gross stiffness (Figure 21), Eq. 44 gives the ratio of total strength v_i taken by bent i, with n columns of diameter D_i, shear height Hs_i and ductility μ_i, required to satisfy force equilibrium. In this trial design, since the column are pinned at the base, $H_s = H$.

$$v_i = (1 - v_a)\frac{\frac{n_i \mu_i D_i^{\,3}}{H_{si}}}{\sum \frac{n_i \mu_i D_i^{\,3}}{H_{si}}} \qquad \mu_i \le 1 \qquad \text{(Eq. 44)}$$

Recognizing that even if the abutments are not designed as part of the earthquake resisting system they can have some effect in the performance of the bridge. As a starting point, it is assumed that the abutments will take 10% of the total seismic forces in the transverse and longitudinal directions. Therefore $v_a = 0.1$ and $v_2 = 0.46$ and $v_3 = 0.44$ with Eq. 44

Design in Transverse Direction

Design in the transverse direction will account for interaction between the superstructure, bents and abutments. The superstructure section shown in Fig. 24 has an out-of-plane inertia I = 222 m4, an elastic modulus E_s = 26500 MPa, and a weight W_s = 260 kN/m.

The abutments are assumed to have an elasto-plastic response. The transverse strength or yield force for the abutments is computed considering there are sacrificial shear keys that will brake during the design earthquake. The residual strength in the abutment comes from friction between the superstructure and the abutment. Assuming a friction coefficient of 0.2, with a normal force equal to the tributary superstructure weight carried by the abutments, the transverse strength of the abutments is 1300 kN. It is assumed that the yield displacement is 50mm.

Step 1. Target displacement profile. Since the bridge is regular and the superstructure is stiff, the abutments are not expected to restrain the displacement of the super-structure and a rigid body displacement patter will be used (Section 2.2) (Suarez and Kowalsky, 2008a). All substructures displace the same amount and the amplitude of the displacement profile is given by the bent 2, which is the one with the least target displacement (Table 12).

Step 2. Equivalent single degree of freedom system. With then bents and abutments displacing the same amount is the transverse direction Eq. 1 and Eq. 2 reduce to Eq. 45 and Eq. 46. The generalized displacement equals the target design displacement of bent 2 so Δ_{sys} = 640 mm. Also the effective mass of the bridge is the sum of the total mass of the superstructure, integral bent-caps and one third of the weight of the columns, M_{eff} = 3808 t.

$$\Delta_{sys} = \Delta_T \qquad \text{(Eq. 45)}$$

$$M_{eff} = \sum_{i=1}^{i=n} M_i \qquad \text{(Eq. 46)}$$

Step 3. Equivalent damping. The ductility at target displacement level is μ_1 = 12.80, μ_2 = 3.59, μ_3 = 3.16, μ_4 = 12.80. These values are obtained as ratios between Δ_{sys} and the yield displacement of each substructure. Equivalent damping is computed for each bent as a function of ductility using Eq. 3. Assuming the abutments respond with 10% of critical damping, ξ_1 = 10%, ξ_2 = 15.2%, ξ_3 = 14.7%, ξ_4 = 10%. The damping combined with Eq. 38 in terms of work done by each element, results in ξ_{sys} = 14.4%.

Step 4. Required strength. The level of damping in the bridge results in a displacement demand reduction factor $R_\xi = 0.65$ and the required period is $T_{eff} = 4.1$ s (Eq. 29). Finally, the required strength for the bridge in the transverse direction is V = 5700 kN (Eq. 31).

Step 5. Checking assumed strength distribution. At the target displacement, both abutments develop their strength, V_a = 2600 kN. Therefore the proportion of the total strength taken by the abutments is v_a = 45% (Eq. 42). This is 4.6 times the value assumed at the beginning of the process, therefore ξ_{sys} must be re-evaluated to obtained a new V. After a few iterations V = 6447 kN and the participation of the abutments is 39 %, as shown in Table 13.

Table 13. Transverse Design. CA-1

Iteration	Δ_{sys}	M_{eff}	ξ_{sys}	T_{eff}	V	(V1+V4)/V
1	0.64	3808.1	14.4	>Tc	5879.8	0.1
2	0.64	3808.1	13.3	3.9	6313.3	0.45
3	0.64	3808.1	13.1	3.87	6417.2	0.38
4	0.64	3808.1	13	3.86	6447.8	0.39

It is important to note that iteration was required since it was chosen to consider the strength of the abutments. Accounting for the strength of the abutments has significantly reduced the demand on the piers. However whether the abutments are able to contribute this strength after several cycles of displacements as large as 0.6 m might be questioned.

Longitudinal Direction

The design process along the longitudinal direction is similar to design in transverse direction. Since the columns are pinned to the foundation and they are integral with the superstructure, the target displacement in the longitudinal direction is the same as the capacity in the transverse direction. Also, since the superstructure is stiff and continuous, the displacement at the location of the bents and abutments are constrained to be the same. Therefore, Δ_{sys} and M_{eff} are the same as in transverse direction.

As in the transverse design case, abutments were considered to provide strength to the bridge. Since the longitudinal direction the abutments are designed with knock-off walls, their strength comes from soil mobilization behind the wall pushed by the superstructure. In the LRFD-Seismic report, the soil passive strength was computed as 6058 kN at a yield displacement of 76mm. An elasto-plastic compression only response based on those values is used here for this design. The equivalent damping of the abutments is assumed constant, equal to 10%

Table 14. Longitudinal Design parameters. Trial design CA-1

Iteration	Δ_{sys}	M_{eff}	ξ_{sys}	T_{eff}	V	(V1+V4)/V
1	640	3808.1	14.5	>Tc	5699.9	0.1
2	640	3808.1	11	3.69	7247.1	0.8
3	640	3808.1	10.8	3.66	7349.5	0.84
4	640	3808.1	10.9	3.67	7316	0.82

Table 14 summarizes the values of the main design parameters during longitudinal design. A few iterations were required as it was found that the abutments contribute with as much as 82% of the total strength in this direction. In the first iteration, it was assumed that the contribution of the abutments was 10%. This yielded a total required strength of 5699 kN, which is actually less than the capacity of the abutment that resist the movement of the superstructure. Therefore that solution is not possible. Repeating the process but starting with 80% as abutment contribution, increases the strength demand since the damping is reduced. After three iterations the solution converges, V = 7316 kN and the contribution of the abutments is 82%.

Element Design

In DDBD, the flexural reinforcement is designed using moment-curvature analysis to provide the required strength at a level of curvature compatible with the ductility demand in the element. Table 15 shows the design moments in the transverse M_t and longitudinal direction M_l that resulted from DDBD. It is observed that these values are the same for bents 2 and 3,

as it was chosen in the strength distribution. These values are followed by the combined moment M_E. This resulted from the largest of the values obtained with Eq. 47 and Eq. 48, using the 100%-30% combination rule.

$$M_E = \sqrt{Mt^2 + 0.3Ml^2} \quad \text{(Eq. 47)}$$

$$M_E = \sqrt{Ml^2 + 0.3Mt^2} \quad \text{(Eq. 48)}$$

Table 15. Bent design. Trial design CA-1

BENT	M_T (kN.m)	M_L (kN.m)	$M_{t\ P\text{-}\Delta}$ (kN.m)	$M_{l\ P\text{-}\Delta}$ (kN.m)	θ_t	θ_l	M_E (kN.m)	P (kN)	ρ (%)	Shear D/C ratio
2	14975	4446	4408	4408	0.29	0.29	17238	7547	1.1	0.24
3	14975	4446	4304	4304	0.29	0.29	17238	7547	1.1	0.25

Also shown in Table 15 are the P-Δ moments in the transverse P-Δ_t and longitudinal P-Δ_l direction along with the stability indexes calculated as the ratio of the P-Δ moments and the combined moment. In DDBD allows that stability indexes less than 30%. However, if the stability index is larger than 8%, the design moment must be increased adding 50% of the P-Δ moment to account for strength reduction caused by P-Δ effects (Priestley et al, 2007). These increased moments are shown in Table 11 along with the design axial force that results from gravity loads only.

At the design displacements, the strain in the concrete reaches values of 0.011 for bent 2 and 0.010 for bent 3. These design strains are computed using the plastic hinge method. By section analysis at the design strains, it is found that all columns in the bridge require 20D44 bars as flexural reinforcement, which is a 1.1% steel ratio.

Finally, using the modified UCSD shear model (Eq. 32) (Kowalsky and Priestley, 2000), the shear capacity of the section is computed and compared to shear demand at flexural over-strength. The shear demand/capacity ratios are shown in Table 15.

6.3 Analysis and Comparison

A summary of results of the two designs for this bridge is presented in Table 16. The following observations are made:

- The displacement capacity in LRFD-Seismic is larger than the target displacement used in DDBD. In LRDF-Seismic, the displacement capacity was obtained by pushover analysis without accounting for P-Δ effects. However P-Δ effects were later checked in terms of displacement demand. In DDBD the target displacement was controlled by P-Δ effects and it was obtained using simple calculations.
- DDBD design accounted by the strength of the abutments in the design directions. This lead to a reduction in the amount of reinforcement required in the piers.

Table 16. Summary of LDFD-Seismic and DDBD designs

LRFD-Seismic							
BENT	Δ_{Ct} (mm)	Δ_{Cl} (mm)	Δ_{Dt} (mm)	Δ_{Dl} (mm)	ρ (%)	Rebar	Spiral
2	882	947	564	599	1.5	26D44	D25@125
3	988	1063	601	599	1.5	26D44	D25@125
DDBD							
BENT	Δ_{Ct} (mm)	Δ_{Cl} (mm)	Δ_{Dt} (mm)	Δ_{Dl} (mm)	ρ (%)	Rebar	Spiral
2	640	640	640	640	1.1	18D44	D25@125
3	640	640	640	640	1.1	18D44	D25@125

- In the LRFD-Seismic design, the contribution of the abutments to the strength of the bridge is ignored. The argument is that the abutment displacement coefficient R_a is greater than four and therefore the abutments have an insignificant effect on the response of the bridge (Ibsen, 2007; Caltrans 2006). However the same LRFD-Design shows that the displacement demand increased 60% when the abutments were ignored.
- In the DDBD design, it was chosen include the abutments as part of the earthquake resistant system. It was noted that the contribution of the abutments was substantial in both directions

- DDBD required less effort than LRFD-Seismic since pushover analysis was not required. As it has been mentioned for the other bridges, the effort required to obtain an optimum design in LRFD-Seismic is directly related to the experience of the designed to guess the reinforcement of the sections and avoid iteration.

7. SUMARY CONCLUSIONS

DDBD has been used to design four bridges that have been designed by others following the new LRFD-Seismic guide. The results of the application of both procedures have been compared and the following conclusions are advanced:

- DDBD produces optimum designs in which the bridge reaches a predefined level of performance in the critical direction. To obtain a comparable design in LRFD-Seismic, iteration is needed, varying the amount of reinforcement, until displacement demand equal displacement capacity.
- The application of DDBD requires less effort than the application of LRFD-Seismic
- DDBD is compatible with the design philosophy in the new LRFD-Seismic guide. Therefore DDBD can be used as an alternative method.

8. REFERENCES

AASHTO, 2004, LRFD Bridge design specifications, fourth edition, American Association of State Highway and Transportation Officials, Washington, D.C.

ATC, 2000, NCHRP 12-49 Recommended LRFD Guidelines for the Seismic Design of Highway Bridges, http://www.ATCouncil.org, (accessed June, 2008)

Blandon Uribe C., Priestley M. 2005, Equivalent viscous damping equations for direct displacement based design, "Journal of Earthquake Engineering", Imperial College Press, London, England, 9, SP2, pp.257-278.

Caltrans, 2006, Seismic Design Criteria, Caltrans, http://www.dot.ca.gov/hq/esc/earthquake_engineering, (accessed April 18, 2008)

Calvi G.M. and Kingsley G.R., 1995, Displacement based seismic design of multi-degree-of-freedom bridge structures, Earthquake Engineering and Structural Dynamics 24, 1247-1266.

Dwairi, H. and Kowalsky, M.J., 2006, Implementation of Inelastic Displacement Patterns in Direct Displacement-Based Design of Continuous Bridge Structures, Earthquake Spectra, Volume 22, Issue 3, pp. 631-662

Dwairi, H., 2004. Equivalent Damping in Support of Direct Displacement - Based Design with Applications To Multi - Span Bridges. PhD Dissertation, North Carolina State University

EuroCode 8, 1998, Structures in seismic regions – Design. Part 1, General and Building", Commission of European Communities, Report EUR 8849 EN

FEMA, 2003, NEHRP Recommended Provisions and Commentary for Seismic Regulations for New Buildings and Other Structures (FEMA 450).

Imbsen, 2007, AASHTO Guide Specifications for LRFD Seismic Bridge Design, AASHTO, http://cms.transportation.org/?siteid=34&pageid=1800, (accessed April 18, 2008).

Kowalsky M. J., 2000, Deformation Limit States for Circular Reinforced Concrete Bridge Columns. Journal of Structural Engineering

Kowalsky M.J. 2000, Improved Analytical Model for Shear Strength of Circular Reinforced Concrete Columns in Seismic Regions, ACI Structural Journal, V 97 no 3

Kowalsky M.J., 2001, "RC Structural Walls Designed According to UBC and Displacement-Based Methods". Journal Of Structural Engineering.

Kowalsky M.J., 2002, A Displacement-based approach for the seismic design of continuous concrete bridges, Earthquake Engineering and Structural Dynamics 31, pp. 719-747.

Kowalsky M.J., Priestley M.J.N. and MacRae G.A. 1995. Displacement-based Design of RC Bridge Columns in Seismic Regions, Earthquake Engineering and Structural Dynamics 24, 1623-1643.

Mander, J.B., Priestley, M.J.N. and Park, R., 1988, Theoretical Stress Strain Model of Confined Concrete Journal of Structural Engineering, ASCE, Vol. 114, No.8, August,

Ortiz, J., 2006, Displacement-Based Design of Continuous Concrete Bridges under Transverse Seismic Excitation". European School for Advanced Studies in Reduction of Seismic Risk (ROSE School).

Priestley, M. J. N., 1993, Myths and fallacies in earthquake engineering-conflicts between design and reality, Bulletin of the New Zealand Society of Earthquake Engineering, 26 (3), pp. 329–341

Priestley, M. J. N., Calvi, G. M. and Kowalsky, M. J., 2007, Direct Displacement-Based Seismic Design of Structures, Pavia, IUSS Press

Priestley, M.J.N. and Grant, D. N. 2005 “Viscous damping in analysis and design” Journal of Earthquake Engineering, Vol.9, No. Special Issue 1.

Shibata A. and Sozen M. Substitute structure method for seismic design in R/C. Journal of the Structural Division, ASCE 1976; 102(ST1): 1-18.

Suarez, V.A. and Kowalsky M.J. 2007, Displacement-Based Seismic Design of Drilled Shaft Bents with Soil-Structure Interaction, Journal of Earthquake Engineering, Volume 11, Issue 6 , pp. 1010 – 1030

Suarez, V.A., 2006, Implementation of Direct Displacement Based Design for Pile and Drilled Shaft Bents, Master Thesis, North Carolina State University

Suarez, V.A., 2008, Implementation of the Direct Displacement Based Design Method for Highway Bridges, PhD Dissertation, North Carolina State University.

Suarez, V.A., Kowalsky, M. J., 2008a, Displacement Patterns for Direct Displacement Based Design of Conventional Highway Bridges, Earthquake Spectra, In press.

Suarez, V.A., Kowalsky, M. J., 2008b, Determination of a Stability-Based Target Displacement for Direct Displacement-Based Design of Bridges, Journal of Earthquake Engineering, in press.

Veletzos, A. and Newmark, N. M., 1960, Effect of inelastic behavior on the response of simple systems to earthquake motions”, Proceedings of 2nd World Conference on Earthquake Engineering, pp. 895 – 912.

PART IV

Displacement Patterns for Direct Displacement Based Design of Conventional Highway Bridges

Vinicio A. Suarez [a] and Mervyn J. Kowalsky [b]

Formatted for submission to Earthquake Spectra

This paper studies the use of different displacement patterns and solution algorithms for application of the Direct Displacement-Based Design (DDBD) method to the most common types of highway bridges. The research focuses on determining under what conditions DDBD can be applied using predefined linear patterns as this greatly reduces the design effort. The objectives of the research are achieved by applying DDBD to a variety of bridge configurations and then assessing the performance of the bridges by means of Inelastic Time History Analysis. Bridge frames, continuous bridges with integral and seat-type abutments and bridges with expansion joints are included. One of the most important conclusions of the study is that bridge frames and bridges with seat-type abutments that comply with the balanced mass and stiffness recommendations of AASHTO, can be effectively designed with DDBD, with minimum effort, using rigid body translation patterns.

[a] Graduate Research Assistant, North Carolina State University, Campus-Box 7908, Raleigh, NC-27695, USA
[b] Associate Professor, North Carolina State University, Campus-Box 7908, Raleigh, NC-27695, USA

INTRODUCTION

After the Loma Prieta earthquake in 1989, extensive research has been conducted to develop improved seismic design criteria for bridges, emphasizing the use of displacements rather than forces as a measure of earthquake demand and damage in bridges. Several Displacement-Based Design (DBD) methodologies have been developed. Among them, the Direct Displacement-Based Design Method (DDBD) (Priestley 1993) has undergone extensive research and has proven to be effective for seismic design of bridges, buildings, and other types of structures (Priestley et al 2007).

DDBD differs from other DBD procedures for bridges, such as the Seismic Design Criteria of Caltrans (2004) or the newly proposed AASHTO Guide Specification for LRFD Seismic Bridge Design (Imbsen 2007), in the use of an equivalent linearization approach and in its execution. DDBD starts with the definition of a performance-based target displacement for the structure and returns the stiffness and strength required to meet the target performance under the design earthquake.

This research studies the use of different displacement patterns and solution algorithms for application of the Direct Displacement-Based Design DDBD method to the most common types of highway bridges. The main objective of the research is to determine under what conditions DDBD can be applied using rigid body translation patterns for continuous bridges or linear patterns for bridges with expansion joints, since this greatly reduces the design effort. The objectives of the research are achieved by applying DDBD to sets of different types of bridges and then by assessing the performance of the bridges by means of Inelastic Time History Analysis. Bridge frames, continuous bridges with integral and seat-type abutments, bridges with expansion joints and curved bridges are included.

REVIEW OF THE DDBD METHOD

DDBD was first proposed by Priestley (1993) as a tool for Performance-Based Seismic Engineering. DDBD uses an equivalent linearization approach (Shibata and Sozen, 1976) by which, a multi degree of freedom system at maximum response, is modeled by an equivalent

single degree of freedom system. The substitution is based on work equivalence and is given by Eq. 1 and Eq. 2 , where Δ_{sys} and M_{eff} are the system displacement and effective mass of the equivalent single degree of freedom system. Δ_i and M_i are the displacements and lumped masses at the locations of piers and abutments in the multi degree of freedom system (Fig. 1) (Calvi and Kingsley 1995).

$$\Delta_{sys} = \frac{\sum_{i=1}^{i=n} \Delta_i^{\,2} M_i}{\sum_{i=1}^{i=n} \Delta_i M_i} \tag{1}$$

$$M_{eff} = \frac{\left(\sum_{i=1}^{i=n} \Delta_i M_i \right)^2}{\sum_{i=1}^{i=n} \Delta_i^{\,2} M_i} \tag{2}$$

The main steps of the design procedure are presented in Fig. 2. The bridge is previously designed for non-seismic loads and the configuration, superstructure section and foundation are known. A design objective is proposed by defining the expected performance and the seismic hazard. Then, the target displacement profile for the bridge is determined. After that DDBD is applied in the longitudinal and transverse axes of the bridge, the results are combined, P-Δ effects are checked and reinforcement is designed and detailed following capacity design principles.

The flowcharts in Fig. 3 show the procedure for DDBD in the transverse and longitudinal direction, as part of the general procedure shown in Fig. 1. As seen in Fig. 3, there are three variations of the procedure: (1) If the displacement pattern is known and predefined, DDBD is applied directly; (2) If the pattern is unknown but dominated by the first mode of vibration, the First Mode Shape (FMS) iterative algorithm is used (Calvi and Kingsley 1995); (3) If the pattern is unknown but dominated by modal combination, the Effective Mode Shape (EMS) algorithm is applied (Kowalsky 2002). The direct application of DDBD for bridges, when the displacement pattern is known, requires substantially less effort than the FMS or EMS

algorithms. Details about the determination of displacement patterns and solution algorithms are give in the following section.

TRANSVERSE DISPLACED PATTERNS FOR DDBD

As was mentioned before, much of the effort in the application of DDBD for transverse design of bridges is in the selection or determination of the target displacement profile. Previous research conducted by Dwairi and Kowalsky (2006) focused on the identification of displacement patterns for symmetric and asymmetric bridge configurations using Inelastic Time History Analysis (ITHA). Three types of displacement patterns were identified, namely: Rigid Body Translation (RBT), Rigid Body Translation with Rotation (RBTR) and flexible pattern. These patterns were found to be highly dependent on the superstructure to substructure stiffness ratio, bridge regularity and type of abutment. It was also found that only symmetrical regular bridges with stiff superstructures and free abutments respond with a RBT pattern.

The application of DDBD for bridges that respond with a RBT pattern is direct and simple, since an RBT pattern can be determined at the beginning of the process (Fig. 2). With an RBT pattern, all piers and the abutments displace the same amount, Eq. 1 reduces to Eq. 3 and Eq. 2 reduces to Eq. 4

$$\Delta_{sys} = MIN_{i=1}^{i=n}(\Delta_i) \tag{3}$$

$$M_{eff} = \sum_{i=1}^{i=n} M_i \tag{4}$$

When the displacement pattern is a RBTR or flexible, DDBD requires iteration with static or modal analyses. Two iterative algorithms have been proposed to deal with bridges with flexible transverse displacement patterns. The most simple, proposed by Calvi and Kinsley (1997) and also used by Alvarez (2005), Ortiz (2006), Priestley et al (2007), uses static analysis to find iteratively the displacement pattern that matches the first mode inelastic shape of the structure. This First Mode Shape (FMS) algorithm is therefore appropriate for bridges in which the first mode of vibration dominates the response (Fig. 3). The second

algorithm, proposed by Kowalsky (2002) and studied by Dwairi and Kowalsky (2005) uses an Effective Mode Shape (EMS) analysis to define the displacement profile accounting for the participation of higher modes of vibration (Fig. 3). The EMS algorithm showed to be accurate for design of regular and irregular bridges. However, since its application requires more effort, its use should be avoided in the cases where the other solutions are applicable.

BRIDGE FRAMES AND BRIDGES WITH WEAK ABUTMENTS.

Bridge frames are found in long bridges and viaducts connected to other frames by expansion/movement joints. Design specifications such as the Seismic Design Criteria by Caltrans (2005), requires bridge frames to meet all design requirements as a stand-alone structures.

Continuous bridges with seat type abutments are probably the most common type of bridge. Seat-type abutments are usually designed to fuse in the transverse direction under the design earthquake, therefore their contribution to the strength of the bridge might be low or comparable with the adjacent piers.

Bridge frames, continuous bridges with seat type abutments or other types of abutments that do not contribute substantially to the strength of the bridge, are likely to respond with an RBT displacement pattern if three conditions are met: (1) the superstructure is stiffer than the substructure; (2) there is a balanced distribution of mass and stiffness among the piers; (3) the configuration of the bridge is symmetrical.

The first condition was studied by Dwairi and Kowalsky (2007) and can be quantified using a relative stiffness index RS. This index is the ratio of superstructure to substructure stiffness given by Eq. 5. Where K_{pi} is the gross stiffness of the pier i and E_s, I_s and L_s are the elastic modulus, out-of-plane inertia and length of the superstructure. This equation assumes that the superstructure responds as a simply supported beam with a point load acting at the middle. This equation differs from the one originally proposed by Dwairi and Kowalsky in the use of gross instead of cracked stiffness properties. This change was made since cracked

properties depend on the amount of reinforcement in the section which is unknown at the beginning of design.

$$RS = \frac{48 E_s I_s}{L_s^{\,3}} \sum_{i=1}^{n} \frac{1}{K_{pi}} \tag{5}$$

The second condition can be quantified by the index BMS proposed in The AASHTO LRFD Seismic Guide (Imbsen, 2007), to check for balanced mass and stiffness distribution. This index, shown in Eq. 6, where M is the effective mass, K_p is the stiffness and the subscripts *i* and *j* refer to two piers in the bridge. This index is evaluated twice: once comparing adjacent piers and the second between all the combinations of any two piers.

$$BMS = \frac{M_i K_{p\,j}}{M_j K_{p\,i}} \tag{6}$$

If the bridge is asymmetrical and the two first conditions given for symmetrical bridges are maintained, the response will exhibit an RBTR pattern. The magnitude of the rotation should be related to the stiffness eccentricity KEC, given by Eq. 7, where *x* is the location of the pier or abutment (Fig. 1).

$$KEC = \frac{\dfrac{\sum_{i=1}^{i=n} K_{pi} x_i}{\sum_{i=1}^{i=n} K_{pi}} - \dfrac{\sum_{i=1}^{i=n} M_i x_i}{\sum_{i=1}^{i=n} M_i}}{L_s} \tag{7}$$

If the magnitude of the rotation could be estimated before design, an RBTR displacement profile would be defined such that no bent or abutment exceeds its target performance. In absence of a means to predict the rotation in an RBTR pattern, asymmetric bridges could be designed as symmetric bridges using an RBT displacement pattern. If the pier that controls the design is on the stiff side of the bridge, Δ_{sys} calculated with Eq. 1 will always be less than the same parameter computed with Eq. 3, assuming an RBTR pattern. This assumption leads to a conservative design and might be appropriate for bridges with small stiffness

eccentricities. The case in which the pier with the least target displacement is on the stiff side of the bridge is the most common since generally short piers have less displacement capacity and higher stiffness than taller piers.

In summary, bridge frames or bridges with weak abutments can be designed assuming an RBT pattern. However this assumption might be accurate only within a range of values for the indexes RS, BMS and KEC. In order to assess the limits on these indexes, a total of 13 bridge frames and 13 bridges with seat type abutments, shown in Tables 1 and 2, were designed with DDBD and then subjected to Inelastic Time History Analysis (ITHA). These bridges include symmetrical and asymmetrical configurations. For comparison, each bridge was designed using an FMS pattern and also using an RBT pattern based on the minimum pier target displacement (Eq. 3). These resulted in 26 different designs for bridge frames and 26 different designs for bridges with seat type abutments. The results from ITHA are used as the benchmark for assessment of the effectiveness of DDBD.

Design and ITHA

DDBD was applied using the computer program DDBD-Bridge (Suarez, 2008). The bridges were designed to reach the damage-control limit state (Priestley et at, 2007) under the seismic hazard represented by the displacement design spectrum shown in Fig. 4. Where PGA is the peak ground acceleration, PGD is the peak ground displacement, PSD is the peak spectral displacement and Tc is the corner period. In each bridge, the single column piers are designed to have the same diameter and reinforcement. Design for each displacement pattern was performed as shown in the flowchart in Fig. 3

Tables 1 and 2 show the configuration of the bridge frames and bridges with seat-type abutments. These bridges have between two and seven spans. The pier heights vary from 7 m to 30 m. The piers are monolithically connected to the superstructure and foundation. The superstructure for all bridges is a preestressed concrete box girder with the properties shown in Fig. 5 where: *Ws* is the unit weight, *Es* is the elastic modulus, *Iz* and *Iy* are the out-of-plane and in-plane inertias, *hs* is the distance from the centroid to the bottom of the section, *Hs* is

the total depth of the section and *ws* is the total width. The concrete in the columns has a unit weight of 23.5 kN/m^3 and an expected compressive strength of 35.1 MPa. The reinforcing steel has an expected yield strength of 450 MPa, the maximum strength is 607 MPa and the strain at maximum stress is 0.1.

The seat-type abutments have knock-off walls and sacrificial shear keys. The transverse strength of the abutments was taken as 20% of the tributary weight the abutments support. This was assumed to be equal to the residual friction between superstructure and abutment once the shear keys fail.

The ITHA were performed using OpenSees (Mazzoni et al, 2005) and a pre-processor and post-processor for OpenSees called ITHA-Bridge (Suarez, 2008). The bridges were modeled using 3D finite elements. The columns were modeled with fiber sections. Nonlinear stress-strain models were used for unconfined concrete, confined concrete and reinforcing steel. The superstructure was modeled as a series of elastic frame elements. The abutments were modeled as elasto-plastic springs.

With each bridge model, seven ITHAs were performed using seven earthquake acceleration records that are compatible with the design spectrum shown in Fig. 4 (Earth Mechanics Inc. 2004). During each ITHA, the maximum concrete compression strains were monitored in the fibers at the section in the base of all columns. The output of each ITHA consists of the displacement profiles of the bridge at the time in which maximum strains were reached. For comparison with the design displacement profiles, the ITHA profiles were averaged.

The comparison between DDBD and ITHA was based on several performance indexes. An Average Displacement Ratio ADR (Eq. 8) was computed as an index that compares the mean displacement in the ITHA profile with the mean displacement in the design profile.

A maximum demand/capacity ratio D/C was also computed as maximum of the ratios between the displacements from the ITHA and the target displacement for each pier, estimated during design. If the D/C ratio is greater than 1, there is at least one pier suffering

more damage that considered in design. Finally, a Shape Error SE index (Eq. 9) was also computed to compare shape of the ITHA displacement pattern with the one used in DDBD. If SE equals zero then the displacement patterns are identical. In Eq. 8 and Eq., Δ_{ITHAi} is the ITHA displacement for pier *i*, Δ_{DDBDi} is the DDBD target displacement for pier *i* and n is the number of points at which displacements are sampled.

$$ADR = \frac{\frac{1}{n}\sum_{i=1}^{i=n}\Delta_{ITHAi}}{\frac{1}{n}\sum_{i=1}^{i=n}\Delta_{DDBDi}} \tag{8}$$

$$SE = \frac{\sqrt{\sum_{i=1}^{i=n}(ADR\cdot\Delta_{DDBDi}-\Delta_{ITHAi})^2}}{n} \tag{9}$$

Analysis of results

Figures 6 and 7 show the relative stiffness index RS, balanced mass and stiffness index BMS and stiffness eccentricity index KEC for the bridge frames and bridges with seat type abutments showed in Tables 1 and 2 respectively. The figures have two columns sorting the bridges according to the displacement pattern used in design. Two values are presented for the BMS index (Eq.6): BMS-1 results from all the combinations of any two piers and BMS-2 from al the combinations of adjacent piers. For seismic design category "D", AASHTO (Imbsen 2007) considers a bridge as regular if BMS-1 > 0.75 and BMS-2 > 0.5. These limits are marked in the figures with thick dot lines.

By looking at the data in Figures 6 and 7, it is observed that most bridges have BMS-1 > 0.5 and BMS-2 > 0.75, therefore they can be considered regular according to AASHTO. The ratio between superstructure and substructure stiffness RS varies greatly between 0.10 to more that 10 as a result of the variation of pier height. The stiffness eccentricity varies from 0 in the symmetrical bridges to 13% for asymmetrical bridges. There is low correlation between the indexes. The indexes are independent of the displacement pattern used in design

(i.e. the indexes for bridge 1.12 are the same as those for 1.12.1), since the indexes are computed based on gross section properties.

Figures 8 and 9 show the results of the comparison between the ITHA and DDBD. It is observed that for all asymmetric bridges (i.e. bridges with KEC > 0), the shape error SE is much less when an RBT pattern was used in design. This means that for asymmetric regular bridges, the RBT pattern better reproduces the displaced shape of the bridge. For regular symmetric bridges, the use of RBT pattern or FMS pattern produces similar results.

By looking at the D/C ratios, the bridges designed with and RBT pattern have D/C ratios close to 1, with minimum variation. The D/C ratios for bridges designed with FMS patterns are more variable than those for the bridges designed with RBT patterns. ADR is also more variable and in some cases greater than 1, when FMS was used. The ADR shows more variability for bridges where SE is greater.

There are not enough results to relate the D/C variability to the configuration indexes RS, BMS and KEC. However, the data seems conclusive to show that using a RBT pattern is appropriate for design of bridges with weak abutments that have BMS-1 > 0.75 and BMS-2 > 0.50. It is also concluded that using FMS algorithm for bridges with free or weak abutments is only appropriate for symmetric bridges.

The FMS algorithm always converges to the first inelastic mode of vibration of the bridge. However, the first mode does not control the response the response of asymmetric bridges. This explains the large variations between the shape of the ITHA profile and the FMS profiles that have been quantified with the SE index. To demonstrate this, the design and analysis results of two asymmetric bridges are reviewed next.

Figures 10 and 11 show results of design and analysis for the bridge frame 1.7 and the bridge with seat type abutments 3.9 (Table 2). These figures show the configuration of the bridges, a top view of the transverse displacement profiles and free body diagrams. The transverse displacement profiles shown in Fig. 10 (b) and Fig. 11 (b) include the RBT pattern, the FMS pattern used in the first iteration of the algorithm, the FMS pattern that

converged to the first inelastic mode shape, the ITHA pattern that corresponds to the RBT design and the ITHA pattern that corresponds to the FMS design. It is observed in these figures that that RBT and ITHA-RBT profiles agree both in magnitude and shape, whereas the converged FMS profile and the corresponding ITHA-FMS profile differ substantially, proving that the first mode shape does not control the response of asymmetric bridge frames and bridges with weak abutments.

Since each bridge of Table 2 was designed with columns of same diameter and reinforcement, the asymmetric bridges have strength eccentricity (i.e. the location of the resultant of inertial forces does not match the location of the resultant of the column reactions). The FMS algorithm that converges to the first inelastic mode of vibration also converges to a solution in which force equilibrium and moment equilibrium are both satisfied. In Fig 10(c-e) and Fig 11(c-e), the open arrows represent the inertial forces acting at the top of each bent and the closed arrows represent the reactions at the bottom of the columns. The sum of the inertial forces equals the sum column reaction in the three diagrams, meaning that force equilibrium is satisfied. However, only in the last iteration of the FMS algorithm, moment equilibrium is satisfied. This explains why the converged FMS profiles are negative in one side of the bridge, since when this happens, the inertial forces and reaction forces switch directions allowing moment equilibrium. Although the use of a RBT pattern does not satisfy moment equilibrium, force equilibrium is satisfied and the pattern better represent the response of the bridges, which results from the combination of different modes of vibration.

BRIDGES WITH STRONG ABUTMENTS

Abutments in general have considerably less displacement capacity than flexible and ductile piers. In bridges with seat-type abutments there are shear keys designed to break during the design earthquake, allowing the superstructure to displace relative to the abutments and protect them from displacing beyond their capacity. In bridges with integral abutments however, there is not relative displacement between the ends of the superstructure

and the abutments. Therefore, the abutments should be provided with enough strength as to constrain the displacement of the superstructure. As a result of this, bridges with strong abutments exhibit a flexible displacement pattern as shown in Fig. 12

The extent of curvature in the flexible pattern depends on several factors such as the relative stiffness of the superstructure, piers and abutments. Therefore, it is difficult to establish the displacement pattern at the beginning of the design. As a result of this, the iterative FMS algorithm will give the best results for design. When applying the FMS algorithm to bridges with strong abutments, the target displacement of the abutments is enforced in each iteration (Priestley 2007). If the bridge is asymmetric, the procedure will converge to a solution where the abutments require different strengths. In this way, the equilibrium of moments and forces is achieved.

To assess the effectiveness of the FMS algorithm, the set of 10 bridges with integral abutments, presented in Table 3, was designed using the FMS algorithm and then analyzed with ITHA. The design and analysis was conducted as described for the bridge frames and bridges with weak abutments in the previous section. The abutments where designed for a target displacement of 100 mm. Results of design and analysis are presented in Figure 13.

It can be seen in Fig. 13 that the majority of the bridges comply with the balanced mass and stiffness criteria for regular bridges in seismic design category “D”. As prescribed by AASHTO (Imbsen, 2007), the calculation of these indexes has excluded the abutments, although these elements contribute significantly with strength and stiffness. Therefore, even if BMS-1 > 0.75 and BMS-2 > 0.5, these bridges do not respond with an RBT pattern but with a flexible pattern as shown in Fig 12.

The SE index for these bridges is variable and orders of magnitude greater than the same index for the bridges with weak abutments. No clear trends are found in the data to relate the effectiveness of the FMS algorithm to the configuration indexes RS, KEC and BMS. However, judging by the D/C ratios, it is concluded that the FMS algorithm is effective for this type of bridges.

Dynamic amplification of shear in abutments

Higher mode effects in the shape of the displacement pattern are minimal if compared to the effects on forces that develop in elastic components of the bridge. If the abutments are designed to reach their target displacement elastically, higher mode effects can amplify the shear demand substantially (Priestley et al 2007). First mode moments in the superstructure are also amplified by higher modes. The shear in the piers is not amplified since it is likely that these elements develop their full strength with the displacements induced by the first mode (Priestley et al 2007).

The dynamic amplification of shear demand in the abutments can be accounted for in design using the EFM algorithm (Kowalsky, 2002). This process shown in Fig. 3, requires modal superposition analysis of the bridge modeled with secant stiffness.

To determine the extent of dynamic amplification of shear in the abutments, the EMS analysis was used with the bridges in Table 3, using the computer program DDBD-Bridge (Suarez, 2008). It was observed that higher mode effects increase the shear demand in the abutments up to 2.5 times the shear calculated with the FMS design. The results shown in Fig. 12 did not show any correlation between the magnitude of the dynamic amplification and the configuration indexes BMS or KEC.

The ITHAs were performed with the abutments modeled as elasto-plastic springs. These springs were set to yield at the abutment design displacement (100 mm). The yield strength of the springs was the design strength that resulted from the EMS design (i.e. the strength of the abutments was increased to account for higher mode effects). The maximum displacements at the abutments are shown in Fig. 13. It is observed that the displacement for the first three bridges is close to the design displacement, while for the other bridges the displacements reduce substantially. This leads to the conclusion that the EMS predicted the amplification of shear demand for the bridges with two spans well, while it over-predicted the amplification for the bridges with three and four spans.

The general conclusion is that regular bridges with strong abutments can be satisfactory designed with DDBD using the FMS algorithm. However, it should be taken into account that the effectiveness of this approach reduces for asymmetric bridges. It is also concluded that the EMS algorithm in general produces a conservative estimate of the shear demand in the abutments. The use of the EMS can be avoided by the application of a dynamic amplification factor to the shear demand obtained from FMS analysis. The results in Fig. 13 suggest that a factor of 2.5 might be appropriate.

Bridges with strong abutments designed with an RBT pattern.

In cases were the designer decides to ignore any contribution of the abutments to the strength of the bridge, bridges with strong abutments could be designed as described in Section 2.1, for bridges with weak abutments. This would simplify design since a RBT displacement pattern would be used instead of a flexible pattern with the FMS algorithm. Also, the design of the piers would be conservative as all seismic demand is directed to them. However, since a realistic displacement profile is not determined, damage in the abutments and superstructure due to displacement in excess of their capacity would not be assessed. The authors do not recommend ignoring the abutments as they have a significant impact on design of piers and superstructure.

BRIDGES WITH EXPANSION JOINTS IN THE SUPERSTRUCTURE

In order to control expansion due to temperature changes in the superstructure, most bridges are provided with expansion joints at the abutments and less commonly along the superstructure, where the flexural continuity is broken. The transverse displaced shape of a superstructure with expansion joints is similar to an open polygon, with most of the rotation concentrated in the expansion joints.

Expansion joints can be easily implemented in DDBD to be used with the FMS and EMS algorithms. For design in the transverse direction, two main adjustments must be made: (1) during the determination of the equivalent single degree of freedom system, mass and displacement at the location of each internal expansion joint must be included; (2) the

stiffness discontinuity generated at each expansion joint must be accounted for when the displaced shape is refined by static or modal analysis.

However, as is the case of frame bridges and bridges with weak abutments, the FMS algorithm will not work for bridges with expansion joints, since the first mode of vibration will not dominate the response in most cases. Therefore, in order to avoid the use of the EMS algorithm, simple displacement patterns must be studied.

The displacement patterns shown in Fig. 14 are proposed for design of bridges with one or two intermediate expansion joints. These patterns are formed by line segments that can be easily and uniquely defined in terms of the pier with the least performance-based target displacement. In these patterns it is assumed that the displacement at the abutments is zero.

In order to assess the effectiveness to the linear patterns, the three bridges shown in Fig. 15-17, were designed with DDDB using the FMS algorithm and the proposed linear patterns. Then, the performance of these bridges was assessed by ITHA. The design and ITHA was performed as described in section 2.1.1. These figures show the layout of each bridge and the design displacement profiles as well as the ITHA profiles. The design profile based on the proposed linear displacement patterns is shown as LDP DDBD, the design profile showing the last iteration of the FMS algorithm is shown as FMS DDBD, the ITHA profiles corresponding to the two designs are shown as LDP ITHA and FMS ITHA.

The results in Fig. 15 for a symmetric bridge with one expansion joint, show good agreement between the FMS profile (FMS DDBD) and ITHA profile from that design (FMS ITHA). There is also good agreement between the design profile based on a linear pattern (LDP) and the ITHA profile that resulted from that design (LPD ITHA). In fact, the use of FMS and LDP profiles produced similar results for this bridge.

The results shown in Fig. 16 for an asymmetric bridge with one expansion joint, show bad agreement between the FMS profile (FMS DDBD) and ITHA profile from that design (FMS ITHA). The reason is that the first mode of vibration does not control de shape of the displacement profile. However there is good agreement between the design profile based on

a linear pattern (LDP) and the ITHA profile that resulted from that design (LPD ITHA). The same observations apply to the asymmetric bridge with two expansion joints shown in Fig. 17.

It is then concluded that the FMS can only be used for symmetric bridges with one expansion joint, which are likely to be dominated by the first mode of vibration. The proposed linear profiles seem effective for design of bridges with one or two expansion joints, provided that bridge frames are regular as defined in section 2.1. The use of linear displacement patterns greatly simplifies design. However, for bridges with more than two expansion joints the EMS should be used.

SUMMARY AND CONCLUSIONS

The DDBD method can be applied (1) Directly with a predefined displacement pattern; (2) using the First Mode Shape FMS algorithm; (3) using the Effective Mode Shape EMS algorithm. The main objective of this research was to determine under what conditions DDBD can be applied using predefined displacement patterns since this greatly reduces design effort. This objective was achieved by applying DDBD to sets of different types of bridges and then by assessing the performance of the bridges by means of Inelastic Time History Analysis. Bridge frames, continuous bridges with integral and seat-type abutments, bridges with expansion joints were included. This research has lead to the following conclusions:

- DDBD should be applied according to Table 4 for different types of bridges.
- DDBD can be applied directly and effectively, using a RBT pattern, for bridge frames or bridges with weak abutments that have a balanced distribution of mass and stiffness (BMS-1 > 0.75 and BMS-2 >0.5)
- Using the FMS algorithm is not appropriate for design of asymmetric bridge frames, asymmetric bridges with weak abutments and bridges with expansion joints, since the first mode of vibration does not control the shape of their displacement pattern.

- Using the FMS algorithm is appropriate for transverse design of bridges with integral abutments. However, the dynamic amplification of abutment forces requires EMS analysis of the use of a dynamic amplification factor.

ACKNOWLEDGEMENTS

The authors wish to acknowledge the support of North Carolina State University, the North Carolina Department of Transportation, and Universidad Tecnica Particular de Loja and Senacyt.

REFERENCES

Caltrans, 2006, Seismic Design Criteria, Caltrans, http://www.dot.ca.gov/hq/esc/earthquake_engineering, (accessed April 18, 2008)

Calvi G.M. and Kingsley G.R., 1995. Displacement based seismic design of multi-degree-of-freedom bridge structures, Earthquake Engineering and Structural Dynamics 24, 1247-1266.

Dwairi, H. and Kowalsky, M.J., 2006, Implementation of Inelastic Displacement Patterns in Direct Displacement-Based Design of Continuous Bridge Structures, Earthquake Spectra, Volume 22, Issue 3, pp. 631-662

Earth Mechanics Inc., 2004, Technical Memorandum Project 04-129, Dr. Nigel Priestley's personal correspondence

Imbsen, 2007, AASHTO Guide Specifications for LRFD Seismic Bridge Design, AASHTO, http://cms.transportation.org/?siteid=34&pageid=1800, (accessed April 18, 2008).

Kowalsky M.J., 2002, A Displacement-based approach for the seismic design of continuous concrete bridges, Earthquake Engineering and Structural Dynamics 31, pp. 719-747.

Mazzoni, S., McKenna, F., Scott, M. and Fenves, G., 2004, OpenSees command language manual, http://opensees.berkeley.edu, (accessed April 18, 2008)

Ortiz J. 2006, Displacement-Based Design Of Continuous Concrete Bridges Under Transverse Seismic Excitation. European School For Advanced Studies In Reduction Of Seismic Risk.

Priestley, M. J. N., 1993, Myths and fallacies in earthquake engineering-conflicts between design and reality, Bulletin of the New Zealand Society of Earthquake Engineering, 26 (3), pp. 329–341

Priestley, M. J. N., Calvi, G. M. and Kowalsky, M. J., 2007, Direct Displacement-Based Seismic Design of Structures, Pavia, IUSS Press

Shibata A. and Sozen M. Substitute structure method for seismic design in R/C. Journal of the Structural Division, ASCE 1976; 102(ST1): 1-18.

Suarez, V.A. and Kowalsky M.J., Displacement-Based Seismic Design of Drilled Shaft Bents with Soil-Structure Interaction, Journal of Earthquake Engineering, Volume 11, Issue 6 November 2007 , pp. 1010 – 1030

Suarez, V.A., 2008, Implementation of Direct Displacement Based Design for Highway Bridges, PhD Dissertation, North Carolina State University.

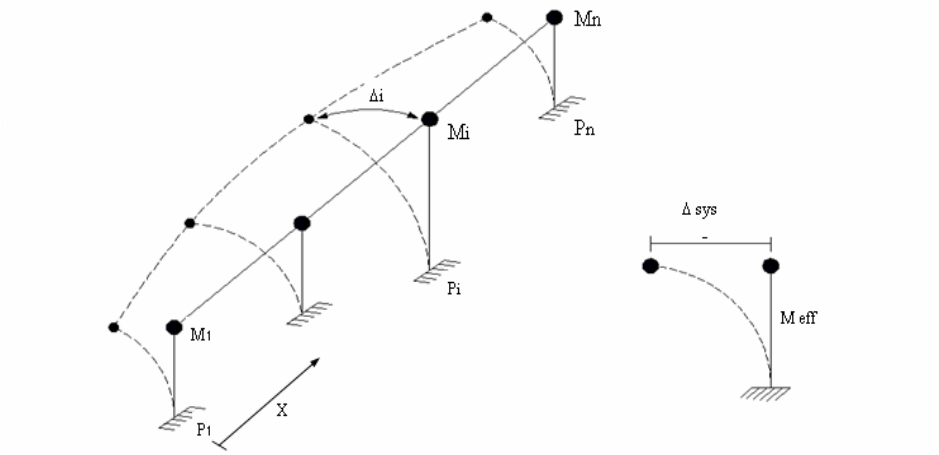

Figure 1. Equivalent single degree of system

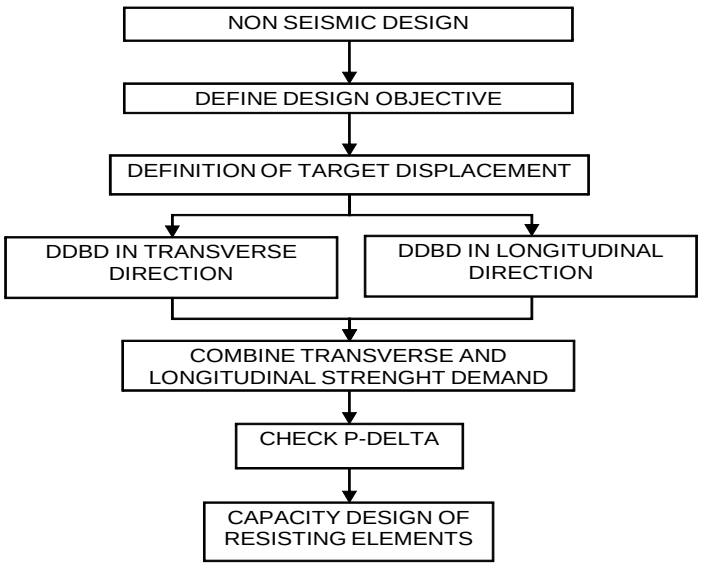

Figure 2. DDBD main steps flowchart

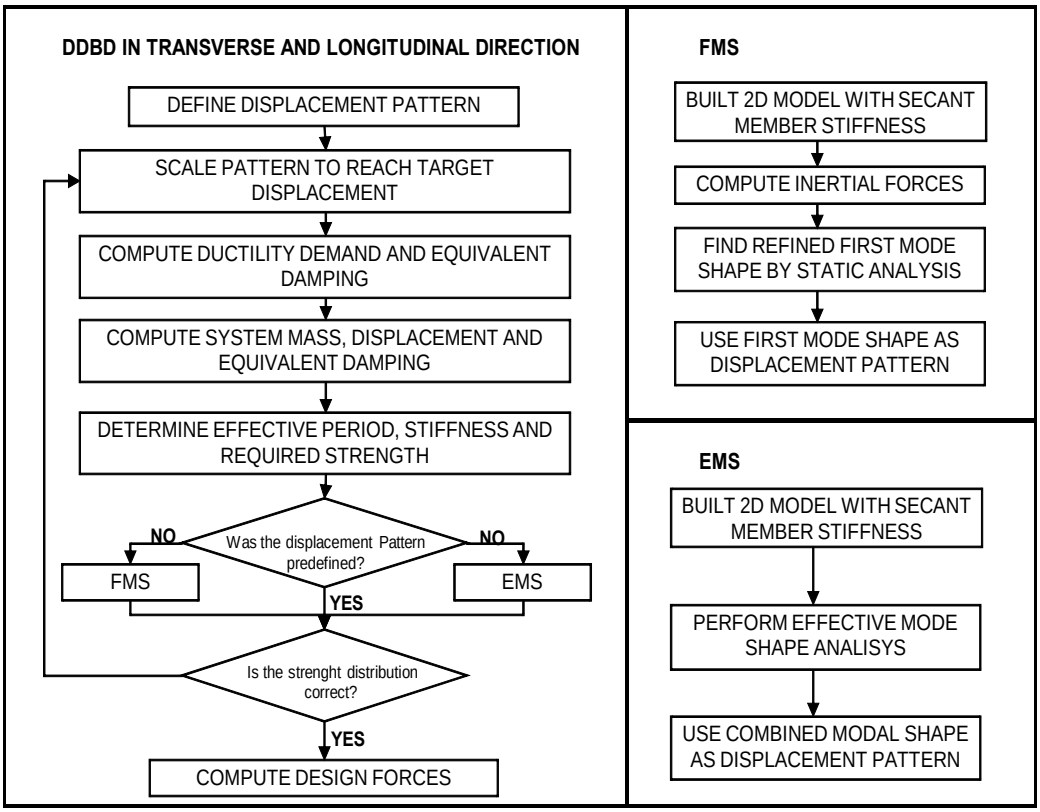

Figure 3. Complementary DDBD flowcharts

SPECTRUM COMPATIBLE RECORDS					
No	Earthquake Event	Year	Station	PGA (g)	PGD (cm)
1	Imperial Valley	1979	Array #7	0.616	17.7
2	Northridge	1994	Sylmar	0.475	14.2
3	Northridge	1994	Rinaldi	0.563	13.2
4	Imperial Valley	1979	Bonds	0.553	25.9
5	Northridge	1994	Van Nuys	0.513	9.7
6	Loma Prieta	1989	Saratoga	0.512	15.7
7	Kobe	1995	Takatori	0.562	16.2

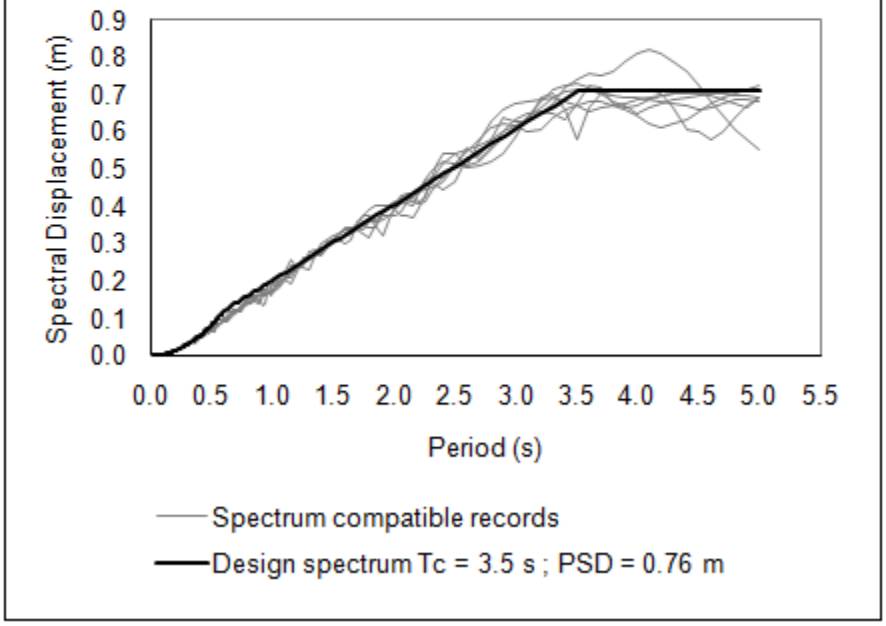

Figure 4. Displacement design spectrum and compatible records

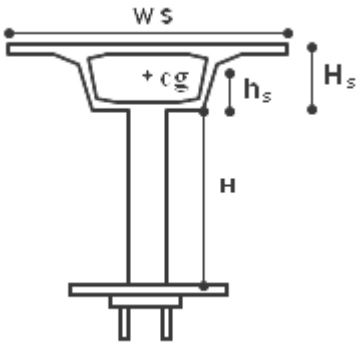

Properties:

Ws	165 KN/m
E	34347 MPa
Iz	73.86 m^4
Iy	5.37 m^4
hs	1.58 m
Hs	2.4 m
ws	13.5 m

Figure 5. Superstructure type and properties

Table 1. Bridge Frames

Bridge Layout

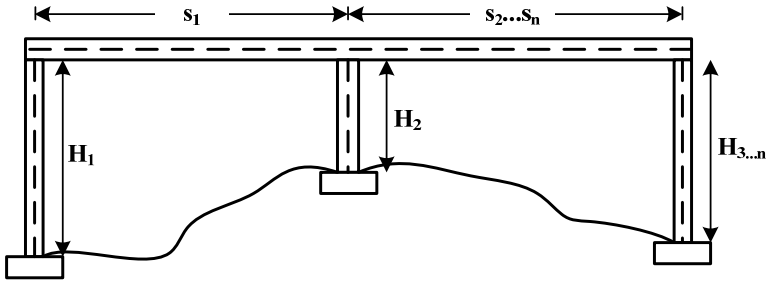

Code	Span length (m)							Pier height (m)								Displacement Pattern
	S_1	S_2	S_3	S_4	S_5	S_6	S_7	H_1	H_2	H_3	H_4	H_5	H_6	H_7	H_8	
1.1	50	50						7	7	7						FMS
1.1.1	50	50						7	7	7						RBT
1.2	50	30						12	13	12						FMS
1.2.1	50	30						12	13	12						RBT
1.3	40	40						12	15	12						FMS
1.3.1	40	40						12	15	12						RBT
1.4	30	30	30					12	12	12	12					FMS
1.4.1	30	30	30					12	12	12	12					RBT
1.5	30	30	30					12	15	15	12					FMS
1.5.1	30	30	30					12	15	15	12					RBT
1.6	25	25	50					10	11	10	11					FMS
1.6.1	25	25	50					10	11	10	11					RBT
1.7	50	50	50	50				20	18	18	20	18				FMS
1.7.1	50	50	50	50				20	18	18	20	18				RBT
1.8	50	50	50	50				15	18	22	18	15				FMS
1.8.1	50	50	50	50				15	18	22	18	15				RBT
1.9	40	40	40	40	40			10	10	10	12	12	12			FMS
1.9.1	40	40	40	40	40			10	10	10	12	12	12			RBT
1.10	40	40	40	40	40			14	15	14	15	14	14			FMS
1.10.1	40	40	40	40	40			14	15	14	15	14	14			RBT
1.11	50	50	50	50	50	50		27	30	27	30	27	30	27		FMS
1.11.1	50	50	50	50	50	50		27	30	27	30	27	30	27		RBT
1.12	50	50	50	50	50	50		20	25	20	25	28	25	20		FMS
1.12.1	50	50	50	50	50	50		20	25	20	25	28	25	20		RBT
1.13	50	50	50	50	50	50	50	18	18	18	18	18	18	18	18	FMS
1.13.1	50	50	50	50	50	50	50	18	18	18	18	18	18	18	18	RBT

Table 2. Continuous Bridges with seat-type abutments

Bridge Layout

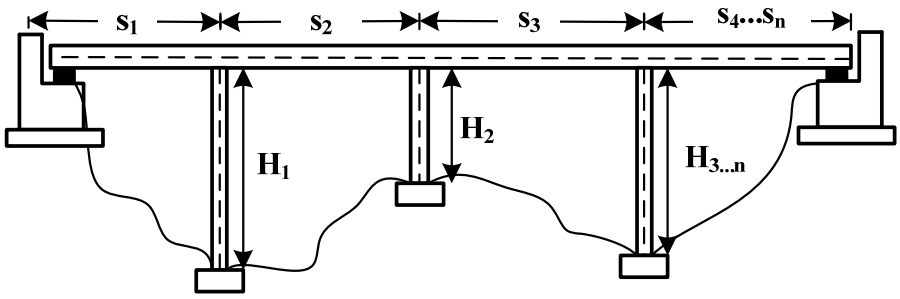

Code	Span length (m)							Pier height (m)						Displacement Pattern
	S_1	S_2	S_3	S_4	S_5	S_6	S_7	H_1	H_2	H_3	H_4	H_5	H_6	
3.1	50	50						7						FMS
3.1.1	50	50						7						RBT
3.2	50	30						13						FMS
3.2.1	50	30						13						RBT
3.3	40	40						15						FMS
3.3.1	40	40						15						RBT
3.4	30	30	30					12	12					FMS
3.4.1	30	30	30					12	12					RBT
3.5	30	30	30					15	15					FMS
3.5.1	30	30	30					15	15					RBT
3.6	25	25	50					11	10					FMS
3.6.1	25	25	50					11	10					RBT
3.7	50	50	50	50				18	18	20				FMS
3.7.1	50	50	50	50				18	18	20				RBT
3.8	50	50	50	50				18	15	18				FMS
3.8.1	50	50	50	50				18	15	18				RBT
3.9	40	40	40	40	40			10	10	12	12			FMS
3.9.1	40	40	40	40	40			10	10	12	12			RBT
3.10	40	40	40	40	40			15	14	15	14			FMS
3.10.1	40	40	40	40	40			15	14	15	14			RBT
3.11	50	50	50	50	50	50		30	27	30	27	30		FMS
3.11.1	50	50	50	50	50	50		30	27	30	27	30		RBT
3.12	50	50	50	50	50	50		25	20	25	28	25		FMS
3.12.1	50	50	50	50	50	50		25	20	25	28	25		RBT
3.13	50	50	50	50	50	50	50	18	18	18	18	18	18	FMS
3.13.1	50	50	50	50	50	50	50	18	18	18	18	18	18	RBT

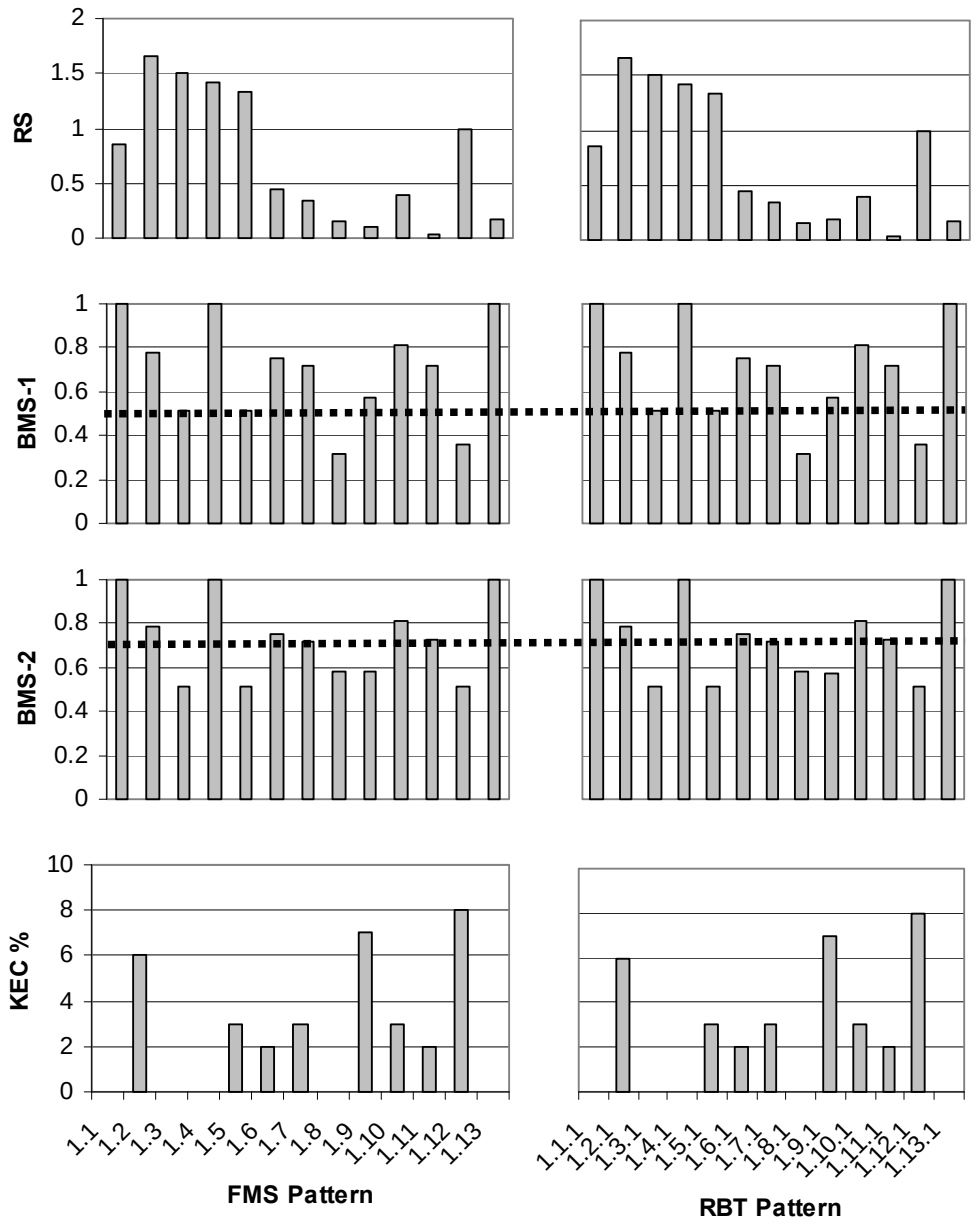

Figure 6. Regularity indexes for bridge frames

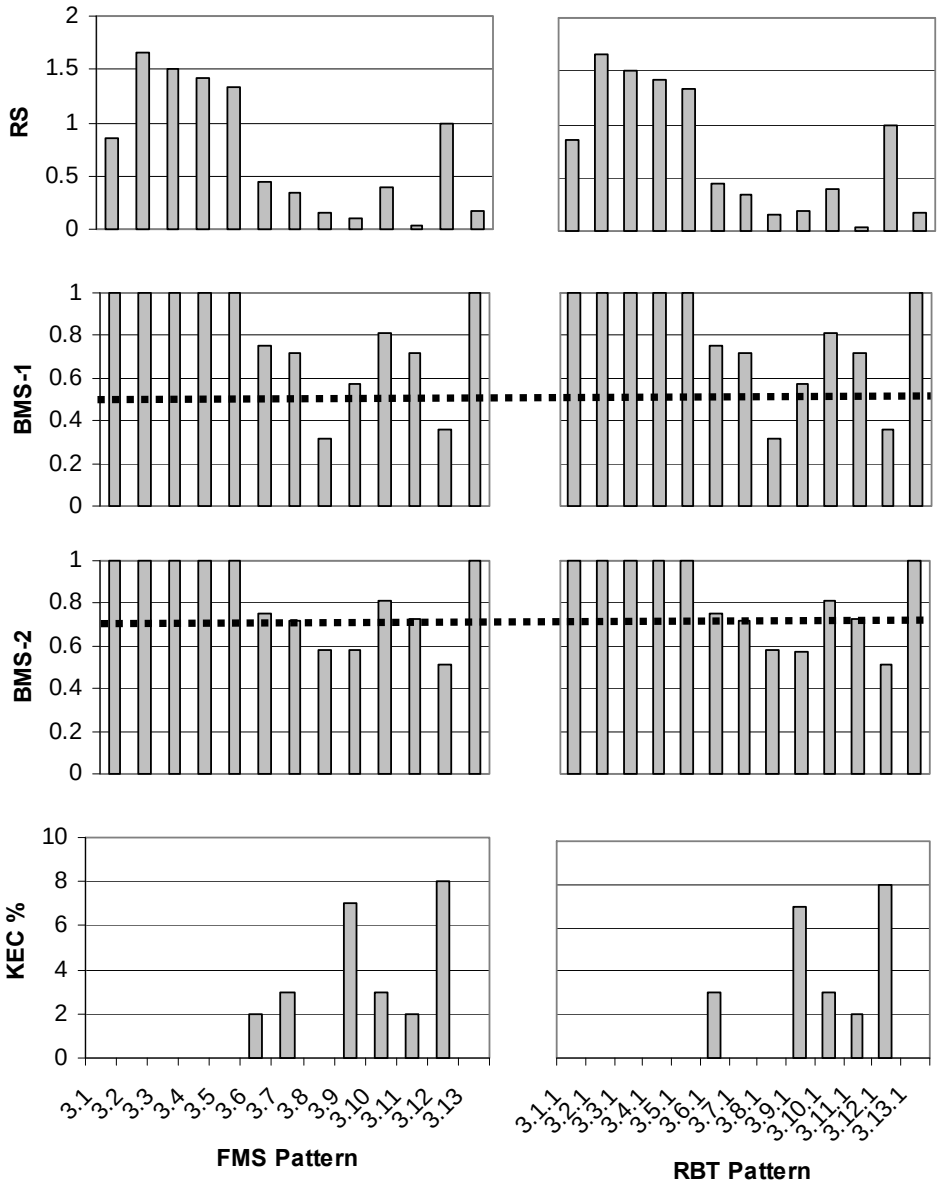

Figure 7. Regularity indexes for bridges with seat-type abutments

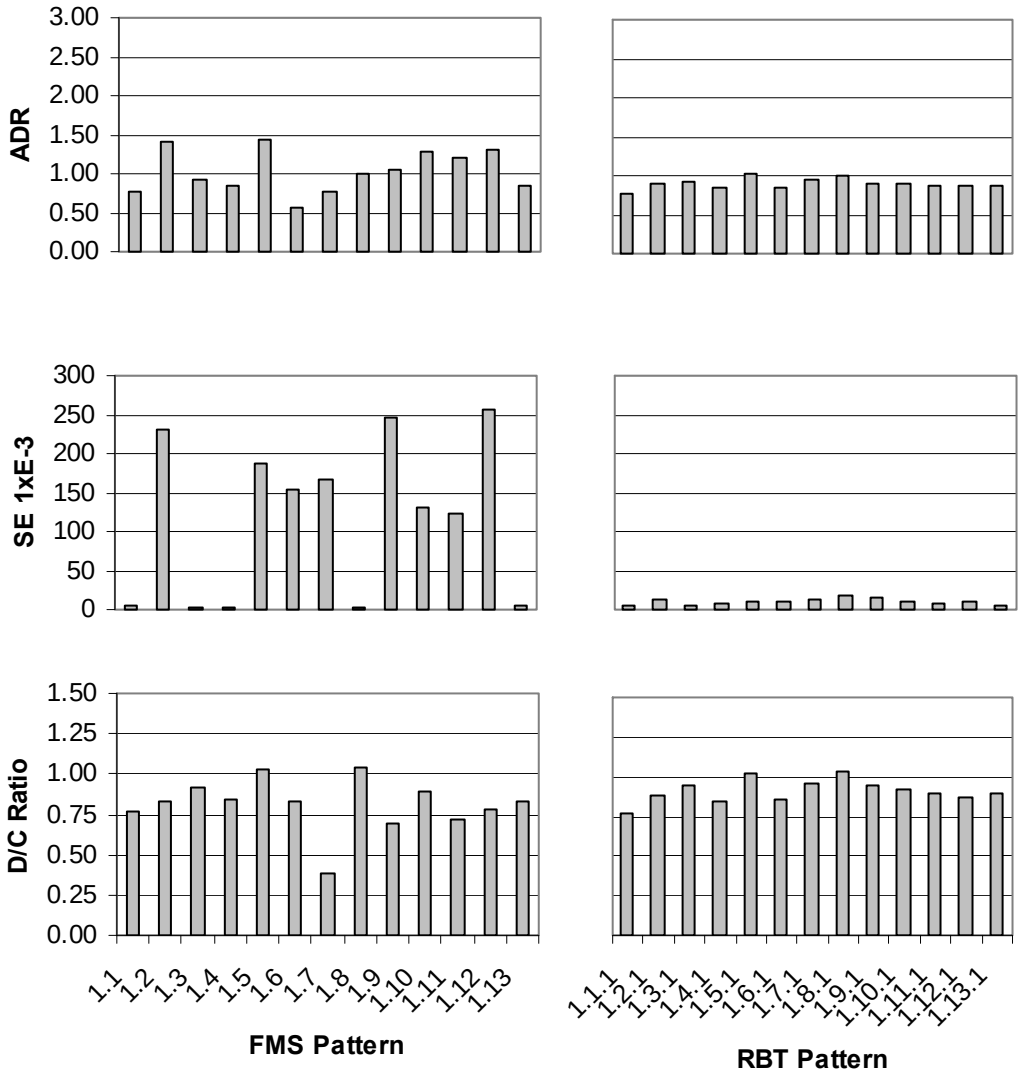

Figure 8. Performance indexes for bridge frames

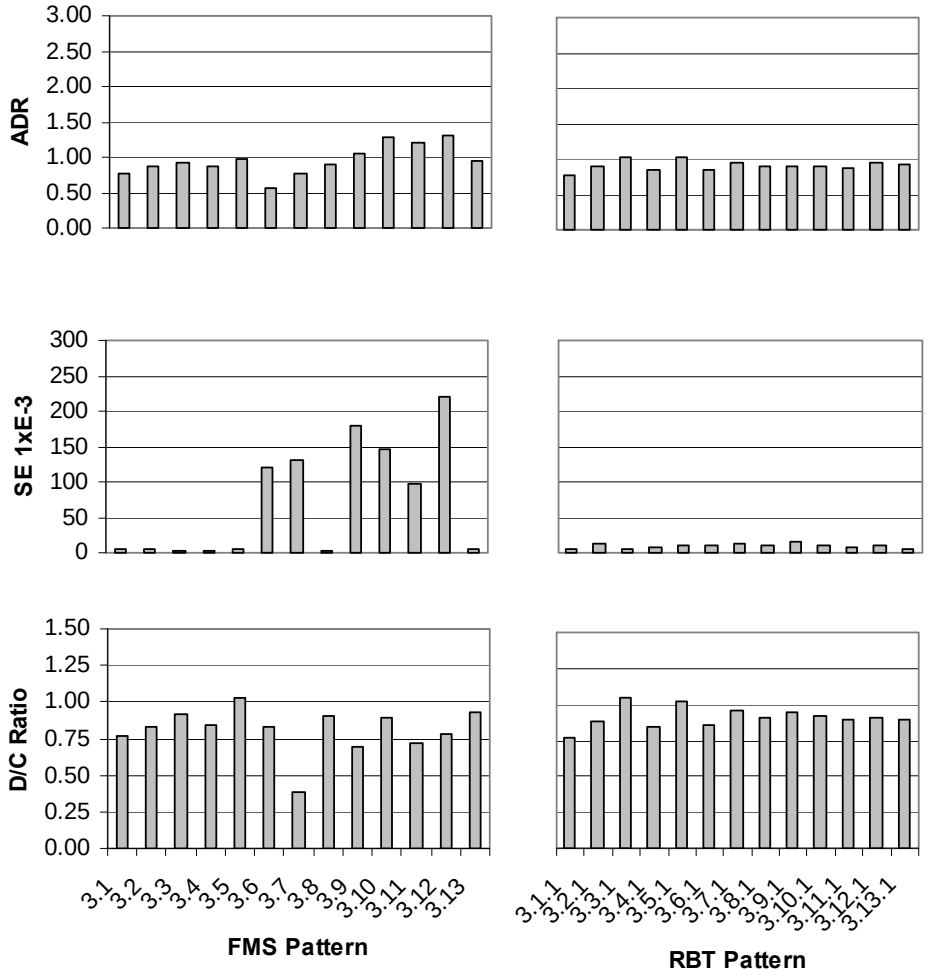

Figure 9. Performance indexes for Bridges with seat-type abutments

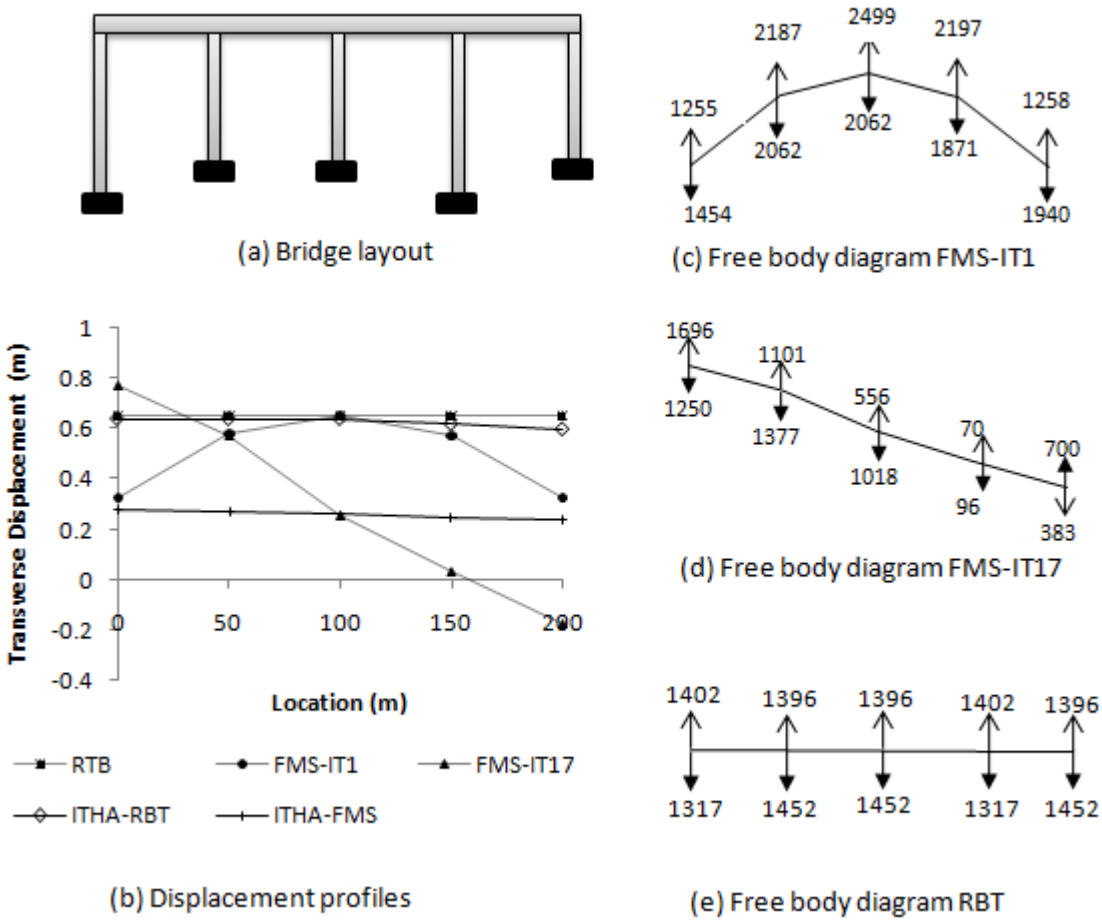

Figure 10. Design and analysis results for bridge 1.7

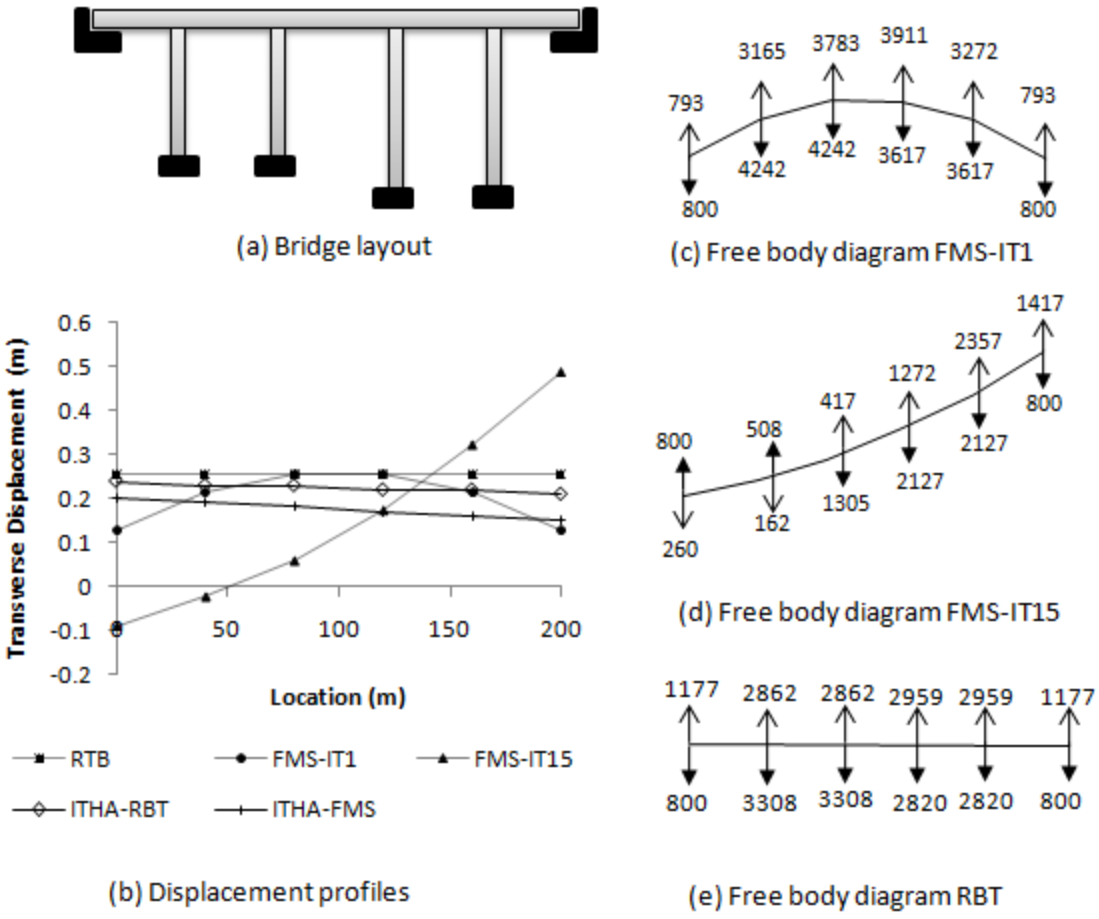

Figure 11. Design and analysis results for bridge 3.9

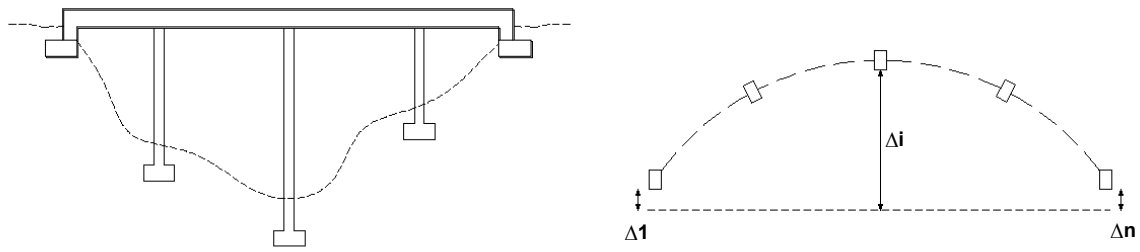

(a) Elevation view **(b) Plan view. Flexible displacement pattern**

Figure 12. Displacement pattern for a bridge with integral abutments

Table 3. Integral abutment bridge table

Bridge Layout

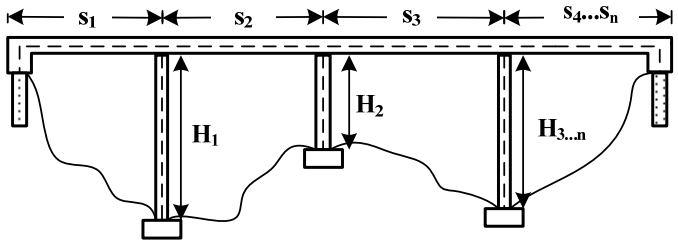

Code	Span length (m)				Pier height (m)			Displacement Pattern
	S_1	S_2	S_3	S_4	H_1	H_2	H_3	
2.1	50	50			7			FMS
2.2	50	50			15			FMS
2.3	30	30	30		12	12		FMS
2.4	50	50	50	50	18	18	20	FMS
2.5	50	50	50	50	6	8	6	FMS
2.6	50	50	50	50	9	8	9	FMS
2.7	50	50	50	50	9	14	9	FMS
2.8	50	50	50	50	12	18	9	FMS
2.9	50	50	50	50	16	18	19	FMS
2.10	50	50	50	50	20	20	20	FMS

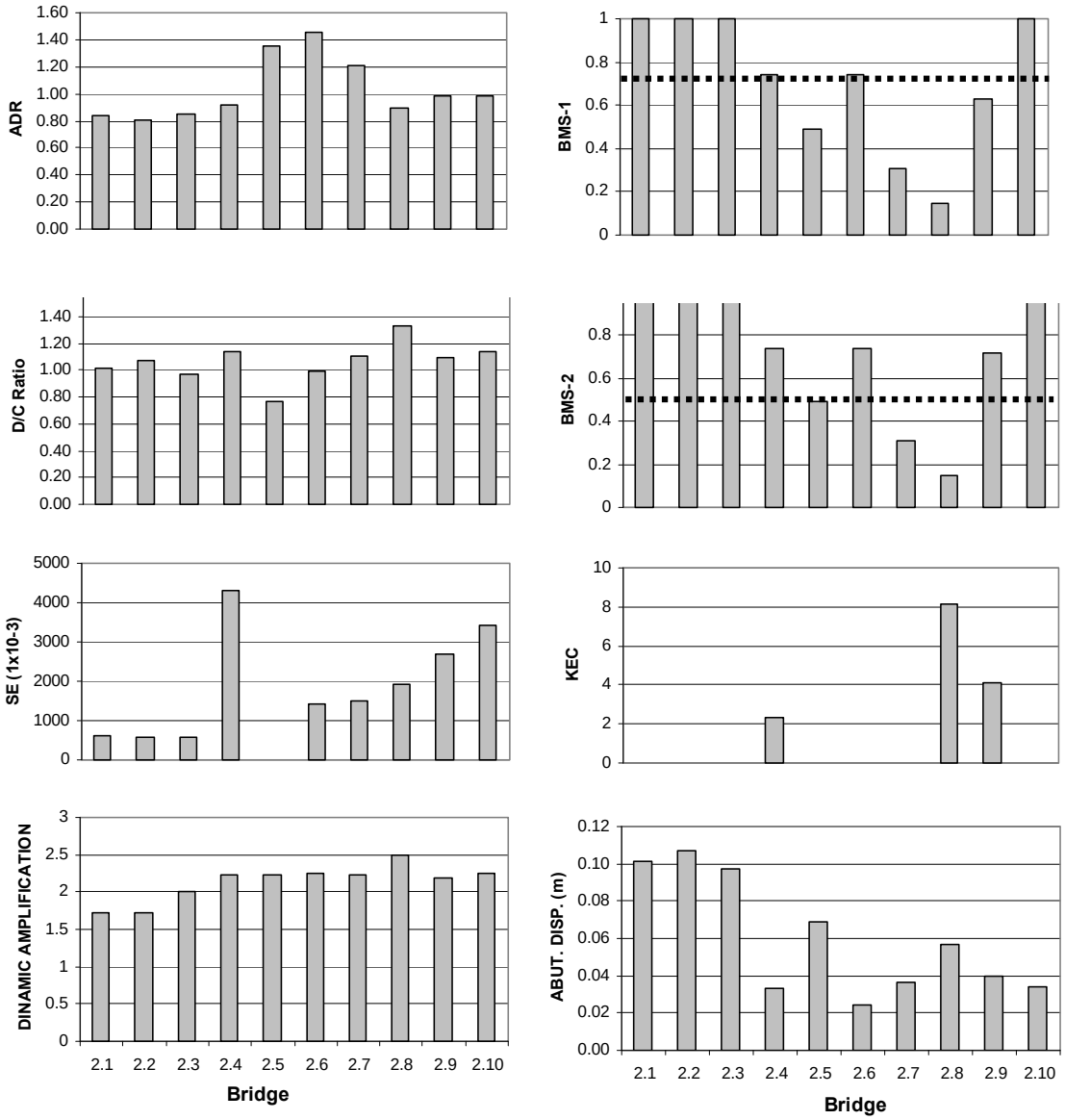

Figure 13. Design and ITHA results for bridges with integral abutments

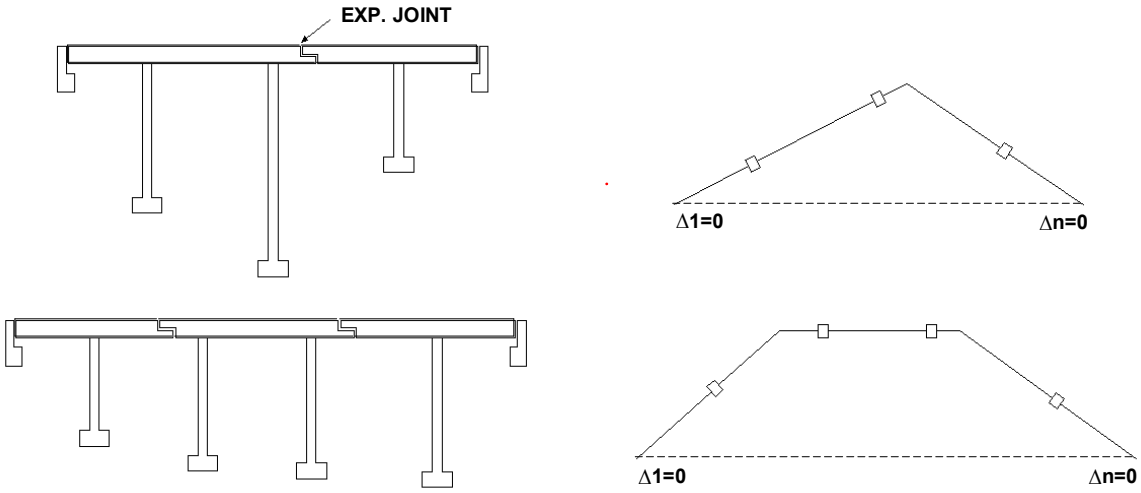

(a) Elevation view **(b) displacement pattern**

Figure 14. Displacement patterns for bridges with expansion joints

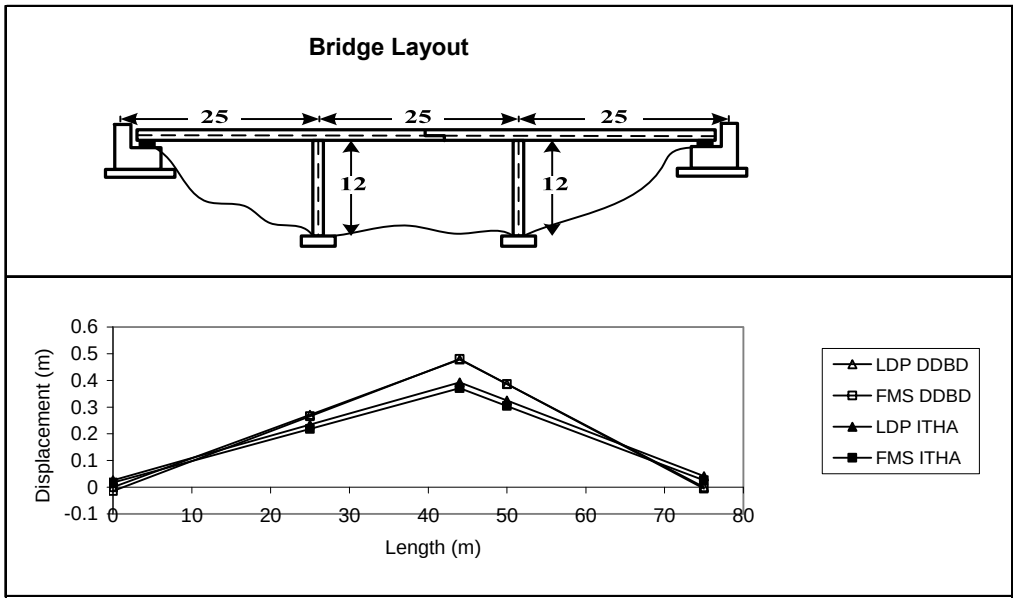

Figure 15. Symmetric bridge with one expansion joint

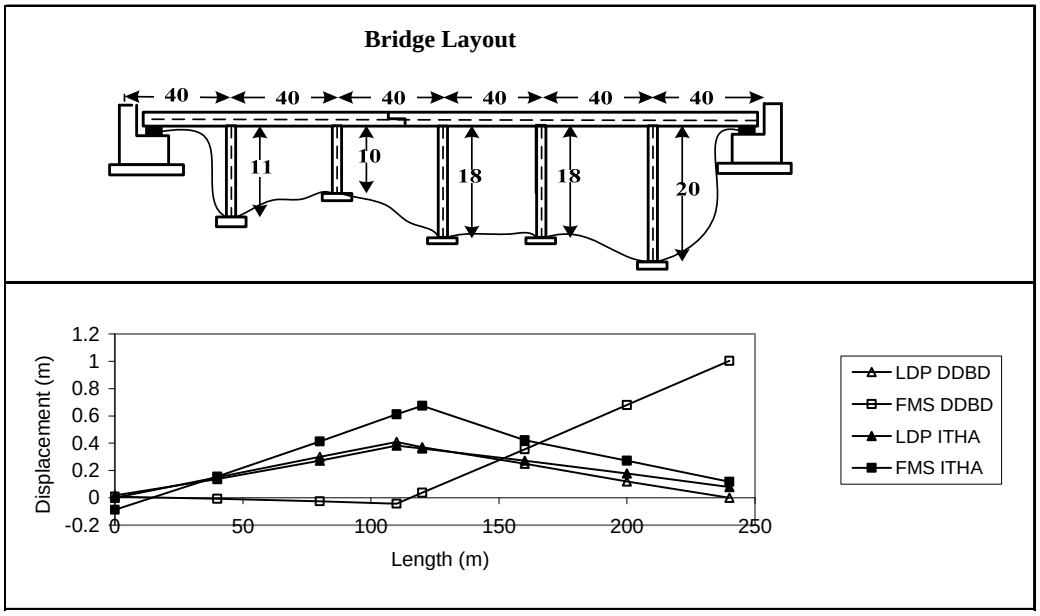

Figure 16. Asymmetric bridge with one expansion joint

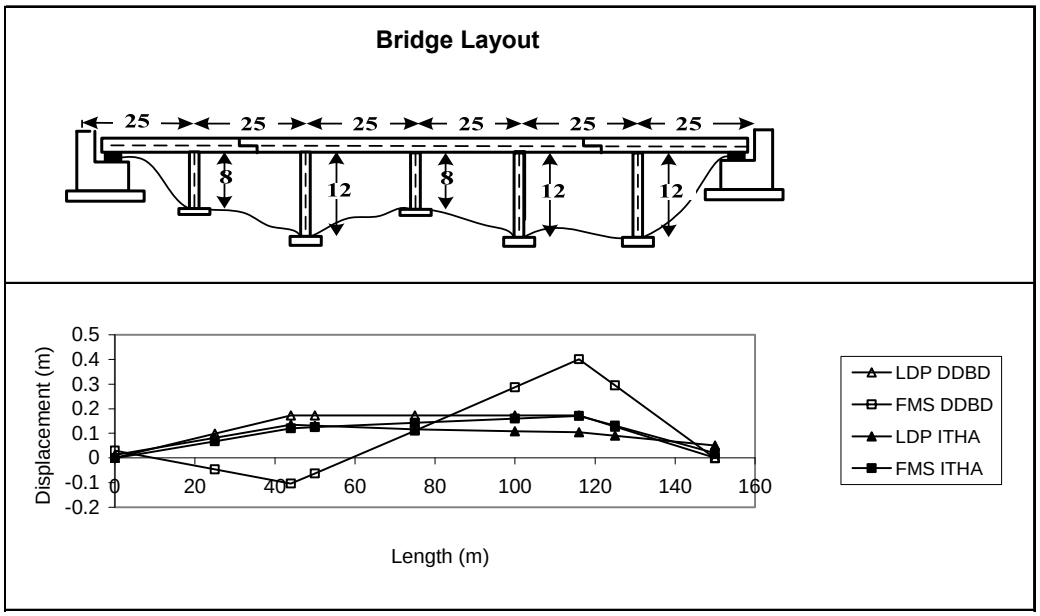

Figure 17. Asymmetric bridge with two expansion joints

Table 4. Displacement patterns for DDDBD of bridges

BRIDGE	BALANCED MASS AND STIFFNESS	NO BALANCED MASS AND STIFFNEES
FRAME	**RBT or EMS**	**EMS**
WEAK ABUTMENTS	**RBT or EMS**	**EMS**
STRONG ABUTMENTS	**FMS or EMS**	**FMS**
ONE EXPANSION JOINT	**LDP1 or EMS**	**EMS**
TWO EXPANSION JOINTS	**LDP2 or EMS**	**EMS**
MORE THAN TWO EXPANSION JOINTS	**EMS**	**EMS**
		

PART V

DETERMINATION OF A STABILITY BASED TARGET DISPLACEMENT FOR DIRECT DISPLACEMENT BASED DESIGN OF BRIDGES

Vinicio A. Suarez and Mervyn J. Kowalsky

Department of Civil, Construction and Environmental Engineering, North Carolina State University, Campus-Box 7908, Raleigh, NC-27695, USA

Formatted for submission to the Journal of Earthquake Engineering

ABSTRACT

This paper presents a model that allows the determination of a target displacement for bridge piers to meet a predefined limit in P-Δ effects. When a bridge is designed using the Direct Displacement-Based Design Method, P-Δ effects are checked at the end of the design process. If P-Δ effects exceed a maximum predefined stability limit, design must be repeated reducing the design target displacement. It is shown that the use of the proposed model eliminates this problem since a stability-based target displacement is computed at the beginning of the design process.

1. INTRODUCTION

The Direct Displacement Based Design method (DDBD) was first proposed by Priestley (1993) as a tool for Performance-Based Seismic Engineering. DDBD starts with a performance-based target displacement and returns the strength required to meet that performance under the design earthquake. The method has undergone extensive research, proven to be effective for performance-based seismic design of bridge piers (Kowalsky et al 1995, Suarez and Kowalsky 2007), continuous bridges (Calvi and Kingsley 1995, Dwairi and Kowalsky 2006, Ortiz 2006, Suarez 2008), buildings and other types of structures (Priestley et al, 2007).

DDBD uses the equivalent linearization approach proposed by Shibata and Sozen (1976) shown in Fig. 1. In this approach, the inelastic structure is substituted by an elastic system with secant stiffness and equivalent viscous damping. This, under earthquake excitation, exhibits the same maximum displacement as the original inelastic system.

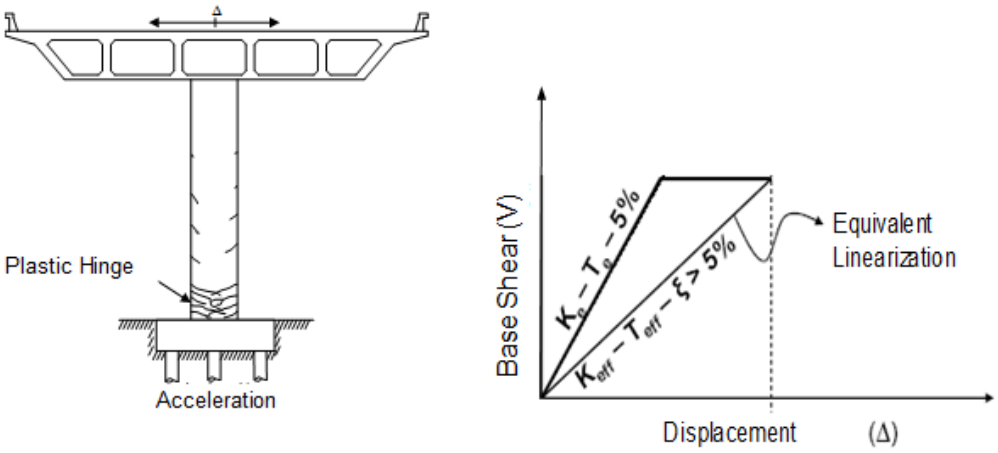

Figure 1 – Equivalent linearization

The main steps of the design procedure are presented in Fig. 2. The bridge is previously designed for non-seismic loads and the configuration, superstructure section and foundation are known. A design objective is proposed by defining the expected performance

and the seismic hazard. Then, the target displacement profile for the bridge is determined. Next, DDBD is applied in the longitudinal and transverse axes of the bridge, the results are combined, P-Δ effects are checked and reinforcement is designed and detailed following Capacity Design principles (Paulay and Priestley 1992).

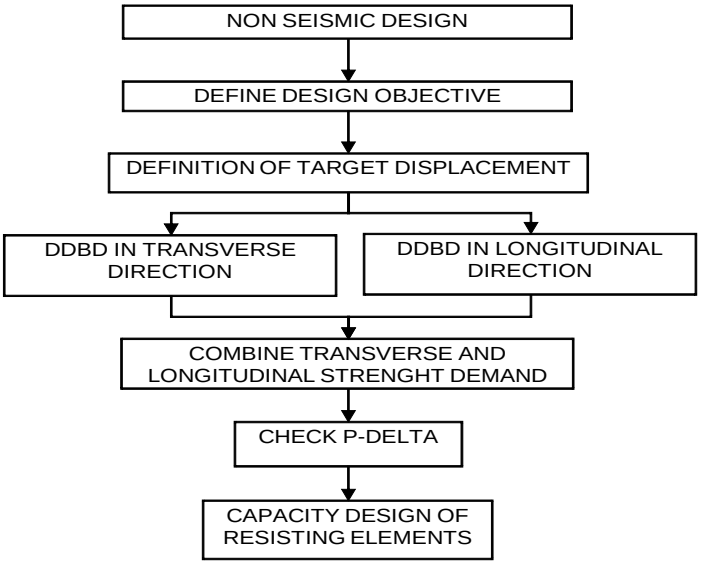

Figure 2 - DDBD main steps flowchart

The flowcharts in Fig. 3 show the procedure for DDBD in the transverse and longitudinal direction, as part of the general procedure shown in Fig. 2. As seen in Fig. 3, there are three variations of the procedure: (1) If the displacement pattern is known and predefined, DDBD is applied directly; (2) If the pattern is unknown but dominated by the first mode of vibration, a First Mode Shape (FMS) iterative algorithm is applied; (3) If the pattern is unknown but dominated by modal combination, an Effective Mode Shape (EMS) iterative algorithm is applied. The direct application of DDBD, when the displacement pattern is known, requires less effort than the FMS or EMS algorithms. Recent research by the authors (Suarez and Kowalsky, 2008) showed that predefined displacement patterns can be effectively used for design of bridge frames, bridges with seat-type of other type of weak abutments and bridges with one or two expansion

joints. These bridges must have a balanced distribution of mass and stiffness, according to AASHTO (Ibsen 2007).

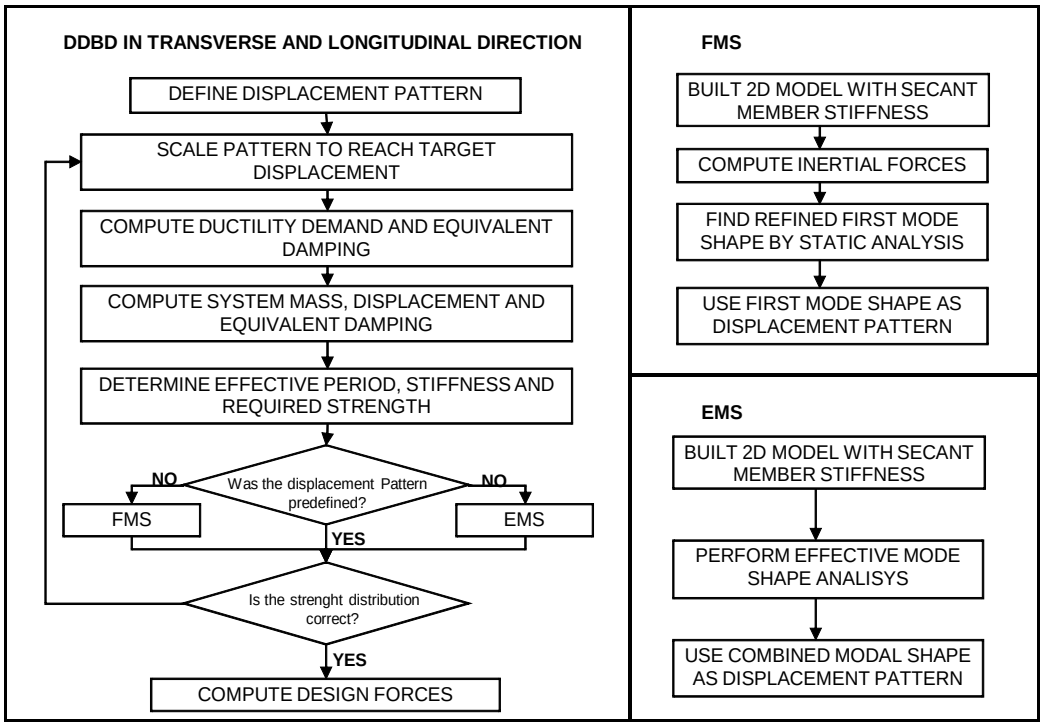

Figure 3 - Complementary DDBD flowcharts

2. P-Δ EFFECTS IN DDBD

Limiting P-Δ effects is necessary to preserve stability under earthquake attack. P-Δ effects can be quantified using a stability index θ_s. When designing a bridge pier, this index relates the P-Δ induced moment $M_{P-\Delta}$ to the flexural strength of the column section M_n (Eq. 1). If θ_s is less than 8%, P-Δ effects are insignificant and no action needs to be taken. If θ_s is greater than 8% but less than 30%, M_n must be increased by one half of $M_{P-\Delta}$ to counteract P-Δ effects. If θ_s is higher that 30% for any individual column of a bridge, DDBD must be repeated reducing the target displacement for that element (Priestley et al 2007). This causes

DDBD to be iterative and increases the design effort. Therefore the main objective of this paper is to develop a model to determine, before design is conducted, a target displacement to meet a predefined θ_s value, in this way eliminating the possibility of iteration in DDBD in the cases where P-Δ is critical.

$$\theta_s = \frac{M_{P-\Delta}}{M_n} \qquad \text{(Eq. 1)}$$

3. STABILITY-BASED TARGET DISPLACEMENT FOR PIERS DESIGNED AS STAND-ALONE STRUCTURES

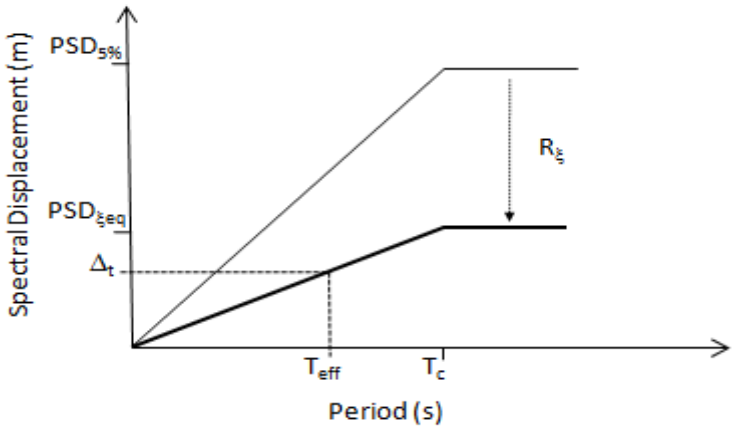

Figure 4 – Determination of the effective period

The DDBD of stand-alone bridge piers follows the general procedure in Fig. 2. If a pier such as the one shown in Fig. 1 is designed to meet a target displacement Δ_t during the design earthquake, the required effective period of the equivalent single degree of freedom system is given by Eq 2. This equation is based on Fig. 4, where the design earthquake is represented by a displacement design spectrum with 5% damping, Peak Spectrum Displacement PSD and corner period Tc that has been reduced to match the equivalent damping of the structure ξ_{eq} using the spectral reduction factor R_ξ.

$$T_{eff} = T_c \frac{\Delta_t}{PSD \cdot R_\xi} \qquad \text{(Eq.2)}$$

Once T_{eff} is known, the required strength V for the system is found with Eq. 3, from the well known relation between period, effective mass M_{eff} and stiffness of single degree of freedom systems.

$$V = \frac{4\pi^2 M_{eff}}{T_{eff}^{\ 2}} \Delta_t \qquad \text{(Eq. 3)}$$

Then, the required flexural strength of the pier is given by Eq. 4, in terms of the height, H_p and the factor Λ that distinguish between single bending or double bending in the pier. If Eq.2 is replaced in Eq. 3 and Eq. 3 is replaced in Eq. 4, Eq.5 is found. This equation allows direct calculation of the required flexural strength for the pier.

$$M_n = VH_p\Lambda \qquad \text{(Eq. 4)}$$

$$M_n = \frac{4\pi^2 M_{eff}}{\Delta_c}\left(\frac{PSD \cdot R_\xi}{T_c}\right)^2 H_p\Lambda \qquad \text{(Eq. 5)}$$

On the other hand, as the pier displaces to Δ_t, supporting an axial load P, the P-Δ moment $M_{P\text{-}\Delta}$ that develops in the pier is given by Eq. 6. If Eq.5 and Eq.6 are replaced in Eq. 1, Eq. 7 is found. In this equation target ductility μ_t has been introduced as ratio of Δ_t and yield displacement Δ_y. In the new equation all the terms on right side are known and can be estimated before design. Therefore, Eq. 7 can be written as Eq.8 where C is given by Eq. 9.

$$M_{P-\Delta} = P\Delta_t\Lambda \qquad \text{(Eq. 6)}$$

$$\frac{R_\xi}{\mu_t} = \frac{T_c\Delta_y}{2\pi PSD}\sqrt{\frac{P}{\theta_s M_{eff} H_p}} \qquad \text{(Eq. 7)}$$

$$\frac{R_\xi}{\mu_t} = C \qquad \text{(Eq. 8)}$$

$$C = \frac{T_c\Delta_y}{2\pi PSD}\sqrt{\frac{P}{\theta_s M_{eff} H}} \qquad \text{(Eq. 9)}$$

The reduction factor R_ξ is given in Eq. 10 to reduce the 5% damping design spectra to higher levels of damping. In this equation ξ_{eq} is the equivalent damping of the system and k is a constant that equals 0.25 for near fault sites and 0.5 for other sites (EuroCode 1998).

$$R_\xi = \left(\frac{7}{2 + \xi_{eq}} \right)^k \qquad \text{(Eq. 10)}$$

Several equivalent damping studies have been performed to obtain equivalent damping models suitable for DDBD (Dwairi 2005, Blandon 2005, Suarez 2006, Priestley et al 2007). These models relate equivalent damping to ductility at target displacement. For reinforced concrete columns supported on rigid foundation ξ_{eq} is computed with Eq. 11 (Priestley, 2007).

$$\xi_{eq} = 5 + 44.4 \frac{\mu_t - 1}{\pi \mu_t} \qquad \text{(Eq. 11)}$$

For extended drilled shaft bents embedded in soft soils, the equivalent damping is computed as a combination of hysteretic damping, $\xi_{eq,h}$, and tangent stiffness proportional viscous damping, ξ_v, with Eq. 12 (Priestley and Grant, 2005). The hysteretic damping is computed with Eq. 13 as a function of the ductility in the drilled shaft. The values of the parameters *p* and *q* are given in Table 1 for different types of soils and boundary conditions (Suarez 2006). In Table 1, clay-20 and clay-40 refer to clay soils with shear strengths of 20 kPa and 40 kPa respectively. Sand-30 and Sand-37 refer to sand with friction angles of 30 and 37 degrees respectively. A fixed head implies that the head of the extended drilled shaft displaces laterally without rotation causing double bending in the element. On the contrary, a pinned head implies lateral displacement with rotation and single bending. To use Eq. 12, ξ_v should be taken as 5%. This value is typically used as by default to develop design spectra.

$$\xi_{eq} = \xi_v \mu^{-0.378} + \xi_{eq,h} \qquad \mu \geq 1 \qquad \text{(Eq. 12)}$$

$$\xi_{eq,h} = p + q\frac{\mu - 1}{\mu} \qquad \mu \geq 1 \qquad \text{(Eq. 13)}$$

Table 1. Parameters for hysteretic damping models in drilled shaft - soil systems

HEAD	SOIL	p	q
Fixed	Clay-20	6.70	8.10
Fixed	Clay-40	5.60	8.70
Fixed	Sand-30	2.40	10.20
Fixed	Sand-37	2.00	9.60
Pinned	Clay-20	15.80	9.40
Pinned	Clay-40	13.70	10.90
Pinned	Sand-30	9.40	11.20
Pinned	Sand-37	8.50	10.40

All damping models are plotted in Fig. 5. This figure shows equivalent damping vs. ductility in the column or shaft. It is observed that when ductility equals one, the equivalent damping for the column on a rigid foundation equals 5% (i.e. the elastic viscous damping level) whereas the equivalent damping for the drilled shafts is higher than 5%. This increment in damping comes from the soil which performs inelastically and dissipates energy at displacements that are less than the displacement that causes yielding of the reinforced concrete section. For cases where the target displacement is less than the yield displacement of the element, a linear relation between damping and ductility seems appropriate. Such a relation is given by Eq. 14.

$$\xi_{eq} = \xi_v + (q - \xi_v)\mu \qquad \mu < 1 \qquad \text{(Eq. 14)}$$

It is observed then that if C is computed before design with Eq. 9, Eq. 8 could be solved for ductility, since R_ξ is a function of ductility only. This results in the target ductility to meet a predefined $\theta_{s,}$ therefore the nomenclature is changed to $\mu_{\theta s.}$ Although there is not a close formed solution for Eq. 8, an approximate solution can be obtained in the form of Eq 15. Where the parameters *a,b,c* and *d* are given in Table 2 and 3 for the different equivalent damping models and for far fault and near fault conditions.

$$\mu_{\theta s} = a + bC + c\frac{C-d}{C} \qquad \text{(Eq. 15)}$$

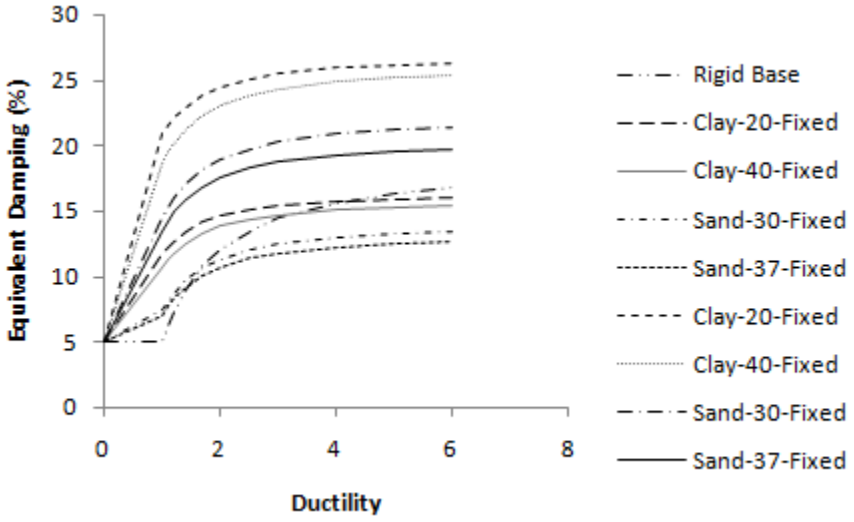

Figure 5. Equivalent damping models for bridge piers

Table 2. Parameters to define Eq.15 for far fault sites

	Rigid Base	Clay-20 Pinned	Clay-20 Fixed	Clay-40 Pinned	Clay-40 Fixed	Sand-30 Pinned	Sand-30 Fixed	Sand-37 Pinned	Sand-37 Fixed
a	1.256	0.839	0.885	0.961	0.909	1.010	1.468	1.105	1.053
b	-0.127	-0.021	-0.034	-0.042	-0.043	-0.047	-0.078	-0.055	-0.061
c	-0.766	-0.657	-0.693	-0.737	-0.697	-0.774	-1.160	-0.847	-0.792
d	0.731	0.724	0.860	0.644	0.877	0.677	0.546	0.620	0.852

Table 3. Parameters to define Eq.15 for near fault sites

	Rigid Base	Clay-20 Pinned	Clay-20 Fixed	Clay-40 Pinned	Clay-40 Fixed	Sand-30 Pinned	Sand-30 Fixed	Sand-37 Pinned	Sand-37 Fixed
a	1.146	0.803	0.924	0.868	0.912	0.963	1.210	0.966	1.053
b	-0.112	0.000	-0.013	-0.015	-0.023	-0.028	-0.035	-0.019	-0.061
c	-0.799	-0.728	-0.833	-0.754	-0.793	-0.814	-1.058	-0.850	-0.792
d	0.917	0.965	0.939	0.920	0.980	0.869	0.759	0.869	0.852

The values for the parameters shown in Tables 2 and 3 were obtained using the optimization tool Solver (Frontline 2008) to minimize the squared error between the values generated from Eq. 8 and those from Eq. 15. The four parameter model shown in Eq. 15 was chosen over other models since it best predicted the values obtained by iterative solution of Eq. 8. The resultant $\mu_{\theta s}$ vs. C relations for the different foundation conditions are plotted for comparison in Fig. 6 and Fig. 7 for far fault and near fault sites respectively. The following observations are made:

- In both figures it is observed than ductility is very sensitive to changes in C when C is less than 0.5
- If two piers have the same value of C, the one with more damping develops less ductility to reach the stability limit. The reason is that the pier with less damping requires more strength.
- The different damping models have less effect in the relation between $\mu_{\theta s}$ and C for near fault sites. This results from the use of k = 0.25 is Eq. 10

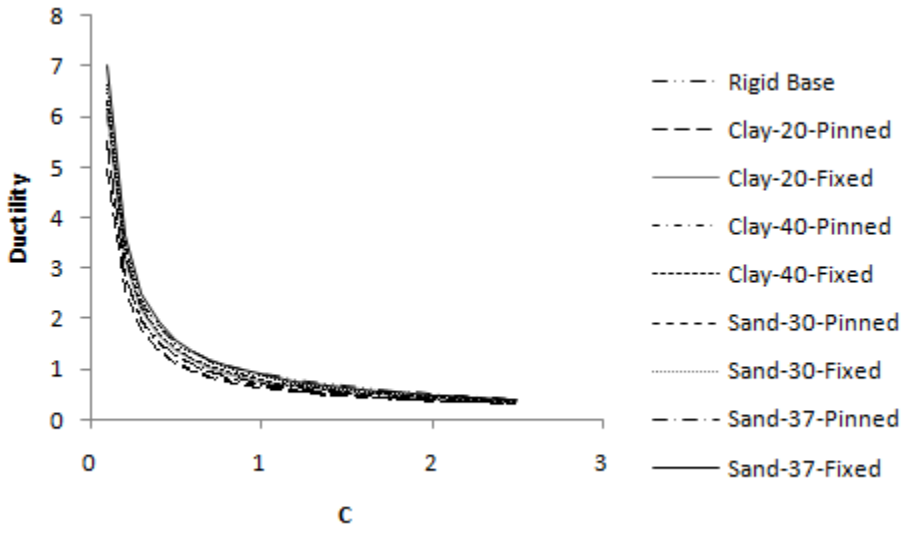

Figure 6. P-Δ Ductility for far fault sites

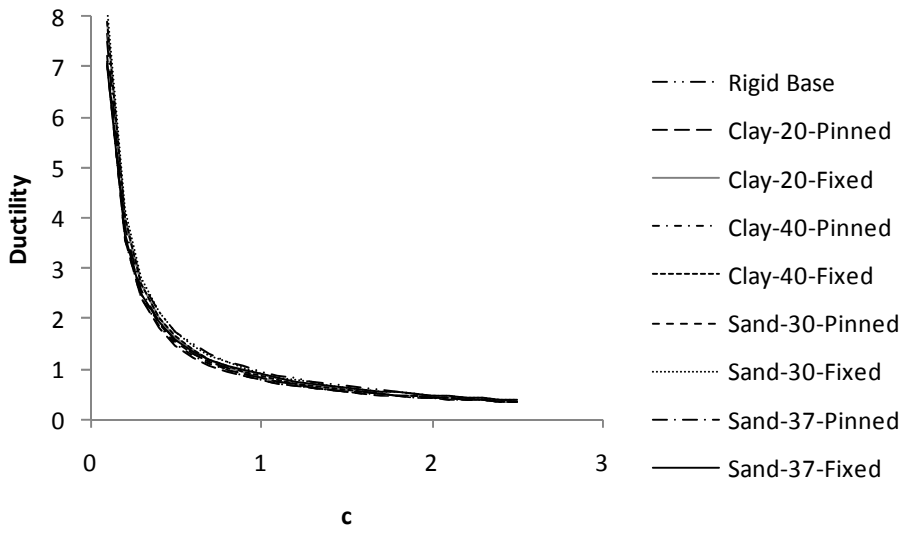

Figure 7. P-Δ Ductility for near fault sites

The use of Eq. 15 avoids the need of iteration in DDBD for designs controlled by P-Δ effects. The proposed model is appropriate for piers in single and double bending since Λ cancels out in the derivation. This model has been derived for piers as stand-alone structures and can be used in the in-plane or out-of-plane direction of the pier. The effective mass M_{eff}, can be computed taking a tributary area of superstructure and adding the mass of the cap-beam and a portion of the mass of the columns. The application of the model is demonstrated in the following examples.

3.1 DDBD of a two-column drilled shaft in sand

The drilled shaft bent shown in Fig. 8 is designed with DDBD using the proposed model in the in-plane and out-of-plane directions. The design is repeated for tree levels of seismic hazard and performance that agree with Seismic Design Categories SDC "D", "C", and "B" of AASHTO Guide Specifications for LFRD Seismic Bridge Design (Imbsen, 2007). For each SDC, the aspect ratio of the bent is varied from 3 to 15. This value is computed as the

ratio between the above ground height *La* of the bent and the diameter *D* of the extended shaft.

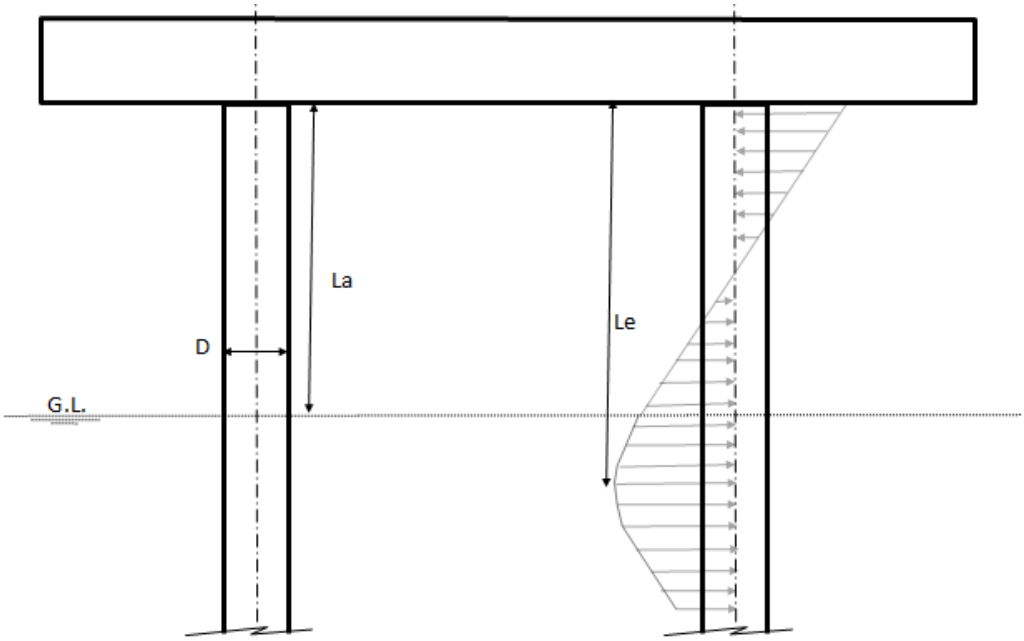

Figure 8. Drilled shaft bent is sand

The diameter and embedded length is supposed to satisfy a geotechnical design. The diameter of the drilled shafts is D =1.2 m. The axial load at the top of each drilled shaft is 2714 kN, which gives an axial load ratio of 10%. The bent is embedded in saturated sand with a friction angle $\phi = 37^{o}$. The reinforced concrete in the extended drilled shafts and cap-beam has an expected compressive strength f'_{ce} = 31.2 MPa. The reinforcing steel has yield stress f_y = 420 MPa and its strain at maximum stress is ε_{su} = 0.1.

The objective of this example are two: 1) Investigate the conditions under which P-Δ effects control design and 2) Observe the effectiveness of the proposed model to produce a stability based target displacement.

Seismic hazard

The displacement spectra corresponding to SDCs “B”, “C” and “D” are shown in Fig. 9. This figure also includes the PSD, Tc, and one second spectral acceleration SD_1 for each spectrum. According to AASHTO (Imbsen, 2007), if SD1 is equal or less than 0.30 g design is given a SDC “B”. If SD1 is less or equal to 0.5 g design is given a SDC “C” and if SD1 > 0.5 g design is given a SDC “D”.

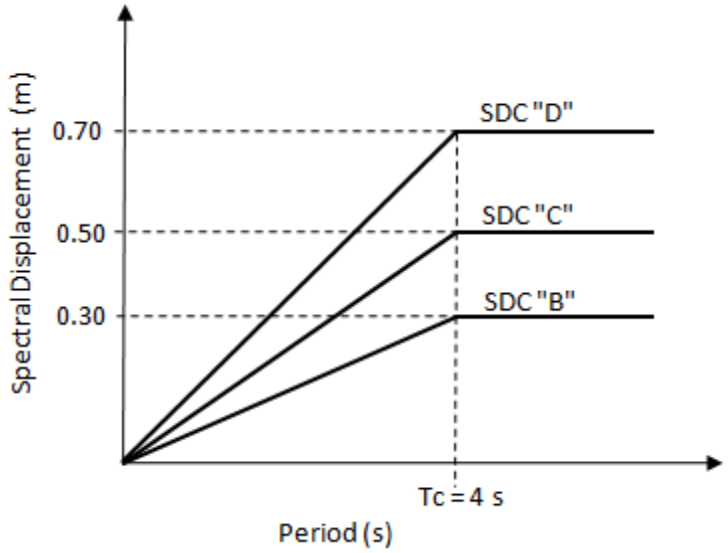

Figure 9 – Displacement design spectra form SDC D, C and B

Damage-based target displacements

The AASHTO Specification links seismic hazard in each SDC to predefined level of damage given as displacement capacity. For SDC “B” the displacement capacity is computed using Eq. 16. This equation implies minimal plastic action with displacement ductility equal or less than two (Imbsen, 2007) . For SDC “C” the displacement capacity is computed using Eq. 17. This equation implies moderate plastic action with displacement ductility equal or less than three (Imbsen, 2007). In this equations H_c is the clear height of the columns and Λ is 1 for columns in single bending and 2 for columns in double bending.

$$\Delta_c = 0.003H_c\left(-2.32\ln\left(\frac{D}{H_c}\Lambda\right)-1.22\right)\geq 0.003H_c \qquad \text{(m)} \qquad \text{(Eq. 16)}$$

$$\Delta_c = 0.003H_c\left(-1.27\ln\left(\frac{D}{H_c}\Lambda\right)-0.32\right)\geq 0.003H_c \qquad \text{(m)} \qquad \text{(Eq. 17)}$$

Structures in SDC "D" are designed for full ductile response. A damage-control displacement for the bent, Δ_{DC} can determined with the plastic hinge method using Eq. 18 and Eq. 19 for the in-plane and out-of-plane directions. In these equations, ϕ_{dc} and ϕ_y are the damage-control and yield curvatures, L_p is the plastic hinge length, H_{in} and H_{out} are the effective heights in the in-plane and out-of-plane directions respectively.

$$\Delta_{DC,in} = \Delta_{y,in} + (\phi_{dc} - \phi_y)L_p H_{in} \qquad \text{(Eq. 18)}$$

$$\Delta_{DC,out} = \Delta_{y,out} + (\phi_{dc} - \phi_y)L_p H_{out} \qquad \text{(Eq. 19)}$$

The yield curvature ϕ_y can be estimated with Eq. 20 in terms of the yield strain of the flexural reinforcement, ε_y, and diameter of the section (Priestley, 2007). The damage-control curvatures ϕ_{dc} is estimated with Eq. 21 in terms of the damage control strain $\varepsilon_{c,dc}$ of the confined concrete core (Eq. 22), diameter of the section, strain at maximum stress of the flexural steel steel ε_{su} , yield stress of the transverse steel f_{yh}, transverse reinforcement volumetric ratio ρ_v, expected compressive strength of concrete f'_{ce} (Eq. 26) and compressive strength of the confined concrete f'_{cc} (Eq. 23). An estimate of the neutral axis depth c is given in Eq. 24. Where A_g is the area of the section and P is the axial load. The damage control strain is based on the model proposed by Mander (1988).

$$\phi_y = 2.25\frac{\varepsilon_y}{D} \qquad \text{(Eq. 20)}$$

$$\phi_{dc} = \frac{\varepsilon_{c,dc}}{c} \qquad \text{(Eq. 21)}$$

$$\varepsilon_{c,dc} = 0.004 + 1.4\frac{\rho_v f_{yh}\varepsilon_{su}}{f'_{cc`}} \quad \text{(Eq.22)}$$

$$f'_{cc} = f'_{ce}\left(2.254\sqrt{1+\frac{7.94 f_1}{f'_{ce}}} - 2\frac{f_1}{f'_{ce}} - 1.254\right) \qquad f_1 = 0.5\rho_v f_{yh} \quad \text{(Eq. 23)}$$

$$c = 0.2D\left(1 + 3.25\frac{P}{f'_{ce} A_g}\right) \quad \text{(Eq. 24)}$$

$$f_{ye} = 1.1 f_y \quad \text{(Eq. 25)}$$

$$f'_{ce} = 1.3 f'_c \quad \text{(Eq. 26)}$$

An equivalent model (Suarez and Kowalsky 2007) is used to replace the soil-bent system for an equivalent bent fixed at its base. The equivalent bent has an effective length L_e to match the location of the underground plastic hinge in the real system. The yield displacement is matched by an appropriate value for α in Eq 27 and Eq 28 for the in-plane and out-of-plane directions respectively. For bents embedded in sand with a friction angle $\phi = 37^o$, L_e is given by Eq. 29 This value valid for the in-plane and out of plane directions. The coefficient alpha is computed with Eq. 30 for pinned head condition and with Eq. 31 for fixed head condition. Assuming pinned head condition is appropriate for out-of-plane response of the bent since the connection between the bent and the superstructure is not integral. Assuming fixed head condition is appropriate for in-plane design since the stiffer cap-beam restrains the rotation of the top of the extended drilled shafts.

$$\Delta_{y,in} = \alpha_{in}\frac{\phi_y L_e^{\,2}}{6} \quad \text{(Eq. 27)}$$

$$\Delta_{y,out} = \alpha_{out}\frac{\phi_y L_e^{\,2}}{3} \quad \text{(Eq. 28)}$$

$$L_e = (3.4 + 0.84\frac{L_a}{D})D \quad \text{(Eq. 29)}$$

$$\alpha_{in} = 1.86 - 0.18 \ln\left(\frac{L_a}{D}\right) \quad \text{(Eq. 30)}$$

$$\alpha_{out} = 3.41 - 0.69 \ln\left(\frac{L_a}{D}\right) \quad \text{(Eq. 31)}$$

The yield strain of the flexural reinforcement is $\varepsilon_y = f_{ye}/E_s = 0.0022$. Therefore the yield curvature of the section is $\phi_y = 0.00375$ 1/m (Eq. 20). The yield displacement and other parameters of the equivalent model are shown in Table 4 for different aspect ratios.

Table 4 – Yield displacement and equivalent model parameters for bent in sand

Aspect Ratio	D (m)	L_a (m)	L_a/D	L_e (m)	In-plane		out-of-plane	
					α_{in}	$\Delta_{y,in}$ (m)	α_{out}	$\Delta_{y,out}$ (m)
3	1.2	3.6	3	7.10	1.6622	0.0524	2.652	0.167
4	1.2	4.8	4	8.11	1.6105	0.0662	2.453	0.202
5	1.2	6	5	9.12	1.5703	0.0816	2.299	0.239
6	1.2	7.2	6	10.13	1.5375	0.0986	2.174	0.279
7	1.2	8.4	7	11.14	1.5097	0.117	2.067	0.320
8	1.2	9.6	8	12.14	1.4857	0.1369	1.975	0.364
9	1.2	10.8	9	13.15	1.4645	0.1583	1.894	0.410
10	1.2	12	10	14.16	1.4455	0.1811	1.821	0.456
11	1.2	13.2	11	15.17	1.4284	0.2054	1.755	0.505
12	1.2	14.4	12	16.18	1.4127	0.231	1.695	0.555
13	1.2	15.6	13	17.18	1.3983	0.2581	1.640	0.605
14	1.2	16.8	14	18.19	1.385	0.2865	1.589	0.657
15	1.2	18	15	19.20	1.3726	0.3162	1.541	0.710

In the in-plane direction, the target displacement Δ_D and the ductility at target displacement μ_D are obtained for the SDC "B" and SDC "C" are computing using Eq. 16 and Eq. 17 with $H_c = L_e$ and $\Lambda = 1$. These results are shown in Table 5 for different aspect ratios. It is observed that ductility is less than the limits intended for the corresponding SDCs. This is because Eq. 16 and Eq. 17 were developed for columns that are fixed at their bases. Therefore, even though the flexibility that the soil adds to the bent is partially accounted by using Le instead of La, these equations do not account for the rotation at the point of maximum moment or the shape of the curvature profile in the real shaft-soil system.

The determination of the damage control target displacement for SDC "D" requires knowledge of the transverse reinforcement in the drilled shaft section. Based on minimum requirements of AASHTO regarding bar size and spacing of reinforcement, a D16 spiral spaced 150 mm is be used. This gives a volumetric ratio ρ_v = 0.48% and a target concrete strain ε_{cd} = 0.012 computed with Eq.22. Next, a neutral axis depth c = 0.3 m is estimated with Eq. 24 and a damage control curvature is ϕ_{dc} = 0.0383 1/m is found with Eq. 21.

In the in-plane direction, the plastic hinge length Lp is computed with Eq. 32. Finally the target displacement Δ_D is computed with Eq. 18. The results of these calculations are summarized in Table 5. Also include in that Table is the ductility at the damage control displacement μ_D.

$$Lp_{in} = k\frac{Le}{2} \qquad k = 0.2\left(\frac{f_u}{f_y} - 1\right) \le 0.07 \qquad \text{(Eq. 32)}$$

Table 5 – In-plane damage-based target displacements for drilled shaft bent in sand

Aspect Ratio	SDC "B"		SDC "C"		SDC "D"		
	Δ_D (m)	μ_D	Δ_D (m)	μ_D	l_p (m)	Δ_D (m)	μ_D
3	0.075	1.4	0.092	1.8	0.284	0.144	2.8
4	0.100	1.5	0.130	2.0	0.324	0.186	2.8
5	0.125	1.5	0.171	2.1	0.365	0.233	2.9
6	0.153	1.6	0.215	2.2	0.405	0.285	2.9
7	0.181	1.6	0.261	2.2	0.445	0.343	2.9
8	0.211	1.5	0.309	2.3	0.486	0.406	3.0
9	0.242	1.5	0.359	2.3	0.526	0.473	3.0
10	0.274	1.5	0.410	2.3	0.566	0.546	3.0
11	0.307	1.5	0.464	2.3	0.607	0.624	3.0
12	0.340	1.5	0.519	2.2	0.647	0.708	3.1
13	0.375	1.5	0.575	2.2	0.687	0.796	3.1
14	0.410	1.4	0.633	2.2	0.728	0.889	3.1
15	0.446	1.4	0.692	2.2	0.768	0.988	3.1

Stability-based target displacements

The stability-based target displacement is computed based on the ductility determined with Eq. 15 and Eq. 9, replacing H by Le. The stability-based displacement is the product of Δ_y and μ_θ. The results of these calculations are presented in Table 6 for the different SDCs y aspect ratios.

Table 6 – In-plane stability-based target displacements for drilled shaft bent in sand

Aspect Ratio	SDC "B"			SDC "C"			SDC "D"		
	C	μ_θ	Δ_θ	C	μ_θ	Δ_θ	C	μ_θ	Δ_θ
3	0.239	2.9	0.150	0.143	4.5	0.238	0.102	6.2	0.327
4	0.282	2.5	0.163	0.169	3.9	0.258	0.121	5.3	0.353
5	0.328	2.2	0.176	0.197	3.4	0.277	0.141	4.6	0.378
6	0.376	1.9	0.189	0.226	3.0	0.296	0.161	4.1	0.402
7	0.426	1.7	0.202	0.255	2.7	0.315	0.182	3.6	0.426
8	0.477	1.6	0.215	0.286	2.4	0.333	0.204	3.3	0.449
9	0.530	1.4	0.228	0.318	2.2	0.351	0.227	3.0	0.473
10	0.584	1.3	0.241	0.350	2.0	0.369	0.250	2.7	0.496
11	0.640	1.2	0.254	0.384	1.9	0.387	0.274	2.5	0.518
12	0.697	1.2	0.266	0.418	1.8	0.405	0.299	2.3	0.541
13	0.755	1.1	0.279	0.453	1.6	0.423	0.324	2.2	0.563
14	0.815	1.0	0.291	0.489	1.5	0.441	0.349	2.0	0.586
15	0.876	1.0	0.304	0.525	1.4	0.458	0.375	1.9	0.608

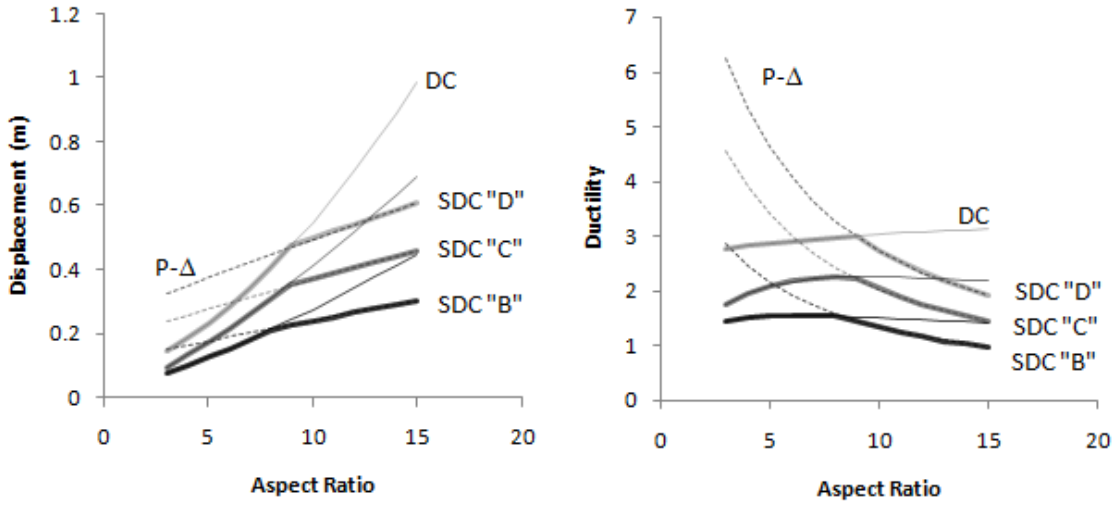

Figure 10 - a) In-plane target displacement vs. aspect ratio. b) In-plane target ductility vs. aspect ratio

Design target-displacement

The design target displacement is the minimum of the damage-based displacement and stability-based displacement. These values are shown in Fig. 10a for the three SDCs. The Damage-Based (DB) displacements are shown with the light continuous lines and the stability-based (SB) displacements are shown with the dotted lines. The design target displacements are shown with the heavy lines. The ductility that correspond to the target displacements are shown in Fig. 10b. In both figures it is observed that the stability based displacements control design for aspect ratios greater than 8. It is also observed that when stability controls, ductility decreases as aspect ratio increases.

Required strength

Continuing DDBD using the envelope of the target displacements shown in Fig 10a, the next step is to compute the equivalent damping of the system using Eq, 12 for the in-plane direction. Then the required effective period is found for each SDC with Eq. 2, the required strength is computed with Eq, 3 and the required flexural strength with Eq. 4. Finally, the stability index is checked (Eq. 1) and the flexural reinforcement is designed. These values are presented in Table 7 and the computed stability indexes are shown in Figure 11. It is observed that the stability index reach the target limit of 0.3 when design is controlled by P-Δ effects. This proves the effectiveness of the proposed model to give a target displacement to meet a predefined stability criterion. Since the predefined limit for the stability index is not exceeded, no iteration is needed.

Repeating DDBD in the out-of-plane direction results in the target ductility shown in Fig. 12a. In this case the stability based target displacement controls design for all aspect ratios in SDC “D” and for aspect ratios greater than four for SDCs “B” and “C”. It is observed that in for the more slender bents, the stability based target displacement is less than the yield displacement of the bent (ductility < 1). This means that the bent is designed to perform elastically. The check of stability index at the end of DDBD shown in Fig. 12b demonstrates that P-Δ effects are effectively controlled by the proposed model and that no

iteration is required. By comparing the required flexural strength in the in-plane and out-of-plane directions, it is found that for small aspect ratios, the flexural reinforcement is controlled by design in the in-plane direction and for larger aspect ratios it is controlled by the out-of-plane design. This means that the stability index computed for the non controlling direction is actually less than what was predicted since the flexural strength provided to the section is higher than required in that direction. This however has no relevance for design since the stability index is exact in the direction controlling design. A similar case occurs when flexural strength is governed by the code minimum steel ratio.

Table 7 – In-plane design results for drilled shaft bent in sand

Aspect Ratio	SDC "B"					SDC "C"					SDC "D"				
	ξ	T_{eff}	V (kN)	M (kN.m	θ	ξ	T_{eff}	V (kN)	M (kN.m	θ	ξ	T_{eff}	V (kN)	M (kN.m	θ
3	9.3	1.3	507	2700	0.04	10.2	1.0	1063	3774	0.03	11.6	1.1	1197	4253	0.05
4	9.5	1.7	375	2700	0.05	10.6	1.4	727	2950	0.06	11.6	1.5	926	3755	0.07
5	9.6	2.2	295	2700	0.06	10.8	1.9	544	2700	0.09	11.6	1.9	737	3361	0.09
6	9.7	2.6	241	2700	0.08	10.9	2.3	430	2700	0.11	11.7	2.3	601	3042	0.13
7	9.7	3.1	203	2700	0.09	11.0	2.8	352	2700	0.13	11.7	2.7	499	2779	0.17
8	9.6	3.6	175	2700	0.11	11.0	3.4	297	2700	0.16	11.7	3.2	421	2700	0.20
9	9.3	3.9	167	2700	0.11	11.0	3.8	262	2700	0.18	11.7	3.8	361	2700	0.24
10	8.9	4.0	164	2700	0.12	10.7	4.0	254	2700	0.19	11.5	3.9	349	2700	0.25
11	8.4	4.1	162	2700	0.13	10.5	4.1	248	2700	0.19	11.3	4.1	339	2700	0.26
12	8.0	4.2	161	2700	0.13	10.2	4.3	242	2700	0.20	11.1	4.2	329	2700	0.27
13	7.6	4.3	161	2700	0.14	9.9	4.4	237	2700	0.21	10.9	4.4	321	2759	0.28
14	7.1	4.4	162	2700	0.15	9.6	4.5	233	2700	0.22	10.7	4.5	314	2855	0.28
15	6.9	4.6	159	2700	0.15	9.3	4.7	230	2700	0.23	10.5	4.6	307	2951	0.28

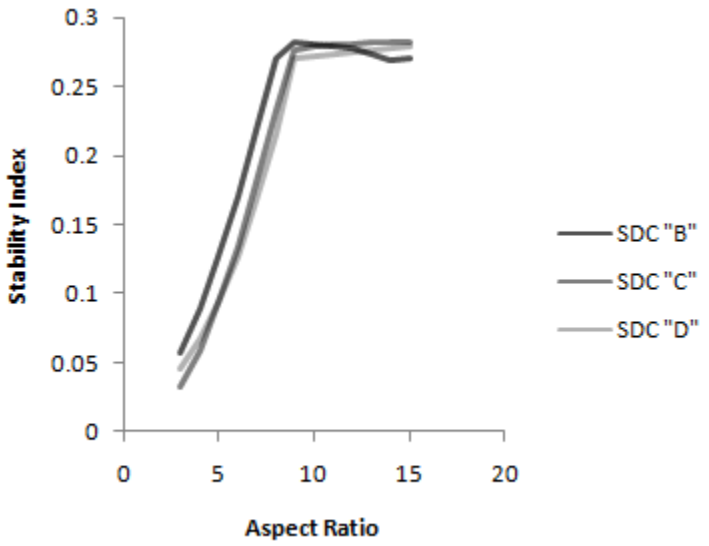

Figure 11 – Stability index computed after DDBD of drilled shaft bent

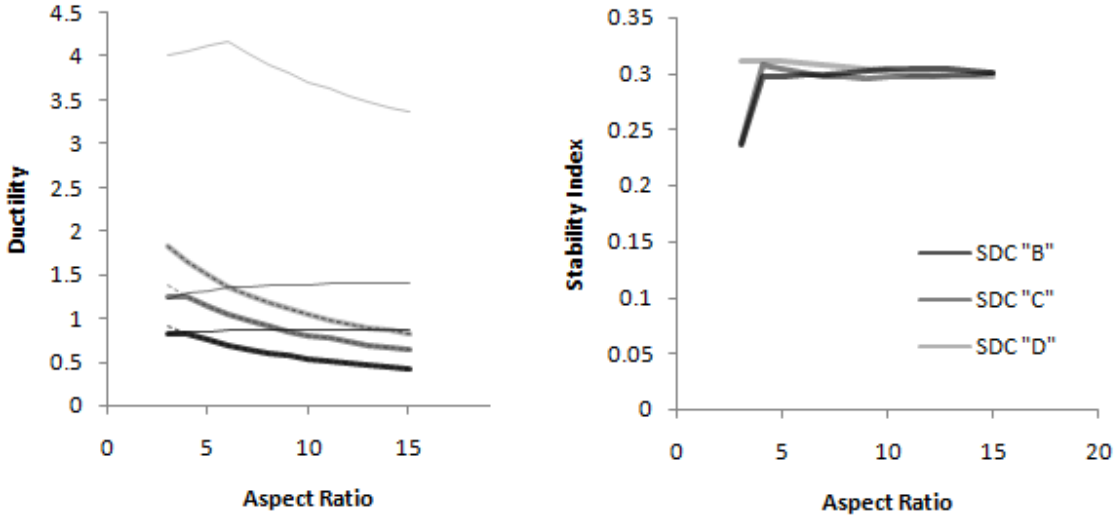

Figure 12 – Design ductility and stability indexes for out-of-plane design of drilled shaft bent

3.2 DDBD of a two-column bent

The column bent shown in Fig. 13 is designed using DDBD and the proposed model in the in-plane and out-of-plane directions. The design is repeated for tree levels of seismic hazard and performance that agree with Seismic Design Categories SDC “D”, “C”, and “B”. The aspect ratio of the bent is also varied from 3 to 15. The diameter of the columns is D =1.2 m. The axial load at the top of each column is 2714 kN, which gives an axial load ratio of 10%. Each column is supported by a pile group that is supposed to provide total fixed at the column base. The reinforced concrete in the extended drilled shafts and cap-beam has an expected compressive strength f'_{ce} = 31.2 MPa. The reinforcing steel has yield stress f_y = 420 MPa and its strain at maximum stress is ε_{su} = 0.1.

Seismic hazard

The displacement spectra corresponding to SDCs “B”, “C” and “D” are shown in Fig. 9, and is the same as for the example in Section 3.1.

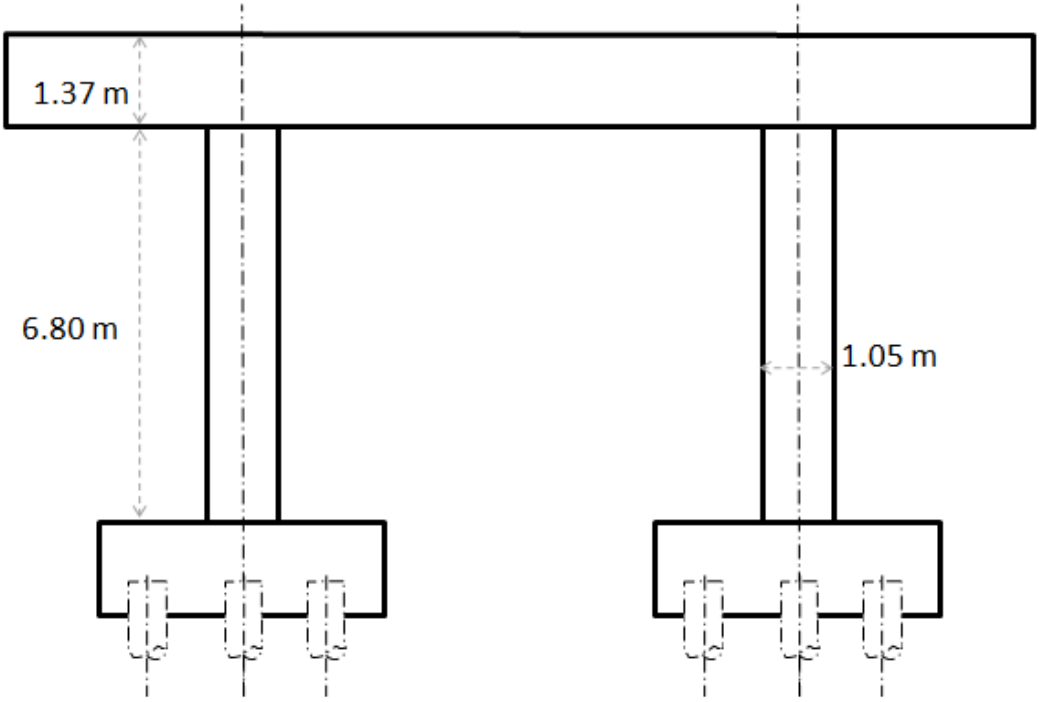

Figure 13 - Two column bent

Damage-based target displacements

Damage-based target displacement for SDC “B” and SDC “C” is directly computed with Eq. 16 and Eq. 17 with H = La and L = 1 for in-plane response and L = 2 for out-of-plane response. The damage control displacement for SDC “D” is computed with the plastic hinge method using Eq. 18 for the in-plane and Eq. 19 for the out-of-plane directions. The yield displacement is estimated with Eq. 27 in the in-plane direction and Eq. 28 for the out of plane direction. In both cases with $\alpha = 1$.

Stability-based target displacements

The stability-based target ductility is computed for the different SDCs and aspect ratios with Eq. using H = La in Eq. 15

Design target-displacement

The design target displacement is the minimum of the damage based displacement and stability based displacement. The ductility that corresponds to the target displacements is plotted in Fig. 14 and Fig 15, for the three SDCs. In both figures that when stability controls, ductility decreases as aspect ratio increases.

Required strength

Continuing DDBD, the next step is to compute the equivalent damping of the system using Eq. 11. Then, the required effective period is found for each SDC with Eq. 2, the required strength is computed with Eq. 3 and the required flexural strength with Eq. 4. Finally, the stability index is checked (Eq.1) and the flexural reinforcement is designed. The computed stability indexes are shown in Fig. 14 for the in-plane direction and in Fig. 15 for the out-of-plane direction. It is observed that the stability index reach the target limit of 0.3 when design is controlled by P-Δ effects. This proves the efficacy of the proposed model to give a target displacement to meet a predefined stability criterion. Since the limit to the stability index is not exceeded, no iteration is needed.

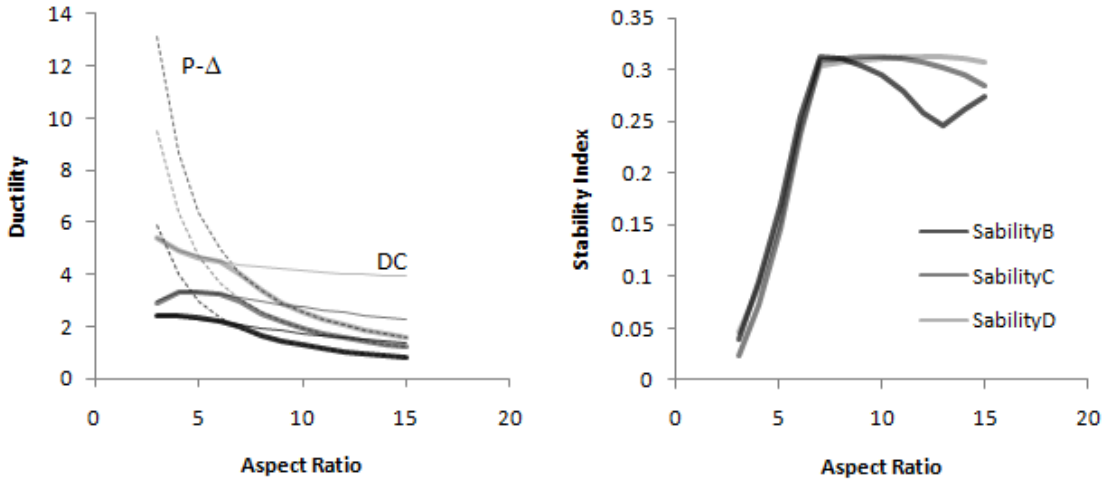

Figure 14 - Ductility and Stability index from design in out-of-plane direction

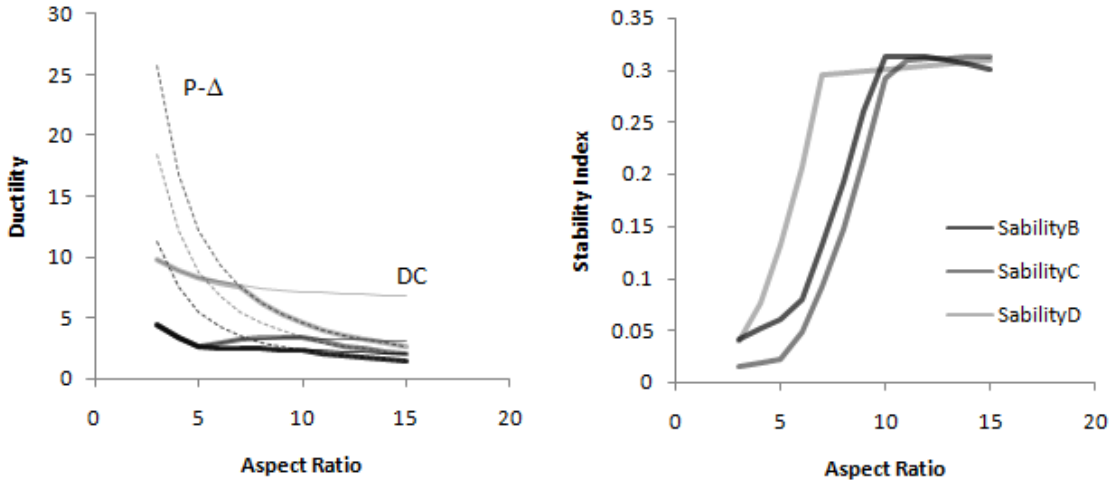

Figure 15 - Ductility and Stability index from design in in-plane direction

The out-of-plane direction controls design in all cases. Therefore, the strength provided in the out-of-plane direction exceeds the requirement is the in-plane direction. This causes that the actual stability index in the in-plane direction be less than those shown in Fig.15. This however has no implication in design.

4. P-Δ EFFECTS IN MULTI SPAN BRIDGES

The model in the previous section was derived from the application of DDBD to the design of bridge piers as stand-alone structures. Therefore some modification is needed for its implementation in the design of bridges. As it was explained in Section xxx, when DDBD is applied to a bridge, the multi-degree of freedom system MDOF is replaced by a substitute single-degree of freedom SDOF system. The substitution is given by Eq. 33 and Eq. 34 where Δ_{sys} and M_{EFF} are respectively the generalized displacement and effective mass assigned to the SDOF system. The substitution is based on an assumed displacement profile for the bridge where Δ_i is the displacement of the pier or abutment i and m_i is lumped mass at the location of each pier or abutment *i*. This is shown schematically in Fig.16. Once the substitution is made, the DDBD follows the same procedure used for stand-alone bents.

$$\Delta_{sys} = \frac{\sum m_i \Delta_i^{\,2}}{\sum m_i \Delta_i} \qquad \text{(Eq. 33)}$$

$$M_{EFF} = \frac{\sum m_i \Delta_i}{\Delta_{sys}} \qquad \text{(Eq. 34)}$$

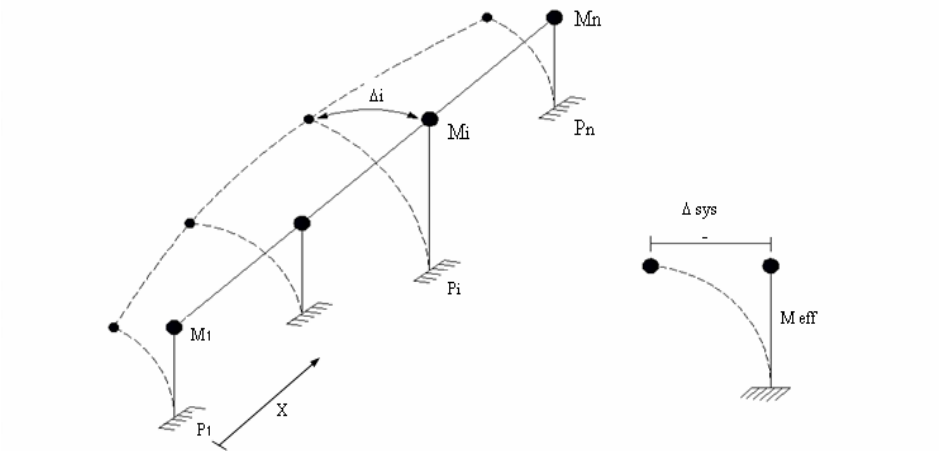

Figure 16 - Equivalent single degree of freedom system

The effective period of the substitute SDOD system is given by Eq.2 . In this Eq. R_ξ is a function of the equivalent damping in the entire bridge ξ_{sys} that results of the combination of the equivalent damping ξ_{eq} in each element of the bridge.

$$T_{eff} = T_c \frac{\Delta_{sys}}{PSD \cdot R_\xi} \qquad \text{(Eq.35)}$$

The required strength for pier i of a multi-span bridge is given by Eq.36. In this equation v_i is the fraction of the total shear V that is taken by pier i, M_{EFF} is the effective mass of the bridge in the direction of design and Δ_{sys} is the generalized displacement related to the displacement profile of the bridge in the direction of design.

$$V_i = v_i \frac{4\pi^2 M_{EFF}}{T_{eff}^{\ 2}} \Delta_{sys} \qquad \text{(Eq. 36)}$$

Since it is likely that all piers develop their strength and perform inelastically during the earthquake, it is possible to distribute strength among piers such that all piers require the same reinforcement ratio. Assuming that bent columns with same reinforcement ratio have the same ratio of cracked to gross inertia, Eq. 37 gives the ratio of total strength v_i taken by bent i, with n columns of diameter D_i, shear height H_{si} and ductility μ_i, required to satisfy force equilibrium. In the case of bridges with seat type abutments the proportion of V taken by the abutments, v_a, must be assumed at the beginning and refined with iteration of DDBD.

$$v_i = (1 - v_a) \frac{\frac{n_i \mu_i D_i^{\ 3}}{H_{si}}}{\sum \frac{n_i \mu_i D_i^{\ 3}}{H_{si}}} \qquad \mu_i \le 1 \qquad \text{(Eq. 37)}$$

Assuming that the bridge displaces with a rigid body pattern, Δ_i is the same for all piers therefore Eq.33 and Eq. 34 reduce to Eq. 38 and Eq. 39 respectively. Assuming rigid body translation is appropriate for design in the longitudinal direction of the bridge where the axial stiffness of the continuous superstructure constrains the displacement of the piers. Assuming rigid body translation is also appropriate in the transverse direction when the bridge has a

balanced distribution of mass and stiffness as defined by AASHTO (Imbsen 2007) (Suarez and Kowalsky 2007)

$$\Delta_{sys} = \Delta_i \quad \text{(Eq. 38)}$$

$$M_{EFF} = \sum m_i \quad \text{(Eq. 39)}$$

Following the same procedure as for stand-alone piers, Eq.40 is derived assuming the target displacement of the pier Δ_t equals $\Delta_{sys,}$ according to Eq.38 for a rigid body translation pattern. The difference between Eq. 5 and Eq. 40 is that the latest is written in terms of the properties of a pier i of the bridge. This has required the inclusion of v_i and the use of M_{EFF} instead of M_{eff}. Eq. 40 can be written as Eq.41 where D (Eq. 42) is a constant that can be calculated at the beginning of DDBD.

$$\frac{R_\xi}{\mu_{t,i}} = \frac{T_c \Delta_{y,i}}{2\pi PSD}\sqrt{\frac{P_i}{\theta_s v_i M_{EFF} H_i}} \quad \text{(Eq. 40)}$$

$$\frac{R_\xi}{\mu_t} = D \quad \text{(Eq. 41)}$$

$$D = \frac{T_c \Delta_{y,i}}{2\pi PSD}\sqrt{\frac{P_i}{\theta_s v_i M_{EFF} H_i}} \quad \text{(Eq. 42)}$$

It is not possible to solve Eq. 41 for ductility of pier *i* since R_ξ is a function of the combined damping ξ_{sys}, which is in turn a function of the ductility in all elements of the bridge. The models proposed in Section 3 are appropriate in the case of regular bridges where the ductility and damping in all piers is the same. In the case of irregular bridges, the models in section can be used and should yield conservative values of target ductility. The reason for this is that as the bridge becomes irregular (piers of different heights), only the critical pier reaches the target ductility. Therefore, the combined damping ξ_{sys} reduces and R_ξ increases. It is observed in Fig. 6 that the curves for the models with less damping (Fixed base columns

vs. drilled shaft in clay) for the same value of C give higher levels of stability-base target ductility.

The use of the proposed model is limited to cases where v_i can be computed before design. This is not possible when DDBD is used for design of bridges with seat-type or integral abutments where these elements are considered part of the earthquake resisting system. In such case DDBD is iterative, and the stability-based ductility should be computed for each pier in each iteration.

4.1 Design Examples.

Six continuous bridge frames are design with DDBD using the proposed model to compute a stability based target displacement for each pier. The superstructure for all bridges is a prestressed concrete box girder supported on single column bents (Fig. 17). The bridges differ in their configuration, number of spans, pier heights and span length as shown in Fig. 17. The variation in configuration results in different Balance Mass and Stiffness ratios BMS. According to AASHTO Guide Specification for LRFD Seismic Bridge Design (Imbsen, 2007) the BMS ratios are computed with Eq. 42, where mi and mj are the lumped mass at piers i and j and k1 and k2 are the stiffness of piers i and j. This index is computed in two ways, BMS1 is the least value that results of all combinations of any two piers and BMS2 is the least value that resulted from all combinations of adjacent piers.

$$BMS = \frac{M_i K_{p\,j}}{M_j K_{p\,i}} \qquad \text{(Eq. 43)}$$

The design of each bridge is performed for the seismic hazard and performance related to SDC B, C and D. The seismic hazard is shown in Fig. 9. For SDCs “B” and “C” the damage-based target displacement for each pier is given by Eq. 16 and Eq. 17. For SDC “D” the damage-based target performance is computed with the plastic hinge method. The stability based target displacement is computed for each pier with Eq. 15.

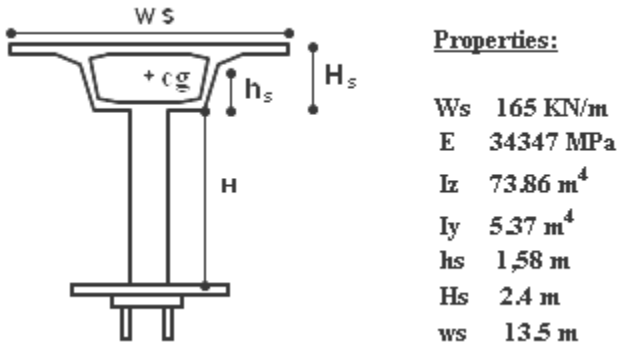

Figure 17 - Superstructure type and properties

DDBD was applied in the longitudinal and transverse directions of the bridges using the computer program DDBD-Bridge (Suarez, 2008). A rigid body translation pattern was used for design in both directions. Design followed the procedure shown in Fig. 2 and detailed in other papers by the authors (Suarez, 2008; Suarez and Kowalsky, 2008). Results of design for the three SDCs are shown in Table 9.

Table 8. Bridge parameter matrix

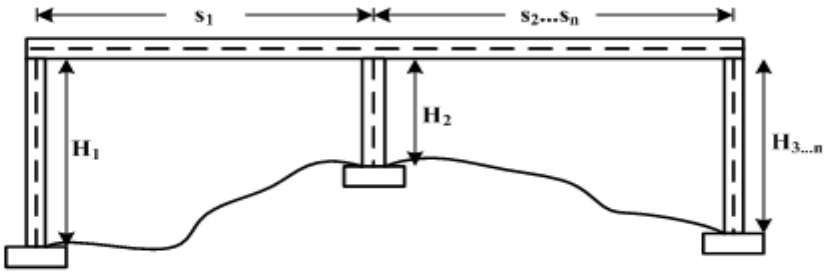

Code	Span length (m)							Pier height (m)								BMS1	BMS2
	S_1	S_2	S_3	S_4	S_5	S_6	S_7	H_1	H_2	H_3	H_4	H_5	H_6	H_7	H_8		
1.1	50	50						12	12	12						1.00	1.00
1.2	50	50						12	13	12						0.81	0.81
1.3	50	50						12	15	12						0.55	0.55
1.4	30	30	30					15	15	15	15					1.00	1.00
1.5	30	30	30					12	15	15	12					0.50	0.55
1.6	30	30	30					17	15	15	12					0.39	0.71

Table 9 shows from left to right: the bridge number with reference to Table 8, the diameter of the piers, the reinforcing ratio of the piers, the maximum stability index calculated for the piers in the transverse direction, the maximum stability index calculated for the piers in the longitudinal direction, and the two last columns shown whether the stability based target displacement controlled design in the transverse or longitudinal directions. By looking at results is Table 9 the following conclusions are advanced:

- The proposed model was effective since the stability index was around the predefined limit for all designs controlled by P-D effects in the three SDCs. No iteration is required

Table 9 - DDBD results for bridge group

SDC "D"						
Bridge	D	ρ (%)	θ_{sT}	θ_{sL}	P-Δ_T	P-Δ_L
1	2.00	1.78	0.11	0.10	no	no
2	2.00	1.98	0.10	0.10	no	no
3	2.00	2.37	0.10	0.09	no	no
4	1.50	2.09	0.31	0.30	yes	yes
5	1.50	3.00	0.17	0.18	no	no
6	1.50	3.91	0.14	0.16	yes	yes
SDC "C"						
Bridge	D	ρ (%)	θ_{sT}	θ_{sL}	P-Δ_T	P-Δ_L
1	1.50	1.82	0.31	0.30	yes	yes
2	1.50	2.00	0.30	0.30	yes	yes
3	1.50	2.28	0.29	0.27	yes	yes
4	1.50	1.46	0.30	0.30	yes	yes
5	1.50	1.46	0.27	0.26	yes	yes
6	1.50	1.82	0.24	0.22	yes	yes
SDC "B"						
Bridge	D	ρ (%)	θ_{sT}	θ_{sL}	P-Δ_T	P-Δ_L
1	1.50	1.10	0.28	0.31	yes	yes
2	1.50	1.20	0.26	0.30	yes	yes
3	1.50	1.37	0.26	0.29	yes	yes
4	1.50	1.10	0.23	0.31	yes	yes
5	1.50	1.00	0.23	0.28	yes	yes
6	1.50	1.18	0.20	0.26	yes	yes

The proposed model gets conservative for irregular bridges. As a bridge becomes irregular (bridge 1, 2 and 3), the required strength increases (reinforcement increases) due to a reduction in damping and the stability index decreases. The proposed model produces underestimate the stability based target displacement.

8. SUMMARY AND CONCLUSIONS

A simple model has been derived to determine a stability-base target displacement for bridge piers. The use of this model avoids the need for iteration when DDBD is controlled by limits in P-Δ effects. The applicability of the model has been assessed in several design examples. The following conclusions were reached:

- Iteration in design of bridges controlled by P-Δ effects can be reduced or avoided by determining a stability-based target displacement at beginning of design.
- The proposed model has proved to effective for determination of a stability-based target displacement
- The proposed model is accurate in cases where the proportion of the total shear taken by the bent can be computed.
- The proposed model gives conservative estimates of stability-based target displacement for irregular bridges.

9. REFERENCES

Blandon Uribe C., Priestley M. 2005, Equivalent viscous damping equations for direct displacement based design, "Journal of Earthquake Engineering", Imperial College Press, London, England, 9, SP2, pp.257-278.

Calvi G.M. and Kingsley G.R., 1995, Displacement based seismic design of multi-degree-of-freedom bridge structures, Earthquake Engineering and Structural Dynamics 24, 1247-1266.

Dwairi, H. and Kowalsky, M.J., 2006, Implementation of Inelastic Displacement Patterns in Direct Displacement-Based Design of Continuous Bridge Structures, Earthquake Spectra, Volume 22, Issue 3, pp. 631-662

Dwairi, H., 2004. Equivalent Damping in Support of Direct Displacement - Based Design with Applications To Multi - Span Bridges. PhD Dissertation, North Carolina State University

EuroCode 8, 1998, Structures in seismic regions – Design. Part 1, General and Building, Commission of European Communities, Report EUR 8849 EN

Frontline, 2008, Solver user manual, http://www.solver.com/, (accessed May 20, 2008)

Imbsen, 2007, AASHTO Guide Specifications for LRFD Seismic Bridge Design, AASHTO, http://cms.transportation.org/?siteid=34&pageid=1800, (accessed April 18, 2008).

Kowalsky M.J., Priestley M.J.N. and MacRae G.A. 1995. Displacement-based Design of RC Bridge Columns in Seismic Regions, Earthquake Engineering and Structural Dynamics 24, 1623-1643.

Ortiz J. 2006, Displacement-Based Design Of Continuous Concrete Bridges Under Transverse Seismic Excitation. European School For Advanced Studies In Reduction Of Seismic Risk.

Paulay, T, Priestley, M.J.N., 1992, Seismic Design of Reinforced Concrete and Masonry Buildings, Wiley, 978-0-471-54915-4

Priestley, M.J.N. and Grant, D.N., 2005, Viscous Damping in Seismic Design and Analysis, Journal of Earthquake Engineering, Vol. 9(SP2), pp. 229-255

Priestley, M. J. N., 1993, Myths and fallacies in earthquake engineering-conflicts between design and reality, Bulletin of the New Zealand Society of Earthquake Engineering, 26 (3), pp. 329–341

Priestley, M. J. N., Calvi, G. M. and Kowalsky, M. J., 2007, Direct Displacement-Based Seismic Design of Structures, Pavia, IUSS Press

Shibata A. and Sozen M. Substitute structure method for seismic design in R/C. Journal of the Structural Division, ASCE 1976; 102(ST1): 1-18.

Suarez, V.A. and Kowalsky M.J., Displacement-Based Seismic Design of Drilled Shaft Bents with Soil-Structure Interaction, Journal of Earthquake Engineering, Volume 11, Issue 6 November 2007 , pp. 1010 – 1030

Suarez, V.A., 2006, Implementation of Direct Displacement Based Design for Pile and Drilled Shaft Bents, Master Thesis, North Carolina State University

Suarez, V.A., 2008, Implementation of Direct Displacement Based Design for Highway Bridges, PhD Dissertation, North Carolina State University.

Suarez, V.A., Kowalsky, M. J., 2008, Displacement Patterns for Direct Displacement Based Design of Conventional Highway Bridges, in preparation.

PARV VI

DIRECT DISPLACEMENT-BASED DESIGN AS AN ALTERNATIVE METHOD FOR SEISMIC DESIGN OF BRIDGES

Vinicio A. Suarez and Mervyn J. Kowalsky

Formatted for submission to an ACI Special Publication

Synopsis:

This paper reviews the Direct Displacement-Based Design Method for seismic design of bridges and compares it to the design procedure implemented in the AASHTO Guide Specification for LRFD Seismic Bridge Design. It is shown by means of examples that DDBD has several advantages that could be put to use as an alternative design method to that proposed in the AASHTO Guide Specification.

Keywords:

DBD DDBD PBSE

Vinicio A. Suarez is a PhD student at North Carolina State University and Professor and Director of the Civil Engineering School and Civil Engineering, Geology and Mining Research Center at Universidad Tecnica Particular de Loja in Ecuador. His research has mainly focused on seismic design of bridges. He is a Professional Engineer in Ecuador and member of several national and international organizations.

Mervyn J. Kowalsky is Associate Professor of Structural Engineering in the Department of Civil, Construction, and Environmental Engineering at North Carolina State University. His research, which has largely focused on the seismic behavior of structures, has been supported by the National Science Foundation, the North Carolina and Alaska Departments of Transportation, and several industrial organizations. He is a registered Professional Engineer in North Carolina and an active member of several national and international committees on Performance-Based Seismic Design

INTRODUCTION

After the Loma Prieta earthquake in 1989, extensive research has been conducted to develop improved seismic design criteria for bridges, emphasizing the use of displacements rather than forces as a measure of earthquake demand and damage in bridges. Several Displacement Based Design (DBD) methodologies have been devolved. Among them, the Direct Displacement-Based Design Method (DDBD) (Priestley 1993) has proven to be effective for performance-based seismic design of bridges, buildings and other types of structures (Priestley et al 2007).

The newly proposed AASHTO Guide Specifications for LRFD Seismic Bridge Design (Imbsen 2007) provides a complete framework for seismic design that is in many ways similar to the Seismic Design Criteria developed by Caltrans (2006a). However, the AASHTO LRFD Seismic Specification recognizes the variability of seismic hazard over the

US specifying four Seismic Design Categories (SDC). Each SDC links seismic hazard to expected performance.

Embedded in the AASHTO LRFD Seismic Specification is a demand/capacity assessment procedure that is used for displacement-based design. Depending on the configuration of the bridge, the demand analysis is performed by the uniform load method for regular bridges, while the spectral modal analysis can be used for all bridges. The capacity verification can be done using implicit equations for SDC B or by pushover analysis for SDCs C and D. As in Caltrans practice, and with the exception of SDC A, the proposed guide requires the use of capacity design principles (Paulay and Priestley 1991) for the detailing of the substructure sections and protected elements.

DDBD differs from the above mentioned DBD procedures, in the use of an equivalent linearization approach and in the way in which it is executed. DDBD starts with the definition of a performance-based target displacement for the structure and returns strength required to meet the target displacement , and hence damage level, under the specified earthquake.

In this paper, DDBD is reviewed and compared to the demand/capacity assessment procedure used for design in the AASHTO LRFD Seismic guide. It is shown that DDBD has several advantages over that procedure; it is also shown that DDBD is compatible with the design philosophy in the AASHTO LRDF Specification, therefore making it suitable as an alternative design method.

OVERVIEW OF THE DIRECT-DISPLACEMENT BASED DESIGN METHOD

DDBD is used for performance-based design of structures. With this method a structure can be designed to meet any level of performance under any level of earthquake. DDBD has undergone extensive research and has been shown to be effective for performance-based

seismic design of bridge piers (Kowalsky et al 1995, Suarez and Kowalsky 2007), multi-span bridges (Calvi and Kingsley 1995, Kowalsky 2002, Dwairi and Kowalsky 2006, Suarez and Kowalsky 2008), buildings and other types of structures (Priestley et al 2007).

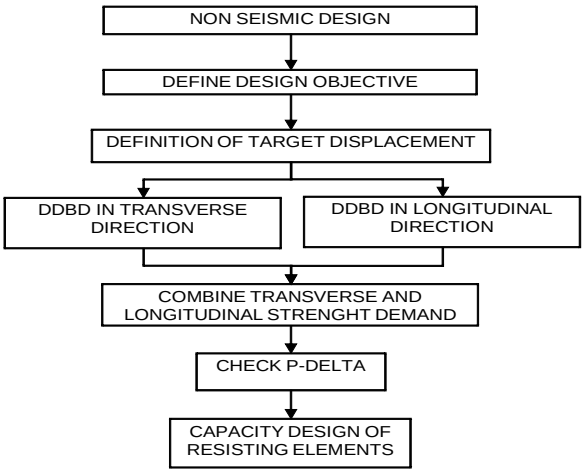

Figure 1 - DDBD main steps flowchart

DDBD uses an equivalent linearization approach (Shibata and Sozen 1976) by which an inelastic multi degree of freedom system at maximum response is substituted by an equivalent single degree of freedom system. The main steps of the design procedure are presented in Fig. 1. The bridge is previously designed for non-seismic loads and the configuration, superstructure section and foundation are known. A design objective is proposed by defining the expected performance and the seismic hazard. Then, the target displacement profile for the bridge is determined. After that, DDBD is applied in the longitudinal and transverse axes of the bridge, the results are combined, P-Δ effects are checked and reinforcement is designed and detailed following capacity design principles.

The flowcharts in Fig. 2 show the procedure for DDBD in the transverse and longitudinal direction, as part of the general procedure shown in Fig. 1. As seen in Fig. 2, there are three variations of the procedure: (1) If the displacement pattern is known and predefined, DDBD is applied directly; (2) If the pattern is unknown but dominated by the first mode of vibration,

the First Mode Shape FMS iterative algorithm is used (Calvi and Kingsley 1995); (3) If the pattern is unknown but dominated by modal combination, the Effective Mode Shape EMS algorithm is applied (Kowalsky 2002).

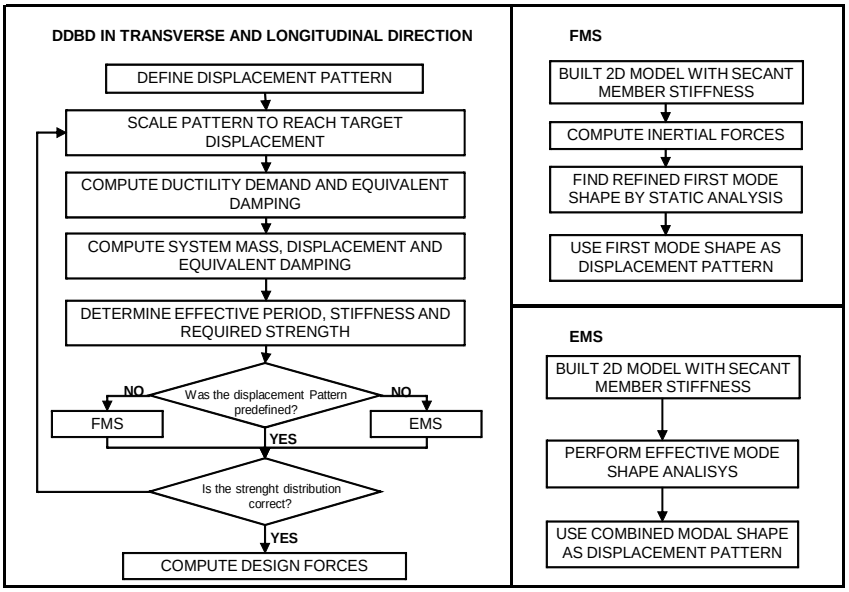

Figure 2 - Complementary DDBD flowcharts

It must be noted that the application of DDBD does not require pushover or other nonlinear analysis. For design of a full bridge with a predefined displacement pattern only hand calculations are required. The FMS algorithm requires 2D static analysis and the EMS algorithm requires 2D modal superposition analysis.

Applicability of DDBD

Extensive research conducted in the last decade has shown that DDBD is effective for the design of most types of highway bridges (Priestley et al 2007). The accuracy and effectiveness of the method depends mainly on the selection of an appropriate displacement pattern. The direct application of DDBD for bridges when the displacement pattern is known requires less effort than the FMS or EMS algorithms. Recent research by the authors (Suarez

and Kowalsky 2008) showed that predefined linear displacement patterns can be effectively used for design of bridge frames, bridges with seat-type or other typse of 'weak abutments' and bridges with one or two expansion joints. These bridges must have a balanced distribution of mass and stiffness, according to the AASHTO LRFD Seismic Specification (Imbsen 2007). Bridges with strong abutments can be designed with the FMS algorithm and any type of bridge can be designed with the EMS algorithm, as shown in table 1.

Table 1- Classification of bridges and design algorithms

BRIDGE	BALANCED MASS AND STIFFNESS	NO BALANCED MASS AND STIFFNEES
FRAME	**RBT or EMS**	**EMS**
WEAK ABUTMENTS	**RBT or EMS**	**EMS**
STRONG ABUTMENTS	**FMS or EMS**	**FMS**
ONE EXPANSION JOINT	**LDP1 or EMS**	**EMS**
TWO EXPANSION JOINTS	**LDP2 or EMS**	**EMS**
MORE THAN TWO EXPANSION JOINTS	**EMS**	**EMS**
		

Real Highway bridges have complexities that limit the applicability of design methods. DDBD can deal with some of these complexities, including: soil-structure interaction, superstructures with low transverse displacement capacity, skew, P-Δ effects, expansion joints (Suarez and Kowalsky 2007, 2008). In order to offer a base for comparison with the design procedure in the AASHTO LRFD Seismic Specifications, the following sections show how DDBD deals with superstructure displacement capacity, P-Δ effects, and skew. A design example is included.

Accounting for superstructure performance in design

A common strategy is to design the superstructure to remain essentially elastic while all inelastic behavior and energy dissipation is directed to well detailed sections in piers and abutments. Current displacement-based practice (Imbsen 2007, Caltrans 2006a) focuses on a

displacement demand-capacity check for piers and ignores the performance of the superstructure. The implication of this is that while piers can have enough displacement capacity to cope with the seismic demand, the superstructure might not. Therefore, a design based purely on pier displacement capacity could lead to bridges in which the superstructure suffers unaccounted for damage.

The superstructure displacement capacity is believed to be an important design parameter for bridges responding with a flexible transverse displacement pattern, including: bridges with strong abutments, bridges with weak and flexible superstructures and bridges with unbalanced mass and stiffness (Suarez and Kowalsky 2008).

The DDBD framework allows easy implementation of superstructure transverse displacement capacity into the design procedure. The transverse target displacement profile of the bridge must be defined accounting for the target performance of the piers and also for target performance of the superstructure.

Determination of a performance-based displacement for the superstructure requires a moment curvature analysis of the superstructure section and double integration of the curvature profile along the length of the superstructure. The yield curvature of a section in mainly dependent on its geometry and it is insensitive to its strength and stiffness (Priestley et al 2007). If it is believed that the lateral displacement of the superstructure should be limited to yielding of the longitudinal reinforcement in the concrete deck, the yield curvature could be estimated with Eq. 1. Where w_s is the width of the concrete deck and ε_y is the yield strain of the steel reinforcement. For other types of superstructure sections or if the target performance is related to some other limit state, a moment-curvature analysis is required. This analysis should account for expected material properties and biaxial bending. An important by-product of the moment-curvature analysis is the flexural stiffness of the superstructure, which is also needed in design.

$$\phi_{ys} = \frac{2\varepsilon_y}{w_s} \qquad \text{(Eq. 1)}$$

Assuming that the superstructure responds in the transverse direction as a simply supported beam, with the seismic force acting as a uniform load (Fig. 3), the double integration of the curvature profile results in Eq. 2 Where L_s is the length of the superstructure and x_i is the location of the point of interest and Δ_1 and Δ_n are the target displacements for the initial and end abutments.

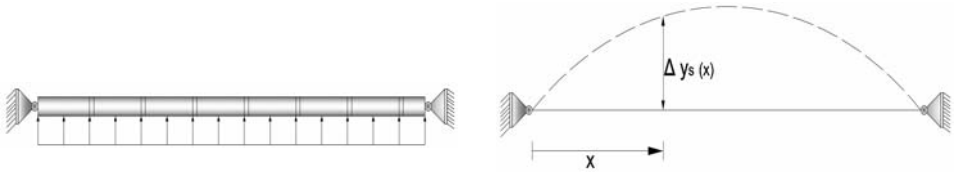

Figure 3- Assumed superstructure displaced shape at yield

$$\Delta_{ys,i} = \phi_{ys}\left[\frac{2x_i^4 - 4L_s x_i^3 + 2L_s^3 x_i}{6L_s^2}\right] + \Delta_1 + \frac{\Delta_n - \Delta_1}{L_s} x_i \qquad \text{(Eq. 2)}$$

When using Eq. 2 in design, x_i is replaced by the location of each pier in the bridge to get the target displacement, $\Delta_{ys,i}$ at that specific point (Eq. 2). If $\Delta_{ys,i}$ is less than the damage based target displacement of the pier, Δ_{ysi} controls design and becomes the target displacement for the pier.

P-Δ Effects

Limiting P-Δ effects is necessary to preserve stability under earthquake attack. P-Δ effects are usually quantified by a stability index, θ_s that relates the P-Δ induced moments with the flexural capacity of the section under consideration. In DDBD, if θ_s exceeds 30%, design must be repeated reducing the target displacement for the element. This causes DDBD to be iterative and increases the design effort substantially. The same happens if the procedure in

the AASHTO LRFD Seismic specification is used, if P-Δ effects exceed the specified limit, reinforcement in the sections must be increased and the whole design process repeated.

To avoid iteration in DDBD, the target displacement to meet a predefined stability index can be estimated at the beginning of design with Eq. 3-4 for concrete piers supported on rigid foundations (Suarez and Kowalsky 2008). The constant C is a function the design displacement spectrum corner period T_c (see Fig. 7), peak spectral displacement *PSD*, yield displacement of the pier Δ_y, axial load *P*, effective mass M_{eff} and height of the pier *H*.

$$\Delta_{\theta s} = 0.85C^{-0.83}\Delta_y \quad \text{(Eq. 3)}$$

$$C = \frac{T_c\Delta_y}{2\pi PSD}\sqrt{\frac{P}{\theta_s M_{eff} H}} \quad \text{(Eq.4)}$$

This model has been derived for piers as stand-alone structures and can be used in the in-plane or out-of-plane direction of the pier. The effective mass M_{eff}, can be computed taking a tributary area of superstructure and adding the mass of the cap-beam and a portion of the mass of the columns. This works well in regular bridges where the seismic mass can be calculated, as in the stand alone case, and where ductility demand is similar for all piers. In any case, it is recommended that P-Δ effect be checked at the end of design. The target displacement computed with this model must be compared to the target displacement to meet other performance limits. The lesser of the values becomes the target displacement for the pier and controls design.

Skewed configurations

It is quite common to see highway bridges in which abutments and piers have been skewed to allow appropriate alignment with under crossings. From a design perspective, the effect of a skewed configuration is that in-plane and out-of-plane response parameters of abutments and piers are no longer oriented in the principal design directions of the bridge (Fig. 4).

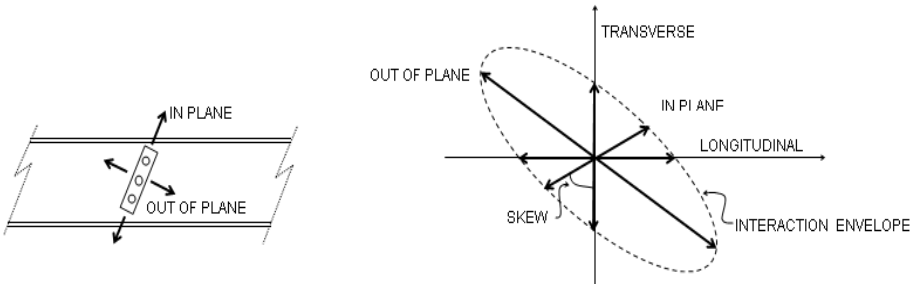

(a) Skewed bent (b) Element and bridge design axis

Figure 4 - Design axes in skewed elements

The effects of skew can be considered in DDBD by determining the projection of any response parameter such as yield displacement Δ_y, displacement capacity Δ_t, shear height H_s and others, with respect to the transverse and longitudinal direction of the bridge. Such determination can be done using an elliptical interaction function between the in-plane and out-of-plane response, as given by the following equations:

$$rp_T = rp_{IN} + skew\frac{rp_{OUT} - rp_{IN}}{90} \quad \text{(Eq. 5)}$$

$$rp_L = rp_{OUT} + skew\frac{rp_{IN} - rp_{OUT}}{90} \quad \text{(Eq. 6)}$$

Where, rp_{IN} is the value of the response parameter in the in-plane direction of the element, rp_{OUT} is the response parameter in the out-of-plane direction of the element, rp_T is the projection of the response parameter in the transverse direction of the bridge and rp_L is the projection of the response parameter in the longitudinal direction of the bridge.

Example 1. DDBD of a multi-column bent

This example shows the design of the central bent of the bridge shown in Fig. 5. This bridge has two spans of 38.20 m and total length of 76.40 m. The width of the superstructure is 13.41 m. The superstructure is continuous, formed by decked bulb-tee girders. The superstructure girders are set side-by-side to form the driving surface. The longitudinal joint

formed between the flanges is filled with non-shrink grout. Because of its configuration, the superstructure is weak in the transverse direction and should not be accounted for transmitting lateral forces to the abutments. The weight of the superstructure is 130 kN/m

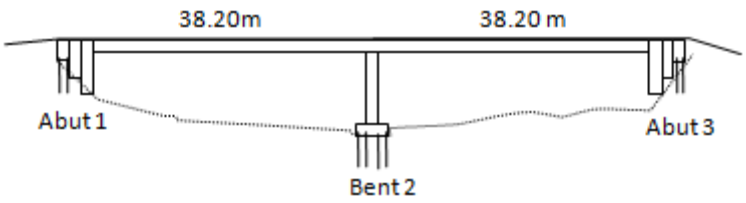

Figure 5 – Two span bridge

The central bent has two reinforced concrete columns supported on pile groups (Fig 6). The diameter of the columns is D = 1.05 m and the free height is H = 6.80 m. The connection between the central bent and the superstructure is pinned. The cap-beam height is 1.37 m and its width is 1.2m. The reinforced concrete in columns has a compressive strength, f'_c = 26.5 MPa. The reinforcing steel has a yield stress, f_y = 414 MPa, a hardening ratio of 1.35 and a damage control strain, $\varepsilon_{s,dc}$ = 0.06. The foundation has cast-in-place reinforced concrete piles. The abutments are integral with the superstructure and are designed as part of the earthquake resisting system. All substructure elements are skewed 18 degrees.

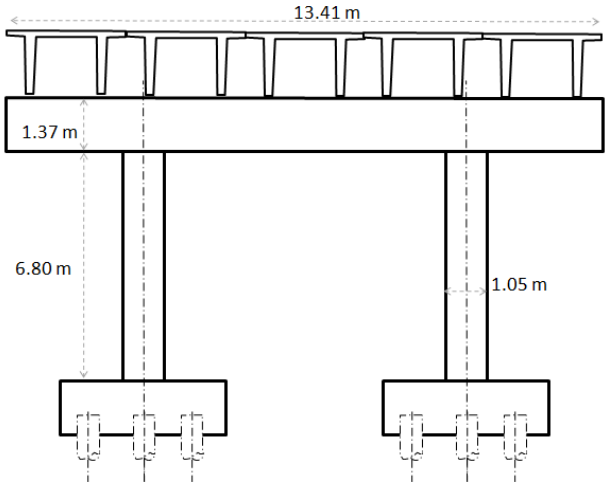

Figure - 6 Central Pier in two span bridge

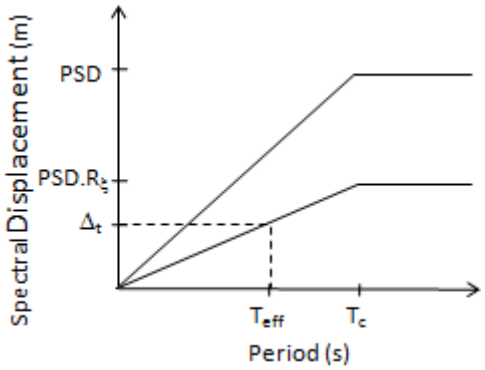

Figure 7 –Displacement Design Spectrum

The seismic hazard at the bridge site is given by the displacement design spectra shown in Fig. 7. The corner period of the displacement spectra is T_c = 4 s, the Peak Spectral Displacement is *PSD* = 0.24 m. This combination results in *SDC* "B" according to the AASHTO LRFD Seismic Specification.

Design Objective: Under the design earthquake represented by the displacement spectra shown in Fig. 7, the bridge must reach one or more of the following performance limits:

- Compression strain in central bent columns is equal to the damage-control strain for confined concrete. This sets the limit beyond which damage cannot be economically repaired.
- The stability index for the central bent is equal to 30%. This sets the limit beyond which the structure might become unstable.
- The superstructure curvature is equal to 0.0003. This value is given from section analysis of the superstructure and sets the limit beyond which longitudinal joints fail.
- The in-plane and out-of-plane displacement of the abutments is 100 mm. This value sets the limit beyond which damage in the abutments is unacceptable.

Assessment of Target Displacement: The definition of a target displacement for the bent requires the assessment of the displacements that will cause the bent to meet the performance limits specified in the design objective. The damage-control displacement for the bent, Δ_{DC} is determined with the plastic hinge method using Eq. 7-8 for the in-plane and out-of-plane directions. The yield displacement, Δ_y is given by Eq. 9-10 in the in-plane and out-of-plane directions. In these equations, ϕ_{dc} and ϕ_y are the damage-control and yield curvatures, L_p is the plastic hinge length given by Eq. 11-12 in the in plane and out of plane directions (Priestley et al 2007), H_{in} is free height of the columns, H_{out} is H_{in} plus the height of the cap-beam. L_{sp} is the strain penetration length given in Eq. 4 in terms if the expected yield strength of the longitudinal reinforcement f_{ye} and the diameter of the reinforcement d_{bl}. The expected material properties are related to the nominal properties as shown in Eq. 13 and Eq. 14 (Priestley et al 2007).

$$\Delta_{DC,in} = \Delta_y + (\phi_{dc} - \phi_y) L_p H_{in} \quad \text{(Eq. 7)}$$

$$\Delta_{DC,out} = \Delta_y + (\phi_{dc} - \phi_y) L_p H_{out} \quad \text{(Eq. 8)}$$

$$\Delta_{y,in} = \frac{\phi_y (H_{in} + 2L_{sp})^2}{6} \quad \text{(Eq. 9)}$$

$$\Delta_{y,out} = \frac{\phi_y (H_{out} + L_{sp})^2}{3} \quad \text{(Eq. 10)}$$

$$Lp_{in} = k\frac{H}{2} + L_{sp} \qquad k = 0.2\left(\frac{f_u}{f_y} - 1\right) \le 0.07 \quad \text{(Eq. 11)}$$

$$Lp_{out} = kH + L_{sp} \qquad k = 0.2\left(\frac{f_u}{f_y} - 1\right) \le 0.07 \quad \text{(Eq. 12)}$$

$$L_{sp} = 0.022 f_y d_{bl} \quad \text{(MPa)} \quad \text{(Eq. 13)}$$

$$f_{ye} = 1.1 f_y \quad \text{(Eq. 14)}$$

$$f'_{ce} = 1.3 f'_c \quad \text{(Eq. 15)}$$

The yield ϕ_y and damage-control curvatures ϕ_{dc} are estimated with Eq. 16 and Eq. 17, in terms of the damage control strain $\varepsilon_{c,dc}$ of the confined concrete core (Eq. 18), diameter of the section *D*, yield strain ε_y and strain at maximum stress of steel ε_{su} , yield stress of the transverse steel f_{yh}, transverse reinforcement ratio ρ_v, expected compressive strength of concrete f'_{ce} and compressive strength of the confined concrete f'_{cc} (Eq. 19). An estimate of the neutral axis depth *c* is given in Eq. 20. Where A_g is the area of the section and *P* is the axial load. The damage control strain is based on the model proposed by Mander (1988).

$$\phi_y = 2.25\frac{\varepsilon_y}{D} \qquad \text{(Eq. 16)}$$

$$\phi_{dc} = \frac{\varepsilon_{c,dc}}{c} \qquad \text{(Eq. 17)}$$

$$\varepsilon_{c,dc} = 0.004 + 1.4\frac{\rho_v f_{yh}\varepsilon_{su}}{f'_{cc`}} \qquad \text{(Eq. 18)}$$

$$f'_{cc} = f'_{ce}\left(2.254\sqrt{1+\frac{7.94 f_1}{f'_{ce}}} - 2\frac{f_1}{f'_{ce}} - 1.254\right) \quad f_1 = 0.5\rho_v f_{yh} \qquad \text{(Eq. 19)}$$

$$c = 0.2D\left(1+3.25\frac{P}{f'_{ce}A_g}\right) \qquad \text{(Eq. 20)}$$

The flexural reinforcement will be provided with D25 bars. A spiral with D13 bars spaced 150 mm, will be used for shear and confinement resulting in a volumetric shear reinforcing ratio, ρ_v = 0.36%. These quantities comply with the requirements for minimum reinforcement and spacing of the AASHTO LRFD Seismic Specification.

Considering a tributary length of 38.2 m, the weight of superstructure acting on the bent is 4966 kN. Adding to that value the weight of the cap-beam and the weight of the columns the axial load at the base of each column is P = 2938 kN. With all parameters having been defined, using Eq. 7-20, ε_{cdc} = 0.0093, $\Delta_{y,in}$ = 67 mm, $\Delta_{y,out}$ = 169, $\Delta_{DC,in}$ = 203 mm, $\Delta_{DC,out}$ = 440 mm.

Next, the target displacements to meet the specified stability factor are computed with Eq. 3-4 for the in-plane and out-of-plane directions. The axial load at the top of each column is P = 2764 kN. The effective mass acting on each column is M_{eff} = 287 t. This value is calculated considering 38.2 m of superstructure tributary length, the mass of the cap-beam and one third of the mass of the column. For θ_s = 0.3, *PSD* = 240 mm and T_c = 4 s: C_{in} = 0.34, C_{out} = 0.81, $\Delta_{\theta s,in}$ = 137 mm and $\Delta_{\theta s,out}$ = 169 mm. It is observed that $\Delta_{DC,in} > \Delta_{\theta s,in}$ and $\Delta_{DC,out} > \Delta_{\theta s,out.}$ Therefore the stability criterion controls response in both directions. The target displacement for the bent is: Δ_{in} = 144 mm and Δ_{out} = 163 mm.

Since the bent is skewed 18 degrees. The local in-plane and out-of-plane axes are rotated with respect to the global transverse and longitudinal axes of the bridge. The response parameters that were obtained in reference to the local axis must be transformed to the global axes using Eq. 5-6. This results in $\Delta_{y,t}$ = 87 mm, $\Delta_{y,l}$ =149 mm, Δ_t = 144 mm, Δ_l = 163 mm, H_t = 8.87 m, H_l = 9.69 m.

Assuming the superstructure displaces transversely like a simple supported beam, for any value of maximum curvature, the displacement at any location is given by Eq. 2. With Δ_1 and Δ_n = 0, L_s = 76.40 m, x_i = 38.2 m and ϕ_{ys} = 0.0003 1/m, the transverse displacement of the superstructure at the location of central bent is Δ_{ys} = 181 mm. This value is greater than the $\Delta_{t,}$ therefore does not control the design of the bent.

The superstructure is transversely weak and does not transfer lateral forces to the abutments. However it is stiff in the longitudinal direction and it is reasonable to assume that the longitudinal displacement of the bent will equal the longitudinal displacement of the integral abutments. Therefore, in order to meet the specified abutment displacement limit, the target displacement of the bent in the longitudinal direction is reduced to Δ_l = 100 mm.

Equivalent damping. The ratio between target displacement and yield displacement gives the target ductility in the bent. In the transverse direction the target ductility is μ_t = 144 mm / 87 mm = 1.65. Ductility greater than one means inelastic energy dissipation and increased damping. The equivalent damping in the transverse direction is $\xi_{eq,t}$ = 10.5% , computed with Eq. 21 (Priestley et al 2007). In the longitudinal direction the bent is expected to respond elastically since the target displacement is less than yield displacement. Therefore, the equivalent damping is $\xi_{eq,l}$ = 5% for the system formed by the bent and the abutments in the longitudinal direction.

$$\xi_{eq} = 5 + 44.4\frac{\mu_t - 1}{\pi\mu_t} \qquad \text{(Eq. 21)}$$

Required Strength. The displacement design spectrum gives the maximum displacement demand for single degree of freedom systems with 5% damping. If the spectrum is reduced to the level of damping of the bent, entering with the Δ_t as displacement demand results in the effective period, T_{eff} required by the structure to meet its target performance (Fig. 7). This has been synthesized in Eq.22, where R_ξ is the spectral reduction due to damping and α is 0.25 for near fault excitation and 0.5 in other cases (Eurocode,1998).

$$T_{eff} = \frac{\Delta_t}{PSD \cdot R_\xi} T_c \qquad R_\xi = \left(\frac{7}{2 + \xi_{eq}}\right)^\alpha \qquad \text{(Eq. 22)}$$

From Eq. 22, in the transverse direction $R_{\xi,t}$ = 0.74 and $T_{eff,t}$ = 3.22 s. Then, using the dynamic properties of single degree of freedom systems, the required secant stiffness $K_{s,t}$ is computed with Eq.23 and the required lateral strength with Eq. 24. This results in V_t = 317 kN for the bent. Therefore, the required flexural strength for each column in double in bending is $M_{E,t}$ = 702 kN-m. In the longitudinal direction, $R_{\xi,l}$ = 1 and $T_{eff,l}$ = 1.67 s. This results in V_l = 1537 kN. The strength in the longitudinal direction is distributed between the bent and the abutments as explained below.

$$K_s = \frac{4\pi^2 M_{eff}}{T_{eff}^{\ 2}} \qquad \text{(Eq. 23)}$$

$$V = K_s \Delta_t \qquad \text{(Eq. 24)}$$

Element Design. Circular columns develop the same flexural strength in any direction. If the column section is provided with 1% steel ratio, under the design axial load will develop an expected moment capacity, M_e = 2688 kN-m. This exceeds $M_{E,t}$ therefore it is appropriate but it is not optimum. However, with minimum reinforcement, the strength of the bent in the longitudinal direction is: $V_{b,l} = 2M_E/H_l$ = 550 kN. Since the total strength required in that direction is V_l = 1537 kN, the integral abutments must be designed to contribute 1537-550 = 986 kN to the longitudinal strength of the bridge.

Once the flexural design has been obtained, the next step is to assess the shear capacity of the columns and compare to a shear demand based on the over-strength flexural capacity of the sections. Finally, the over-strength capacity of the columns is also used to design and detail the cap-beam and foundation.

In summary, DDBD has been used to design the flexural reinforcement of the central pier of a two bent bridge, the required strength for the integral abutments have also been determined. The design was controlled by the abutment displacement limit in the longitudinal direction. The design was rational, simple, direct and accounted for all the specified performance limits.

DDBD vs. LRFD SEISMIC

After introducing DDBD, discussing its applicability and showing how the method deals with several design issues, this section presents a comparison between DDBD and the demand capacity assessment procedure implemented in the AASHTO LRFD Seismic Specification.

Linearization: The displacement demand assessment procedure in AASHTO LRFD Seismic uses elastic analysis and the Equal Displacement Approximation (Veletzos and Newmark 1960) to obtain inelastic displacement demands (An amplification factor is used with short period structures). In the elastic analysis the structure is modeled with cracked section stiffness. DDBD uses an equivalent linearization approach where the inelastic structure at maximum response is substituted by an equivalent single degree of freedom system with properties of effective stiffness to maximum response and equivalent damping to model energy dissipation. Although both approaches are valid (Suarez and Kowalsky 2008), equivalent linearization overcomes the limitations of the Equal Displacement Approximation which can result in significant errors in predicting response.

Execution: The demand/capacity assessment procedure in AASHTO LRFD is iterative in nature since reinforcement in the column sections must be guessed at the beginning. If the displacement capacity is ultimately less than the displacement demand, the process must be repeated increasing the amount of reinforcement. If the inverse occurs, no iteration is needed, however, the resulting design will be overly conservative. In contrast to this, DDBD goes directly from target performance to required strength. The amount of reinforcement does not need to be assumed at any point in design.

Effort: DDBD does not require pushover analysis. When determining a strain-based target displacement, DDBD recognizes that the relation between strain and displacement is rather insensitive to the strength of the section. Other performance specifications, such as P-Δ effects and displacement limits in the superstructure or abutments are accounted directly with the procedures previously described.

For further comparison, the two methods are used next to design a ‘real’ bridge. The design following AASHTO LRFD Seismic was performed by others as a trial design for the implementation of that specification (Caltrans 2006b).

Example 2: Typical California Bridge

This bridge has three spans of 38.41 m, 51.21 m and 35.98 m respectively and a total length of 125.60 m. The superstructure is a continuous prestressed reinforced concrete box girder. The two bents are skewed 20^o and have two 1.83 m diameter columns supported on piles. Column height varies from 13.40 m at bent two to 14.30 m at bent three. The columns are pinned at the bottom and fixed to an integral bent in the superstructure. The abutments are seat type with brake-off walls and therefore are not considered part of the earthquake resisting system. An elevation view of the bridge is presented in Fig.8 and the superstructure section and substructure configuration are shown in Fig. 9. The seismic hazard at the bridge site is given by a design spectra with 5% damping, T_c = 4 s and *PSD* = 0.96 m.

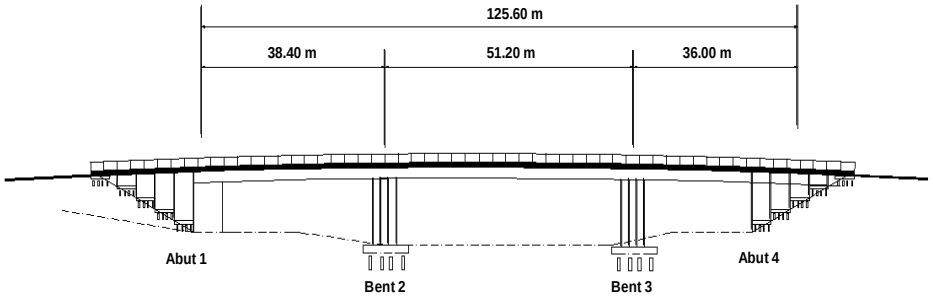

Figure 8 - Elevation view trial design CA-1

Review of design based on AASHTO LRFD Seismic: Design in the transverse direction is carried out for each bent independently (stand-alone design). In the longitudinal direction, the bents were considered linked by the superstructure. In both cases any participation of the abutments was ignored. For a detailed review of this design, the readers are directed to Caltrans (2006b).

Design began by assuming the columns are reinforced with 26D44 bars and a D25 spiral spaced at 125 mm. Next, it was checked that the bridge complies with the balanced mass and stiffness criteria given by AASHTO LRFD Seismic and a preliminary capacity-demand assessment was conducted. In order to do so, moment-curvature analyses were performed to

determine the yield moment, yield curvature and ultimate curvature and cracked section moment of inertia of the column sections. The ultimate curvature was found at a concrete strain equal 0.018.

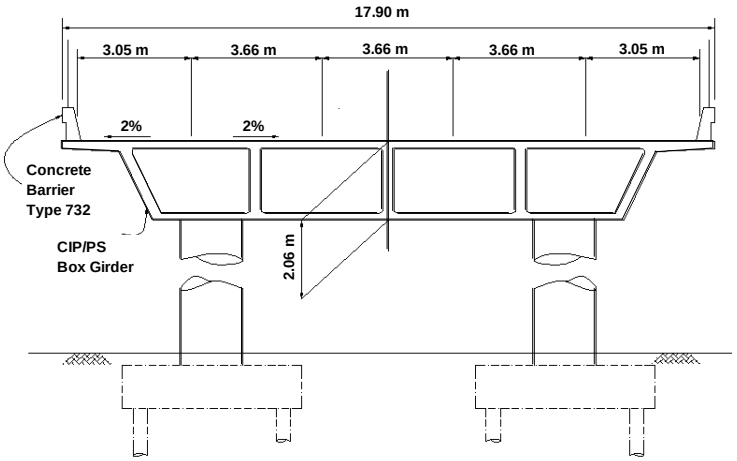

Figure 9 - Superstructure section and interior bent, trial design CA-1

Then, using the plastic hinge method, the yield displacement and ultimate displacement capacity of each bent was estimated. For bent 2, Δ_y = 184 mm and Δ_c = 908 mm and for bent 3, Δ_y = 210 mm and Δ_c = 1026 mm. These values are valid for transverse and longitudinal response. The ductility capacity of these bents is close to 5 exceeds the minimum 3 specified in AASHTO LRFD Seismic.

Next, displacement demand was computed in the transverse direction of the bridge. Each bent was treated separately; the mass that was used corresponded to the weight supported by each bent. These calculations resulted in displacement demands of 478 mm and 524 mm for bents 2 and 3 respectively. The ductility demand is 2.6 and 2.5 for bents 2 and 3 respectively. These values are significantly less than the ductility capacity and less than maximum ductility allowed by AASHTO LRFD Seismic. Therefore, it was concluded that the sections satisfied the minimum design requirements and design was continued with more detailed analyses.

Pushover analyses were then used to get a best estimate of the displacement capacity and stiffness of the bents in the transverse and longitudinal directions of the bridge, now accounting for the flexibility of the integral cap-beam and considering that the columns are partially embedded in soil. In the transverse direction, Δ_c = 882 mm and Δ_D= 564 mm for bent 2. For bent 3, Δ_C = 988 mm and Δ_D= 601 mm. A P-Δ check showed that the stability index was close to 25%. Since 25% is the limit allowed in AASHTO LRFD Seismic, it was concluded that the assumed reinforcement was appropriate and that design was controlled by P-Δ effects rather than by displacement capacity.

The pushover analysis in the longitudinal direction considered all columns in the bridge lumped together and all the mass of the bridge. The participation of the abutments was neglected. In the longitudinal direction, Δ_c = 947 mm for bent two and Δ_c = 1063 mm for bent three. The displacement demand was 599 mm for the two bents since the superstructure acts as a rigid link between them. The ductility demand is 3.11 for bent two and 2.76 for bent three. Since the induced P-Δ moments are 24% of the flexural capacity of the columns the longitudinal design was also controlled by P-Δ effects and the chosen reinforcement was considered appropriate.

Finally, a shear demand-capacity check was performed for the columns. The shear demand was based on the over-strength flexural capacity of the columns, the integral cap-beams were designed and seismic forces developed in the superstructure due to longitudinal displacement of the bridge were determined.

Direct Displacement Based Design: This design is based on the geometry, configuration, materials and section properties as reported in the AASHTO LRFD Seismic Design. Transverse and longitudinal responses are considered.

Design Objective: Under the design earthquake represented by the displacement spectra described previously, the bridge shall reach one or more of the following limits: damage-

control strains in the columns, stability index equal to 30%, superstructure displacement equal to yield limit.

Assessment of Target Displacement: According to AASHTO LRFD Seismic design report, the reinforced concrete in the bents has the following properties: f'_{ce} = 36 MPA, f_{ye} = 455 MPa, ε_y = 455/200000 = 0.0022, ε_{su} = 0.1, f_{yh} = 414 MPA. Complying with minimum reinforcement and spacing requirements, D44 longitudinal bars and a D25 spiral spaced 130 mm are chosen for the columns.

Table 2 - Target displacements Trial design CA-1

	H (m)	D (m)	P (kN)	Δ_y (m)	Damage Control Δ_C (m)	P-Δ Δ_C (m)
Bent 2	13.4	1.83	6714	178	656	640
Bent 3	14.3	1.83	6557	202	737	650

For the given amount of shear and confinement reinforcement, the damage control concrete strain computed with Eq. 18 is 0.014, this is less than the limit strain used in the AASHTO LRFD Seismic design for a life-safety limit state. The damage control displacement of the bents is determined with the plastic hinge method, assuming single bending in the columns. These calculations are valid for the two directions of design. The Yield displacement Δ_y and damage-control displacement Δ_{DC} are shown in Table 2, along with the stability based displacement (Eq. 3-4) and some parameters used in their calculation. It is observed in this table that P-Δ based displacement controls design and becomes the target design displacement. The bents are skewed 20 degrees, however since the target displacement and other response parameters are the same in the in-plane and out-of-plane direction of the bent, these are also the same in the transverse and longitudinal directions of the bridge (Eq.5-6). Also, since the abutments are weak, significant out-of-plane bending it is not expected in the superstructure and therefore its yield displacement is unlikely to control design and is therefore not assessed.

Strength Distribution: The application of DDBD results in the total strength V, required in each design direction, to meet performance specified in the design objective. The strength of seat-type abutments V_a is generally known or can be estimated before design. The contribution of the abutments to the total strength of the bridge is given by Eq. 25. Therefore, satisfying equilibrium of forces, the contribution of the piers to the strength of the bridge is given by Eq. 26.

$$v_a = \frac{V_a}{V} \qquad \text{(Eq. 25)}$$

$$v_p = 1 - v_a \qquad \text{(Eq. 26)}$$

Since it is likely that all piers develop their strength and perform inelastically during the earthquake, it is possible to distribute strength among piers such that all piers require the same reinforcement ratio (Priestley et al, 2007). Assuming that bent columns with same reinforcement ratio have the same ratio of cracked to gross inertia, Eq. 27 gives the ratio of total strength v_i taken by bent i, with n columns of diameter D_i, shear height H_{si} and ductility μ_i, required to satisfy force equilibrium. In this trial design, since the columns are pinned at the base, H_s equals the height of the columns.

$$v_i = (1 - v_a)\frac{\frac{n_i \mu_i D_i^{\,3}}{H_{si}}}{\sum \frac{n_i \mu_i D_i^{\,3}}{H_{si}}} \qquad \mu_i \le 1 \qquad \text{(Eq. 27)}$$

Recognizing that even if the abutments are not designed as part of the earthquake resisting system they can have some effect on the performance of the bridge. As a starting point, it is assumed that the abutments will take 10% of the total seismic forces in the transverse and longitudinal directions.

Design in Transverse Direction: The design in the transverse direction will account for interaction between the superstructure, bents and abutments. The superstructure section,

shown in Fig. 9, has an out-of-plane inertia I = 222 m4, an elastic modulus E_s = 26500 MPa, and a weight W_s = 260 kN/m. The abutments are assumed to have an elasto-plastic response. The transverse strength or yield force for the abutments is computed considering sacrificial shear keys that will break during the design earthquake. The residual strength in the abutment comes from friction between the superstructure and the abutment. Assuming a friction coefficient of 0.2, with a normal force equal to the tributary superstructure weight carried by the abutments, the transverse strength of the abutments is 1300 kN. It is assumed that the yield displacement is 50mm.

Since the bridge is regular and the superstructure is stiff, the abutments are not expected to restrain the displacement of the super-structure and a linear displacement profile will be used (Suarez and Kowalsky 2008). The amplitude of the target displacement profile is given by the bent with the least target displacement so Δ_{sys} = 640 mm. The effective mass comes from the mass of the superstructure, integral bent-caps and one third of the weight of the columns, M_{eff} = 3808 t.

The ductility at target displacement level is μ_1 = 12.80, μ_2 = 3.59, μ_3 = 3.16, μ_4 = 12.80. Equivalent damping is computed and combined resulting in ξ_{sys} = 14.4%. Combination of damping is done in terms of work done by each element (Priestley et al 2007).

The level of damping in the bridge results in a displacement demand reduction factor R_ξ = 0.65 and the required period is T_{eff} = 4.1 s (Eq. 22). Finally, the required strength for the bridge in the transverse direction is V = 5700 kN (Eq. 24). At the target displacement, both abutments develop their strength V_a = 2600 kN and v_a = 45% (Eq. 25). This is 4.6 times the value assumed at the beginning of the process; therefore ξ_{sys} must be re-evaluated to obtain a new V. After a few iterations V = 6447 kN and the participation of the abutments is 39 %, as shown in Table 3.

Table 3 - Transverse Design. CA-1

Iteration	Δ_{sys}	M_{eff}	ξ_{sys}	T_{eff}	V	(V1+V4)/V
1	0.64	3808.1	14.4	>Tc	5879.8	0.1
2	0.64	3808.1	13.3	3.9	6313.3	0.45
3	0.64	3808.1	13.1	3.87	6417.2	0.38
4	0.64	3808.1	13	3.86	6447.8	0.39

Table 4 - Longitudinal Design parameters. Trial design CA-1

Iteration	Δ_{sys}	M_{eff}	ξ_{sys}	T_{eff}	V	(V1+V4)/V
1	640	3808.1	14.5	>Tc	5699.9	0.1
2	640	3808.1	11	3.69	7247.1	0.8
3	640	3808.1	10.8	3.66	7349.5	0.84
4	640	3808.1	10.9	3.67	7316	0.82

It is important to note that iteration was required since it was chosen to consider the strength of the abutments. Accounting for the strength of the abutments has significantly reduced the demand on the piers. However whether the abutments are able to contribute this strength after several cycles of displacements as large as 0.6 m might be questioned.

Design in Longitudinal Direction: The design process along the longitudinal direction is similar to design in transverse direction. Since the columns are pinned to the foundation and they are integral with the superstructure, the target displacement in the longitudinal direction is the same as the capacity in the transverse direction. Also, since the superstructure is stiff and continuous, the displacement at the location of the bents and abutments are constrained to be the same. Therefore, Δ_{sys} and M_{eff} are the same as in transverse direction.

As in the transverse design case, abutments were considered to provide strength to the bridge. Since the longitudinal direction the abutments are designed with knock-off walls, their strength comes from soil mobilization behind the wall pushed by the superstructure. In the AASHTO LRFD Seismic report, the soil passive strength was 6058 kN at a yield displacement of 76mm.

Table 4 summarizes the values of the main design parameters during longitudinal design. A few iterations were required as it was found that the abutments contribute with as much as 82% of the total strength in this direction. After four iterations the solution converges, V = 7316 kN and the contribution of the abutments is 82%.

Element Design: In DDBD, the flexural reinforcement is designed using moment-curvature analysis to provide the required strength at a level of curvature compatible with the ductility demand in the element. Table 5 shows the design moments in the transverse M_t and longitudinal direction M_l that resulted from DDBD. These values are followed by P-Δ moments and stability indexes. If the stability index is larger than 8%, the design moment must be increased adding 50% of the P-Δ moment to account for strength reduction caused by P-Δ effects (Priestley et al 2007). The increased moments are then combined using the 100%-30% rule to get the design moment M_E.

Table 5 - Bent design. Trial design CA-1

BENT	M_T (kN.m)	M_L (kN.m)	$M_{t\ P\text{-}\Delta}$ (kN.m)	$M_{l\ P\text{-}\Delta}$ (kN.m)	θ_t	θ_l	M_E (kN.m)	P (kN)	ρ (%)	Shear D/C ratio
2	14975	4446	4408	4408	0.29	0.29	17238	7547	1.1	0.24
3	14975	4446	4304	4304	0.29	0.29	17238	7547	1.1	0.25

At the design displacements, the strain in the concrete reaches values of 0.011 for bent 2 and 0.010 for bent 3. These design strains are computed using the plastic hinge method. By section analysis at the design strains, it is found that all columns in the bridge require 20D44 bars as flexural reinforcement, which is a 1.1% steel ratio. Finally, using the modified UCSD shear model (Priestley et al 1994), the shear capacity of the section is computed and compared to shear demand at flexural over-strength. The shear demand/capacity ratios are shown in Table 5.

Table 6. Summary of LDFD-Seismic and DDBD designs

LRFD-Seismic							
BENT	Δ_{Ct} (mm)	Δ_{Cl} (mm)	Δ_{Dt} (mm)	Δ_{Dl} (mm)	ρ (%)	Rebar	Spiral
2	882	947	564	599	1.5	26D44	D25@125
3	988	1063	601	599	1.5	26D44	D25@125
DDBD							
BENT	Δ_{Ct} (mm)	Δ_{Cl} (mm)	Δ_{Dt} (mm)	Δ_{Dl} (mm)	ρ (%)	Rebar	Spiral
2	640	640	640	640	1.1	18D44	D25@125
3	640	640	640	640	1.1	18D44	D25@125

*Analysis and Comparison***:** A summary of results of the two designs for this bridge is presented in Table 6. It is observed that accounting by the strength of the abutments in DDBD lead to a reduction in the amount of reinforcement required in the piers. DDBD required less effort than AASHTO LRFD Seismic since pushover analysis was not required. It is also observed that the effort required to obtain an optimum design in AASHTO LRFD Seismic is directly related to the experience of the designed to guess the reinforcement of the sections and avoid iteration.

CONCLUSIONS

- DDBD produces optimum designs in which the bridge meets a predefined level of performance in the critical direction. To obtain a comparable design in AASHTO LRFD Seismic, iteration is needed, varying the amount of reinforcement, until displacement demand equal displacement capacity.
- The application of DDBD requires less effort than the application of AASHTO LRFD Seismic
- DDBD can design a structure for any combination of performance and earthquake intensity. Therefore DDBD can be used to meet the performance requirements AASHTO LRFD Seismic, for design in all SDC.

REFERENCES

Caltrans, 2006a, Seismic Design Criteria, Caltrans, http://www.dot.ca.gov/hq/esc/earthquake_engineering, (accessed April 18, 2008)

Caltrans, 2006b, LRFD Design Example B November 3, 2006 – Version 1.1, AASHTO, http://cms.transportation.org/?siteid=34&pageid=1800, (accessed April 18, 2008).

Calvi G.M. and Kingsley G.R., 1995, Displacement based seismic design of multi-degree-of-freedom bridge structures, Earthquake Engineering and Structural Dynamics 24, 1247-1266.

Dwairi, H. and Kowalsky, M.J., 2006, Implementation of Inelastic Displacement Patterns in Direct Displacement-Based Design of Continuous Bridge Structures, Earthquake Spectra, Volume 22, Issue 3, pp. 631-662

EuroCode 8, 1998, Structures in seismic regions – Design. Part 1, General and Building", Commission of European Communities, Report EUR 8849 EN

Imbsen, 2007, AASHTO Guide Specifications for LRFD Seismic Bridge Design, AASHTO, http://cms.transportation.org/?siteid=34&pageid=1800, (accessed April 18, 2008).

Kowalsky M.J., 2002, A Displacement-based approach for the seismic design of continuous concrete bridges, Earthquake Engineering and Structural Dynamics 31, pp. 719-747.

Kowalsky M.J., Priestley M.J.N. and MacRae G.A. 1995. Displacement-based Design of RC Bridge Columns in Seismic Regions, Earthquake Engineering and Structural Dynamics 24, 1623-1643.

Mander, J.B., Priestley, M.J.N. and Park, R., 1988a, Theoretical Stress Strain Model of Confined Concrete Journal of Structural Engineering, ASCE, Vol. 114, No.8, August, 1988

Mazzoni, S., McKenna, F., Scott, M. and Fenves, G., 2004, OpenSees command language manual, http://opensees.berkeley.edu, (accessed April 18, 2008)

Paulay, T, Priestley, M.J.N., 1992, Seismic Design of Reinforced Concrete and Masonry Buildings, Wiley, 978-0-471-54915-4

Priestley, M. J. N., 1993, Myths and fallacies in earthquake engineering-conflicts between design and reality, Bulletin of the New Zealand Society of Earthquake Engineering, 26 (3), pp. 329–341

Priestley, M. J. N., Calvi, G. M. and Kowalsky, M. J., 2007, Direct Displacement-Based Seismic Design of Structures, Pavia, IUSS Press

Priestley, M. J. N., Verma, R., Xiao, Y., 1994, Seismic Shear Strength of Reinforced Concrete Columns, Journal of Structural Engineering 120(8) (1994) pp. 2310–2328

Shibata A. and Sozen M. Substitute structure method for seismic design in R/C. Journal of the Structural Division, ASCE 1976; 102(ST1): 1-18.

Suarez, V.A. and Kowalsky M.J., Displacement-Based Seismic Design of Drilled Shaft Bents with Soil-Structure Interaction, Journal of Earthquake Engineering, Volume 11, Issue 6 November 2007 , pp. 1010 – 1030

Suarez, V.A., 2008, Implementation of Direct Displacement Based Design for Highway Bridges, PhD Dissertation, North Carolina State University.

Veletsos, A. and Newmark, N. M., 1960, Effect of inelastic behavior on the response of simple systems to earthquake motions", Proceedings of 2nd World Conference on Earthquake Engineering, pp. 895 – 912.

PART VII

SUMMARY AND CONCLUSIONS

1. SUMMARY AND CONCLUSIONS

The main objective of this research is to bridge the gap between existing research on DDBD and its implementation for design of conventional highway bridges with their inherent complexities. This research has addressed issues such as: the limited displacement capacity of superstructures, skew in bents and abutments, displacement patterns, P-Δ effects, increasing the scope and applicability of DDBD substantially.

Products of this research are the programs DDBD-Bridge and ITHA-Bridge. These programs and their documentation can be used online (www.utpl.edu.ec/vlee) to recreate the results presented thru this dissertation and also a tool for future studies.

The most significant contributions of this research are the models for determination of a stability-based target displacement for piers (Part V) and the observations made to the use of different types of displacement patterns in the transverse design of bridges (Part IV). With this new information, the effort in the application of DDBD can be greatly reduced since the need for iteration is eliminated.

Other important contributions are the models to incorporate the superstructure displacement capacity and skew in bents and abutments into DDBD. Also important is the comparison of execution and outcome of DDBD to the design procedure in the AASHTO Guide Specification for Seismic Bridge Design (Part III).

The most relevant conclusions of this research are:

- DDBD can be applied directly and effectively, using a RBT pattern, for bridge frames or bridges with weak abutments that have a balanced distribution of mass and stiffness (BMS-1 > 0.75 and BMS-2 >0.5)
- Using the FMS algorithm is not appropriate for design of asymmetric bridge frames, asymmetric bridges with weak abutments and bridges with expansion joints, since the first mode of vibration does not control the shape of their displacement pattern.

- Iteration in design of bridges controlled by P-Δ effects can be reduced or avoided by determining the proposed stability-based target displacement at beginning of design.
- DDBD produces optimum designs in which the bridge meets a predefined level of performance in the critical direction. To obtain a comparable design in LRFD-Seismic, iteration is needed, varying the amount of reinforcement, until displacement demand equal displacement capacity.
- DDBD is compatible with the design philosophy in the new LRFD-Seismic guide. However DDBD requires less effort than the method in LRFD-Seismic. Therefore DDBD can be used as an alternative method.

PART VIII

APPENDICES

DDBD-BRIDGE
SOFTWARE FOR DIRECT DISPLACEMENT BASED DESIGN OF BRIDGES
USER MANUAL

Vinicio A. Suarez and Mervyn J. Kowalsky

1. INTRODUCTION

DDBD-Bridge has been developed for automation of the DDBD method for highway bridges. In most design cases DDBD can be applied with manual or spreadsheet calculations. However, time in the application of the First Mode Shape (FMS) or Effective Mode Shape (EMS) algorithms and section design can be saved by programming the algorithms into a computer code.

DDBD-Bridge has been programmed following the general procedure presented in a companion paper by the authors entitled "Implementation of DDBD for Highway Bridges".

DDBD-Bridge has the following features:

- DDBD of highway bridges in the transverse and longitudinal directions
- Design using the direct, FMS and EMS algorithms
- Continuous superstructures or superstructures with expansion joints
- Supports Integral or seat-type abutments
- Supports skewed piers and abutments
- All types of piers shown in Figure 1
- Automated section design

The program and its documentation can be accessed and used on-line though the Virtual Laboratory for Earthquake Engineering (VLEE) at: www.utpl.edu.ec/vlee. The VLEE provides an interactive user interface for DDBD-Bridge and other related programs such as ITHA-Bridge.

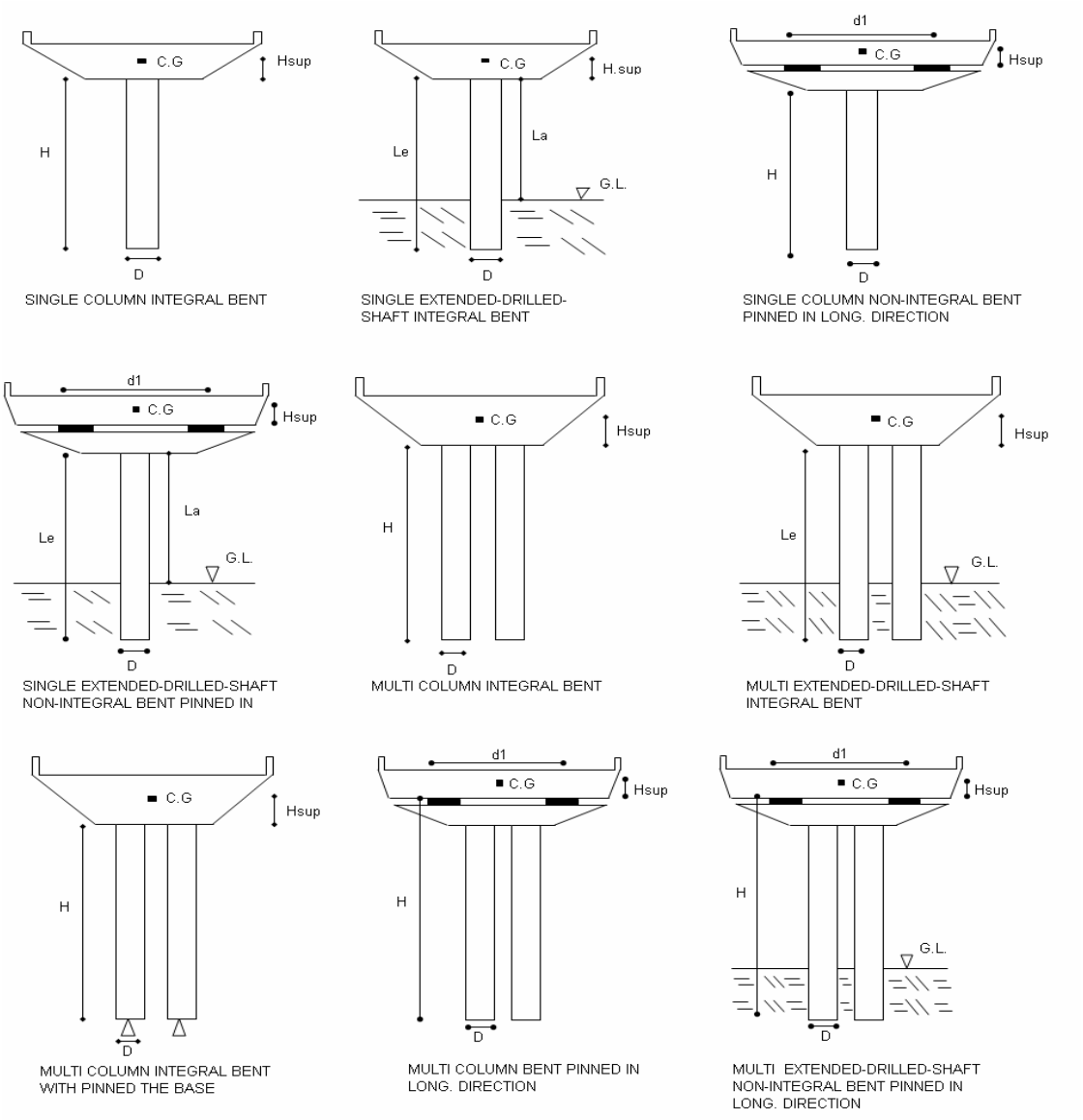

Figure 1 - Pier configurations supported by DDBD Bridge

2. RUNNING DDBD-BRIDGE

To run the program the user must input the data requested in the web interface and run the program on-line. Then, the user can download a design report that is automatically generated.

3. INPUT DATA

When using the web interface, the user inputs a number of design variables. These parameters are defined next

Bridge Configuration

NSPAN	Number of spans **[1-8]**
SLENGTH	Length of the superstructure **[> 0]**
PHIYS	Allowable curvature in superstructure (1/m) **[> 0]**

Superstructure

SWEIGHT	Weight of the superstructure section (kN/m) **[>0]**
SHEIGHT	Distance from the soffit to the centre of gravity of the superstructure section (m) [>0]
SINERTIA	Superstructure inertia around the vertical axis (m^4) [>0]
SEM	Elastic modulus of the superstructure (MPa) [>0]
NSJOINTS	Number of expansion joints in the superstructure (0 if none) [0-3]

Design Spectra

TC	Corner period in displacement design spectra [>0]
MDISP	Maximum spectral displacement [>0]
TB	Period at end of acceleration plateau**.** [>0, TB>TA]
TA	Period at beginning of acceleration plateau**.** [>0]

PSA Peak spectral acceleration (m/s^2) [>0]

PGA Peak ground acceleration (m/s^2) [>0]

ALPHA **0.5** if fault is more than 10 km away from the site

0.25 if fault is less than 10 km away from the site

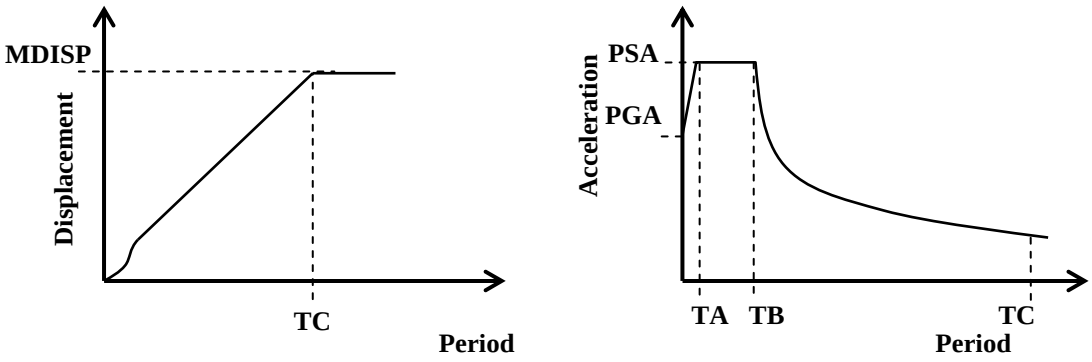

Figure 2 – Design Spectra

DDBD

SDIST **1** To get columns with same reinforcement (typical)

2 To get same shear in all piers (appropriate for seismic isolated piers)

NITER Max number of iterations allowed (10-30)

TOL Tolerance in convergence of displaced shape (0.01-0.1)

SST (Assumed) fraction of total base shear taken by abutments in transverse direction (0-1)

SSL (Assumed) fraction of total base shear taken by abutments in longitudinal direction (0-1)

UDDS 0 Program uses a transverse Rigid Body Translation Patter

1 Program uses a user defined transverse displacement profile. In which case the user must provide the displacement values (m) at each substructure location

2 Program used the First Mode Shape design algorithm

3 Program uses the Effective Mode Shape design Algorithm

Material Properties

WC	Unit weight of concrete (kN/m^3) [>0]
FPC	Specified unconfined compressive strength of concrete (MPa) [>0]
FY	Specified yield stress of longitudinal reinforcement bars (MPa) [>0]
FUR	Ratio between ultimate and yield stress of longitudinal reinforcement bars [>1]
ESU	**S**train at maximum stress of longitudinal reinforcement bars [0.06-0.12]
FYH	Specified yield stress of transverse reinforcement bars (MPa) [>0]
FURH	Ratio between ultimate and yield stress of transverse reinforcement bars [>1]
ESUH	**S**train at maximum stress of transverse reinforcement bars [0.06-0.12]

Substructure Types

Elastic Abutment

STA	Distance from the left end of the bridge to the element (m) [0 or SLENGTH]
SKEW	Skew angle (Degrees measured from axis perpendicular to bridge) [0 a 90]
DTOUT	Out-of-plane displacement capacity (m) [>0]
DTIN	In-plane displacement capacity (m) [>0]
DAMP	Equivalent damping (%)[5%-10%]
AWEIGHT	Effective weight of the abutment [>=0]

Elasto-plastic abutment

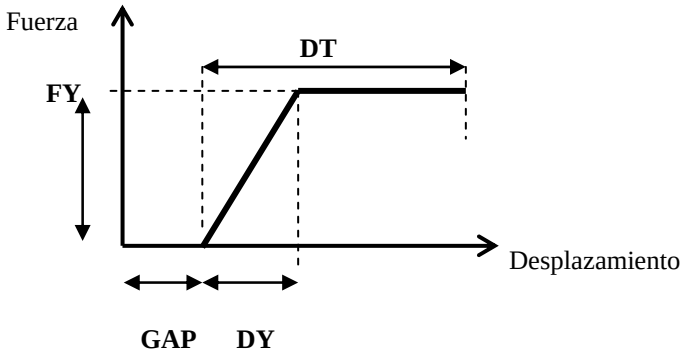

Figure 3 – Elasto-plastic abutment

STA	Distance from the left end of the bridge to the element (m) [0 or SLENGTH]
SKEW	Skew angle (Degrees) [0-90]
DTOUT	Out-of-plane displacement capacity (m) [>0]

DTIN In-plane displacement capacity (m) [>0]

DYOUT Out-of-plane yield displacement (m) [>0]

DYIN In-plane yield displacement (m) [>0]

FYOUT Out-of-plane strength (kN) [>=0]

FYIN In-plane strength (kN) [>=0]

GAP Longitudinal gap between superstructure and abutment (m) [>=0]

B Parameter that defines the equivalent damping, as a function of the ductility demand, for the element. If B >0, B is used in the equation below to compute If B = 0 or omitted then B is taken as 60 as for an elasto-plastic system. If B < 0, the absolute value of B is taken as constant damping for the abutment.

$$\xi = 5 + B\frac{\mu - 1}{\pi\mu}$$

AWEIGHT Effective weight of the abutment [>=0]

Single column integral bent

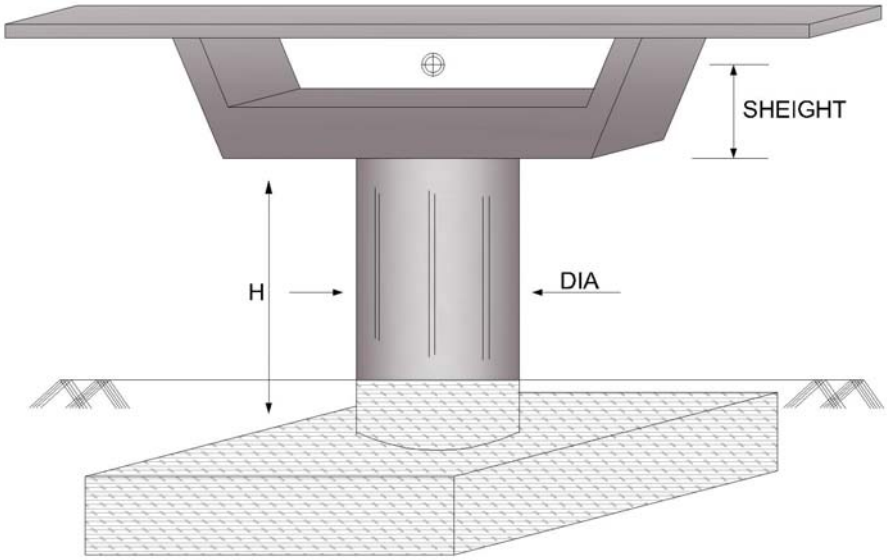

Figure 4 – Single column integral bent

STA	Distance from the left end of the bridge to the element (m) [0-SLENGTH]
DIA	Diameter of the column (m) [>0]
H	Height of the column (m) [>0]
D1 D2	Parameters that control how target displacement is calculated If D1>0 and D2>0 then D1 and D2 are taken as the limit STRAINS for concrete and steel respectively If D1 = -1 then D2 is the target DRIFT value for transverse and longitudinal response (drift is expressed as the ratio of top displacement and height of the column) If D1 = -2 and D2 = 0 then target displacement is found for DAMAGE CONTROL limit state

	If D1 = -3 and D2 = 0 then target displacement is found for moderate plastic action using the implicit procedure in LRFD-Seismic for SDC "B"
	If D1 = -4 and D2 = 0 then target displacement is found for minimal plastic action using the implicit procedure in LRFD-Seismic for SDC "C"
	If D1 = -5 then target displacement is computed for the displacement ductility limit specified in D2
DBL	Diameter of longitudinal rebars (mm). [>=0]. If DBL = 0, program uses minimum reinforcement ratio
DBH	Diameter of spiral (mm). [>=0] If DBH = 0, program uses minimum reinforcement
SHB	Spacing of spiral (mm). [>=0] If SHB = 0, program uses minimum reinforcement
COV	Concrete cover to spiral (mm) [>0]
CAPW	Weight of integral cap built into superstructure (kN) [>=0]
MGT	Moment in plastic hinge regions caused by gravity loads that is to be added to seismic moment in transverse direction (kN.m) [>=0]

Single column bent

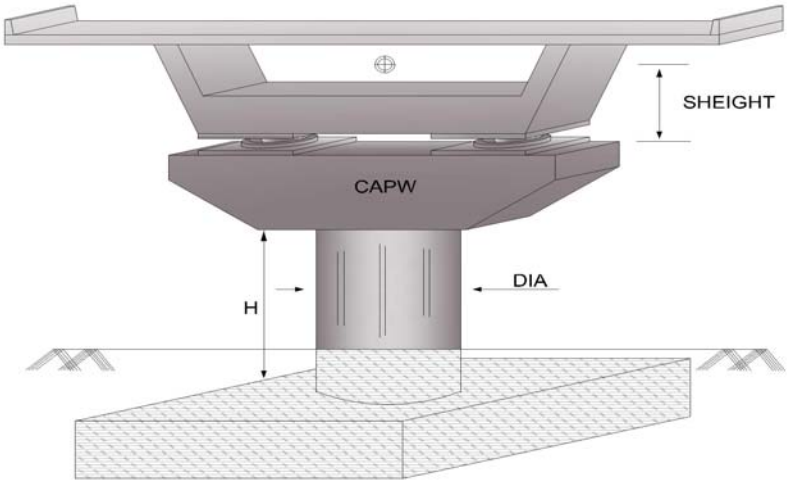

Figure 5 – Single column bent

STA	Distance from the left end of the bridge to the element (m) [0-SLENGTH]
DIA	Diameter of the column (m) [>0]
H	Height of the column (m) [>0]
D1 D2	Parameters that control how target displacement is calculated If D1>0 and D2>0 then D1 and D2 are taken as the limit STRAINS for concrete and steel respectively If D1 = -1 then D2 is the target DRIFT value for transverse and longitudinal response (drift is expressed as the ratio of top displacement and height of the column) If D1 = -2 and D2 = 0 then target displacement is found for DAMAGE CONTROL limit state

	If D1 = -3 and D2 = 0 then target displacement is found for minimal plastic action using the implicit procedure in LRFD-Seismic for SDC "B" If D1 = -4 and D2 = 0 then target displacement is found for moderate plastic action using the implicit procedure in LRFD-Seismic for SDC "C" If D1 = -5 then target displacement is computed for the displacement ductility limit specified in D2
DBL	Diameter of longitudinal rebars (mm). [>=0] If DBL = 0, program uses minimum reinforcement ratio
DBH	Diameter of spiral (mm). [>=0] If DBH = 0, program uses minimum reinforcement
SHB	Spacing of spiral (mm). [>=0] If SHB = 0, program uses minimum reinforcement
COV	Concrete cover to spiral [>0] (mm)
CAPW	Weigtht of integral cap built into superstructure (kN) [>=0]
MGT	Moment in plastic hinge regions caused by gravity loads that is to be added to seismic moment in transverse direction (kN.m) [>=0]

Multi column integral bent

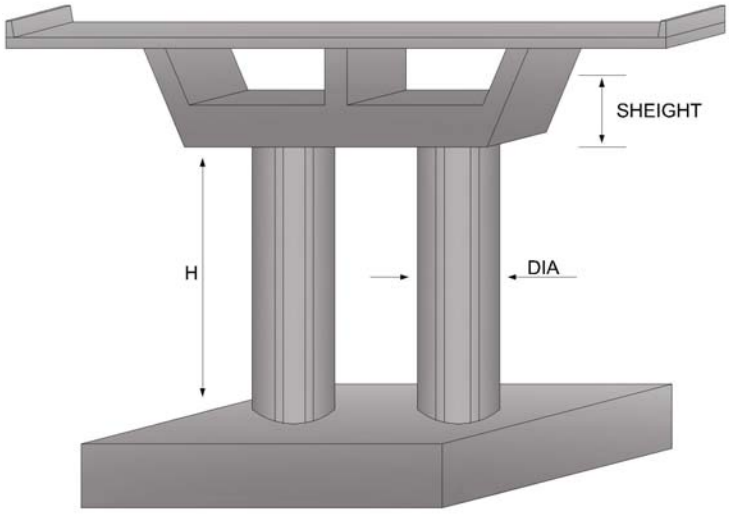

Figure 6 – Multi column Integral bent

STA	Distance from the left end of the bridge to the element (m) [0-SLENGTH]
DIA	Diameter of the column (m) [>0]
H	Height of the column (m) [>0]
NCOLS	Number of column is bent [>1]
D1 D2	Parameters that control how target displacement is calculated If D1>0 and D2>0 then D1 and D2 are taken as the limit STRAINS for concrete and steel respectively If D1 = -1 then D2 is the target DRIFT value for transverse and longitudinal response (drift is expressed as the ratio of top displacement and height of the column) If D1 = -2 and D2 = 0 then target displacement is found for DAMAGE CONTROL limit state

	If D1 = -3 and D2 = 0 then target displacement is found for moderate plastic action using the implicit procedure in LRFD-Seismic for SDC "B" If D1 = -4 and D2 = 0 then target displacement is found for minimal plastic action using the implicit procedure in LRFD-Seismic for SDC "C" If D1 = -5 then target displacement is computed for the displacement ductility limit specified in D2
DBL	Diameter of longitudinal rebars (mm). If DBL = 0, program uses minimum reinforcement ratio [>=0]
DBH	Diameter of spiral (mm). If DBH = 0, program uses minimum reinforcement [>=0]
SHB	Spacing of spiral (mm). If SHB = 0, program uses minimum reinforcement [>=0]
COV	Concrete cover to spiral (mm) [>0]
CAPW	Weigtht of integral cap built into superstructure (kN) [>=0]
MGT	Moment in plastic hinge regions caused by gravity loads that is to be added to seismic moment in transverse direction (kN.m) [>=0]

Multi column integral bent with pinned base

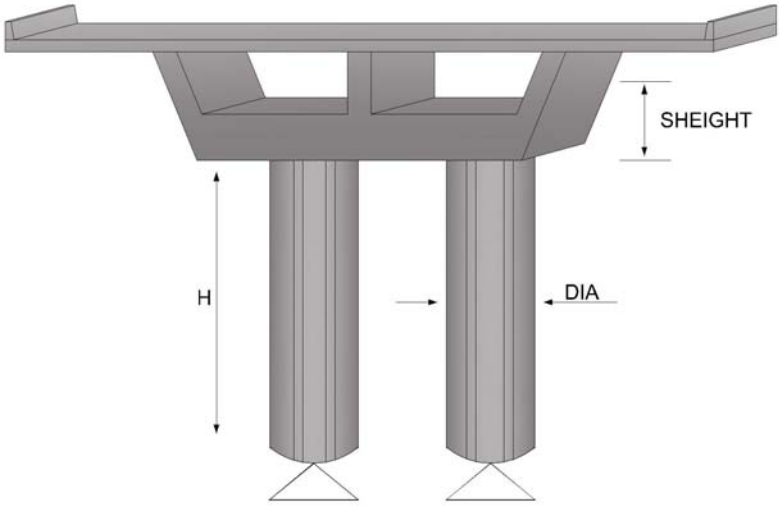

Figure 7 – Multi column integral bent with pinned base

STA	Distance from the left end of the bridge to the element (m) [0-SLENGTH]
DIA	Diameter of the column (m) [>0]
H	Height of the column (m) [>0]
NCOLS	Number of column is bent [>1]
D1 D2	Parameters that control how target displacement is calculated If D1>0 and D2>0 then D1 and D2 are taken as the limit STRAINS for concrete and steel respectively If D1 = -1 then D2 is the target DRIFT value for transverse and longitudinal response (drift is expressed as the ratio of top displacement and height of the column) If D1 = -2 and D2 = 0 then target displacement is found for DAMAGE CONTROL limit state

	If D1 = -3 and D2 = 0 then target displacement is found for moderate plastic action using the implicit procedure in LRFD-Seismic for SDC "B" If D1 = -4 and D2 = 0 then target displacement is found for minimal plastic action using the implicit procedure in LRFD-Seismic for SDC "C" If D1 = -5 then target displacement is computed for the displacement ductility limit specified in D2
DBL	Diameter of longitudinal rebars (mm). If DBL = 0, program uses minimum reinforcement ratio [>=0]
DBH	Diameter of spiral (mm). If DBH = 0, program uses minimum reinforcement [>=0]
SHB	Spacing of spiral (mm). If SHB = 0, program uses minimum reinforcement [>=0]
COV	Concrete cover to spiral (mm) [>0]
CAPW	Weigtht of integral cap built into superstructure (kN) [>=0]
MGT	Moment in plastic hinge regions caused by gravity loads that is to be added to seismic moment in transverse direction (kN.m) [>=0]

Multi column bent

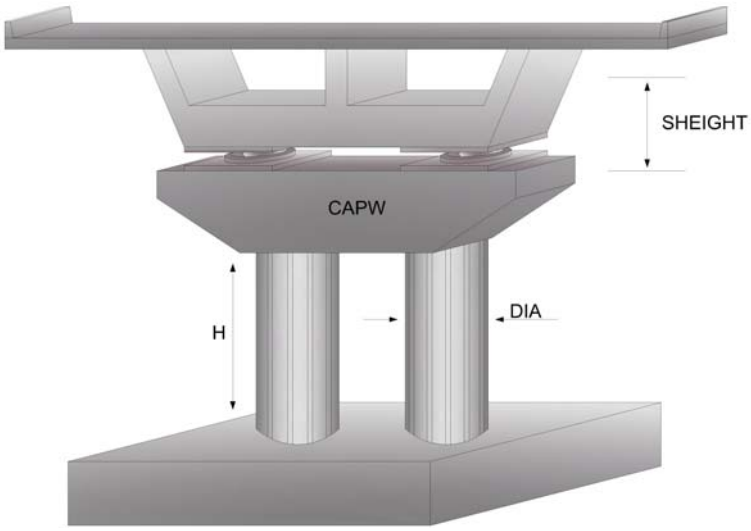

Figure 8 – Multi column bent

STA	Distance from the left end of the bridge to the element (m) [0-SLENGTH]
DIA	Diameter of the column (m) [>0]
H	Height of the column (m) [>0]
NCOLS	Number of column is bent [>1]
D1 D2	Parameters that control how target displacement is calculated If D1>0 and D2>0 then D1 and D2 are taken as the limit STRAINS for concrete and steel respectively If D1 = -1 then D2 is the target DRIFT value for transverse and longitudinal response (drift is expressed as the ratio of top displacement and height of the column) If D1 = -2 and D2 = 0 then target displacement is found for DAMAGE CONTROL limit state

	If D1 = -3 and D2 = 0 then target displacement is found for moderate plastic action using the implicit procedure in LRFD-Seismic for SDC "B"
	If D1 = -4 and D2 = 0 then target displacement is found for minimal plastic action using the implicit procedure in LRFD-Seismic for SDC "C"
	If D1 = -5 then target displacement is computed for the displacement ductility limit specified in D2
DBL	Diameter of longitudinal rebars (mm). If DBL = 0, program uses minimum reinforcement ratio [>=0]
DBH	Diameter of spiral (mm). If DBH = 0, program uses minimum reinforcement [>=0]
SHB	Spacing of spiral (mm). If SHB = 0, program uses minimum reinforcement [>=0]
COV	Concrete cover to spiral (mm) [>0]
CAPW	Weigtht of integral cap built into superstructure (kN) [>=0]
SKEW	Skew angle [0-90]
HCBEAM	Height of the cap-beam [>0]
MGT	Moment in plastic hinge regions caused by gravity loads that is to be added to seismic moment in transverse direction (kN.m) [>=0]

General Pier

STA Distance from the left end of the bridge to the element (m) [0-SLENGTH]

DYT Yield displacement in transverse direction (m) [>0]

DYL Yield displacement in longitudinal direction (m) [>0]

DTT Displacement capacity in the transverse direction (m) [>0]

DTL Displacement capacity in the longitudinal direction (m) [>0]

B Parameter that defines the equivalent damping, ξ, as a function of the ductility demand, μ, for the element. If B >0, B is used in the equation below to compute ξ. If B = 0 or omitted then B is taken as 60 as for an elasto-plastic system. If B < 0, the absolute value of B is taken as constant damping for the abutment.

$$\xi = 5 + B\frac{\mu - 1}{\pi\mu}$$

AWEIGHT Effective weight of the pier [>=0]

Expansion Joint

STA Distance from the left end of the bridge to the element (m) [0-SLENGTH]

GAP Longitudinal gap provided at the expansion joint (m) **[>=0]**

ITHA-BRIDGE
SOFTWARE FOR INEASTIC TIME HISTORY ANALYSYS OF BRIDGES
PRE-PROCESSOR AND POST-PROCESOR OF OPENSEES

Vinicio A. Suarez and Mervyn J. Kowalsky

1. INTRODUCTION

The program ITHA-Bridge has been developed to perform Inelastic Time History Analysis (ITHA) of highway bridges. This program is a pre-processor and post-processor of OpenSees and has the following features:

- From a basic input automatically generates the bridge model files for OpenSees.
- Supports the substructures shown in Figure 1, integral and seat-type abutments. Also supports superstructure joints and plan curvature.
- Multiple acceleration records can be run in batch mode automatically.
- Checks convergence errors in solution and adjusts the analysis time step if necessary to achieve convergence.
- Produces and output file combining the output of the different acceleration records that were run.

ITHA-Bridge and its documentation can be accessed and used on-line though the Virtual Laboratory for Earthquake Engineering (VLEE) at www.utpl.edu.ec/vlee. The VLEE provides an interactive user interface for ITHA-Bridge and other related programs such as DDBD-Bridge.

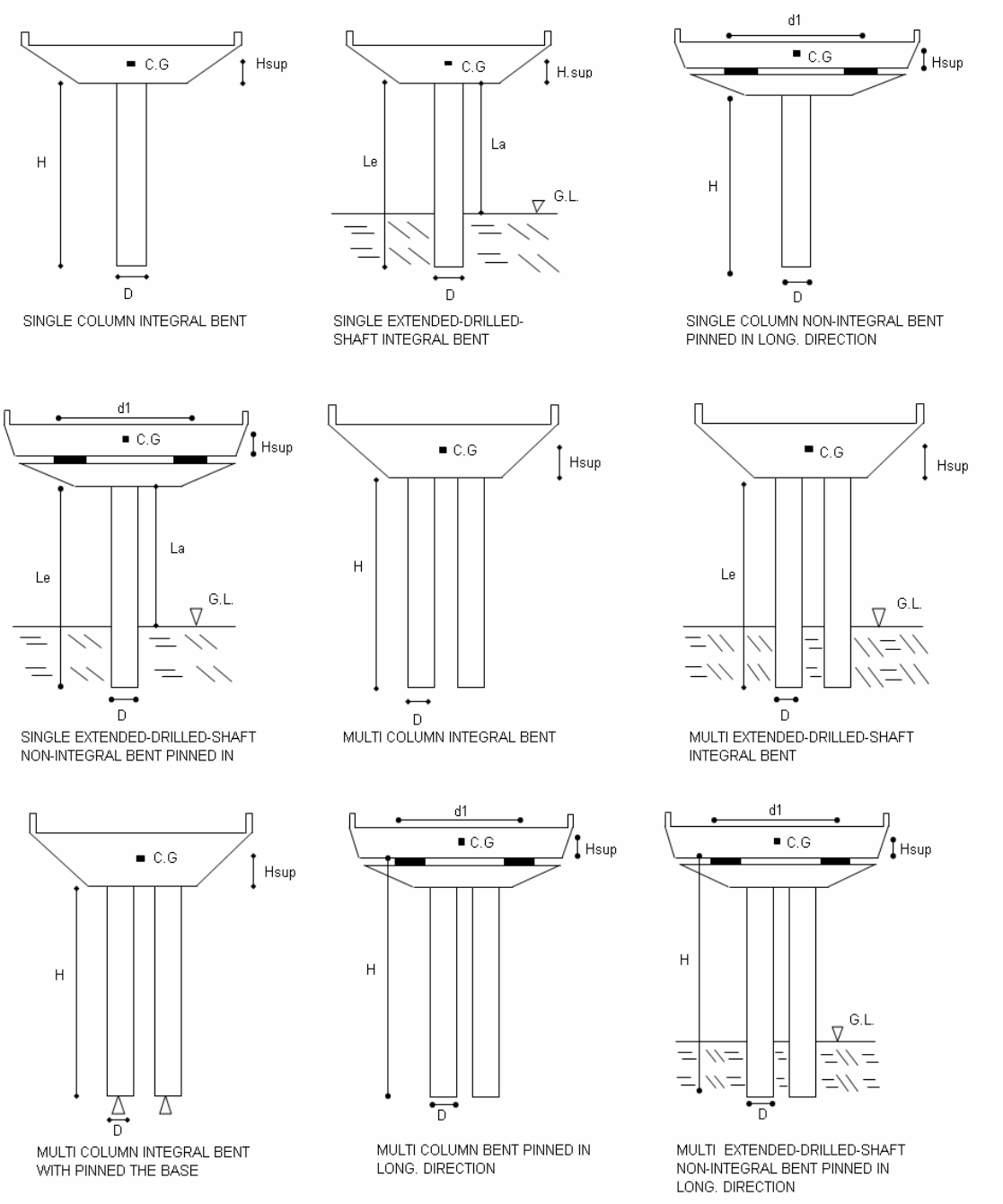

Figure 9 - Pier configurations supported by ITHA-Bridge

2. RUNNING DDBD-BRIDGE

To run the program the user must input the data requested in the web interface and run the program on-line. Then, the user will receive an email with the report of the simulation.

3. INPUT DATA

When using the web interface, the user inputs a number of design variables. These parameters are defined next.

Bridge Configuration

NSPAN	Number of spans **[1-8]**
SLENGTH	Total length of the superstructure (m) **[> 0]**
SANGLE	Subtended angle that gives plan curvature (deg) **[> 0]**

Superstructure

SW	Weight of the superstructure (kN/m) **[>0]**
SH	Distance from the centroid to the bottom of the superstructure section (m) [>0]
IZ	Out-of-plane inertia of the superstructure section (m4)
IY	In-plane inertia of the superstructure section (m4)
EC	Elastic modulus of the superstructure (MPa)
A	Area of the superstructure section (m2)
J	Torsion constant of superstructure (m3)
NPS	Number of frame elements each span is divided in

NEJ	Number of expansion joints in the superstructure

Earthquake records

NEQ	Number of acceleration records to be applied
TOL	Tolerance in the ITHA solution (0.0001 - 0.000001)
PDELTA	0 to turn off P-Delta effects in the analysis 1 to turn on P-Delta effects in the analysis
ACCX	Name of the file that has the acceleration record to be applied in the X direction
ACCY	Name of the file that has the acceleration record to be applied in the Y direction
DUR	Duration of the record (s)
DT	Time step of the record (s)
FX	Factor applied to the record in the X direction
FY	Factor applied to the record in the Y direction

Material Properties

WC	Unit weight of concrete (kN/m^3) [>0]
FPC	Specified unconfined compressive strength of concrete (MPa) [>0]
FY	Specified yield stress of longitudinal reinforcement bars (MPa) [>0]
FUR	Ratio between ultimate and yield stress of longitudinal reinforcement bars [>1]
ESU	**S**train at maximum stress of longitudinal reinforcement bars [0.06-0.12]
FYH	Specified yield stress of transverse reinforcement bars (MPa) [>0]
FURH	Ratio between ultimate and yield stress of transverse reinforcement bars [>1]

ESUH **S**train at maximum stress of transverse reinforcement bars [0.06-0.12]

Substructure Types

Abutment

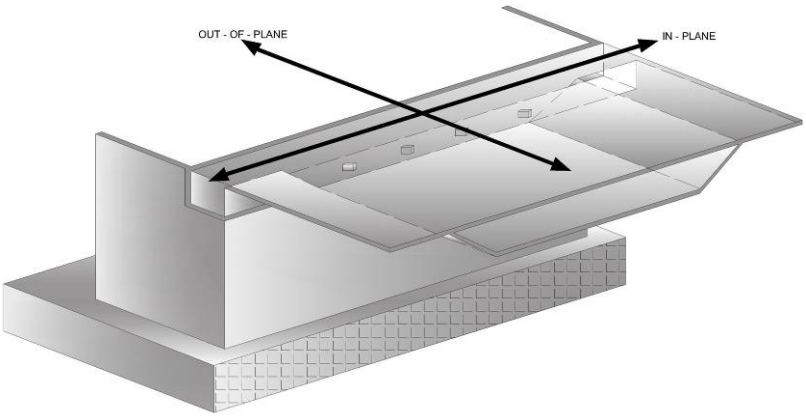

Figure 10 – Abutment

STA Distance from the left end of the bridge to the element (m) [0 or SLENGTH]

SKEW Skew angle (Degrees measured from axis perpendicular to bridge) [0 a 90]

DYOUT Out-of-plane yield displacement (m)

DYIN In-Plane yield displacement (m)

VYOUT Out-of-plane yield force of the abutment (kN)

VYIN In-plane yield force of the abutment (kN)

GAPOUT Expansion gap in the longitudinal direction of the abutment

DAMP Viscous damping (%) [5%-10%]

W Weight of the abutment (kN**)** [>=0]

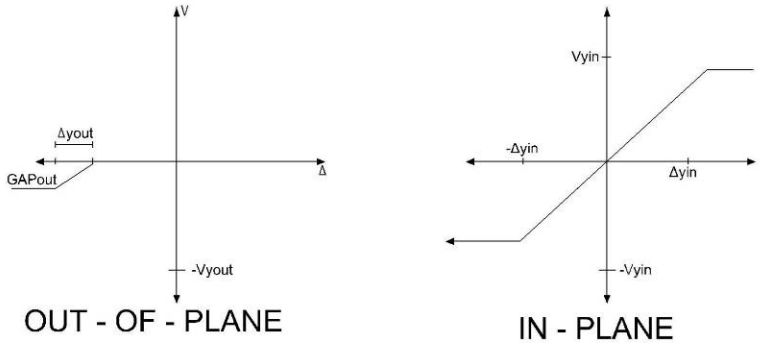

Figure 11 – Out-of-plane and in-plane response of abutment model

Expansion Joint

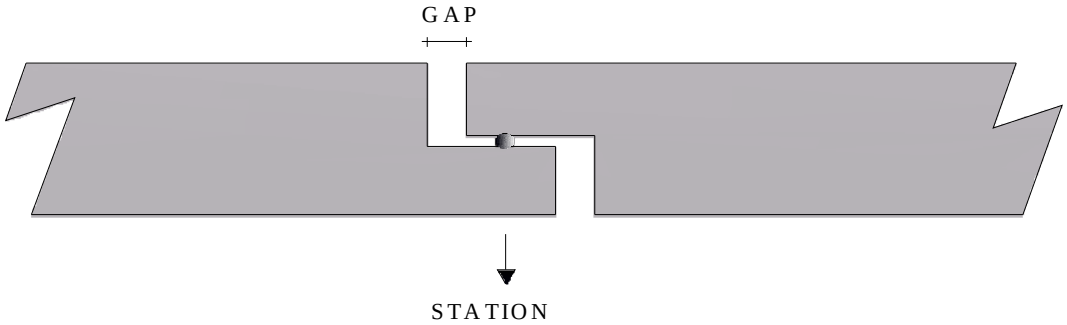

Figure 12 – Expansion joint model

STA Distance from the left end of the bridge to the element (m) [0-SLENGTH]

GAP Size of the expansion gap (m) [>=0]

Single column integral bent

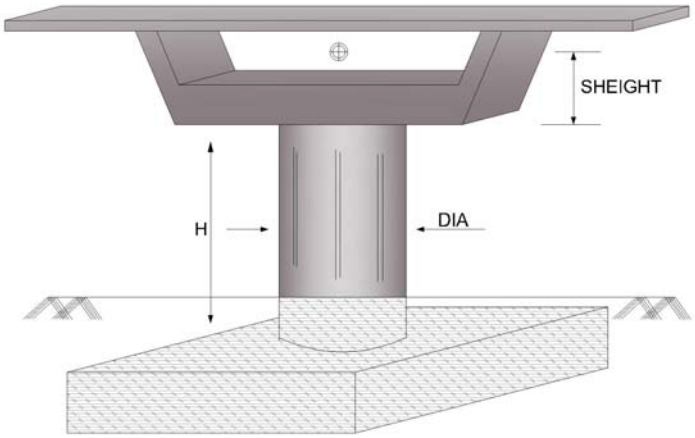

Figure 13 – Single column integral bent

STA	Distance from the left end of the bridge to the element (m) [0-SLENGTH]
DIA	Diameter of the column (m) [>0]
H	Clear height of the column (m) [>0]
NLBAR	Number of longitudinal bars
DLBAR	Diameter of the longitudinal bars (m) [>0]
DHBAR	Diameter of the transverse reinforcement (mm) [>0]
HBARS	Spacing of the transverse reinforcement (mm)
COV	Concrete cover to the transverse reinforcement (mm)
NPC	Number of elements in which the column is divided [1 – 5]
CBW	Weight of the Capbeam (kN)

Single column bent

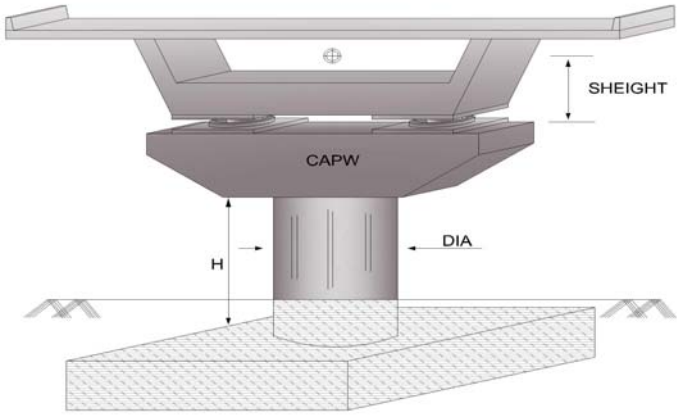

Figure 14 – Single column bent

STA	Distance from the left end of the bridge to the element (m) [0-SLENGTH]
DIA	Diameter of the column (m) [>0]
H	Clear height of the column (m) [>0]
NLBAR	Number of longitudinal bars
DLBAR	Diameter of the longitudinal bars (m) [>0]
DHBAR	Diameter of the transverse reinforcement (mm)
HBARS	Spacing of the transverse reinforcement (mm)
COV	Concrete cover to the transverse reinforcement (mm)
NPC	Number of elements in which the column is divided [1 – 5]
CBW	Weight of the Capbeam (kN)
SKEW	Skew angle [0-90]

Multi column integral bent

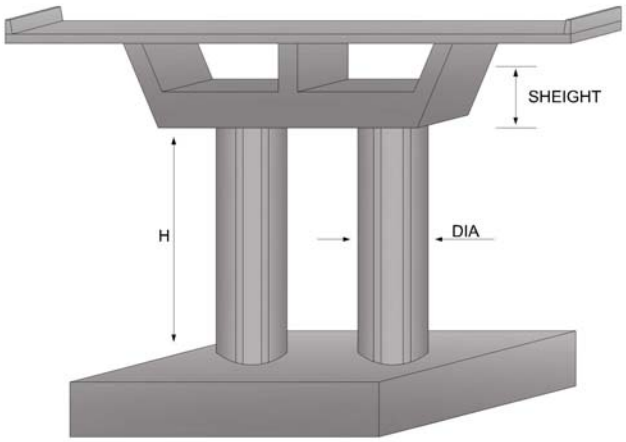

Figure 15 – Multi column integral bent

STA	Distance from the left end of the bridge to the element (m) [0-SLENGTH]
DIA	Diameter of the column (m) [>0]
H	Clear height of the column (m) [>0]
NLBAR	Number of longitudinal bars
DLBAR	Diameter of the longitudinal bars (m) [>0]
DHBAR	Diameter of the transverse reinforcement (mm) [>0]
HBARS	Spacing of the transverse reinforcement (mm)
COV	Concrete cover to the transverse reinforcement (mm)
NPC	Number of elements in which the column is divided [1 – 5]
NCOLS	Number of columns in the bent
SCOL	Spacing of the columns
CBW	Weight of the Capbeam (kN)

Multicolumn integral bent with pinned base

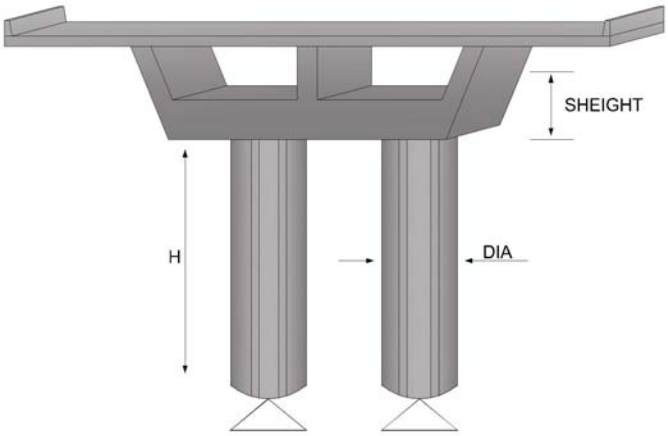

Figure 16 – Multi column integral bent with pinned base

STA	Distance from the left end of the bridge to the element (m) [0-SLENGTH]
DIA	Diameter of the column (m) [>0]
H	Clear height of the column (m) [>0]
NLBAR	Number of longitudinal bars
DLBAR	Diameter of the longitudinal bars (m) [>0]
DHBAR	Diameter of the transverse reinforcement (mm) [>0]
HBARS	Spacing of the transverse reinforcement (mm)
COV	Concrete cover to the transverse reinforcement (mm)
NPC	Number of elements in which the column is divided [1 – 5]
NCOLS	Number of columns in the bent
SCOL	Spacing of the columns
CBW	Weight of the Capbeam (kN)

Multi column bent

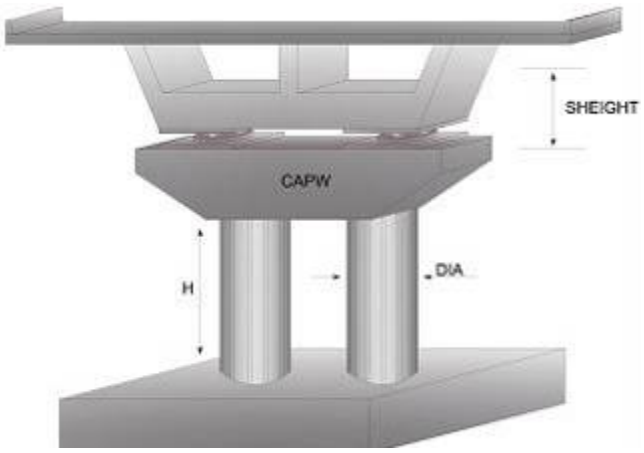

Figure 17 – Multi column bent

STA	Distance from the left end of the bridge to the element (m) [0-SLENGTH]
DIA	Diameter of the column (m) [>0]
H	Clear height of the column (m) [>0]
NLBAR	Number of longitudinal bars
DLBAR	Diameter of the longitudinal bars (m) [>0]
DHBAR	Diameter of the transverse reinforcement (mm) [>0]
HBARS	Spacing of the transverse reinforcement (mm)
COV	Concrete cover to the transverse reinforcement (mm)
NPC	Number of elements in which the column is divided (1 – 5)
NCOLS	Number of columns in the bent
SCOL	Spacing of the columns
CBW	Weight of the Capbeam (kN)
SKEW	Skew angle[0-90]
CAPH	Height of the capbeam (m)